17633

NATIONAL LIBRARY
OTTAWA

BIBLIOTHÈQUE NATIONALE
OTTAWA

NAME OF AUTHOR........Muzik Ivan

TITLE OF THESIS........State Variable Model of Surface Runoff from a Laboratory Catchment

UNIVERSITY........of Alberta

DEGREE FOR WHICH THESIS WAS PRESENTED........Ph. D.

YEAR THIS DEGREE GRANTED........1973

Permission is hereby granted to THE NATIONAL LIBRARY OF CANADA to microfilm this thesis and to lend or sell copies of the film.

The author reserves other publication rights, and neither the thesis nor extensive extracts from it may be printed or otherwise reproduced without the author's written permission.

(Signed)........Ivan Muzik

PERMANENT ADDRESS:

11807 - 76 Ave.
Edmonton
Alta

DATED........June 14........1973

NL-91 (10-68)

THE UNIVERSITY OF ALBERTA

STATE VARIABLE MODEL OF SURFACE RUNOFF FROM A LABORATORY CATCHMENT

by

Ⓒ IVAN MUZIK

A THESIS

SUBMITTED TO THE FACULTY OF GRADUATE STUDIES AND RESEARCH

IN PARTIAL FULFILMENT OF THE REQUIREMENTS FOR THE DEGREE OF

DOCTOR OF PHILOSOPHY

DEPARTMENT OF CIVIL ENGINEERING

EDMONTON, ALBERTA

FALL, 1973

UNIVERSITY OF ALBERTA

FACULTY OF GRADUATE STUDIES AND RESEARCH

The undersigned certify that they have read, and recommend to the Faculty of Graduate Studies and Research, for acceptance, a thesis entitled "STATE VARIABLE MODEL OF SURFACE RUNOFF FROM A LABORATORY CATCHMENT" submitted by Ivan Muzik, in partial fulfilment of the requirements for the degree of Doctor of Philosophy.

Dr. J.P. Verschuren Supervisor

Dr. T. Blench

Dr. G.S. Christensen

John B. Nuttall
Professor J.B. Nuttall

Dr. S.H. Simmonds

Date April 24, 1973

D. M. Gray
Dr. D.M. Gray
External Examiner
University of Saskatchewan
Saskatoon, Saskatchewan

ABSTRACT

The response of a well defined impervious surface to a specified input of rainfall was studied by means of a laboratory catchment. Under natural conditions these responses are affected by many random factors such as evaporation and infiltration losses. Under laboratory conditions such factors are eliminated or negligible. Thus the laboratory experiments enable investigation of deterministic processes in hydrology.

A mathematical model of overland flow has been developed using the state variable approach to system analysis. The model was tested by simulating the experimental hydrographs of surface runoff from the laboratory catchment for uniform, and time and space variable rainfall inputs. A mathematical relationship describing the raindrop impact effect was developed by the method of dimensional analysis and subjected to empirical evaluation.

The experimental hydrographs were also simulated by two existing mathematical models of overland flow: the instantaneous unit hydrograph and the kinematic wave model. The purpose of the investigation was to study nonlinearity of the rainfall-runoff relationship, to examine the theoretical assumptions of the above mathematical models, and to provide a basis for comparison of the results obtained by the state variable model.

The results of experiments indicated that the rainfall-runoff process is highly nonlinear, and thus the linear system analysis methods have limited application. The kinematic wave model was found to provide fairly consistent results but has a tendency to over-estimate the time to peak and the peak discharge. Results obtained with the state variable model compared favourably with those obtained experimentally by means of the laboratory catchment. It is believed that the output of this mathematical model may be helpful in urban runoff calculations, and that the concept of state and state variables should find a wide application in general hydrologic simulation.

ACKNOWLEDGEMENTS

The author wishes to express his appreciation to Professor J. P. Verschuren for his suggestions and guidance provided throughout the course of the work.

Sincere appreciation is expressed to the Hydraulics Laboratory staff for their help in fabricating the apparatus in various phases of the work.

The work upon which this thesis is based was supported by the National Research Council of Canada through a grant to Professor J. P. Verschuren.

TABLE OF CONTENTS

Page

Title Page i

Approval Sheet ii

Abstract iii

Acknowledgements v

Table of Contents vi

List of Tables ix

List of Figures xi

List of Symbols xxi

Chapter

I INTRODUCTION 1

History 1
Rainfall - Runoff Relationship 2
  Traditional Analysis 3
  New Approaches 5
Statement of the Problem 10
Objectives and Scope 11

II LABORATORY CATCHMENT: EXPERIMENTAL EQUIPMENT AND TECHNIQUES 13

Introduction 13
Requirements 14
  Test Basin 14
  Input Control and Output Measurement 14
Experimental Equipment 16
  Apparatus 16
  Rainfall Simulator 16
  Timing Device 25
  Test Basin 25
  Discharge Measuring Device 26
  Data Acquisition System 27
Experimental Techniques 27

TABLE OF CONTENTS (continued)

Chapter | Page

III NONLINEARITY PROBLEM IN HYDROLOGIC SIMULATION 36

Introduction 36
Linearized Hydrologic System 36
Comparison of Measured and Computed Responses . . 41

IV EXISTING MODELS OF SURFACE RUNOFF 44

Introduction 44
The Instantaneous Unit Hydrograph 45
The Convolution Integral 45
Conceptual Models of IUH 46
Direct Determination of IUH 51
Comparison of Experimental and Theoretical Results 52
Nonlinearity of Runoff Distribution 55
The Kinematic Wave Model 63
Kinematic Waves 63
Kinematic Wave Theory of Overland Flow 64
Comparison of Simulated and Observed Hydrographs 70

V STATE VARIABLE MODEL OF SURFACE RUNOFF 79

Introduction 79
State Space Analysis of Systems 80
Dynamic Systems 81
State and State Variables 82
State Space 82
State Space Representation of Systems 82
Second Order Systems and the Phase Plane 86
State Variable Model of Spatially Varied Overland Flow 97
Unsteady Spatially Varied Flow - Basic Equations 97
Unsteady Spatially Varied Flow - Approximation by Lumped Parameters 99
The State Variable Model 108
Modification of the Dynamic Equation for Raindrop Impact Effect 110
General 110
The Relationship Between Rainfall Intensity and Friction Factor 111
Comparison of Results with Existing Knowledge . . 124
Comparison of Predicted and Measured Hydrographs . . 126
Experiments with Uniformly Distributed Rainfall Input 129

TABLE OF CONTENTS (continued)

Chapter Page

Experiments with Temporally Varied Rainfall Input 138
Experiments with Spatially Varied Rainfall Input 138

VI DISCUSSION OF EXPERIMENTAL RESULTS AND SIMULATION METHODS 144

General 144
Accuracy of Experimental Techniques 145
Cumulative Outflow Hydrographs 145
Instantaneous Outflow Hydrographs 149
Comparison of the Studied Models 150
The Instantaneous Unit Hydrograph Model 151
Kinematic Wave and State Variable Models 154
Application of the State Variable Approach in Hydrologic Simulation 163
Traditional Approach 164
Modern Approach - Digital Hydrologic Simulation . . 165
Potential of the State Variable Approach 167

VII CONCLUSIONS AND RECOMMENDATIONS 173

Conclusions 173
Recommendations 175

LIST OF REFERENCES 177

APPENDICES

A LOAD BEAM: STRAIN-RESISTANCE RELATIONSHIP 186

B DERIVATION OF A UNIT IMPULSE RESPONSE OF (1) SINGLE RESERVOIR, (2) SERIES OF RESERVOIRS . . . 191

C RAINDROP IMPACT EFFECT ANALYSES - TABLES OF MEASURED AND CALCULATED FLOW PARAMETERS 198

D LIST OF COMPUTER PROGRAMS USED IN THE ANALYSIS 203

E MEASURED AND SIMULATED HYDROGRAPHS BY THE STATE VARIABLE MODEL, RUNS NO. 1 TO 6, AND 10 TO 24 213

F SAMPLE STATISTICAL ANALYSES 235

G EXAMPLES OF THE PHASE PLANE REPRESENTATION OF SYSTEMS 242

LIST OF TABLES

Table		Page
4-1	Apparent time to equilibrium, t_e, as function of rainfall intensity and bed slope for a runoff plane of length 91.4 cm.	60
4-2	Comparison of the empirical apparent time to equilibrium, t_e, and the time to equilibrium, t_s, predicted by the kinematic wave model.	72
5-1	Phase plane analysis of a laboratory reservoir for the case of receding outflow and zero inflow: approximate slopes of isoclines calculated by Equation (5-36) from measured values of discharge.	92
5-2	Summary of laboratory catchment experiments with uniformly distributed rainfall inputs	130
6-1	Estimated maximum errors in cumulative outflow	147
6-2	Differentiation of the depth of flow in the segments of the 7-order state variable model during surface runoff simulation for test 4	161
C-1	Flow parameters for slope $S_o = 0.2079$	200
C-2	Flow parameters for slope $S_o = 0.1051$	201
C-3	Flow parameters for slope $S_o = 0.05143$	202
F-1	Sample calculation of the confidence band of the cumulative outflow hydrograph, run 7.	239
F-2	Sample calculation of the confidence band of the instantaneous outflow hydrograph, run 7.	240

LIST OF TABLES (continued)

Table		Page
F-3	Sample calculation of the truncation error of the theoretical instantaneous outflow hydrograph, run 7.	241

LIST OF FIGURES

Figure		Page
2-1	Sketch of the laboratory catchment apparatus installation.	19
2-2	Side view of the laboratory catchment installation.	20
2-3	Front view of the laboratory catchment installation.	20
2-4	Rainfall simulator with a constant head tank and a rain-intercepting tray used to time the duration of rainfall applied to the laboratory catchment.	21
2-5	View of the 2 by 3 feet rainfall simulating unit showing 532 stainless steel tubes (I.D. = 0.012 inch) spaced at 1 1/4 inch intervals.	21
2-6	Formation of raindrops.	22
2-7	Arrangement of a movable constant head tank supplying water into the rainfall simulator.	22
2-8	Time sequence of formation of drops from capillary stainless tubes (I.D. = 0.012 inch) at the rainfall intensity of approximately 3 inches per hour. Average maximum drop diameter d is 2.5 mm.	23
2-9	Fall velocity versus fall distance (Wenzel, 1970).	24
2-10	Laboratory catchment (size 2 by 3 feet) and runoff collecting trough resting on two steel beams.	30
2-11	Sheet flow over the laboratory catchment runoff plane under simulated rainfall.	30

LIST OF FIGURES (continued)

Figure		Page
2-12	Sketch of the load beam.	31
2-13	Installation of the strain gauge transducer.	32
2-14	Arrangement of the collecting trough and the load beam.	32
2-15	Load beam - arrangement of strain gauges into a full Wheatstone bridge, and the bridge circuit diagram.	33
2-16	Flowchart of the data acquisition system.	34
2-17	Calibration curve of the load beam.	35
3-1	Definition sketch of a reservoir.	38
3-2	Graphical interpretation of linearization of a function around a steady state operating point, $O(q_*,S_*)$, by means of a Taylor series expansion.	40
3-3	Comparison of responses of a nonlinear reservoir to two step function inputs, and those predicted by a linear model of the reservoir.	42
4-1	Characteristic responses of non-interacting first-order linear systems to unit step function input.	48
4-2	Illustration of the physical analog of the Nash IUH model as the response, q_nk of a series of n non-interacting linear reservoirs to a unit impulse input I.	50
4-3	Recorded S-hydrographs, S_1 and S_2, of runoff from the laboratory catchment, and the corresponding derived instantaneous unit hydrographs, IUH-1 and IUH-2.	54

LIST OF FIGURES (continued)

Figure		Page
4-4	Reproduction of hydrographs by the Instantaneous Unit Hydrograph model when IUH-1 was used as the unit impulse response function (IUH-1 was derived from the S_1 hydrograph (Figure 4-3) for which the rainfall intensity was the same as for the reproduced hydrographs).	56
4-5	Simulated hydrographs by the Instantaneous Unit Hydrograph model when IUH-2 was used as the unit impulse response function (IUH-2 was derived from the S_2 hydrograph (Figure 4-3) for which the rainfall intensity was different (approximately 3 times higher) than for the simulated hydrographs).	56
4-6	Recorded hydrographs (runs no. 1, 4, 7) resulting from rainfalls of different intensities, and hydrographs derived by superposition of ordinates of the observed hydrograph corresponding to rainfall intensity $i = 3.84$ cm/hr.	58
4-7	Cumulative outflow from a runoff plane of length 91.4 cm with uniform slope $S_o = 9$ degrees as a function of rainfall intensity i (plotted by X-Y recorder).	61
4-8	Relationship of apparent time to equilibrium, t_e, rainfall intensity, i, and bed slope, determined experimentally for a runoff plane of length 91.4 cm.	62

LIST OF FIGURES (continued)

Figure **Page**

4-9 Kinematic wave solution of surface runoff by the method of characteristics: (a) definition sketch, (b) development of flow profiles: AM_1N_1 at time t_1, AM_2N_2 at time t_2, steady state profile $AM_1M_2M_3$ at time t_s. Broken lines represent y-x curves corresponding to the paths traced by imaginary observers who started to move along the plane AB at time t = 0 with velocity, c, from their starting positions 1, 2, 3, and 4. 67

4-10 Outflow q - t curves. 69

4-11 Observed and predicted hydrographs (kinematic wave model) for test 1, $(t_o>t_s)$. 73

4-12 Observed and predicted hydrographs (kinematic wave model) for test 2, $(t_o \doteq t_s)$. 74

4-13 Observed and predicted hydrographs (kinematic wave model) for test 3, $(t_o<t_s)$. 75

4-14 Observed and predicted hydrographs (kinematic wave model) for test 4, $(t_o>t_s)$. 76

4-15 Observed and predicted hydrographs (kinematic wave model) for test 5, $(t_o \doteq t_s)$. 77

4-16 Observed and predicted hydrographs (kinematic wave model) for test 6, $(t_o<t_s)$. 78

LIST OF FIGURES (continued)

Figure Page

5-1 Graphical solution of storage equation of a nonlinear reservoir by the method of isoclines for the case of zero inflow and three initial storages, S_1, S_2, S_3. 90

5-2 Phase plane solution of storage equation of a nonlinear reservoir for the case of zero inflow. 93

5-3 Comparison of measured responses of a nonlinear reservoir to two step function inputs, and those predicted by the phase plane method (nonlinear solution). 96

5-4 Definition sketch for surface flow over a sloping plane. 98

5-5 Surface runoff over a sloping plane: (a) definition sketch, (b) simulation by a 4th-order lumped system of interacting reservoirs in series, (c) simulation by a 4th-order lumped system consisting of hypothetical uniform flow reaches. 102

5-6 Energy in gradually varied overland flow. 105

5-7 Definition sketch for comparison of: (a) actual flow, and (b) flow simulated by noninteracting reaches. 106

5-8 Definition sketch for steady discharge condition ($Q = BiX = B\alpha y^3/C_r$) from a plane of length X and width B. 117

LIST OF FIGURES (continued)

Figure		Page
5-9	Definition sketch for determination of storage terms S_n ($n = 1, 2, 3, 4$).	120
5-10	Determination of the amount of stored water, S_T, on the runoff plane by means of mass curves of inflow and outflow.	121
5-11	Best fit line of the relationship between the intensity factor Ci and the dimensionless parameter $i\nu/U^2y$.	122
5-12	Friction factor, f_r, for laminar sheet flow under rainfall versus Reynold's number Re.	122
5-13	Comparison between hydrographs generated by the state variable model for the case: (a) raindrop impact effect not included, (b) raindrop impact effect included.	128
5-14	Responses of state variable models of nth-order ($n = 1, 2, 4, 7, 10$, and 15) to idential inputs of uniform rainfall with duration of 50 seconds.	128
5-15	Observed and predicted hydrographs (state variable model) for test 7 with uniform rainfall input.	132
5-16	Observed and predicted hydrographs (state variable model) for test 8 with uniform rainfall input.	133
5-17	Observed and predicted hydrographs (state variable model) for test 9 with uniform rainfall input.	134
5-18	Observed and predicted hydrographs (state variable model) for test 25 with uniform rainfall input.	135

LIST OF FIGURES (continued)

Figure		Page
5-19	Observed and predicted hydrographs (state variable model) for test 26 with uniform rainfall input.	136
5-20	Observed and predicted hydrographs (state variable model) for test 27 with uniform rainfall input.	137
5-21	Observed and predicted hydrographs (state variable model) for test with temporally varied rainfall input (ramp function).	139
5-22	Observed and predicted hydrographs (state variable model) for test with temporally varied rainfall input (double pulse function).	140
5-23	Observed and predicted hydrographs (state variable model) for test with spatially varied rainfall input (stationary rainstorm).	143
6-1	95% confidence bands of experimental hydrographs for test 7.	148
6-2	Instantaneous unit hydrograph (corresponding to unit rainfall intensity i = 7.42 cm/hr) derived from test 13.	152
6-3	Instantaneous unit hydrograph (corresponding to unit rainfall intensity i = 3.91 cm/hr) derived from test 16.	152
6-4	Comparison of simulated hydrographs for test 13.	155
6-5	Comparison of simulated hydrographs for test 14.	156
6-6	Comparison of simulated hydrographs for test 15.	157

LIST OF FIGURES (continued)

Figure		Page
6-7	Block diagram of the state variable model simulating natural watershed.	169
6-8	Definition sketch for application of the state variable model in simulating surface runoff from a natural watershed.	171
A-1	Definition sketch of a beam in bending.	188
A-2	Stress distribution diagram.	188
B-1	Definition sketch of a single linear reservoir.	192
B-2	Definition sketch of a series of linear non-interacting reservoirs.	195
E-1	Observed and predicted hydrographs (state variable model) for test 1 with uniform rainfall input.	214
E-2	Observed and predicted hydrographs (state variable model) for test 2 with uniform rainfall input.	215
E-3	Observed and predicted hydrographs (state variable model) for test 3 with uniform rainfall input.	216
E-4	Observed and predicted hydrographs (state variable model) for test 4 with uniform rainfall input.	217
E-5	Observed and predicted hydrographs (state variable model) for test 5 with uniform rainfall input.	218
E-6	Observed and predicted hydrographs (state variable model) for test 6 with uniform rainfall input.	219
E-7	Observed and predicted hydrographs (state variable model) for test 10 with uniform rainfall input.	220

LIST OF FIGURES (continued)

Figure		Page
E-8	Observed and predicted hydrographs (state variable model) for test 11 with uniform rainfall input.	221
E-9	Observed and predicted hydrographs (state variable model) for test 12 with uniform rainfall input.	222
E-10	Observed and predicted hydrographs (state variable model) for test 13 with uniform rainfall input.	223
E-11	Observed and predicted hydrographs (state variable model) for test 14 with uniform rainfall input.	224
E-12	Observed and predicted hydrographs (state variable model) for test 15 with uniform rainfall input.	225
E-13	Observed and predicted hydrographs (state variable model) for test 16 with uniform rainfall input.	226
E-14	Observed and predicted hydrographs (state variable model) for test 17 with uniform rainfall input.	227
E-15	Observed and predicted hydrographs (state variable model) for test 18 with uniform rainfall input.	228
E-16	Observed and predicted hydrographs (state variable model) for test 19 with uniform rainfall input.	229
E-17	Observed and predicted hydrographs (state variable model) for test 20 with uniform rainfall input.	230
E-18	Observed and predicted hydrographs (state variable model) for test 21 with uniform rainfall input.	231
E-19	Observed and predicted hydrographs (state variable model) for test 22 with uniform rainfall input.	232

LIST OF FIGURES (continued)

Figure **Page**

E-20 Observed and predicted hydrographs (state variable model) for test 23 with uniform rainfall input. 233

E-21 Observed and predicted hydrographs (state variable model) for test 24 with uniform rainfall input. 234

G-1 Phase trajectories for a system described by $\ddot{z} + z = 0$. 244

G-2 Construction of a trajectory (ABCD) using isoclines. 247

G-3 Phase plane diagram showing isoclines and a typical trajectory for a system described by $\ddot{x} + \dot{x} + x = 0$. 249

G-4 Phase plane diagram for a system described by $\ddot{x} + x\dot{x} + x = 0$. 250

LIST OF SYMBOLS

A	cross-sectional area of a reservoir
$\underline{A}$	matrix in the state equation
a_i	coefficients of a differential equation ($i = 1, 2, \ldots, n$)
B	width of a runoff plane
	area of a discharge orifice
$\underline{B}$	matrix coupling the input to the state variables
C	constant in a friction factor equation for laminar flow without rainfall, $f = \frac{C}{R_e}$
$\underline{C}$	matrix coupling the state variables to the output
C_1	Chezy coefficient, $C_1 = U/\sqrt{RS_o}$
C_2	Manning coefficient, $C_2 = 1.49/n$
C_1, C_2	constants of partial fraction expansion
C_i	dimensionless raindrop-impact-effect coefficient, $C_i = F_n(\frac{i\,\nu}{U^2 y})$
C_r	coefficient in a friction factor equation for flow under rainfall, $f_r = C_r/R_e$
$\overline{C_r}$	equivalent coefficient to C_r for uniform steady flow
c	velocity of a wave relative to the bank
	discharge coefficient of an orifice
D	inside diameter of a pipe
d	mean drop size
e	equivalent surface roughness
F_n	function
F_r	Froude number, $F_r = U/\sqrt{gy}$
f	Darcy friction factor

f_r	modified friction factor for raindrop impact effect
f	vector-valued function
g	gravitational constant
$\underline{g}$	vector-valued function
H_j	total energy at the channel section j
h	vertical depth of flow
h_f	head loss
$h(t)$	unit impulse response function
I	deviation variable of inflow, $I = i-i_*$
	rainfall intensity in the summation form of convolution
i	rainfall intensity
	volumetric rate of inflow
i_*	steady state rate of volumetric inflow
K	coefficient of a reservoir, $K = cB\sqrt{2g/A}$
K_r	recession constant
k	constant of a linear reservoir, $k = S/Q$
L	length of runoff plane
m	exponent
N	slope of a local tangent of a phase trajectory
n	Manning's resistance coefficient
	exponent
O	lumped volumetric outflow
P	lumped volumetric inflow
	precipitation number, $P = iL^2/Uy^2$
Q	volumetric rate of discharge
q	discharge per unit width

q_*	steady state rate of volumetric outflow
R_e	Reynolds number, $R_e = Uy/\nu$, $R_e = VD/\nu$
R	hydraulic radius
S	storage, $S = Ah$
	total energy line gradient
S_o	bed slope, $S_o = \sin\theta$
S_f	friction slope, $S_f = U^2/C^2R$
S_w	water surface slope
S_*	steady state storage
s	Laplace transform variable
T	time interval
t	time
t_o	duration of rainfall
t_e	apparent time to equilibrium
t_p	duration of constant outflow during recession, kinematic wave model
t_s	time to equilibrium of inflow and outflow
U	mean flow velocity in the x-direction
u	velocity component of the lateral inflow along x-direction
$\underline{u}$	input vector
$u(t)$	instantaneous unit hydrograph
u_r	raindrop impact velocity
V	mean flow velocity in a pipe
W	Weber number, $W = U^2\rho L/\sigma$
X	length
$\underline{x}$	state vector

y	depth of flow normal to bottom
$\bar{y}$	equivalent depth of uniform steady flow
Z	deviation variable of volumetric outflow, $Z = q - q_*$
	height above datum
$\underline{z}$	output vector
α	parameter in discharge equation
$\Gamma(z)$	Gamma function
ε	equivalent surface roughness
η	dimensionless coefficient
θ	angle of bed slope
λ	dimensionless coefficient
μ	fluid dynamic viscosity
ν	fluid kinematic viscosity
ρ	fluid mass density
σ	fluid surface tension
τ	time constant
	time

CHAPTER I

INTRODUCTION

1-1 History

Natural sciences are observational sciences. The first flood observations which were made, according to biblical accounts about 2957 B.C. on the Euphrates, may thus properly indicate the beginning of hydrology. However, it was not until the 20th century A.D. that hydrology developed into a truly scientific discipline.

In antiquity it was considered that stream flow was supplied from huge subterranean reservoirs and that water somehow returned from the oceans to the reservoirs through subterranean channels. No direct link was considered to exist between rainfall and runoff.

The first recorded attempts at measuring the adequacy of precipitation to provide runoff were made in the 17th century by Perrault (1674) and Mariotte (1686), who measured the flow and precipitation of the Seine basin in France and concluded that precipitation falling in this basin was sufficient to supply the stream flow.

From then onwards, in the 17th and 18th centuries, many observations were made of hydrological phenomena and the period was marked by the development of important measuring equipment, such as the current meter for the measurement of velocity in streams.

From the beginning of the 19th century to about 1930, hydrology went through the period of coefficients. This was, in a way, an empirical approach, in which "universal propositions were made about causal connections" (Toebes, 1968). Propositions were usually expressed in a simple equation in which one or more coefficients expressed the universality and had to be selected by judgement based on experience.

The excessive use of simple formulae, the results of which were not always found satisfactory, forced engineers to increase hydrological investigations to find more rational methods, based on a reasoning process rather than on judgement.

From about 1930 hydrology went through a period of great advance. The hydrological cycle in all its aspects became the central concept of the science, and rather than the restricted view of hydrology held before as a subject largely dealing with stream flow, it became a science which dealt with water in all its aspects. Definitions of hydrology such as "Hydrology is an earth science which is concerned with the laws governing the time and space distribution, circulation, and properties of the waters of the earth" were made and the sphere of hydrological interest has become interrelated in many aspects with other sciences, ranging from meteorology to chemistry and geology.

1-2 Rainfall - Runoff Relationship

Engineers are often concerned with only part of the hydrologic cycle which manifests itself as river runoff. Because rainfall is a prime cause of runoff in many parts of the earth, understanding of the rainfall-runoff relationship is essential for engineering analysis. The present emphasis on the development of water resources accelerates the need to develop reliable theories for the solution of problems such as the prediction of the future runoffs from watersheds altered by man-made changes, the design of a reservoir capacity for irrigation or waterpower development, and the prediction of flood flows in rivers. Although a large number of theories and methods now exists, there is a general lack of confidence concerning their ability to produce reliable solutions to the above type of engineering problem.

River runoff phenomena, besides their relation to rainfall as their sources, are the result of a highly complex combination of processes taking part at the surface and in layers of the ground. These processes in general are non-stationary because of temporal changes in the parameters governing them. Some of these parameters, such as soil moisture potential, soil permeability, and land-surface roughness, are variable over short periods of time.

Like all physical phenomena on the earth the processes which transform rainfall into runoff conform to the laws of physics and in this sense are completely regular. However, the extraordinary variety of conditions under which these processes occur, the non-uniformity of their spatial and temporal development, and finally the random character of fluctuations and combinations of different factors cause the analysis of the rainfall-runoff relationship to be a difficult task.

1-2-1 Traditional Analysis

Classical hydrology has attempted to solve the relation between rainfall and runoff on a given catchment with records through a study of the dependence of the volume of effective rainfall in an individual event on the volume and duration of actual rainfall, the time of year, etc., usually expressed in co-axial graphical correlation. For attenuation the unit hydrograph method was used. For ungauged catchments the traditional approach has been to relate the unit hydrograph to the catchment characteristics, such as the catchment area and shape, the length and slope of the main stream, etc.

The unit hydrograph concept was proposed by Sherman (1932) as a means of transforming effective rainfall (i.e. rainfall from which all losses due to evaporation, deep seepage, etc., have been deducted) into a runoff hydrograph. The unit hydrograph of a drainage basin is defined as a hydrograph of direct runoff (i.e. that part of runoff which enters the stream promptly after rainfall) resulting from a unit depth of effective rainfall generated uniformly over the basin area at a uniform rate during a specified period of time. It is assumed that the direct runoff is derived from the effective rainfall by a linear operation. Hence, if the unit hydrograph for the drainage basin is known, the hydrograph due to any effective rainfall distribution can be derived by applying principles of proportionality and superposition of causes and effects, which are valid for linear processes.

Derivation of the unit hydrograph from an observed hydrograph requires estimates of the depth and duration of the effective rainfall. Traditionally the observed total runoff hydrograph has been separated into the direct runoff and base flow. Parameters of the effective rainfall are then determined from the amount of the direct runoff. However, because the total runoff hydrograph consists of a continuum of components (surface runoff, subsurface runoff, and groundwater runoff) it is virtually impossible to distinguish them and thus the separation of the hydrograph becomes extremely arbitrary. This arbitrariness of the base flow separation necessarily destined further rainfall-runoff analysis, and the relationships thus derived to be somewhat haphazard.

1-2-2 New Approaches

The strength of hydrology lies in the excellence of the basic and derived sciences on which it is founded and the capability with which hydrologists can apply findings of these sciences to solve hydrological problems. Both the rapid development of related sciences such as mathematics, engineering and computing sciences, and the concentrated effort during the International Hydrological Decade have prompted introduction of new techniques into the rainfall-runoff analysis. The majority of these techniques can be categorized into one of the following general classifications: (1) system approach to the rainfall-runoff relationship, and (2) laboratory catchment studies of the rainfall-runoff relationship.

1-2-2-1 System Approach

The difficulty of applying known physical laws to hydrological phenomena lies in the ignorance of boundary and input conditions (Nash, 1969). Modern hydrology has attempted to circumvent these difficulties by a system approach. In the system approach, instead of studying the laws governing the operation and applying these to the boundary conditions, the operation itself, as manifest in previously recorded events, is studied.

The concept of a system, borrowed from electrical engineering, found widespread use by hydrologists. A system can be defined (Naslin, 1965) to be an assembly of physical components which experience mutual actions and reactions under the influence of their own behaviour and the external excitations acting upon the system as a whole. Essentially, a system consists of three parts (Vemuri, 1970): (1) the input signal, (2) the output signal, and (3) the plant. The plant of a system contains a mathematical characterization of the process that relates the inputs and outputs.

Problems solved by system engineering can be broadly classified as direct and inverse problems. Direct problems are characterized by a complete specification of a system and the task is to study or predict the response of the system to any specified input. The inverse problems are much more complex. Here the response to a particular input or inputs is known, but either the equations describing the process are unknown, or the inputs themselves are unknown. Depending upon the specific circumstance, an inverse problem may present itself as (1) design problem, (2) control problem, and (3) identification or modeling problem.

The task of analysing the rainfall-runoff relationship and simulating the runoff process by a mathematical model is a typical identification problem of systems analysis. In general, an identification problem is characterized by a specification of a finite set of observations on the input and output signals of a system and the goal is to find a mathematical characterization of the system. There are two principal lines of attack in attempting to characterize a system (Vemuri, 1970):

(1) The dynamical (or differential) equation approach. The unknown system is assumed to be characterized by a known set of dynamic (often differential) equations of a given order but with unknown coefficients. State variable and transfer function methods belong to this class.

(2) The kernel function approach. No assumption is made about the unknown system which is characterized by an analytic function over a function space and represented by the associated power series expansion (Balakrishnan, 1963). Identification of the inputs response essentially belongs to this class.

A basic advantage of the system approach lies in the possibility for standardization of analytical and computational techniques. Once a handful of techniques are mastered, it becomes only necessary to extend the arguments to be applicable to any physical system (Vemuri, 1970). Furthermore, the system representation helps to identify analogous situations which may otherwise escape attention. General as it may seem, the system approach is not a substitute for the lack of understanding of the governing laws of the studied process. There are two aspects of the system approach which must be realized.

Firstly, the form of the equation, or the model of a system, cannot be found through analysis of the input and the output (black box approach), but must be assumed. The system analysis says very little about the choice of the model, or about how a specific system should be characterized. Rather, it demonstrates the application of mathematical tools after the system has been properly represented by a mathematical model.

Secondly, the identification problem may lead to a multitude of mathematically acceptable solutions out of which one physically acceptable solution, if any such solution exists, has to be selected. However, it is almost practically impossible to verify the validity of an identified model. Two main reasons for this are: (1) in an identification problem the input is not generally under the control of the observer, and (2) the period of observation is always limited and therefore the validity of the model is correspondingly limited to the range of variation of input signals which appeared within the observation interval. The wording "identification of a system from input and output measurements" is therefore not strictly correct; the best one can do is to make an estimate, from the measurements, of the best "representative" in a given class (Balakrishnan, 1967).

1-2-2-2 Laboratory Catchment Studies

The conventional approach to study the rainfall-runoff relationship of a watershed uses historical data to fit a mathematical model for simulation of watershed hydrologic behaviour. Historical data, however, are collected from natural phenomena that can be measured and observed only once and then will not occur again. Furthermore, the available data usually cover too short a period and contain too limited a range of events to provide a thorough test of mathematical models of the runoff process. For these reasons there has been growing interest in the studies of the rainfall-runoff relationship under controlled conditions, by means of laboratory catchments.

Amorocho (1965) defined a laboratory catchment as a physical system of comparatively small size, in which the input and the output occur in the form of flowing water, and appropriate controls and measurement devices are provided to regulate the input as desired and to measure the output with adequate accuracy. The majority of laboratory catchments can be categorized into one of the following general classifications: (1) model catchments, (2) hydromechanic prototypes, and (3) prediction analysis prototypes.

The first type of laboratory catchment is used in studies of the rainfall-runoff relationship, which involve construction of a scale model of an actual watershed. The aim of such studies is to predict the prototype behaviour from observations made on the model, according to Newton's law of similitude. Several studies with model catchments of this type have been reported (Grace, 1965, 1967; Chery, 1965, 1966, 1967), however, the complexity of the hydrologic processes poses very difficult problems with regard to the establishment of dynamic similitude. Not only does it appear unlikely that even the most significant requirements of similitude may be satisfied simultaneously, but it is a hard task to characterize rigorously most watershed parameters.

The second of the above classifications includes laboratory catchments which are used for experimental investigation of flow mechanisms and are part of the field of study sometimes called "watershed hydraulics" (Amorocho, 1965; Chow, 1967). With the use of this type of a laboratory catchment as a research tool, a number of studies on the rainfall-runoff relationship have been made, including studies of the time distribution of the runoff process (Harbaugh, 1966), the conceptual watershed roughness (Harbaugh and Chow, 1967), and the effect of the storm movement (Yen and Chow, 1968). There are numerous other problems that can be studied systematically using this experimental approach. The experimentation may include changes in physical variables of the catchment, such as the shape, roughness, slope, size, and channel pattern. The study may not be limited to the surface runoff only. The laboratory catchment may be built with perforated bottom and provided with a layer of porous material. Thus, subsurface flow can be developed, tested, and analyzed. Information obtained from such experiments is otherwise unobtainable in the case of natural hydrological data.

The type of a laboratory catchment depicted in the third classification serves the purpose of providing laboratory data for the tests of mathematical models of the rainfall-runoff relationship built on the basis of the system approach, i.e., to provide data necessary for identification of the system. When this type of a laboratory catchment is used, no attempt is made to simulate the detailed inner behaviour of any specific watershed. The only requirement is that the laboratory catchment should have significant nonlinearities of the same kind presumed to exist in natural basins, and the prime purpose is to gain knowledge on methods for establishing the input-output relationship applicable to the general class of nonlinear systems of which watersheds are a part (Amorocho, 1965). Most experimental investigations dealing with this type of a laboratory catchment have been done by Amorocho and Orlob (1961), Amorocho and Hart (1965) and Amorocho (1971).

1-3 Statement of the Problem

The present study has evolved from a need to improve on the existing methods of the rainfall-runoff relationship analysis, which is part of a general problem of hydrograph forecasting. A host of mathematical models simulating rainfall input and runoff output from a watershed are available but there is as yet no general theory to explain the course of mechanics of flow from input to output. It is not unusual to obtain predictions from different models that differ, to an unacceptable degree, both with each other and with the truth. Some of the more obvious causes of this lack of reliability are the following (1., 2., 3. after Amorocho, 1967):

(1) Time variability of watersheds due to man-made changes, and due to the natural processes of weathering, erosion, climatic change, etc.

(2) Uncertainty with respect to the space and time distribution of the inputs and outputs of hydrologic systems, and with respect to the states and properties of the interior elements of the system in time.

(3) The inherent nonlinearity of the processes of mass and energy transfer that constitute the hydrologic cycle.

(4) The use of natural data which limits the rainfall-runoff analysis to derivation of only empirical and statistical relationships. The basic laws or principles involving a certain factor cannot be readily determined.

1-4 Objectives and Scope

The purpose of the present study has been to extend and improve the existing knowledge concerning the relationship between rainfall and runoff. The primary objective was to apply state space theory of systems analysis to formulate a general mathematical model of watershed runoff. In the state space formulation of an n-th order physical system, the future performance of the system can be related to the values of n state variables which are defined at any given time. The attractiveness of the state space method to mathematical simulation in hydrology lies in the (1) flexibility and the systematic manner with which the method handles any number of inputs and outputs, (2) clear physical interpretation of the state variables, and (3) applicability of the method to both linear and nonlinear systems. Specific objectives were:

(1) To develop and test a state variable model, able to simulate surface runoff generated by temporally and spatially distributed rainfall.

(2) To compare the state variable model with two existing theories of surface runoff: (a) the instantaneous unit hydrograph theory, and (b) the kinematic wave theory.

(3) To investigate the degree of nonlinearity involved in the rainfall-runoff relationship, with the aim to assess the feasibility of using the theory of linear systems (eg., the unit hydrograph method) in the analysis of the rainfall-runoff relationship.

Because of the weaknesses of the conventional approaches to the rainfall-runoff relationship studies (due to the use of natural data), the analysis in the present study has been based on the results of laboratory catchment experiments. The investigation has been limited to rainfall-generated surface sheet runoff from a uniformly sloping impervious plane of uniform roughness. These restrictions, which can be removed in the future when the mechanics of the surface runoff becomes clearer, do not impair the validity of the present approach of analysis. On the contrary, the controlled laboratory experiments eliminate the uncertainty embedded in natural data, and the nonstationarity of natural watersheds. The use of an impervious surface eliminates the arbitrariness of the base flow separation. Therefore, the concepts and theories concerning the rainfall-runoff relationship can be readily examined from the results obtained by this research.

CHAPTER II

LABORATORY CATCHMENT: EXPERIMENTAL EQUIPMENT AND TECHNIQUES

2-1 Introduction

Dimensional analysis is a well established technique in engineering fluid mechanics. A useful practical by-product of such analysis has been the discovery of how, within practical limits, to devise and run models so that quantitative predictions can be made about prototype behaviour despite total ignorance of the dynamically correct formulas for the phenomena at work (Blench, 1969).

The use of dynamically similar models to solve hydrologic problems has been an attractive possibility for many years. In such studies the topographic features of a natural (prototype) catchment are reproduced to an approximate scale in a laboratory model from which predictions of prototype behaviour are obtained by application of similarity criteria. Unfortunately, studies of overland flow conducted by Chery (1966), Grace (1967), et. al., show that true hydraulic similitude between a prototype basin and a scale model is very difficult if not impossible to obtain.

An alternative approach, used in this study and previously employed by Amorocho (1961), is to study a laboratory basin, which although not representative of any specific prototype, still retains some of the qualitative characteristics of natural catchments. By analyzing experiments on such basins the aim is to develop a method equally well applicable for analysis of natural catchments.

2-2 Requirements

Laboratory study of a small catchment involves a number of requirements pertinent not only to the instrumentation necessary to control the input and to measure the output, but also to the characteristics of the catchment itself. Such requirements are discussed in this chapter. Also the designed equipment and the applied experimental techniques are described.

2-2-1 Test Basin

The size of a laboratory basin should be such that the use of simple and reliable instrumentation is possible. The accuracy of the outflow measurement increases with the size of the test basin. However, with increasing catchment area the difficulty arises in providing adequate rainfall input control.

Depending on the scope of experiments the test basin should provide for the possibility to vary the slope, and roughness of the runoff surface. In the case of experiments including the subsurface flow, the test basin should provide a layer of porous material and allow for measurements of the subsurface outflow.

2-2-2 Input Control and Output Measurement

The objectives of using a laboratory catchment demand that any spatial variation of input rainfall should be reflected in the runoff hydrograph. Thus the ability to produce controlled inputs both in time and space is a prerequisite for the detection of such effects.

The simplest input is a uniformly distributed rainfall in space and time. The uniformity of input rainfall is closely related to the method used to simulate rainfall. Basically there are two types of rainfall simulators. One type uses sprinklers or nozzles to form raindrops, the other type employs capillary tubes. Sprinklers and nozzles produce raindrops of variable sizes comparable to the drop size distributions observed in natural rainfalls (Hall, 1970). However, it is difficult to achieve uniform areal distribution. To maintain the uniformity of the inputs and to investigate the effect of raindrop impact on sheet flow, it is desirable to limit the experiments to one drop size at a time.

In summary, the input installation should have the following features:

(1) Drop sizes comparable with those occurring in natural rainfall.

(2) Allow variation in rainfall intensity.

(3) Assure uniform application over the test basin.

(4) Ability to produce time and space variable inputs.

(5) Quick response to on-off inflow commands.

From the existing methods of simulating rainfall (Hall, 1970) only the method employing capillary tubes to form raindrops appears to satisfy the above requirements.

The outflow measuring device should be simple, reliable, and accurate. It is desirable to measure outflow directly, however, no such method, applicable to sheet flow, is available. Instead, the cumulative volume or weight of outflowing water is usually measured. Relatively simple transducers of the cumulative amount of outflow can be constructed by utilizing strain gauges (Byards, 1969; Stein, 1962).

2-3 Experimental Equipment

All devices used in the laboratory catchment experiments, except the data acquisition system, were designed and made for the purpose of this investigation. A full description of these devices is given in the following sections.

2-3-1 Apparatus

The general arrangement of the experimental set up is shown schematically in Figure 2-1. The photographs of the installation are shown in Figures 2-2 and 2-3.

2-3-2 Rainfall Simulator

The rainfall simulator, for reasons given earlier, was of the type in which drops are formed by a large number of short length fine-bore capillary tubes. Mechanics of drop formation from a capillary tube was described by Chow (1965) and need not be discussed here.

The unit, shown in Figure 2-4, consisted of a closed box, 24 1/4 inches by 37 1/2 inches, constructed of 3/16 inch thick plexiglass. The height of the box increased diagonally from 7/8 inch to 3 1/8 inch. The sloping ceiling allowed concentration of air bubbles in one corner of the box where a vertical tube served both as an air vent and an open manometer.

The water supply was provided by a 3/4 inch copper pipe, placed inside, across the width of the box, at the higher end. Drilled holes along the pipe faced the top of the box to minimize the effect of inflow velocity.

The raindrop producing tubes were 1 inch long, made of stainless steel, with 0.012 inch I.D. They were placed at 1 1/4 inch centers in the bottom face of the box, (Figures 2-5 and 2-6) totalling to 532 tubes.

The unit rested on an aluminum rectangular frame provided with four levelling screws. The frame was placed on top of an overall framework.

Pressure inside the unit was controlled by a constant head tank, shown in Figure 2-7, movable along four vertical rods. Maximum possible difference in pressure head, between the water level in the tank and the tips of the capillary tubes, was 3 feet. This installation was suitable for generation of steady rainfall inputs and a ramp function type of inputs.

It was intended to monitor the pressure inside the unit by a pressure transducer, calibrated in terms of rainfall intensity. However, the pressure transducer was found to be temperature sensitive, and since the daily temperature fluctuations in the laboratory were up to 10°F in summer, this idea was abandoned. Instead, rainfall intensity was determined from measured steady outflow during experiments.

The rainfall intensity range of the described simulator was from 0.75 inches per hour (19.05 mm/hr) to 6 inches per hour (152.4 mm/hr). Since the unit consisted of 532 tubes with inside diameter = 0.012 inches (0.3048 mm) and covered an area of 6 square feet (5574.1824 cm^2), the average flow velocity in cm per second through the tubes was

$$V = \frac{5574.1824 \times i}{3600 \times 532 \times \pi \frac{.03048^2}{4}} = 0.3988\ i \qquad (2\text{-}1)$$

where i is the rainfall intensity in mm per hour. For the proposed range of rainfall intensities, the average flow velocity in the tubes varied from 7.58 cm/sec. to 60.79 cm/sec. The maximum Reynolds number ($Re = \frac{VD}{\nu}$), was thus about 200, well within the range of laminar flow, and the flow was therefore assumed to be laminar. This in turn assured a linear relationship between applied pressure to the unit and the resulting rainfall intensity (Amorocho, 1965).

The length of the capillary tubes, L, was found to be an important factor, greatly influencing the speed with which the individual drops are formed. For laminar flow the friction head loss, h_f, is expressed by the Hagen-Poiseuille equation

$$h_f = \frac{32\nu LV}{g\,D^2} \qquad (2-2)$$

where ν is the kinematic viscosity of water and g is the acceleration of gravity. For maximum velocity of 60.79 cm/sec the head loss per 1 mm of a tube's length is h_f = 1.98 cm. This represents about 4% of the total pressure range used in the experiments (about 50cm), or 4% change in the corresponding range of rainfall intensity. It is therefore important that the tubes are as much as possible of the same length to assure spatially uniform rainfall distribution.

The average height of the rain simulator above the test basin was 4.4 feet (134 cm), and the average diameter, d, of a drop was 2.5 mm. The average drop diameter was estimated from a sequence of photographs taken by a movie camera as illustrated in Figure 2-8. By interpolation from Wenzel's data (1970), shown in Figure 2-9, giving the relationship of drop size, fall height and fall velocity, the impact raindrop velocity in the present study was approximately 15 ft/sec.

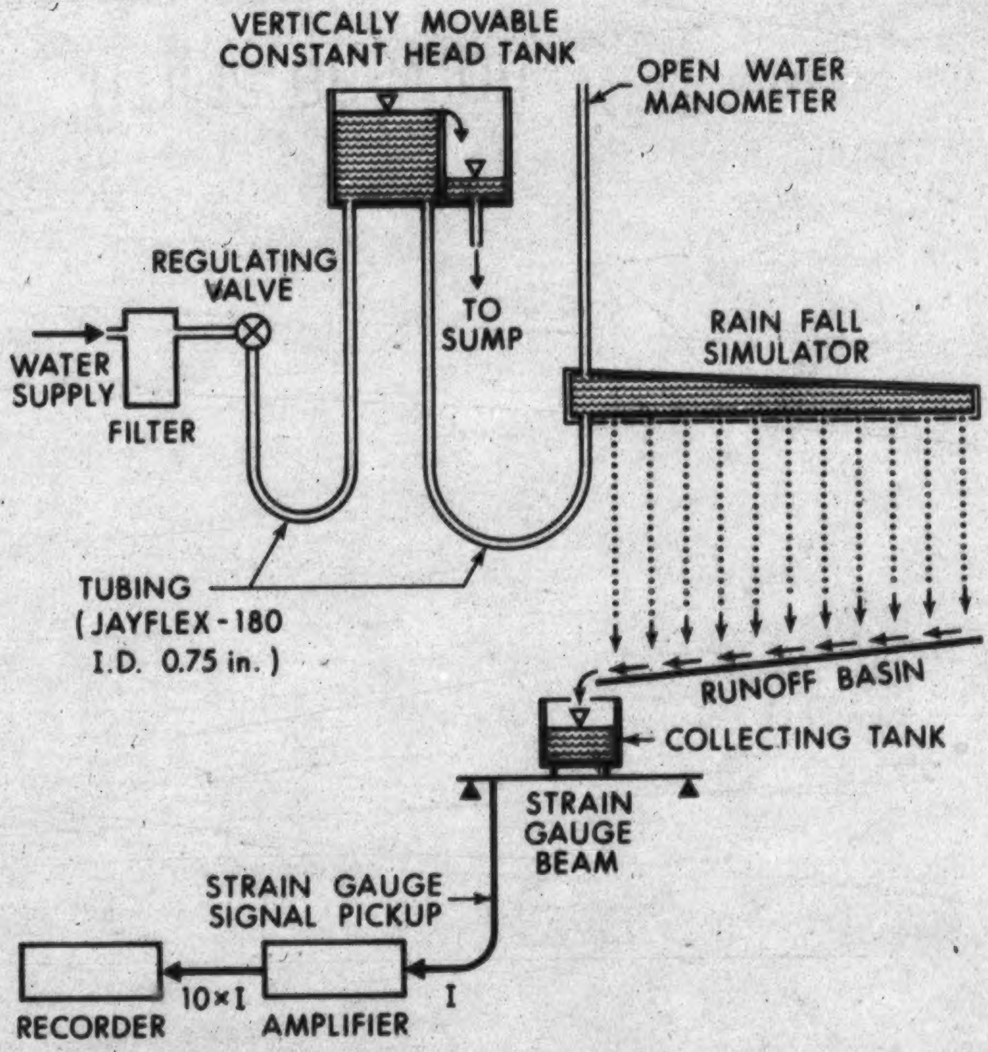
VERTICALLY MOVABLE CONSTANT HEAD TANK
OPEN WATER MANOMETER
REGULATING VALVE
TO SUMP
RAIN FALL SIMULATOR
WATER SUPPLY
FILTER
TUBING (JAYFLEX-180 I.D. 0.75 in.)
RUNOFF BASIN
COLLECTING TANK
STRAIN GAUGE BEAM
STRAIN GAUGE SIGNAL PICKUP
RECORDER
10×I
AMPLIFIER
I

Figure 2-1. Sketch of the laboratory catchment apparatus installation.

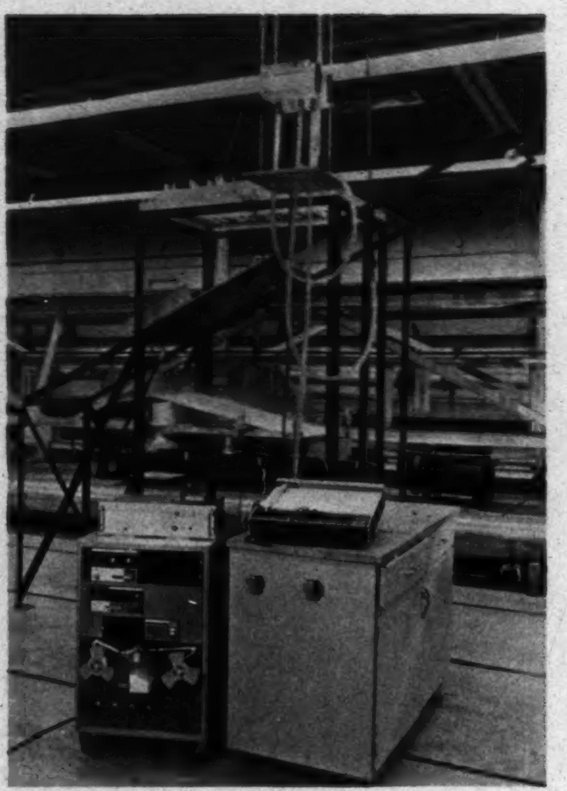

Figure 2-2. Side view of the laboratory catchment installation.

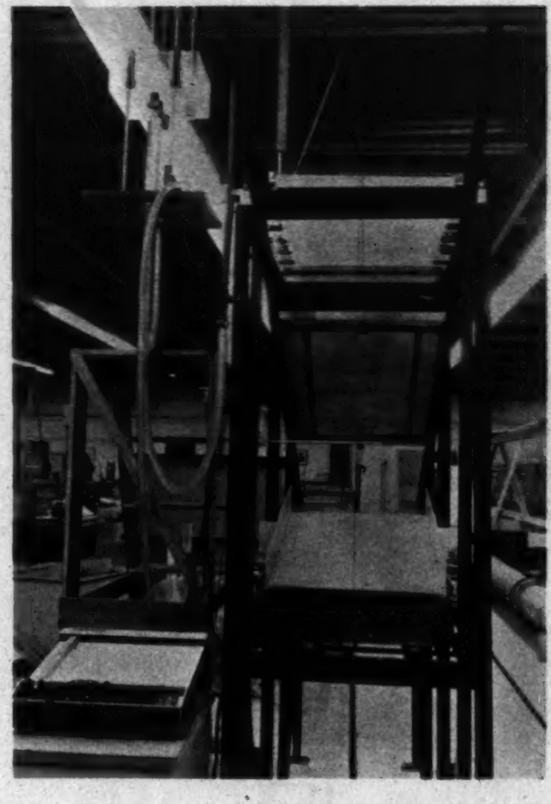

Figure 2-3. Front view of the laboratory catchment installation.

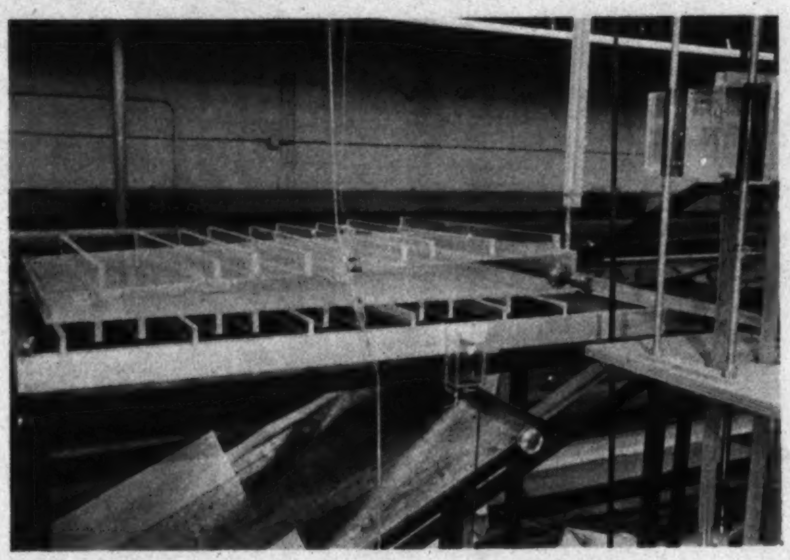

Figure 2-4. Rainfall simulator with a constant head tank and a rain-intercepting tray used to time the duration of rainfall applied to the laboratory catchment.

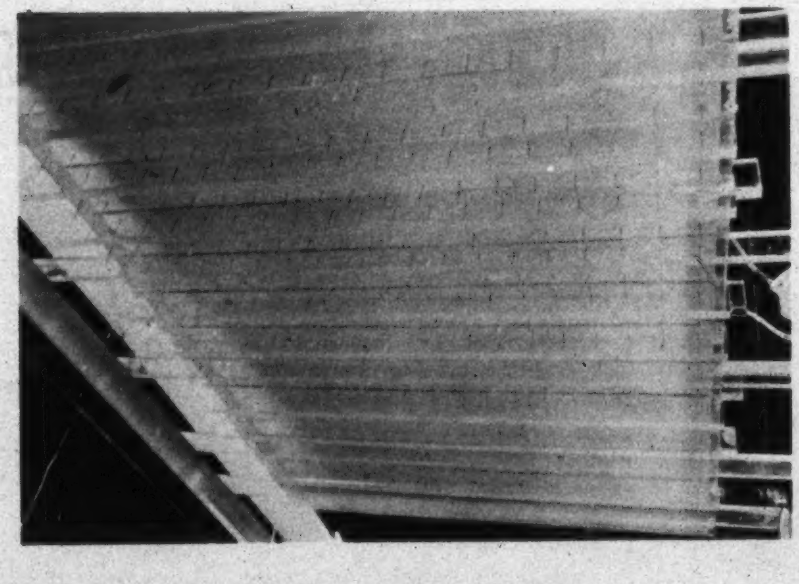

Figure 2-5. View of the 2 by 3 feet rainfall simulating unit showing 532 stainless steel tubes (I.D.=0.012 inch) spaced at 1 and 1/4 inch intervals.

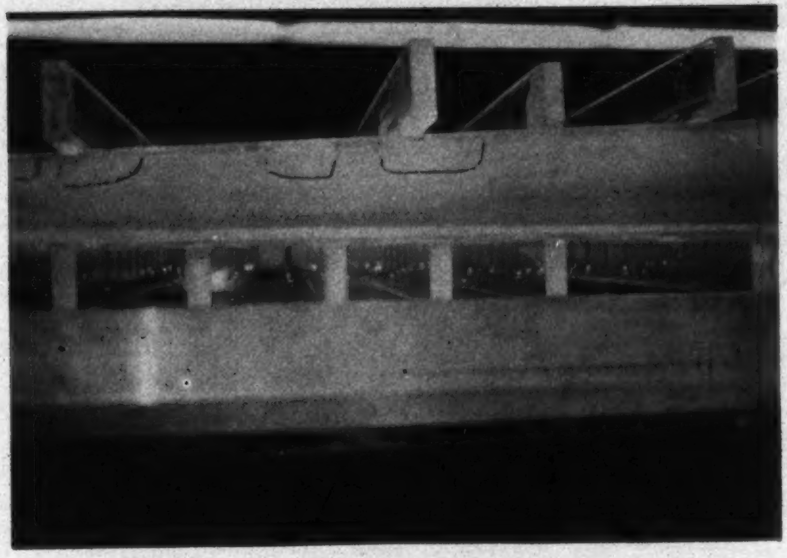

Figure 2-6. Formation of raindrops.

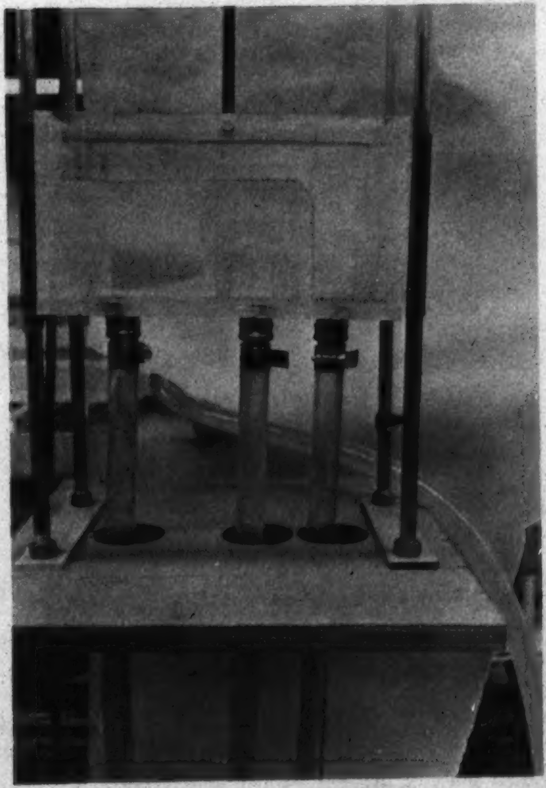

Figure 2-7. Arrangement of a movable constant head tank supplying water into the rainfall simulator.

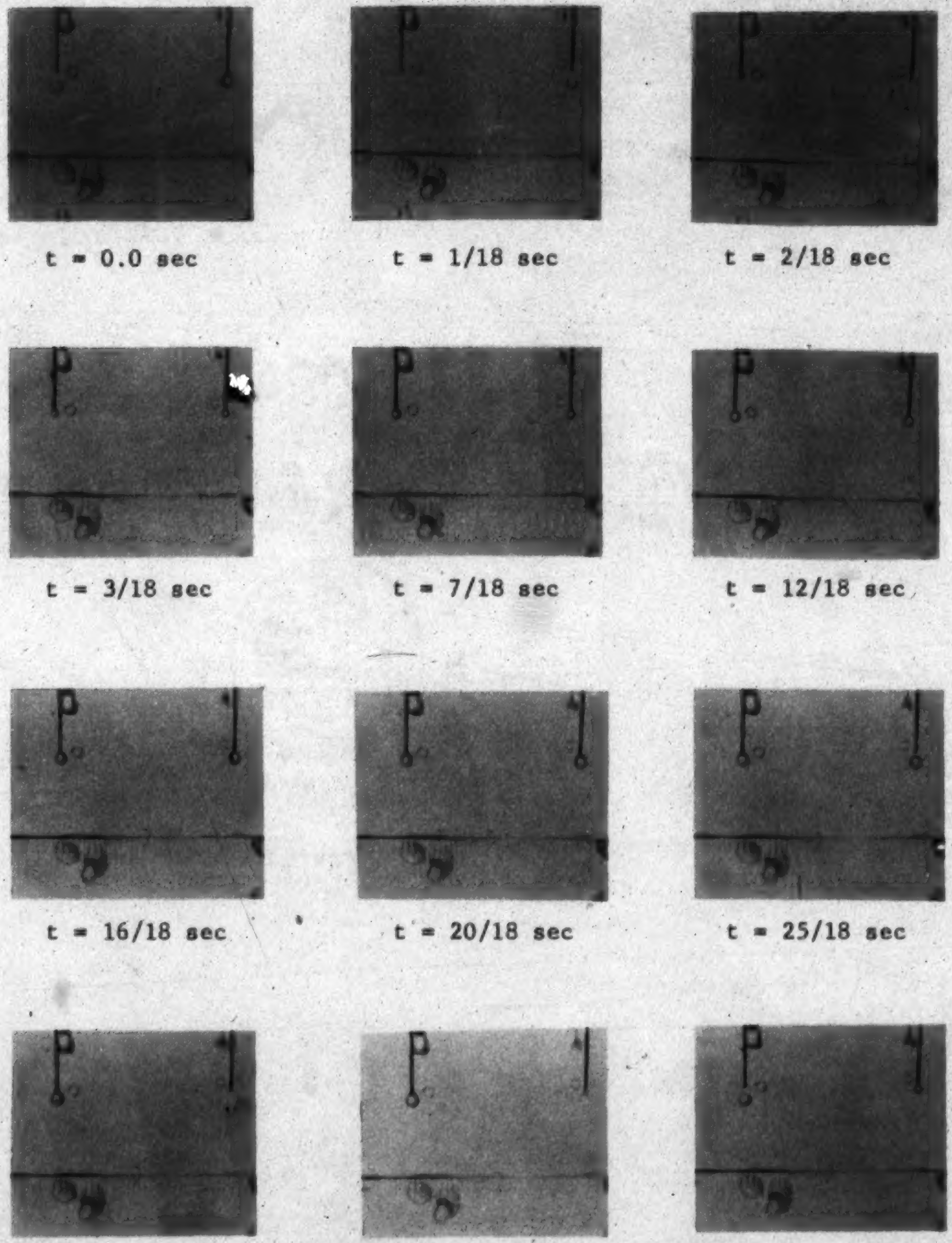

t = 0.0 sec
t = 1/18 sec
t = 2/18 sec
t = 3/18 sec
t = 7/18 sec
t = 12/18 sec
t = 16/18 sec
t = 20/18 sec
t = 25/18 sec
t = 26/18 sec
t = 27/18 sec
t = 28/18 sec

Figure 2-8. Time sequence of formation of drops from capillary stainless steel tubes (I.D.=0.012 inch) at the rainfall intensity of approximately 3 inches per hour. Average maximum drop diameter d is 2.5 mm.

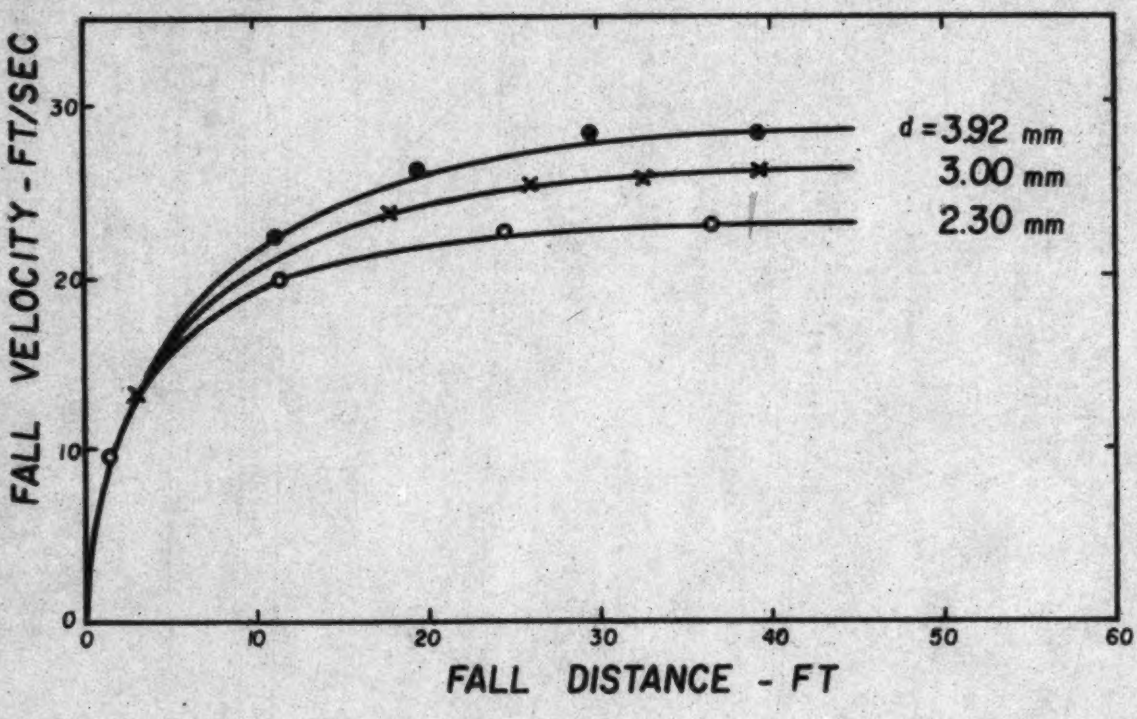

Figure 2-9. Fall velocity versus fall distance (Wenzel, 1970).

2-3-3 Timing Device

Starting and stopping of rainfall application was done manually using a rain intercepting tray, shown in Figures 2-2, 2-3, and 2-4. The tray, provided with four wheels, was placed between the rain simulator and the test basin, on a separate frame with two leading rails. The slope of the rails was 0.49, which enabled the released tray to slide down fast by the action of gravitational pull alone. To clear or screen the test basin took on the average 0.5 second.

Water intercepted by the tray was discharged elsewhere by a plastic tube. This type of rain interception was also suitable for simulation of moving storms over the test basin.

2-3-4 Test Basin

A rectangular shape of the test basin, with uniformly sloping runoff plane, as shown in Figures 2-10 and 2-11, was used exclusively. The basin, made of 1/4 inch plexiglass, was supported by an aluminum frame allowing variation of the slope of the basin within the range from 0 to 20 degrees.

The runoff plane was made of galvanized sheet metal, treated with diluted solution of hydrochloric acid. This treatment changed the originally non-wetting metal surface into a wetting surface.

Experiments with non-wetting surfaces showed that water formed on the surface as small globules. The globules grew, and when they became of sufficient size, they would suddenly leave their place and flow over the surface as a small slug of water. As a result, the runoff hydrographs were of undesirable shape in the form of cumulative stepwise increments.

2-3-5 Discharge Measuring Device

The choice of the method of measuring the discharge from the test basin was primarily dictated by the amount of outflowing water. Since the discharge from the test basin was relatively small and occurred as sheet flow with shallow depth, the only practical method was to record cumulative outflow continuously. The instantaneous rates of discharge were then determined by numerical differentiation.

Discharge from the test basin was received in a painted sheet metal trough, supported by two steel beams. The arrangement of the trough and beams is shown in Figures 2-12, 2-13, and 2-14. The design permitted only one position of the trough with respect to the beams (important for calibration), and minimized friction during bending of the beams.

Only one of the beams was active, with two strain gauges attached centrally both at the top and the bottom. The strain gauges, type Budd C-6-141-1000, gauge factor 2.02 ± 0.5%, were cross - connected into a full Wheatstone bridge, as shown in Figure 2-15. The input voltage into the bridge was 24V. The adopted strain gauge measuring system was based on the linear relationship between weight applied to a beam and the resulting strain. This method was preferred to others because the use of strain gauges permits to construct relatively simple measuring devices, with high sensitivity and accuracy. Also calibration of such devices does not change appreciably with time, and modern strain gauges are temperature compensated.

The strain-resistance relationship, as well as the criteria important for choice of strain gauges are discussed in the Appendix A.

2-3-6 Data Acquisition System

The signal from the Wheatstone bridge was either continuously recorded by a Hewlett-Packard 7004A X-Y recorder or punched on a paper tape in form of a discrete time series, using Digitec Data Acquisition System.

The X-Y recorder was used only in a few experiments, dealing with the effect of raindrop impact on runoff. For the main series of runoff experiments the discrete data system was used exclusively. A flow chart of the discrete data acquisition system is shown in Figure 2-16.

The Wheatstone bridge signal was first amplified ten times before the data were punched on a paper tape in ASCII code. The fastest possible rate of data punching was about one nine-digit reading per 1.6 sec. This was much slower than the manufacturer's suggested rate of reading (personal communication), however, it was observed that with increased frequency of reading the system malfunctioned.

For further processing the data were copied on a nine-track magnetic tape, which was subsequently used in IBM-360 digital computer. The final output was a printout of cumulative and instantaneous outflows as functions of time, and computer plotted hydrographs of instantaneous discharge.

Despite a certain noise level present in the electronic system, the load readings on the digital system could be made to within ± 3g.

2-4 Experimental Techniques

Timing of the rain application to the test basin was done manually by releasing or pulling up the intercepting tray. This technique inevitably introduced random errors into the measurement. Each experiment was therefore repeated seven times to obtain an estimate of the average runoff values with respect to the assumed beginning and end of the rainfall.

This, in turn, required that the initial conditions, with respect to the amount of water present on the runoff surface before each repetition, were the same. To start each run with initially dry surface would have been too time consuming. Morgali (1970) concluded from his analysis of the scatter of the data obtained in laboratory catchment experiments, that the ideal condition is for the runoff plane to have neither free water on the surface, which would add to the flow, nor dryness, which would cause water to be absorbed by the plane. Hence, five minutes drying interval was allowed after each run before the next run was started. This period was sufficient for the runoff from a previous test to cease to zero, within the limits of the recording device.

Calibration of the outflow measuring system was done for weight increments of 500 grams by adding 500 cc of water into the collecting trough. The relationship between applied weight and the Wheatstone bridge voltage output, shown in Figure 2-17, was found to be linear within the working range from 0. to 11,000. grams. The calibration was checked before and after each experimental period, and was found to be stable.

The noise in the recorded signal was partly due to the fluctuations of the reference voltage applied to the Wheatstone bridge. The fluctuations were observed to be within the range 24.00 ± 0.02 volts. Another source of noise was a slight vibration of the beams caused by the impact of inflowing water into the trough.

The experimental runs were conducted in the following manner:

(1) Approximately 20 minutes warm up period preceded the beginning of an experimental period. During this period the electronic parts of the system were allowed to stabilize.

(2) The constant head tank was secured in position for a desired rainfall intensity, while the sliding tray was in position intercepting the rain.

(3) After the warm up period the sliding tray was released and the test basin was wetted completely.

(4) When a steady outflow was reached the rain was interrupted. After a five minutes drying period the first experimental run started. The initial voltmeter reading was recorded and an electric stop watch and the paper tape punch were started. Simultaneously the sliding tray was released to begin the rain application.

(5) After a specified duration of rain, the sliding tray was pulled up and the receding runoff continued to be recorded for another 150 seconds.

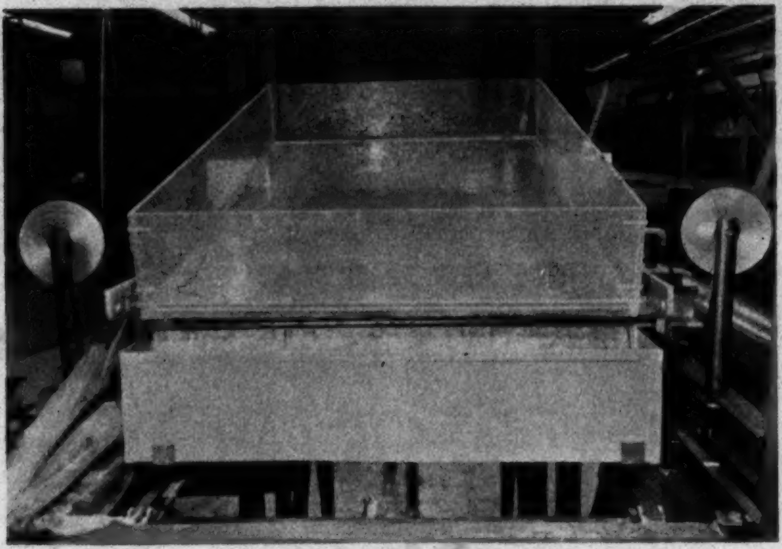

Figure 2-10. Laboratory catchment (size 2 by 3 feet) and runoff collecting trough resting on two steel beams.

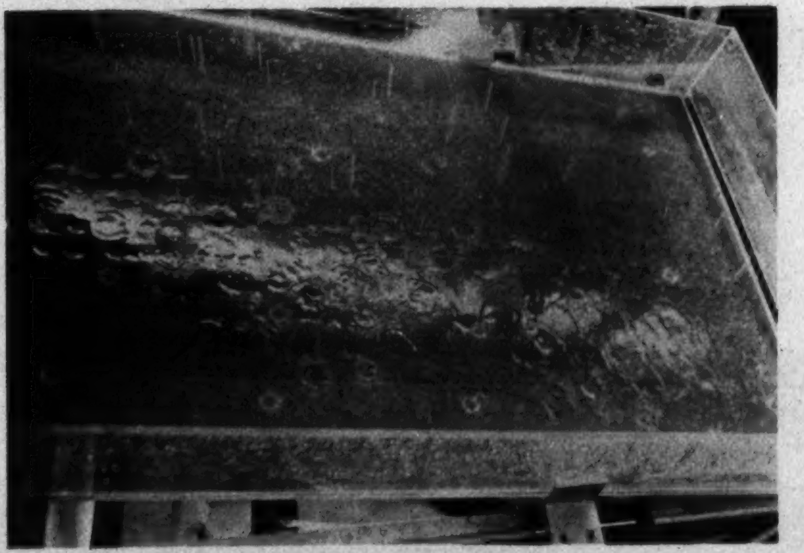

Figure 2-11. Sheet flow over the laboratory catchment runoff plane under simulated rainfall.

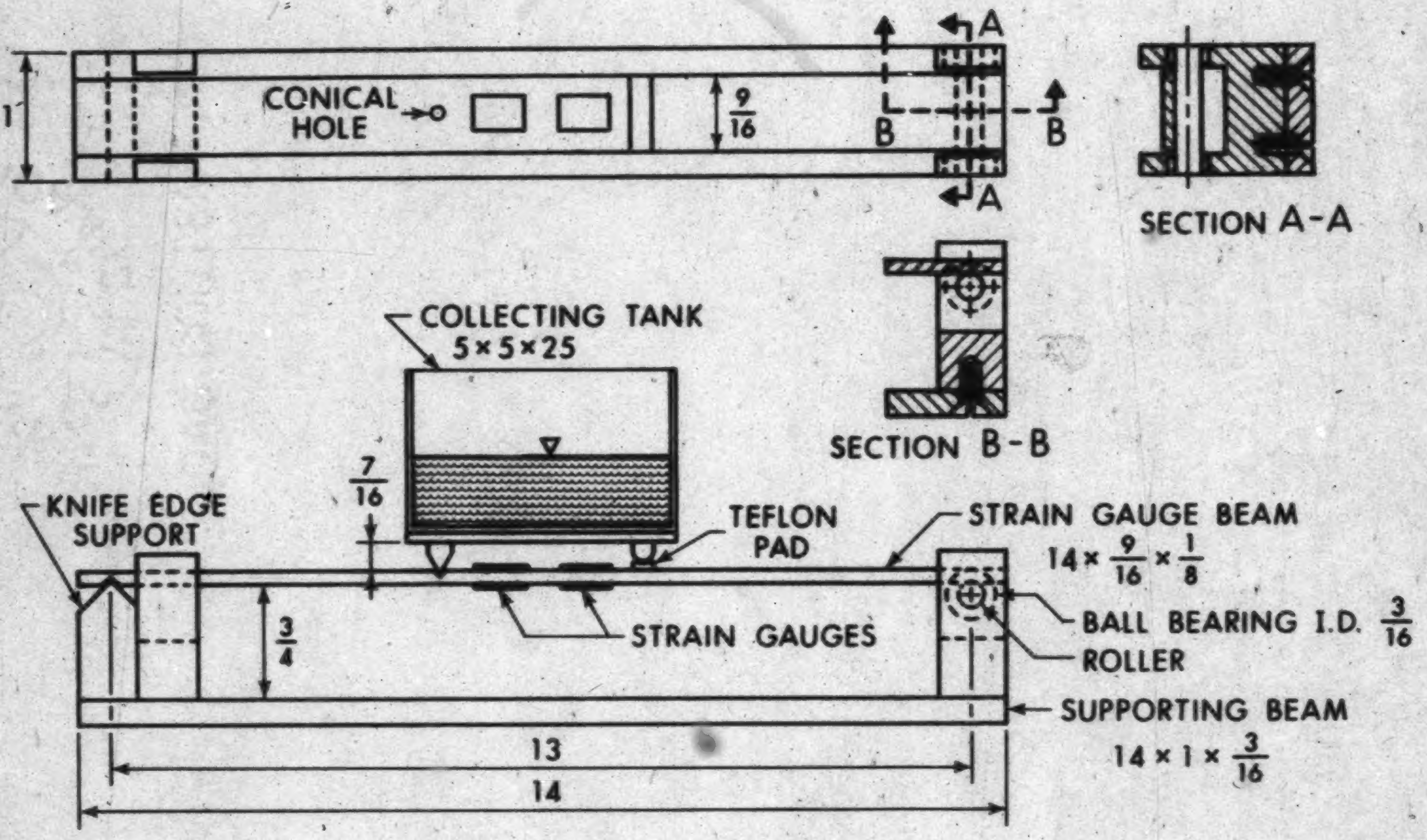

1
CONICAL HOLE
9/16
A
A
B
B
SECTION A-A
SECTION B-B
COLLECTING TANK 5×5×25
7/16
KNIFE EDGE SUPPORT
TEFLON PAD
STRAIN GAUGE BEAM 14× 9/16 × 1/8
BALL BEARING I.D. 3/16
ROLLER
3/4
STRAIN GAUGES
SUPPORTING BEAM 14 × 1 × 3/16
13
14

Figure 2-12. Sketch of the load beam.

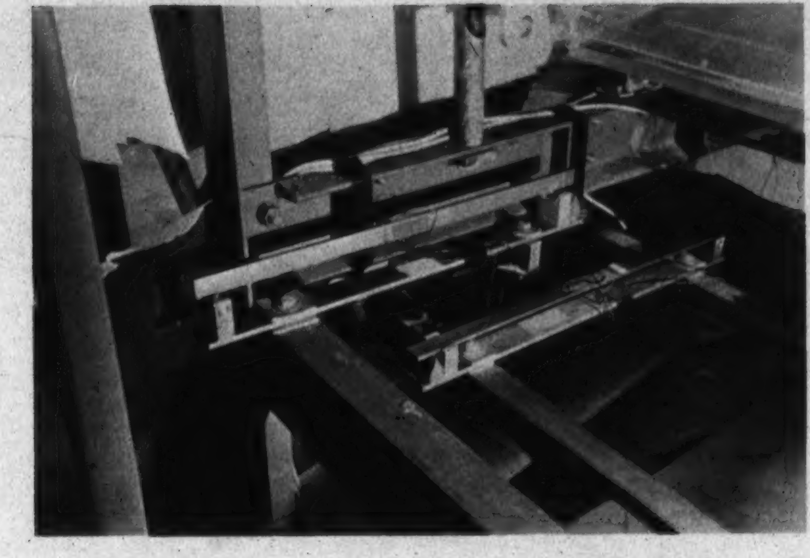

Figure 2-13. Installation of the strain gauge transducer.

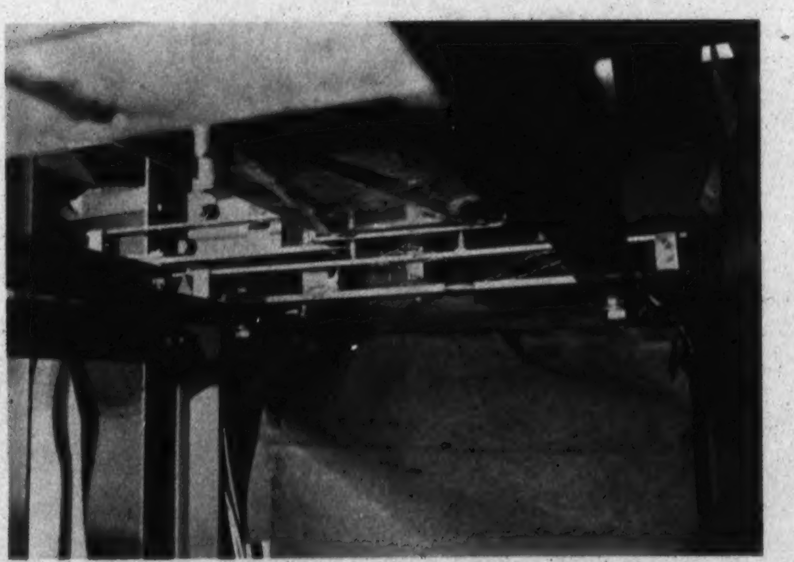

Figure 2-14. Arrangement of the collecting trough and the load beam.

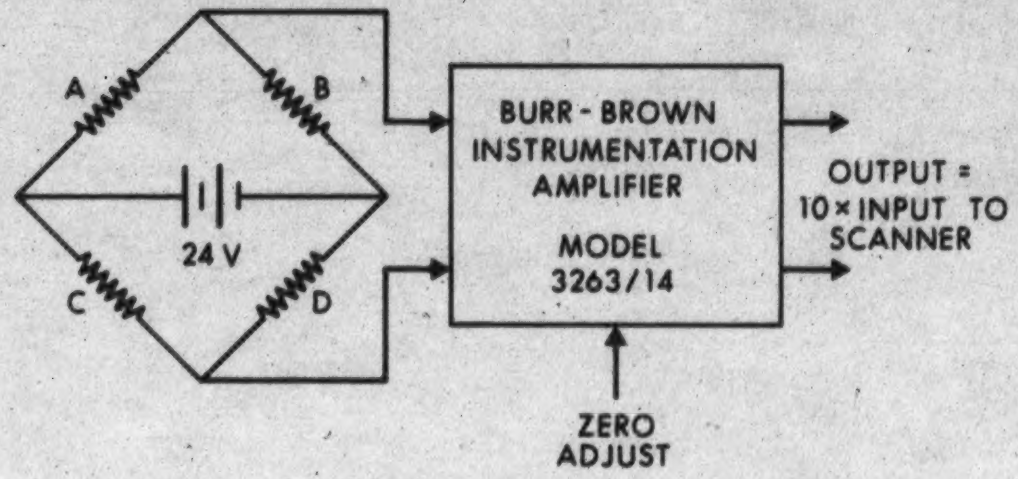
A
B
C
D
24 V
BURR - BROWN
INSTRUMENTATION
AMPLIFIER
MODEL
3263/14
OUTPUT =
10 × INPUT TO
SCANNER
ZERO
ADJUST

WHEATSTONE BRIDGE

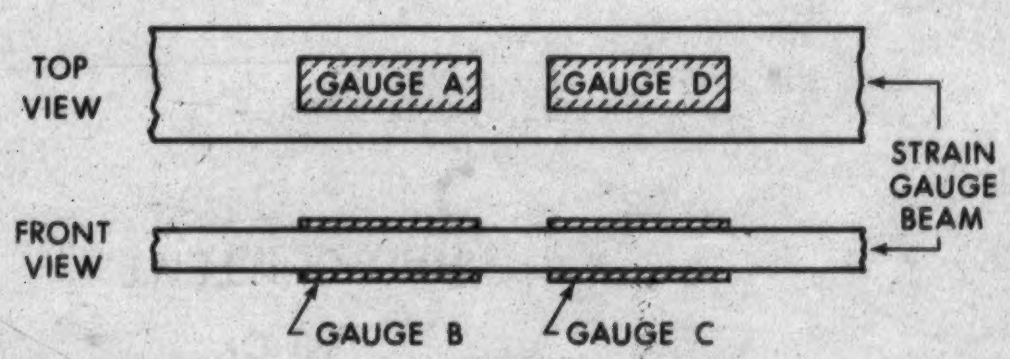
TOP
VIEW
GAUGE A
GAUGE D
STRAIN
GAUGE
BEAM
FRONT
VIEW
GAUGE B
GAUGE C

LOAD BEAM

Figure 2-15. Load beam - arrangement of strain gauges into a full Wheatstone bridge, and the bridge circuit diagram.

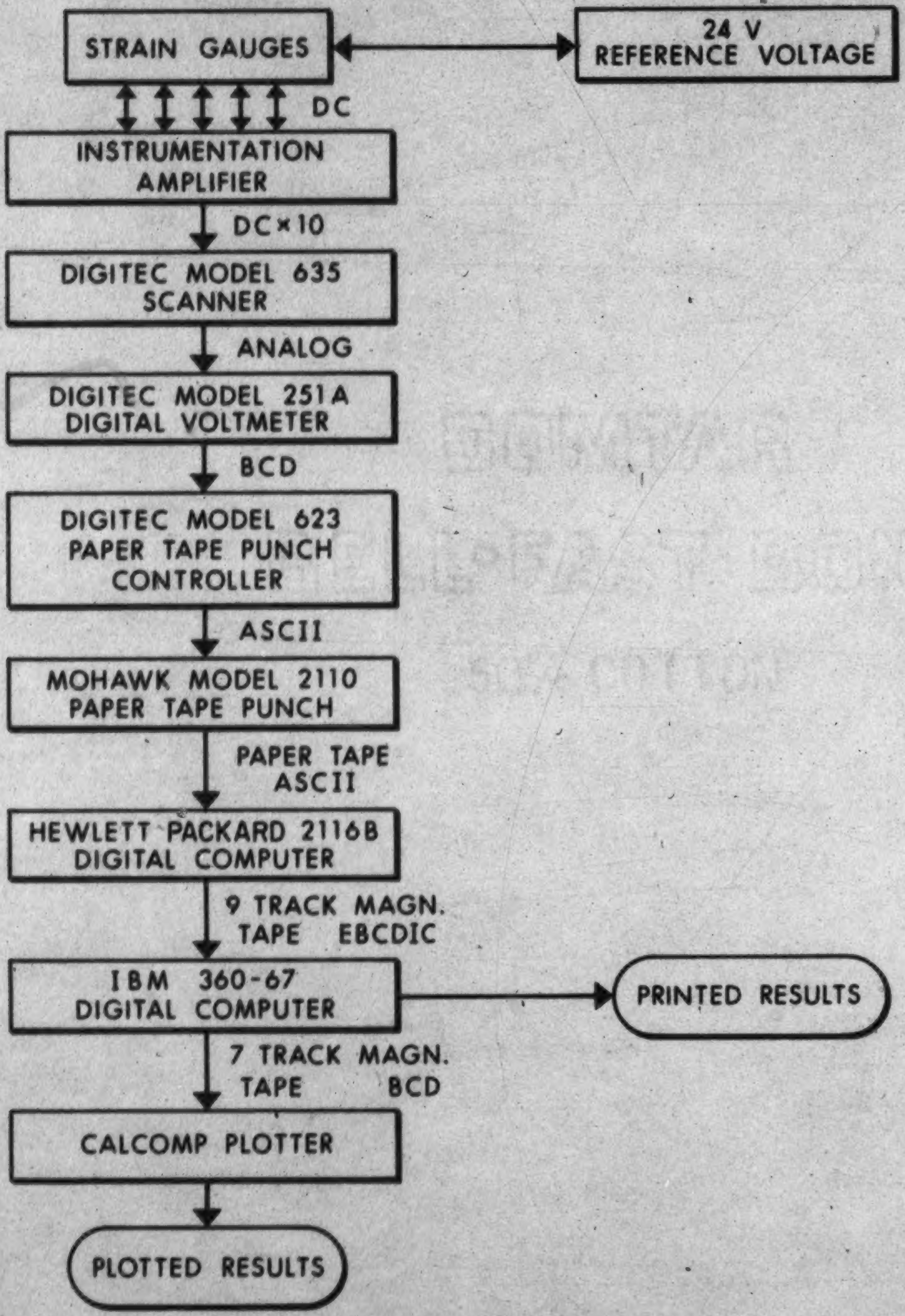
STRAIN GAUGES
24 V
REFERENCE VOLTAGE
DC
INSTRUMENTATION AMPLIFIER
DC×10
DIGITEC MODEL 635 SCANNER
ANALOG
DIGITEC MODEL 251A DIGITAL VOLTMETER
BCD
DIGITEC MODEL 623 PAPER TAPE PUNCH CONTROLLER
ASCII
MOHAWK MODEL 2110 PAPER TAPE PUNCH
PAPER TAPE ASCII
HEWLETT PACKARD 2116B DIGITAL COMPUTER
9 TRACK MAGN. TAPE EBCDIC
IBM 360-67 DIGITAL COMPUTER
PRINTED RESULTS
7 TRACK MAGN. TAPE BCD
CALCOMP PLOTTER
PLOTTED RESULTS

Figure 2-16. Flowchart of the data acquisition system.

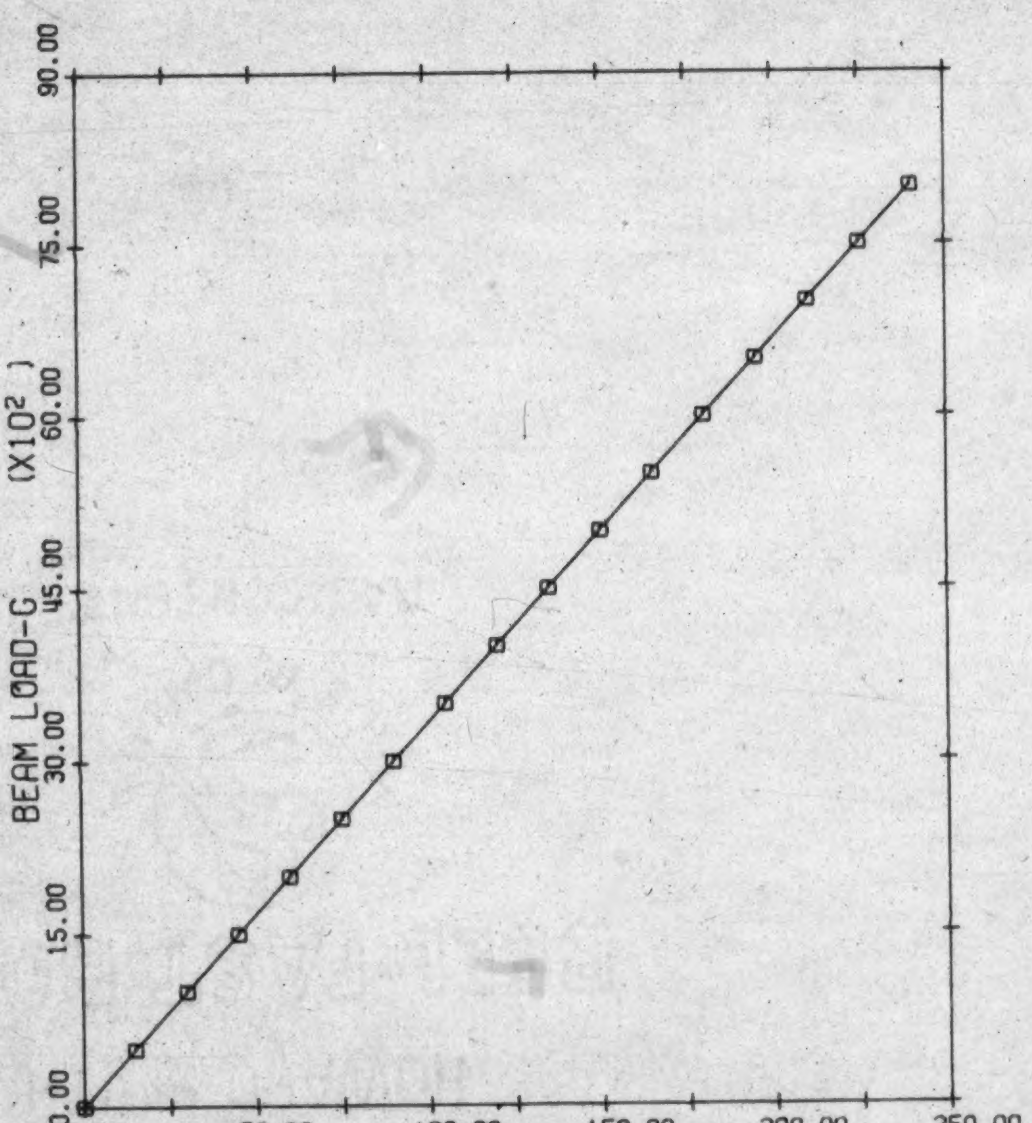

Figure 2-17. Calibration curve of the load beam.

CHAPTER III

NONLINEARITY PROBLEM IN HYDROLOGIC SIMULATION

3-1 Introduction

The nonlinear nature of watersheds behaviour has been observed and reported in recent years by many authors (Minshall, 1960; Amorocho, 1961, 1971; Diskin, 1964; Kulandaiswamy, 1964; Proceedings of the International Hydrology Symposium, Fort Collins, Colorado, 1967; Chiu, 1970; First U.S.-Japan Seminar in Hydrology, 1971). Because there is no general theory of analysis applicable to nonlinear systems, "identification" of a nonlinear system proves to be a formidable task in most cases. Because of the theoretical and practical difficulties associated with the treatment of nonlinear systems most hydrologic analysis have been directed towards the formulation of procedures for the linear approximation of these systems (Amorocho, 1967). How close such approximations may be is a problem which has not been given much attention in hydrology.

In the following sections the risk associated with the use of linear models approximating nonlinear systems is discussed in qualitative terms.

3-2 Linearized Hydrologic System

Three basic equations are available for the deterministic simulation of the relationship between rainfall and runoff. These are: (1) equation of continuity, (2) momentum equation, and (3) energy equation. When the operation of the rainfall-runoff process of the hydrologic cycle is approximated by a linear model, it is assumed that the momentum equation is linear. As a very simple example the effect of linearization in the case of a single nonlinear reservoir, as shown in Figure 3-1, can be used as an illustration. The single reservoir system is similar in some or all respects to other hydrologic-hydraulic systems for which the solutions involve relation between storage and discharge, such as small dams, ponds, overland flow, and individual reservoirs in the reservoir cascade approach to watershed hydrograph models.

The equation of continuity for the single reservoir is

$$\frac{dS}{dt} = i(t) - q(t) \qquad (3\text{-}1)$$

where S is the amount of stored water in the reservoir at time t, i and q are time varying inflow and outflow rates respectively.

The dynamic equation can be written as

$$q(t) = K\sqrt{S} \qquad (3\text{-}2)$$

where $K = cB\ 2g/A$ is a constant; c is the discharge coefficient, B is the area of discharge orifice, g is the acceleration of gravity, and A is the area of the reservoir.

Substituting Equation (3-2) into Equation (3-1) gives

$$\frac{dS}{dt} = i(t) - K\sqrt{S} \qquad (3\text{-}3)$$

Response of the nonlinear reservoir to an arbitrary input i(t) can be found by solving Equation (3-3). It is interesting to compare responses of the nonlinear reservoir and its linear model to a simple input such as a step function input.

Linear model of the reservoir requires that the q-S relationship be linearized. Mathematically, linearization of the q-S relation may be done

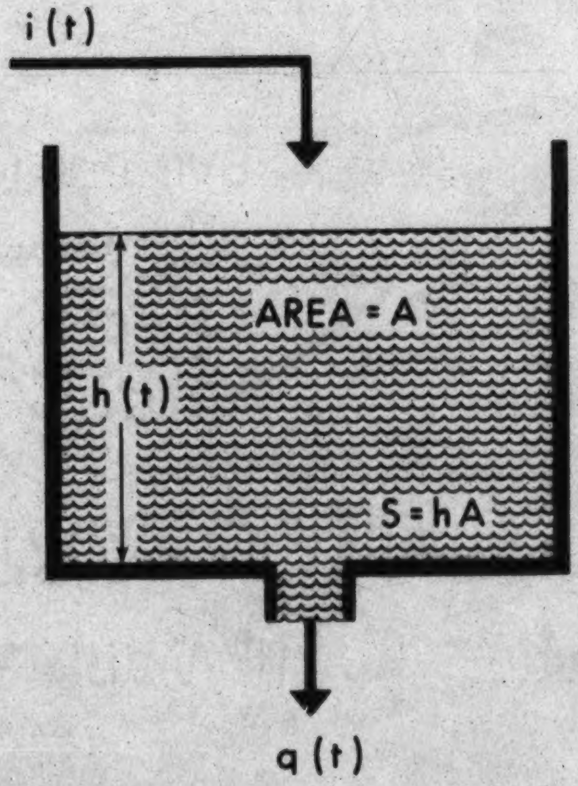
i (t)
AREA = A
h (t)
S = hA
q (t)

Figure 3-1. Definition sketch of a reservoir.

by means of a Taylor series expansion of the function q(s), given by Equation (3-2), around the steady state value S_*; thus

$$q(S) = q(S_*) + q'(S_*)(S-S_*) + q''(S_*)\frac{(S-S_*)^2}{2!} + \ldots. \qquad (3\text{-}4)$$

where $q'(S_*)$ is the first derivative of q evaluated at S_*, $q''(S_*)$ is the second derivative, etc. Truncating the series after the last linear term, the result is

$$q = q_* + q_*'(S - S_*) \qquad (3\text{-}5)$$

where $q = q(S)$, and $q_* = q(S_*)$. The first derivative of q_* is $q_*' = \frac{1}{2}KS_*^{-\frac{1}{2}}$, which after substituting into Equation (3-5) gives

$$q = q_* + \frac{S - S_*}{\tau} \qquad (3\text{-}6)$$

where the parameter $\tau = \frac{2}{K} S_*^{\frac{1}{2}}$ is called the time constant of the system and has the units of time. (Physically this parameter represents the time elapsed since the beginning of a step input applied to a first order system operating at a steady state, until the system's response reaches 63.2 percent of its ultimate value. When the time elapsed is 2τ, 3τ, and 4τ, the percent response is 86.5, 95, and 98, respectively (Coughanowr, 1965).) Substituting Equation (3-6) into Equation (3-3) yields

$$\frac{dS}{dt} = i - q_* - \frac{S - S_*}{\tau} \qquad (3\text{-}7)$$

Equation (3-7) is a linearized version of the nonlinear relationship given by Equation (3-3) and represents a tangent line passing through the point of operation $O(q_*, S_*)$, as illustrated in Figure 3-2. Solution of Equation (3-7) for a step input of magnitude I (Coughanowr, 1965) is

$$S(t) = S_* + \tau I(1 - e^{-t/\tau}) \qquad (3\text{-}8)$$

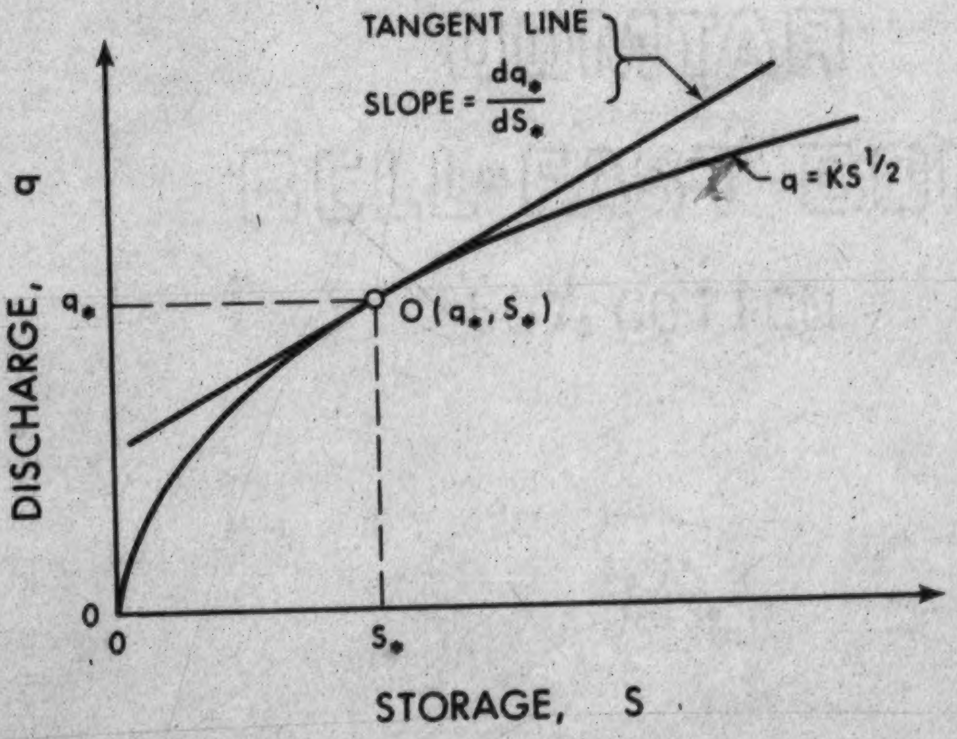

Figure 3-2. Graphical interpretation of linearization of a function around a steady state operating point, $O(q*,S*)$, by means of a Taylor series expansion.

3-2-4 Comparison of Measured and Computed Responses

Predicted responses by the linear model to step function inputs, were compared to the true nonlinear responses determined by measuring the changes of storage in a small plexiglass tank whose nonlinear function of outflow was given by Equation (3-2) with $K = 0.74$. The tank was placed on two beams, one of which was fitted with strain gauges, thus acting as a weight transducer (Chapter II). The signal from the transducer was recorded in time intervals of 4 seconds. Outflow from the tank occurred through a circular orifice centered in the bottom of the tank, and the inflow was regulated by a valve.

The experimental measurements consisted of two step inputs applied to the tank initially operating at a steady state (same for both inputs) given by: $S_* = 1955$ cm^3, $i_* = q_* = 33$ cm^3/sec. The corresponding value of the time constant of the linear model was $\tau = 119.5$ sec. In the first experiment the inflow was suddenly increased to 35.6 cm^3/sec, which represents 7.9 percent of the initial value of inflow i_*. In the second experiment the inflow was increased to 37.4 cm^3/sec, or by 13.4 percent of the initial value. Measured responses to these two step inputs, and the predicted responses by the linear model are shown in Figure 3-3. At time $t = 4\tau$ the predicted responses are 13 percent and 19.4 percent respectively less than the true values, in terms of the measured increase in storage from the time $t = 0$ to $t = 4\tau$.

The results show that even when the inputs varied within a relatively small range (less than 14 percent) around the operating point, linearization of the system's equation resulted in the loss of ability

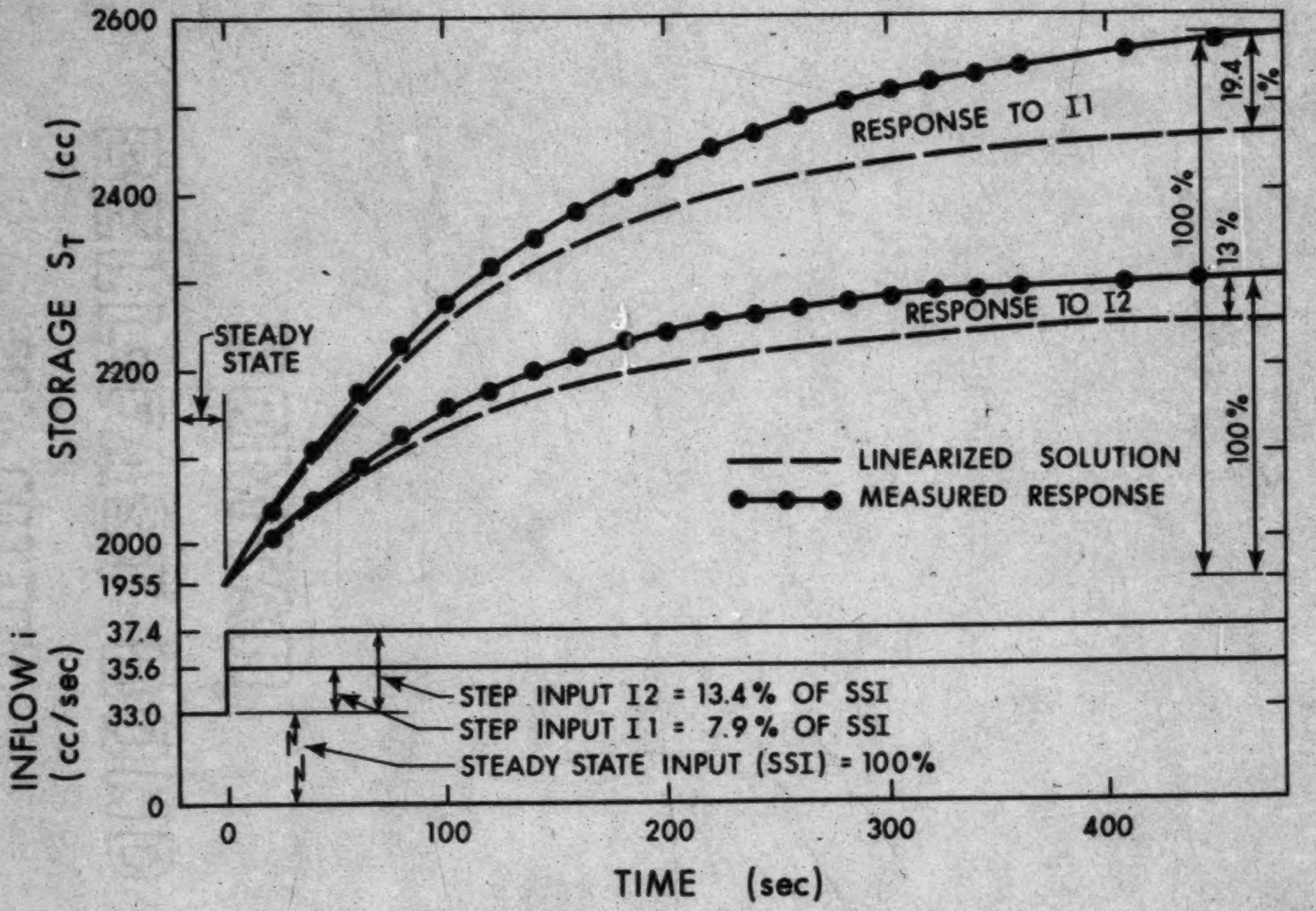

Figure 3-3. Comparison of measured responses of a nonlinear reservoir to two step function inputs, and those predicted by a linear model of the reservoir.

to predict responses of the system quantitatively. Similar situations arise when dealing with the rainfall-runoff relationship. It is shown in Chapter IV that the instantaneous unit hydrograph derived for the laboratory catchment is a linear model based on the rainfall-runoff relationship linearized for a particular rainfall intensity input. When the rainfall intensity changes the particular instantaneous unit hydrograph becomes a poor model of the rainfall-runoff process.

CHAPTER IV

EXISTING MODELS OF SURFACE RUNOFF

4-1 Introduction

In the study of surface runoff from watersheds numerous attempts have been made to formulate the relationship that is required for the simulation of overland flow. These efforts have resulted in the development of a multitude of mathematical models describing the runoff phenomenon(International Hydrology Symposium, Fort Collins, Colorado,1967).

The models can be classified into two categories. The first of these categories covers the runoff models which assume a linear relationship between rainfall and runoff. Most of the linear models are based on the unit hydrograph theory. In the second category fall the models which are nonlinear.

In the present chapter two of the more popular concepts of surface runoff are reviewed and performance of mathematical models based on these concepts was tested experimentally. These two concepts are the instantaneous unit hydrograph and kinematic wave concepts.

The IUH model was chosen to represent all linear models of the surface runoff in this study, primarily because the unit hydrograph theory has become very familiar to most hydrologists. If the investigation reveals that the nonlinearity of the surface runoff is a significant reason for the IUH failure, then it can be concluded that any linear model is susceptible to the same degree of failure. The kinematic wave model is a nonlinear model based on the kinematic wave theory. The attractiveness of the model lies in the relatively easy solution of a simplified hydrodynamic equation governing the runoff.

The unit hydrograph and the kinematic wave have been considered theoretically for many years. Both concepts have been used quite extensively in attempts to solve practical problems. However, there seems to be a lack of experimental investigation of their validity and properties. Review of the requirements and conditions assumed in the unit hydrograph and kinematic wave theory indicates that these concepts can be best tested by means of a laboratory catchment.

4-2 The Instantaneous Unit Hydrograph

The instantaneous unit hydrograph (IUH), designated in the following by u(t), is a unit hydrograph resulting from an effective precipitation of infinitesimally small duration. In other words, for an IUH the effective precipitation is applied to the drainage basin in zero time, and the input is in the form of a unit impulse. This rather fictitious hydrograph has a major advantage in comparison with a unit hydrograph. It is independent of the duration of effective precipitation, thereby eliminating one variable in hydrograph analysis. Furthermore, the IUH is better suited for the needs of theoretical investigations of the rainfall and runoff relationship because it allows the use of the linear theory of systems analysis.

4-2-1 The Convolution Integral

It is known from the systems analysis (Zadeh, 1963; Bendat, 1966) that the dynamic characteristics of a constant parameter linear system can be described by a unit impulse response, h(t), defined as the output of the system at any time t to a unit impulse input applied at time t-τ. If a catchment is considered to be a linear system with the surface runoff as an output, then the IUH, or u(t), is the system's unit impulse response and the effective rainfall of the IUH corresponds to the unit impulse input.

Usefulness of the unit impulse response for description of the system is due to the fact that for any arbitrary input i(t), the system's output Q(t) at any time t is given by the convolution integral

$$Q(t) = \int_{0}^{t} i(\tau)\, u(t-\tau)\, d\tau \qquad (4\text{-}1)$$

According to Equation (4-1) the value of the output Q(t) at time t is given as a weighted linear sum over the entire history of the input i(t). Once the unit impulse response, sometimes called the weighting function of the system, is known the system is "identified", and the system's output can be predicted for any input by Equation (4-1). The prediction property of the convolution integral led to its use in hydrograph forecasting. The assumption of linearity of the surface runoff process was essential. In this approach the problem of runoff simulation was then reduced to finding the unit impulse response of a catchment.

4-2-2 Conceptual Models of IUH

There have been many conceptual models proposed to delineate an IUH. They were composed of simulated components such as linear reservoirs (Nash, 1960), linear channels (Dooge, 1959) or time area diagrams (Ross, 1921). The theoretical development of the IUH models composed of linear reservoirs has been derived in the following sections using the transfer function method of linear systems theory. The method, as well as the conclusions about the reservoir type model, generally apply to any linear model. The reservoir type model was chosen merely because it can be compared with the nonlinear state variable runoff model derived in Chapter V, and which is also composed of reservoirs.

4-2-2-1 Single Reservoir

The simplest conceptual model of a catchment is a fictitious reservoir in which the outflow q is directly proportional to the storage S(Amorocho, 1961), or

$$S = kq \tag{4-2}$$

where k is constant for the reservoir and has units of time. The inflow i into the reservoir and the outflow q are related to the rate of change of storage by the continuity equation

$$\frac{dS}{dt} = i - q \tag{4-3}$$

The unit impulse response, u(t), of the reservoir (Appendix B) is

$$u(t) = \frac{1}{k} e^{-t/k} \tag{4-4}$$

Substituting Equation (4-4) into the convolution integral, Equation (4-1), and assuming a constant input i, gives the outflow function as

$$q(t) = i(1 - e^{-t/k}) \tag{4-5}$$

If the inflow terminates at time t_o since the outflow began, then

$$q(\tau) = q_o e^{-\tau/k} \tag{4-6}$$

where $\tau = t - t_o$, and q_o is the outflow at time t_o.

The disadvantage of a one stage first-order system, such as the single reservoir, in runoff simulation is that the rate of change of the

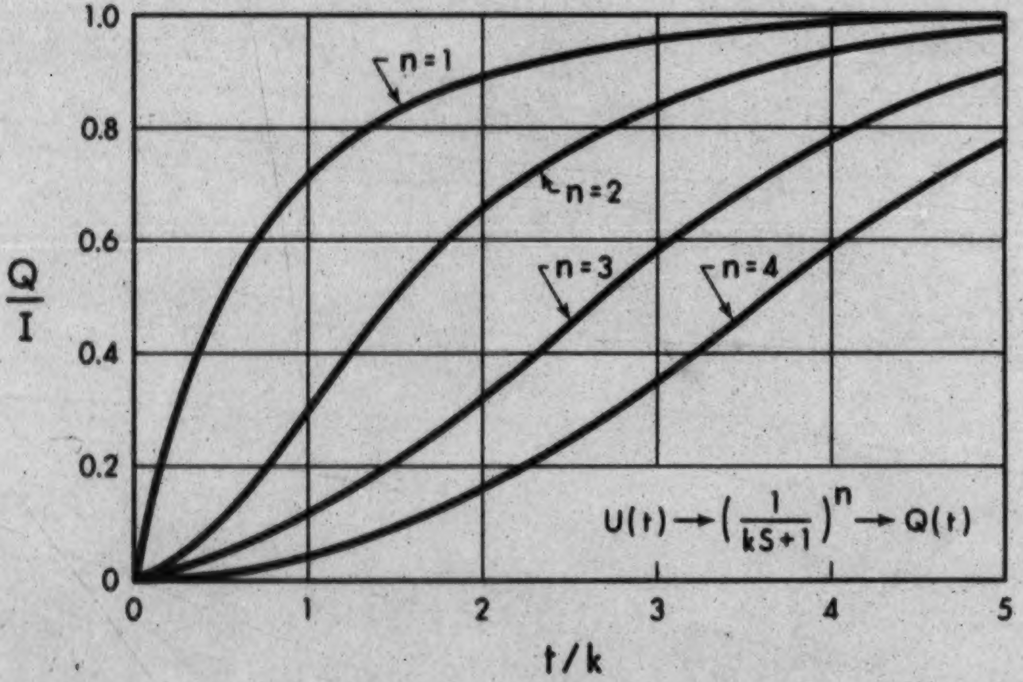

Figure 4-1. Characteristic responses of non-interacting first-order linear systems to unit step function input.

response (slope of response curve) is maximal at $t = 0$. In order to compensate for this, conceptual models composed of a series of reservoirs have been suggested. Step response of a system consisting of two or more first-order systems is S-shaped and the response changes very slowly just after introduction of the step input. This sluggishness or delay is sometimes called transfer lag (Coughanowr, 1965), and is always present when two or more first-order systems are connected in series. Figure 4-1 illustrates the step input response curves for several systems composed of one or more linear reservoirs in series.

4-2-2-2 Series of Reservoirs

Nash (1960) made a significant contribution to the unit hydrograph theory by presenting a conceptual model composed of a series of n identical linear non-interacting reservoirs, as shown in Figure 4-2. All reservoirs have the same storage characteristic, $S = kq$. Response of such a system to a unit impulse input (Appendix B) is

$$Q_n(t) = \frac{t^{n-1}}{k^n} \frac{1}{(n-1)!} e^{-t/k} \tag{4-7}$$

where $Q_n(t)$ is a deviation variable of the outflow from the n-th reservoir at time t. Nash substituted the factorial in Equation (4-7) by a Gamma function to account for continuous values of n. Thus the Nash's equation of the IUH is

$$u(t) = \frac{1}{k\Gamma(n)} \left(\frac{t}{k}\right)^{n-1} e^{-t/k} \tag{4-8}$$

Values of k and n can be evaluated by the method of moments from the knowledge of past hydrographs.

There are several basic objections to the Nash model and the unit hydrograph concept generally. Firstly, there is the problem of assessing

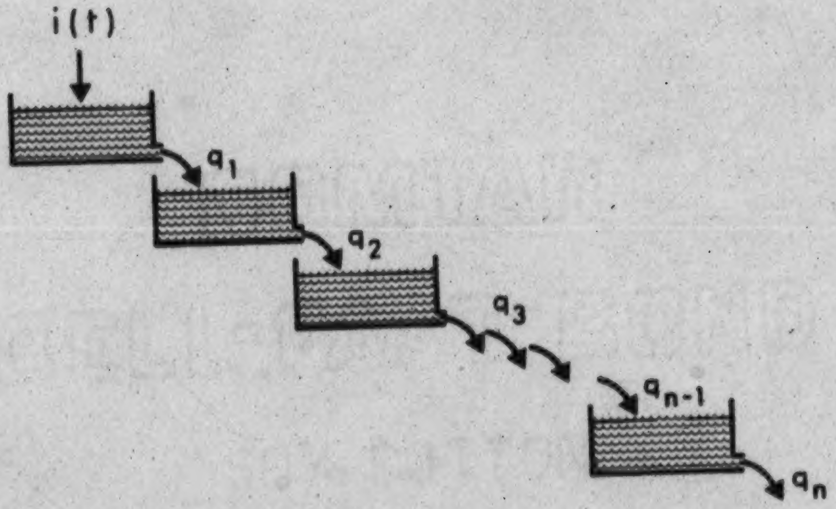

Figure 4-2. Illustration of the physical analog of the Nash IUH model as the response, q_n, of a series of n non-interacting linear reservoirs to a unit impuls input i(t).

the correct amount of the effective rainfall as an input into the system. Secondly, the IUH method is a black box type of analysis, and as such it disregards any information about the mechanics of water motion. A good fit is the sole objective of the analysis and the only physical argument may be that the runoff process is a heavily damped linear system.

The Nash model does not provide for spatial distribution of rainfall since all the input into the system enters only through the first reservoir. Another criticism that can be made is that the model allows for reservoir storage effects but not for channel translation effects present in any catchment (O'Donnell, 1966).

The spatial distribution of the input rainfall and the channel translation effects were subjects of later proposed IUH models (Dooge, 1959; Singh, 1964; Diskin, 1964). However, the single main drawback of all IUH models remains the assumption of linearity as can be seen from the experimental results presented in the following sections.

4-2-3 Direct Determination of IUH

Deriving a catchment IUH by invoking the aid of some catchment model is bound to lead to an approximation of the real IUH, the goodness of the approximation being dictated by the goodness of the model simulating reality. One would like to use methods of deriving an IUH that by-pass the need for a model, i.e. operate directly on the rainfall excess and direct runoff data to yield the IUH. Such methods have, in fact, been used (O'Donnell, 1966) and require only that the system be linear and time-invariant.

The method of deriving the IUH used in the present study was first proposed by Chow (1962). It is based on the fact that an S-hydrograph is an integral curve to the IUH. The IUH ordinate at time t is thus simply equal to the slope of the S-hydrograph at time t.

4-2-4 Comparison of Experimental and Theoretical Results

The experimental apparatus, described in Chapter 2, was well suited for experimental testing of the unit hydrograph theory because the two most basic assumptions of the theory were satisfied: (1) the input rainfall was uniformly distributed over the experimental basin, and (2) the measured hydrographs resulted from direct runoff only.

The aim of the experiments was not to test particularly any of the IUH conceptual models. Rather, the objective was more general: to depict clearly nonlinearity of the runoff process and thus to prove invalidity of the unit hydrograph method generally. This amounted basically to:

(1) Derivation of an IUH from a recorded experimental S-hydrograph caused by a rainfall of specific intensity.

(2) Recording a number of experimental hydrographs resulting from rainfalls of different intensities and durations.

(3) Simulation of the experimental hydrographs by means of the convolution integral, using the derived IUH as the unit impulse response of the laboratory catchment.

(4) Comparison of the experimental and the simulated hydrographs.

4-2-4-1 IUH of the Laboratory Catchment

The method of direct determination of the IUH described in Section 2-3 was used to derive the IUH of the laboratory catchment. The method requires that a continuous record of cumulative outflow from the catchment, i.e. S-hydrograph, be available. An S-hydrograph was easily obtained experimentally by letting the duration of rainfall be longer than the time to equilibrium. A smooth curve was then fitted to the experimental data and the IUH was obtained by numerical differentiation of the curve.

Two recorded S-hydrographs, S_1 and S_2, resulting from 3.84 cm/hr and 11.53 cm/hr rainfall intensities, and the corresponding derived IUH's, IUH-1 and IUH-2, are shown in Figure 4-3. The two IUH's were adjusted to the common "unit" rainfall intensity of 10 cm/hr. A linear rainfall - runoff process would have resulted in derivation of exactly identical IUH's from both S-hydrographs. The actually derived IUH's show remarkable differences in peak values, time to peak, and the total duration. Hence, the sheet runoff caused by rainfall must be classified as a highly nonlinear process.

4-2-4-2 Comparison of Simulated and Observed Hydrographs

Hydrographs simulating recorded runoffs from the laboratory catchment, generated by rainfalls of various intensities, were calculated by convolution of the derived IUH's with the input rainfall intensities. Since the experimental data were discrete, summation form of the convolution integral (Chow, 1964) was used, expressed as

$$Q_{(t)} = \sum_{j=1}^{n} u[t - (j - 1)\Delta t] I_j \Delta t \tag{4-9}$$

where t represents any time after the beginning of effective rainfall. The input rainfall may be considered to consist of n blocks of different intensities I_j and of the same duration t; the subscript j denotes the number representing a block. A computer program performing the convolution given by Equation (4-9) is listed in Appendix D.

The convolution results provided an interesting insight into the

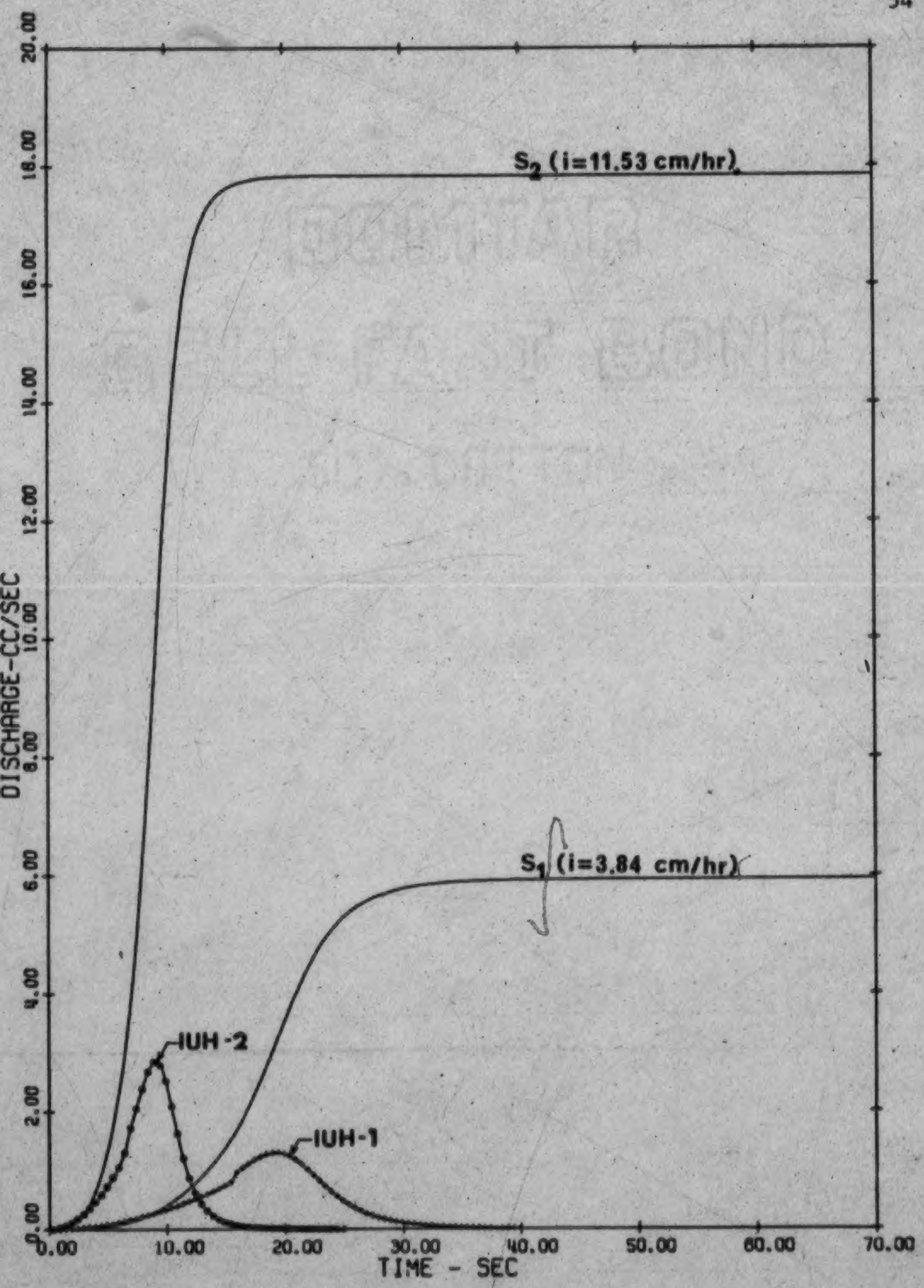

Figure 4-3. Recorded S-hydrographs, S_1 and S_2, of runoff from the laboratory catchment, and the corresponding derived instantaneous unit hydrographs IUH-1 and IUH-2.

IUH simulation method. Typical results are shown in Figures 4-4 and 4-5. Three experimental hydrographs resulting from the rainfall input of the same intensity as for the S_1-hydrograph were simulated. The rainfall input durations for the three hydrographs were 20, 25, and 50 seconds.

Firstly, the hydrographs were simulated using the IUH-1 as a unit impulse response in the convolution equation. To repeat the earlier comment, this was actually a simulation of hydrographs caused by the same rainfall intensity as was the S_1-hydrograph from which the IUH-1 was derived. Figure 4-4 shows that the rising parts of the hydrographs were reproduced exactly up to the time equal to rainfall durations. However, the recession curves were extremely poorly simulated and the times to peak and the peak values were grossly overestimated.

The overshoot of the simulated hydrographs is due to the shape of the IUH-1. The IUH-1 peaks approximately at $t = 19$ sec, as can be seen in Figure 4-3. Thus the past inputs are weighted more heavily than an immediate input.

Secondly, the same three hydrographs were simulated using the IUH-2 as a unit impulse response in the convolution. Figure 4-5 shows the results which strikingly demonstrate nonlinearity of the runoff process. The simulated hydrographs in this case do not even partly resemble the experimental curves.

4-2-5 Nonlinearity of Runoff Distribution

Comparison between measured hydrographs and those predicted by the IUH method indicates clearly that the runoff phenomenon cannot be analyzed successfully by linear methods. To illustrate further the nonlinearity

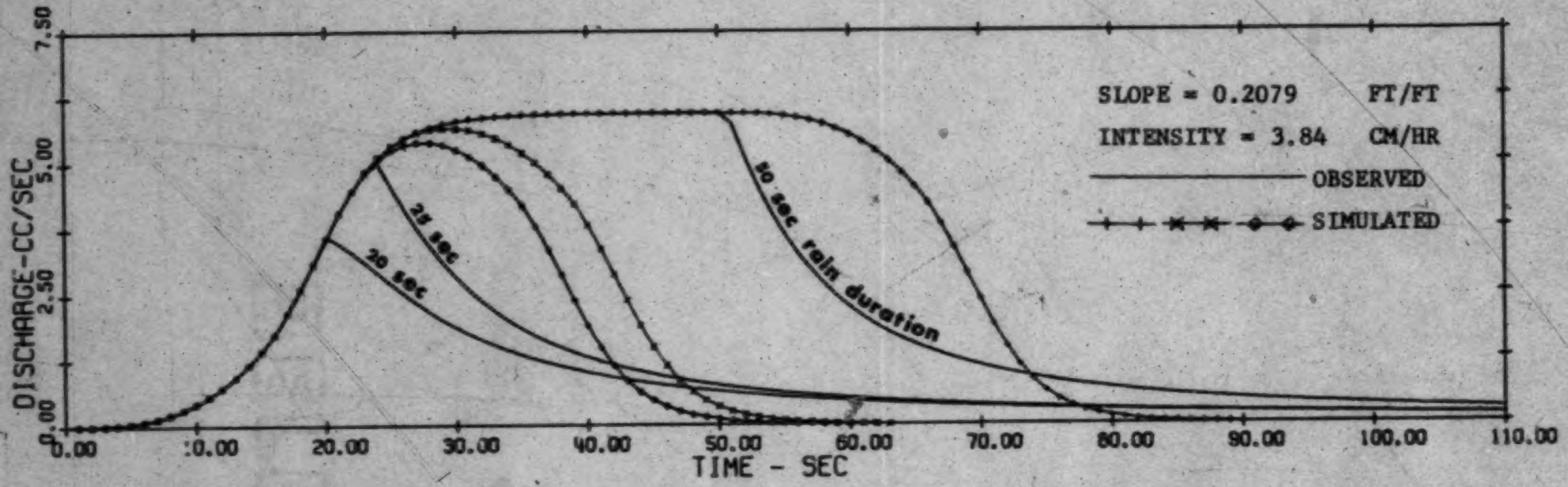

Figure 4-4. Reproduction of hydrographs by the Instantaneous Unit Hydrograph model when IUH-1 was used as the unit impulse response function (IUH-1 was derived from the S_1 hydrograph (Fig. 4-3.) for which the rainfall intensity was the same as for the reproduced hydrographs).

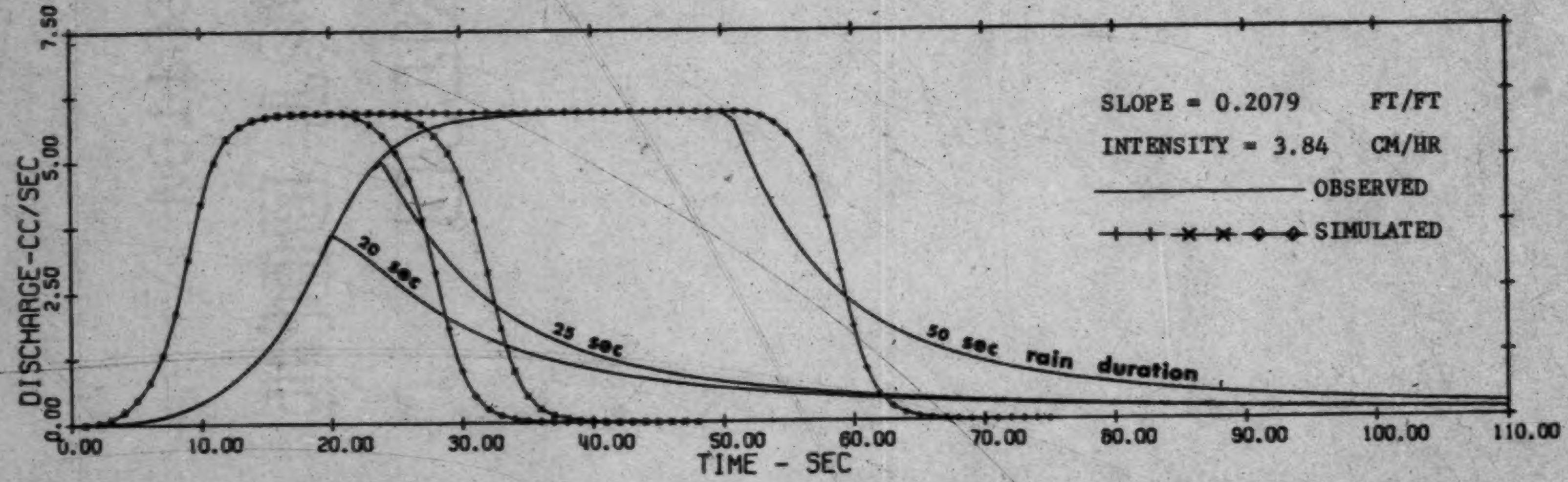

Figure 4-5. Simulated hydrographs by the Instantaneous Unit Hydrograph model when IUH-2 was used as the unit impulse response function (IUH-2 was derived from the S_2 hydrograph (Fig. 4-3.) for which the rainfall intensity was different (approx. 3 times higher) than for the simulated hydrographs).

of the rainfall-runoff relationship the following experiment was performed. The runoff plane of the laboratory catchment was fixed in the position such that the bed slope was $S_o = 0.2079$. Hydrographs of surface runoff from the catchment were recorded for the following three rainfall intensities: 3.84 cm/hr, 7.77 cm/hr, and 11.53 cm/hr. The rainfall intensities were approximately in ratios 1:2:3. Duration of rainfall for all events was 50 seconds. Average observed hydrographs for each rainfall intensity are shown in Figure 4-6. In the same figure are plotted two hydrographs, corresponding to rainfall intensities of 7.77 cm/hr and 11.53 cm/hr respectively, derived by superposition of the ordinates of the recorded hydrograph generated by rainfall of 3.84 cm/hr intensity. These two derived hydrographs represent in effect a linear relationship between rainfall input and runoff output. The actual rainfall-runoff relationship, however, is highly nonlinear as can be seen from comparison of the recorded hydrographs with those derived by superposition.

4-2-5-1 Time Distribution of Runoff

In design flood estimation characteristic times are required for the determination of hydrograph parameters and critical durations of flood-producing rainfall. The rise time, time of concentration, time to equilibrium and volume/peak ratio have all been suggested as appropriate characteristic times (Bell, 1969). These are influenced to a great degree by the physical configurations of the catchments concerned. Many of the suggested formulas in fact define the characteristic response times only in terms of catchment parameters, such as the slope and length (Snyder, 1938; Kirpich, 1940; Taylor, 1952). The unit hydrograph theory in effect

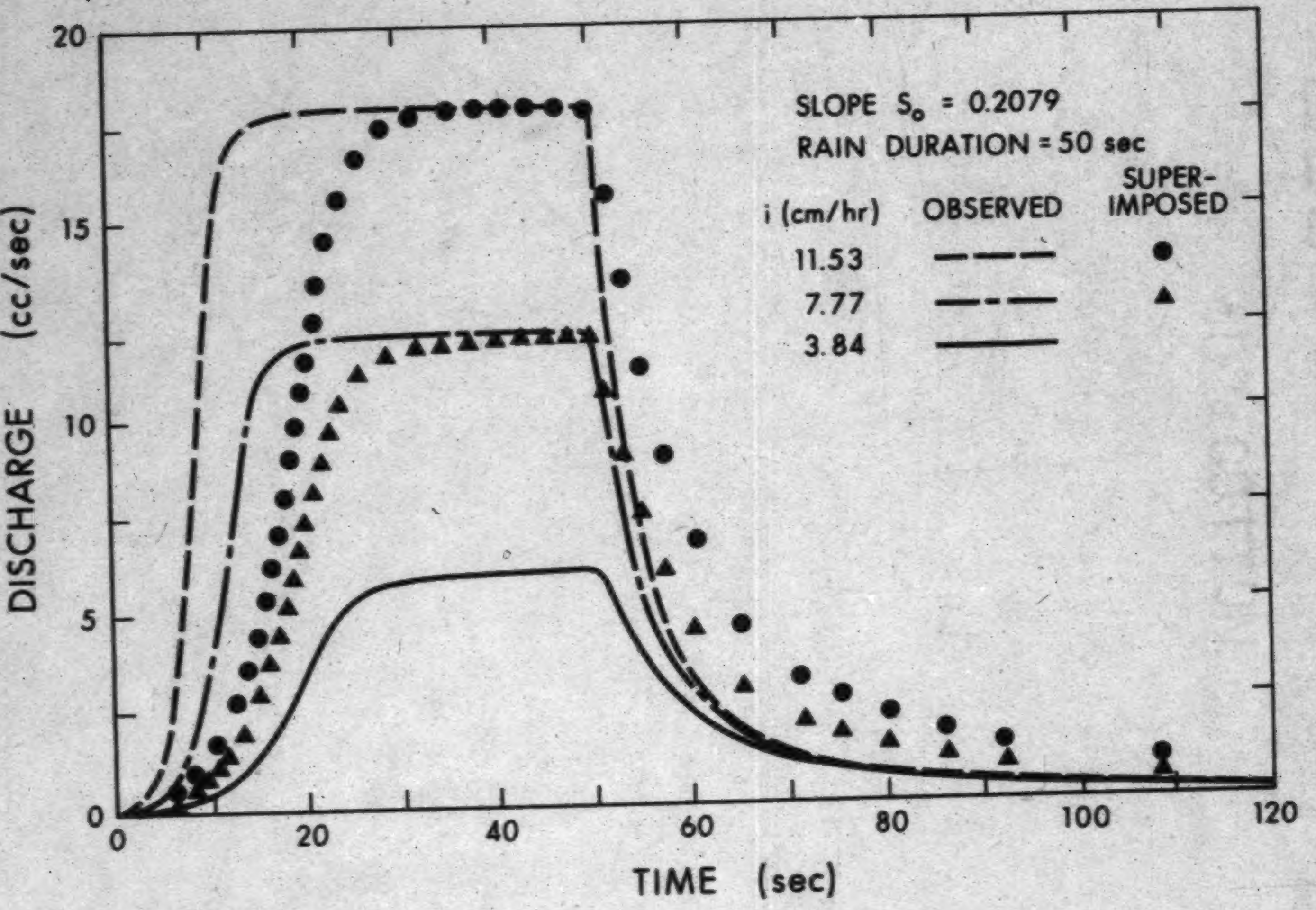

Figure 4-6. Recorded hydrographs (runs no. 1, 4, 7) resulting from rainfalls of different intensities, and hydrographs derived by superposition of ordinates of the observed hydrograph corresponding to rainfall intensity i = 3.84 cm/hr.

also assumes a constant response time. However, because the rainfall-runoff relationship is nonlinear, the time distribution of runoff is a function of the input amplitude, i.e. the rainfall intensity, besides the catchment parameters.

To support this reasoning by experimental evidence the relationship of the apparent time to equilibrium, rainfall intensity and the runoff surface slope was investigated experimentally. Five different slopes of the runoff surface were tested. For each slope the apparent times to equilibrium were measured for between 23 and 26 different rainfall intensities within the range from 1.7 cm/hr to 14 cm/hr. The results are given in Table 4-1. The apparent times to equilibrium were determined from cumulative curves of runoff plotted by an X-Y recorder. Typical cumulative curves of runoff are given in Figure 4-7. A tangent was drawn to each cumulative curve at the point of equilibrium. The intercept of this tangent on the abscissa was taken as the apparent time to equilibrium.

Analysis of the experiments show that the relationship between the apparent time to equilibrium, t_e, and the rainfall intensity, i, can be expressed in the form of an equation of a hyperbola, i.e., in general by the equation

$$t_e = a\, i^{-n} \qquad (4\text{-}10)$$

where the coefficient a is a function of the slope S_o. The effect of the length of the runoff plane was not investigated. The experimental data for each slope were fitted by least square method with best fit lines and plotted on logarithmic paper as straight lines, as shown in Figure 4-8. Equations of these lines are also given in the same figure.

TABLE 4-1

APPARENT TIME TO EQUILIBRIUM, t_e, AS FUNCTION OF RAINFALL INTENSITY, i, AND BED SLOPE FOR A RUNOFF PLANE OF LENGTH 91.4 cm

Slope (ft/ft)	0.05124		0.07870		0.10510		0.15838		0.21256	
Run	i cm/hr	t_e sec	i cm/hr	t_e sec	i cm/hr	t_e sec	i cm/hr	t_e sec	i cm/hr	t_e sec
1	1.80	58.6	1.79	47.0	1.91	40.0	1.84	41.0	1.47	32.0
2	1.87	54.0	1.81	43.0	1.96	40.0	1.97	36.0	1.88	35.0
3	1.91	47.4	2.01	45.1	2.72	37.0	2.54	29.8	2.65	28.0
4	2.63	42.0	2.57	39.0	2.75	31.4	2.75	31.2	2.76	29.0
5	3.45	32.9	2.75	34.0	3.53	26.0	3.59	24.5	3.26	24.0
6	4.07	31.0	3.51	30.0	4.18	25.3	4.01	23.0	3.40	22.4
7	4.82	26.8	4.08	29.0	5.02	22.0	4.23	21.8	4.21	20.4
8	5.06	29.2	4.20	26.0	5.62	20.4	4.68	20.5	4.82	18.6
9	5.49	26.0	4.78	26.0	6.40	18.9	5.06	18.8	5.60	16.4
10	6.21	24.0	5.02	24.0	6.99	18.0	5.38	18.1	6.25	16.0
11	6.84	21.8	5.40	23.8	7.73	16.0	5.91	18.0	7.03	14.8
12	7.33	21.2	5.68	21.5	8.29	16.0	6.42	16.2	7.59	14.0
13	8.04	20.0	6.36	21.0	9.09	15.1	6.99	15.5	8.31	13.1
14	8.75	19.2	6.96	18.0	9.49	14.4	7.81	14.2	8.86	12.2
15	9.33	17.8	7.72	18.5	10.35	13.4	8.30	14.0	9.65	11.4
16	10.04	17.0	8.30	17.2	10.77	13.2	9.18	12.8	10.16	11.0
17	10.56	16.6	8.98	16.8	11.53	10.8	9.57	12.6	10.83	10.4
18	11.11	15.8	9.45	15.1	11.92	12.0	10.27	11.2	11.44	10.0
19	11.75	14.8	10.21	14.6	12.69	10.8	10.80	11.0	12.02	9.3
20	12.30	14.6	10.63	13.7	13.11	10.7	11.50	10.8	12.69	9.2
21	12.87	14.0	11.50	14.0	13.82	10.2	11.98	10.6	12.78	9.0
22	13.33	14.1	11.82	12.6	14.21	10.9	12.22	10.0	13.72	8.3
23	14.30	13.5	12.57	12.3	14.79	10.0	13.19	10.0	14.27	8.1

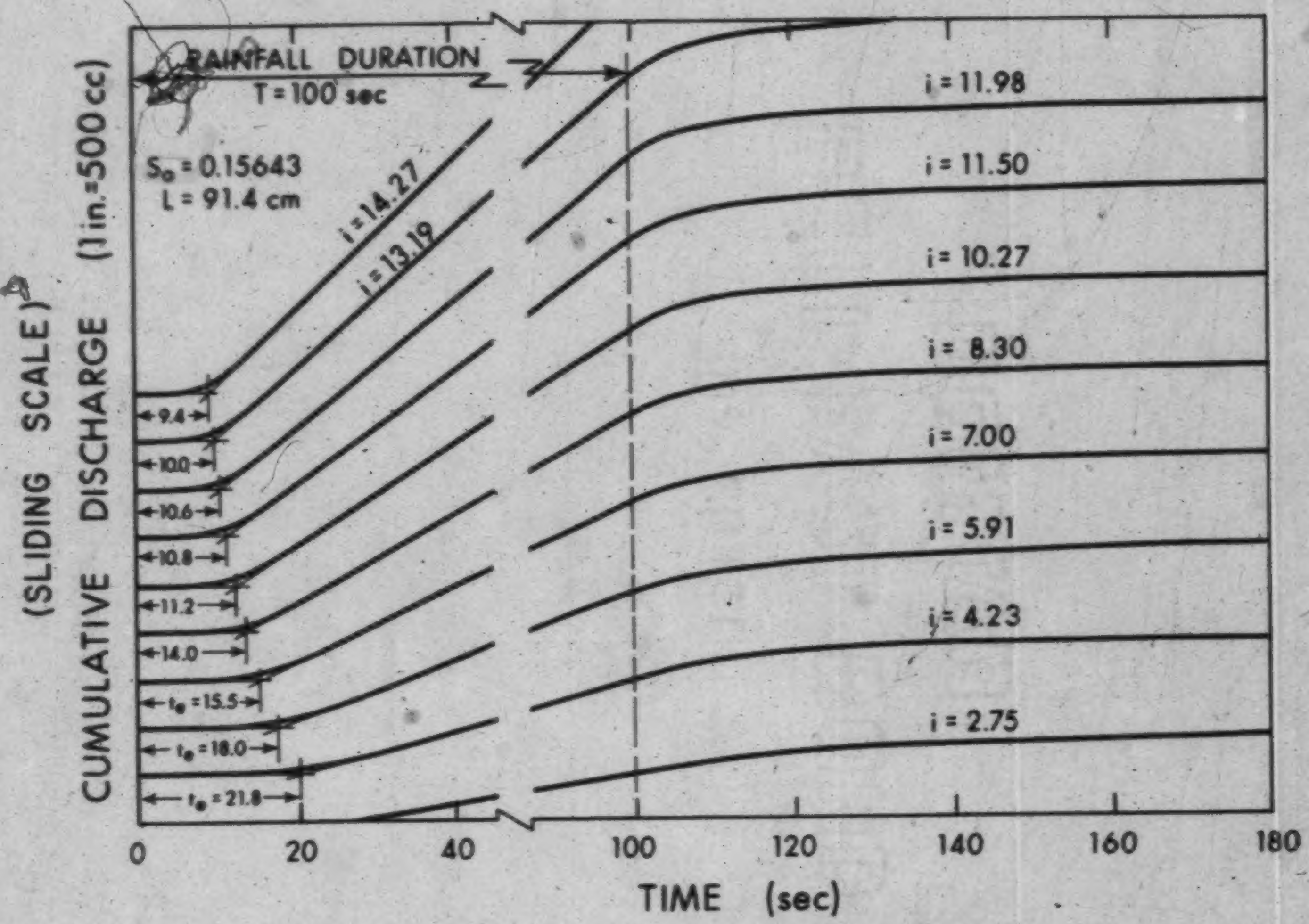

Figure 4-7. Cumulative discharge hydrographs for different rainfall intensities i (cm/hr) as plotted by X-Y recorder.

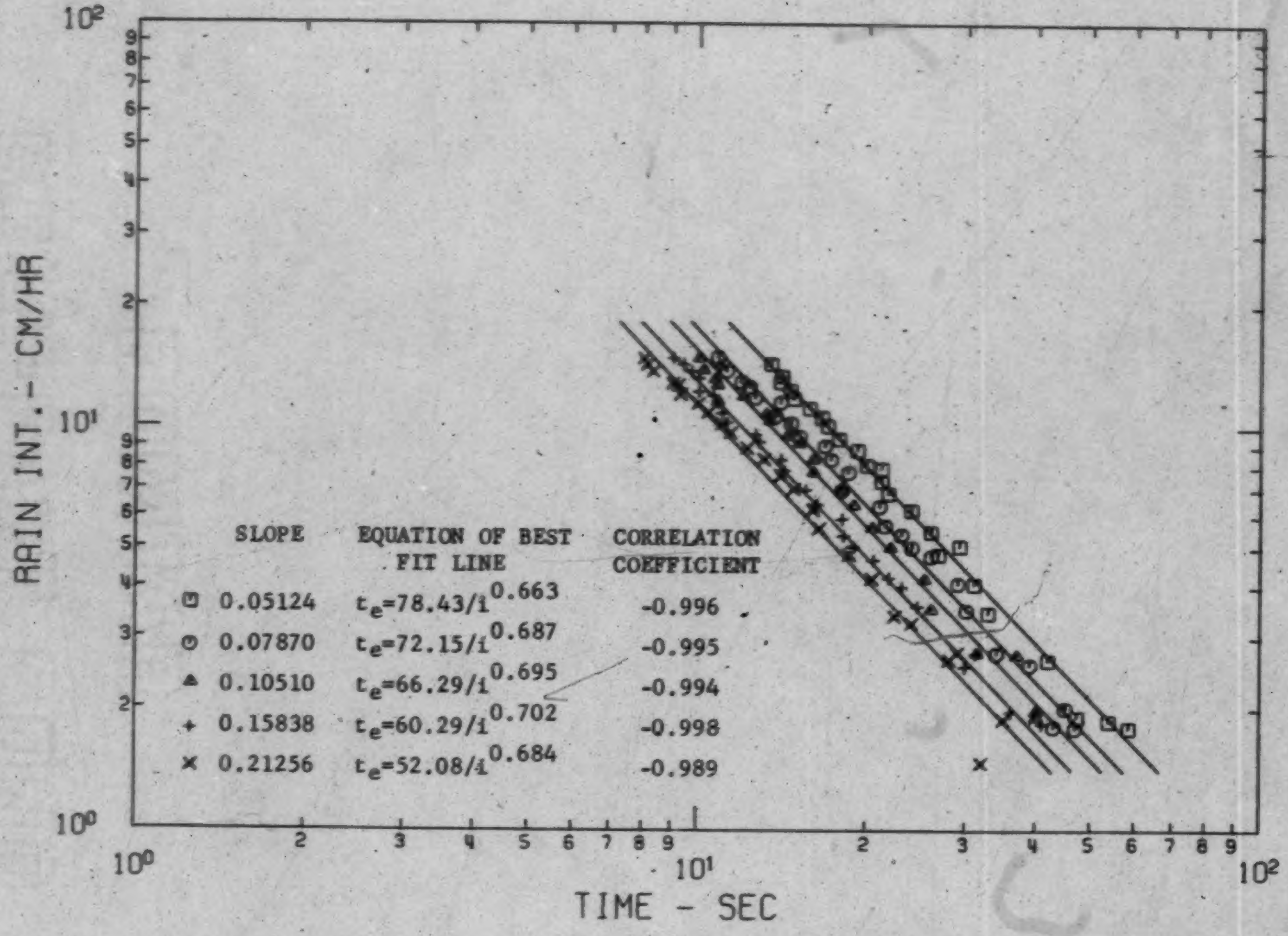

Figure 4-8. Relationship of apparent time to equilibrium, t_e, rainfall intensity, i, and bed slope, determined experimentally for a runoff plane of length 91.4 cm.

The significant result of these experiments is that the time distribution of overland flow is a function of rainfall intensity, in addition to slope, surface roughness, length, etc. Hence, any relationship for catchment characteristic times, such as "time of concentration", "basin lag", "time to equilibrium", and "time-area concentration curve (Nash, 1958)", which all have been used as measures of the speed of a catchment response to rainfall, in fact depends on the rainfall intensity. Many of the published relationships (Snyder, 1938; Taylor, 1952; Kerby, 1959; reviewed by Bell, 1969) failed to recognize this.

4-3 The Kinematic Wave Model

4-3-1 Kinematic Waves

Certain properties of a distinct type of wave motion, normally referred to as kinematic waves, were known already at the turn of this century. The velocity, c, measured relative to the bank of such waves was observed by Seddon (1900) to be given by the slope of the discharge - area curve, i.e.,

$$c = \frac{dQ}{dA} = \frac{1}{B}\frac{dQ}{dy} \qquad (4\text{-}11)$$

where Q is the discharge, A is the cross-sectional area of flow, B is the channel width, and y is the depth of flow. The validity of Equation (4-11), known as Seddon's Law (Linsley, 1958), was demonstrated by Seddon on the Mississippi River.

However, the first proof of the existence of the kinematic wave was given by Lighthill and Whitham (1955), who derived its properties mathematically. The authors provided the theory for this type of wave motion, which arises in any one-dimensional flow problem when there is an approximate functional relation at each point between the flow Q (quantity passing a given point in unit time) and concentration k (quantity per unit distance). The wave property then follows directly from the equation of continuity satisfied by Q and k. In view of this, the authors suggested calling these waves "kinematic" as distinct from the classical wave motions, which depend also on Newton's second law of motion and are therefore called dynamic.

The kinematic wave theory is based on the assumption that Q is a function of y only. Then the total derivative, dQ/dy, in Equation (4-11) has a unique meaning derived from the uniform flow condition, i.e., that the friction slope S_f and the bed slope S_o are equal (Henderson, 1969). The assumption that the discharge is a function of depth only is most likely satisfied when S_o is large. Thus, the kinematic wave theory appears to be particularly suited for the surface runoff problem, because of the steep slopes in the upper catchment regions where overland flow exists.

4-3-2 Kinematic Wave Theory of Overland Flow

Henderson and Wooding (1964) applied the kinematic wave theory to an elementary case of surface runoff illustrated in Figure 4-9(a). The runoff occurs from an impermeable uniformly sloping plane, and is caused by a uniformly distributed rainfall of constant intensity i. Following the derivation given by Henderson and Wooding, the equation of continuity for unsteady spatially varied flow caused by rainfall is

$$\frac{\partial q}{\partial x} + \frac{\partial y}{\partial t} = i \qquad (4\text{-}12)$$

where q is the discharge per unit width, y is the normal depth of flow, x is the distance in the main direction of flow, t is the time, and i is the rainfall intensity. Equation (4-12) can be written as

$$\frac{dq}{dy}\frac{\partial y}{\partial x} + \frac{\partial y}{\partial t} = i \tag{4-13}$$

or

$$c\frac{\partial y}{\partial x} + \frac{\partial y}{\partial t} = i \tag{4-14}$$

where

$$c = \left(\frac{dq}{dy}\right) \text{ for constant } x \tag{4-15}$$

Equation (4-15) is the Seddon Law and expresses the assumption that the discharge at a fixed distance x depends only on the depth at x.

Since y = fn(x,t) the total derivative of y is

$$\frac{dy}{dt} = \frac{dx}{dt}\frac{\partial y}{\partial x} + \frac{\partial y}{\partial t} \tag{4-16}$$

Comparing Equation (4-14) and Equation (4-16) one can see that if

$$\frac{dx}{dt} = c \tag{4-17}$$

then the two equations are identical, and

$$\frac{dy}{dt} = i \tag{4-18}$$

Physical interpretation of this result is that, to an observer moving with velocity $\frac{dx}{dt} = c$, the relation given by Equation (4-18) appears to be true, as well as the following relations:

(1) $y = it$ (4-19)

there being no constant of integration if the surface is initially dry, i.e., y = 0 at t = 0 for all x.

(2) $\frac{dq}{dy}\frac{dy}{dt} = \frac{dq}{dt} = ci$ (4-20)

and

$$\frac{dq}{dt}\frac{dt}{dx} = \frac{dq}{dx} = i \tag{4-21}$$

hence

$$q = ix + \text{constant} \tag{4-22}$$

As a result of the assumption that $S_f = S_o$ the discharge q is related to the depth y by the uniform flow equation of the general form

$$q = \alpha y^m$$

where $\alpha = \frac{gS_o}{3\nu}$, m = 3 for laminar flow, and $\alpha = C_1 S_o^{\frac{1}{2}}$, m = 3/2 for turbulent flow (Chezy equation). ν is the kinematic viscosity of water, and g is the acceleration of gravity. (For details see Chapter 5, Section 3-2-2.)

When a steady state is reached, the flow profile is given by

$$q = ix \tag{4-23}$$

Henderson (1964, 1969) discussed further solution in terms of a method of characteristics, i.e., tracing of the wave motion on the x-t plane. The resulting curve, called a characteristic, can be visualized as a path traced on the x-t plane by an observer moving with velocity c. Tracing the movements of many such observers, all starting to move at time t = 0 but from different starting positions along the runoff plane, will result in a set of characteristics. There is only one set of characteristics on the x-t plane, since the kinematic wave motion proceeds only in one direction, i.e. downstream.

Corresponding to each characteristic there is a curve in the physical y-x plane. Comparison of Equation (4-22) and Equation (4-23) shows that all these curves are identical with the steady state profile but displaced from it by an amount depending on the starting position of the observer at t = 0. By joining up points on these curves having the same value of t, one obtains an instantaneous profile of the water surface appropriate to that value of t, as illustrated in Figure 4-9(b).

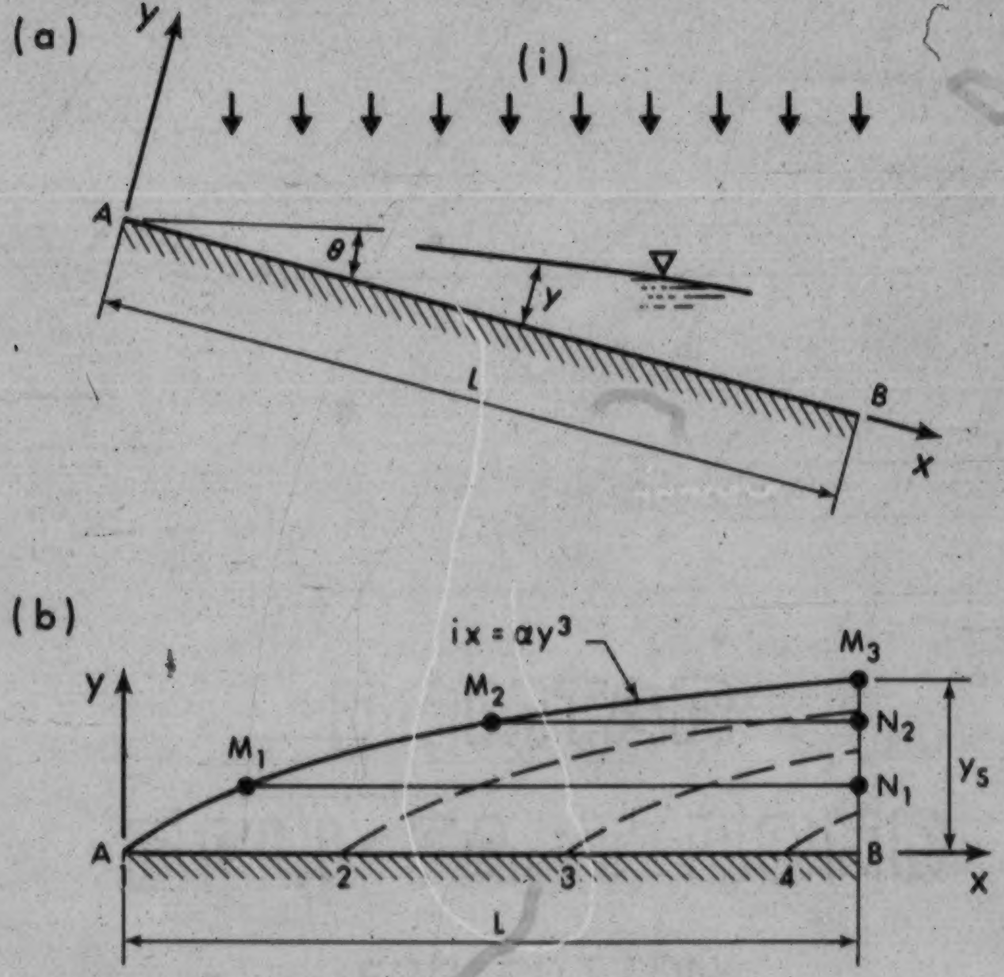

Figure 4-9. Kinematic wave solution of surface runoff by the method of characteristics: (a) definition sketch, (b) development of flow profiles: AM_1N_1 at time t_1, AM_2N2 at time t_2, steady state profile $AM_1M_2M_3$ at time t_s. Broken lines represent y-x curves corresponding to the paths traced by imaginary observers who started to move along the plane AB at time t = 0 with velocity c, from their starting positions 1, 2, 3, and 4.

Since Equation (4-19) appears true to all observers it follows that the successive profiles MN in Figure 4-9(b) are parallel to the surface AB in the region to the right of the steady state profile. The plateau MN rises with constant velocity i until a steady state is reached after a time

$$t_s = \frac{y_s}{i} = \left(\frac{L}{\alpha\ i^{m-1}}\right)^{1/m} \qquad (4\text{-}24)$$

Discharge q at the lower end, B, of the runoff plane is given by

$$q = \alpha y^m = \left\{\begin{array}{ll} \alpha i^m t^m & (t<t_s) \\ Li & (t\geq t_s) \end{array}\right\} \qquad (4\text{-}25)$$

The relation for discharge given by Equation (4-25) is valid for the duration of rainfall, t_o, equal to infinity. For finite durations the following two cases of discharge subsidence, after cessation of rainfall can be distinguished (derivation of formulas can be found in Henderson [1964, 1969]):

(1) $t_o \geq t_s$. The initial profile is a steady state profile. The depth y at B at a given time, t_a, after the cessation of rainfall can be computed from

$$L = \alpha y^{m-1}\ \left(\frac{y}{i} + mt_a\right) \qquad (4\text{-}26)$$

and the discharge is given by $q = \alpha y^m$.

(2) $t_o < t_s$. The greatest depth at B reached during the rising period is $y_o = it_o$. This depth remains constant during the recession for the time $t_a < t_p$, where t_p is given by

$$t_p = \frac{L - \dfrac{\alpha y_o^m}{i}}{m\alpha y_o^{m-1}} = \frac{1}{m}(t_{os} - t_o) \qquad (4\text{-}27)$$

where $t_{os} = L/\alpha y_o^{m-1}$. From Equation (4-24) it follows that $t_{os} = t_s$ when

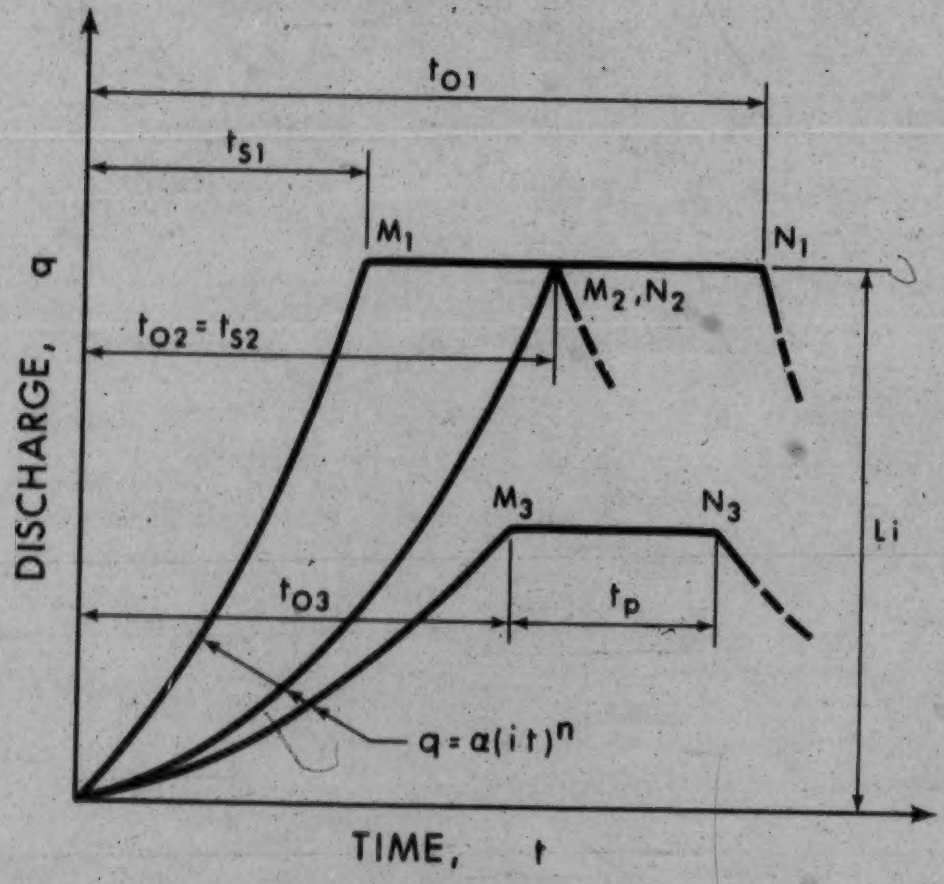

Figure 4-10. Outflow q - t curves.

Crest	Hydrograph
M_1N_1	typical case when $t_o > t_s$
M_2N_2	typical case when $t_o = t_s$
M_3N_3	typical case when $t_o < t_s$

$t_o = t_s$. When $t_a \geq t_p$, Equation (4-26) holds and the outflow is then identical with that given in case (1) with the same value of i.

In summary, three types of hydrographs can be distinguished when the surface runoff is simulated by the kinematic wave model. The criterion governing the occurrence of a particular type is given by the relation of the rainfall duration, t_o, to the time to equilibrium, t_s, i.e. whether t_o is greater, equal or less than t_s. Typical hydrographs for each case are shown schematically in Figure 4-10. A characteristic property of the kinematic wave model is the sharp crest of the simulated hydrograph. This property follows from Equation (4-19), according to which the depth of flow increases with constant velocity until a steady state is reached or until the rain input ceases.

4-3-3 Comparison of Simulated and Observed Hydrographs

In Section 4-3-2 the concept of kinematic wave was used to develop the relationships given by Equations (4-24) to (4-27), specifying the temporal and spatial distribution of discharge from a uniformly sloping plane under rainfall. These equations, which together form the kinematic wave model of overland flow, were used for development of a computer program for performing digital simulation of experimental hydrographs. The computer program is listed in Appendix D. The simulation included six events of runoff, from the laboratory catchment with the bed slope $S_o = 0.20791$, generated by rainfalls of intensities of 11.53 cm/hr and 7.77 cm/hr (runs number 1 to 6 given in Table 5-2, Chapter 5).

The case when the rainfall duration is longer than the time to equilibrium, i.e. $t_o > t_s$, is shown in Figures 4-11 and 4-14. The simulated hydrographs fit the experimental data quite well except near the hydrograph crest. Larger discrepancies in peak discharge values are apparent for the case when $t_o = t_s$, shown in Figures 4-12 and 4-15 and the case when $t_o < t_s$, shown in Figures 4-13 and 4-16. In these two cases, i.e. when $t_o \leq t_s$, the predicted peak discharges are considerably higher than the observed ones. There are two possible reasons for these discrepancies, besides the errors in measurement. Firstly, it is a property of the kinematic wave model, given by Equation (4-19), that a steady rate of increase of flow depth at a given cross-section occurs until a steady state of discharge at the same cross-section is reached. This property results in sharp crested hydrographs, contrary to the assymptotical approach to a steady flow in natural hydrographs. Consequently, the simulated values of discharge near the peak are overestimated. Secondly, the raindrop impact effect was neglected in the kinematic wave model. As a result, the simulated hydrographs are rising faster and the peak discharges are again overestimated. Complete discussion of the raindrop impact effect is given in Chapter 5, Section 4.

The duration t_s, sometimes called the "time to equilibrium", appears, in one form or another, in all standard hydrological theories or methods. In many cases it is assumed to be independent of i, as it was discussed in Section 4-2-5-1 of this Chapter. It was found experimentally in the same section that the apparent time to equilibrium, t_e, is in fact a function of rainfall intensity i, and has the form given by Equation (4-10). The empirical equations, given in Figure 4-8, specifying t_e for different values of S_o as a function of i are compared in Table 4-2 to the time to equilibrium, t_s, predicted by the kinematic wave model. The time to equilibrium, t_s, is given by Equation (4-24) which may be written for the case of laminar flow from the laboratory catchment (L = 3 feet, m = 3) as

$$t_s = \left(\frac{3L\nu}{gSi^{m-1}}\right)^{1/m} = 32.29 \left(\frac{1}{S}\right)^{1/3} \frac{1}{i^{0.666}} \tag{4-28}$$

The predicted values of t_s compare closely with the empirical values of t_e. Because t_e is of a shorter duration than t_s by definition the constants in the empirical equations are generally smaller than the constants in the corresponding equations for t_s. The relationship specifying the time to equilibrium, t_s, follows from the assumption of the kinematic wave theory that the discharge is a function of the flow depth only. The results in Table 4-2 support the validity of this assumption or at least give the evidence of a good approximation for the given conditions.

TABLE 4-2

COMPARISON OF THE EMPIRICAL APPARENT TIME TO EQUILIBRIUM, t_e, AND THE TIME TO EQUILIBRIUM, t_s, PREDICTED BY THE KINEMATIC WAVE MODEL

S_o	t_s (sec)	t_e (sec)
0.05117	$86.93\ i^{-0.666}$	$78.43\ i^{-0.663}$
0.0787	$75.37\ i^{-0.666}$	$72.15\ i^{-0.687}$
0.1045	$68.46\ i^{-0.666}$	$66.29\ i^{-0.695}$
0.1583	$59.22\ i^{-0.666}$	$60.29\ i^{-0.702}$
0.20791	$54.12\ i^{-0.666}$	$52.08\ i^{-0.684}$

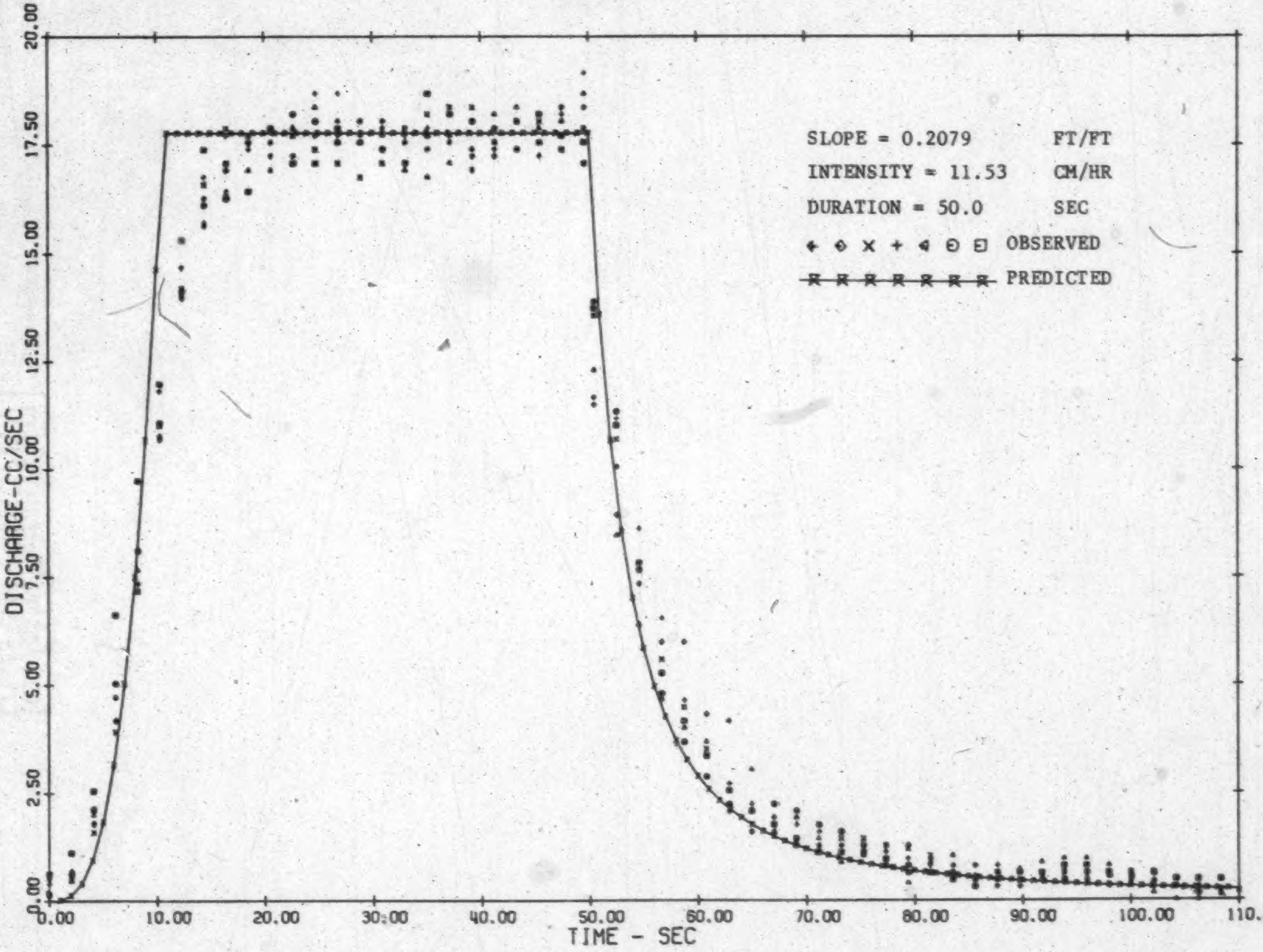

Figure 4-11. Observed and predicted hydrographs (kinematic wave model) for test 1, $(t_o > t_s)$.

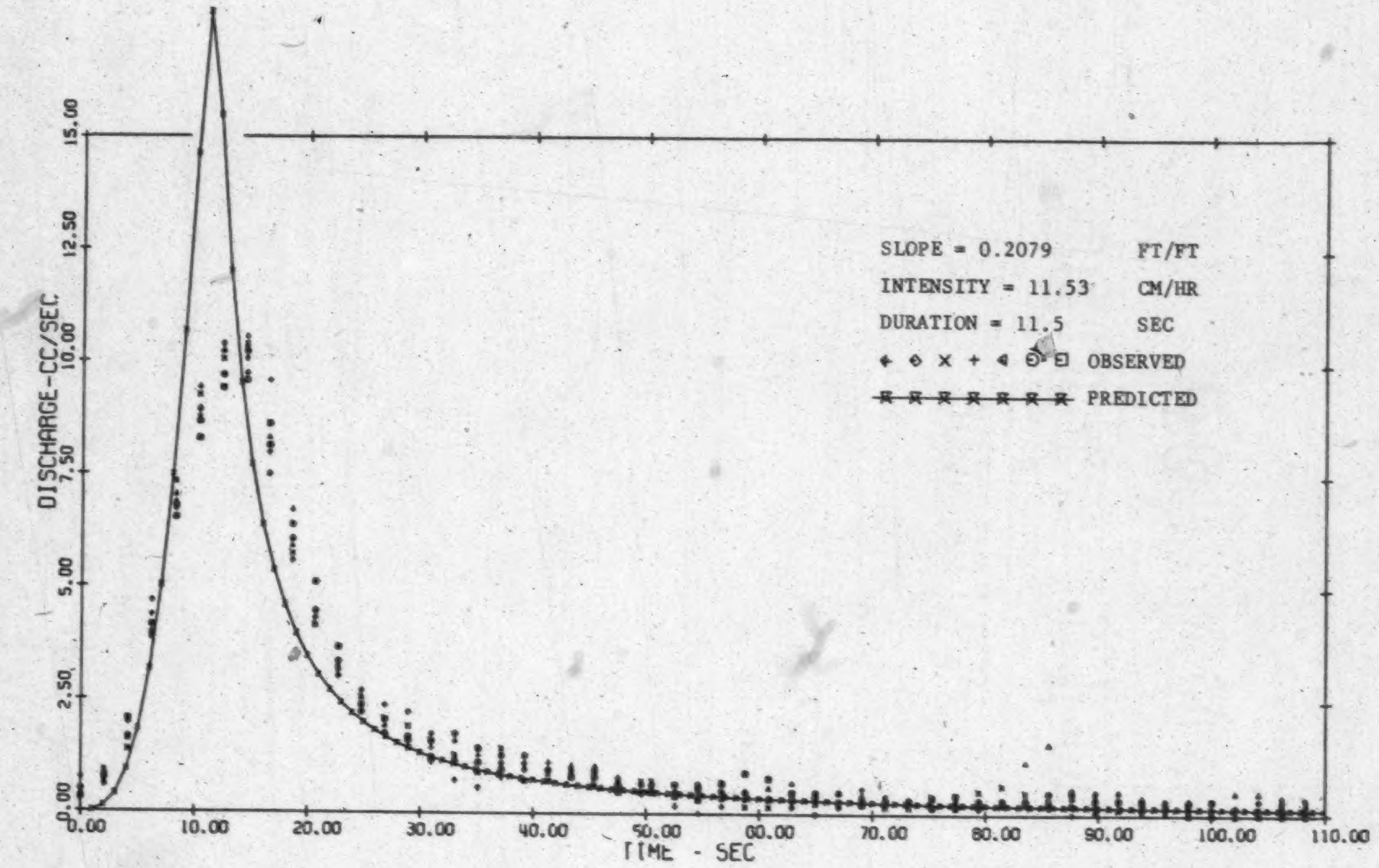

Figure 4-12. Observed and predicted hydrographs (kinematic wave model) for test 2, ($t_o \doteq t_s$).

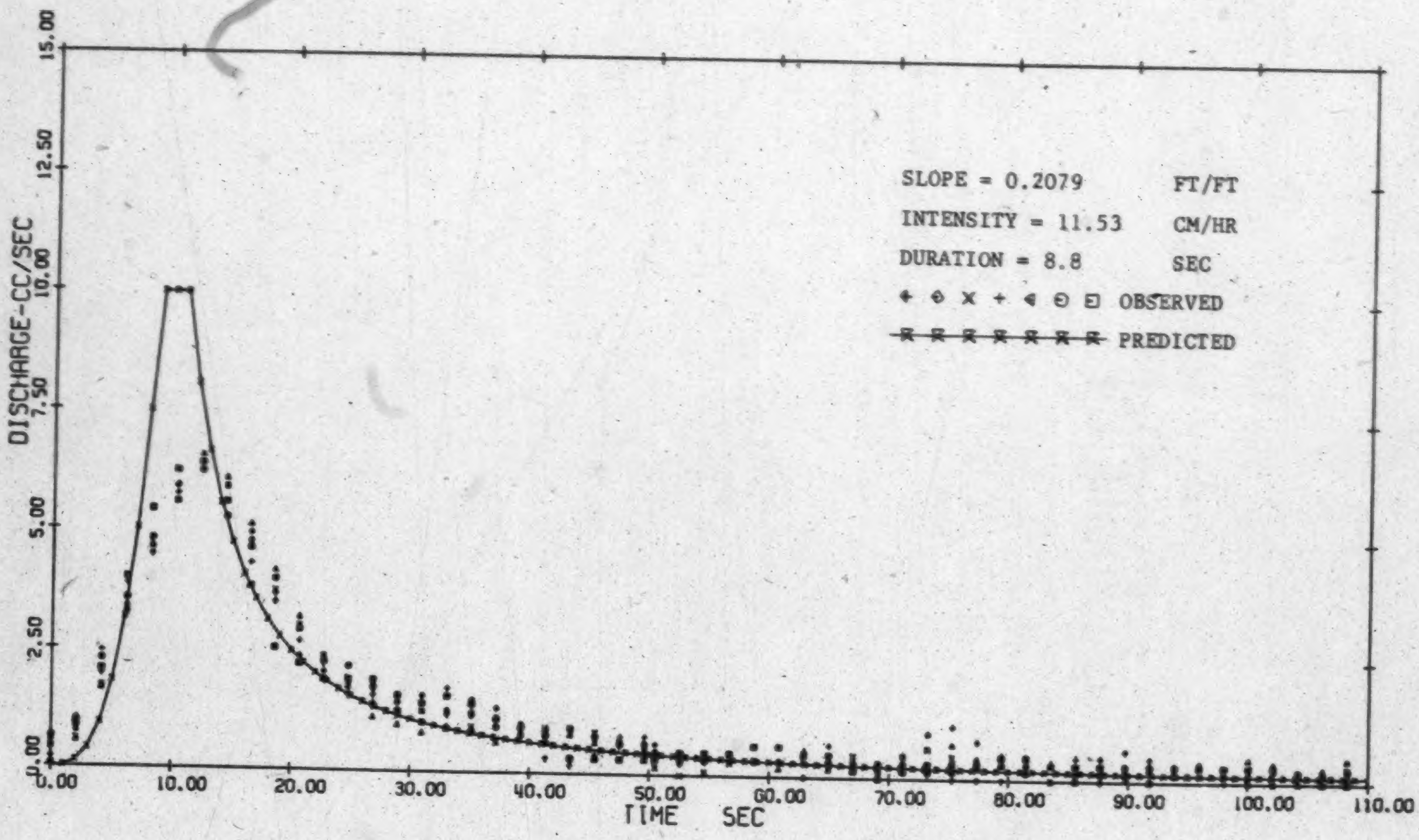

Figure 4-13. Observed and predicted hydrographs (kinematic wave model) for test 3, $(t_o < t_s)$.

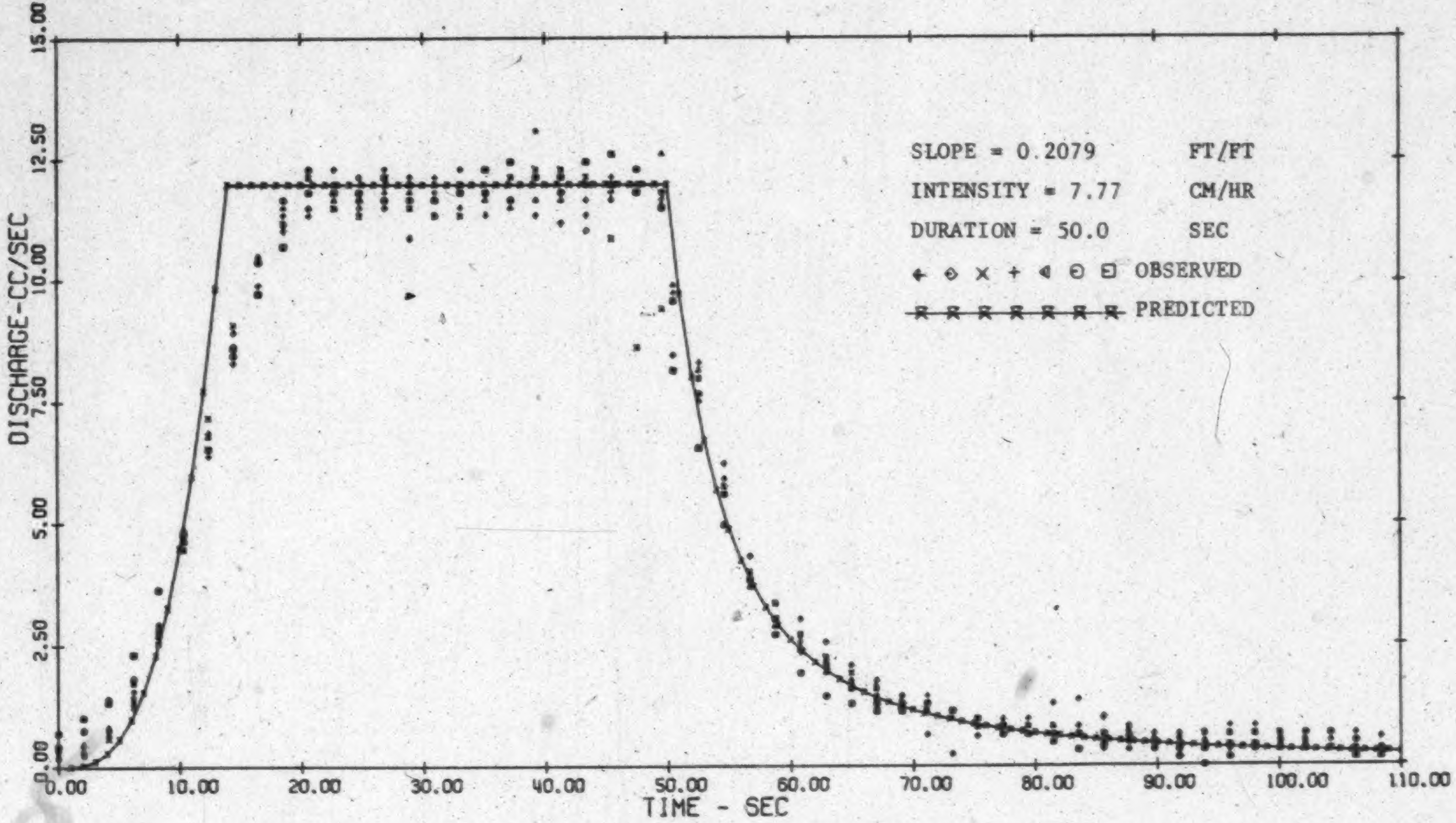

Figure 4-14. Observed and predicted hydrographs (kinematic wave model) for test 4, ($t_o > t_s$).

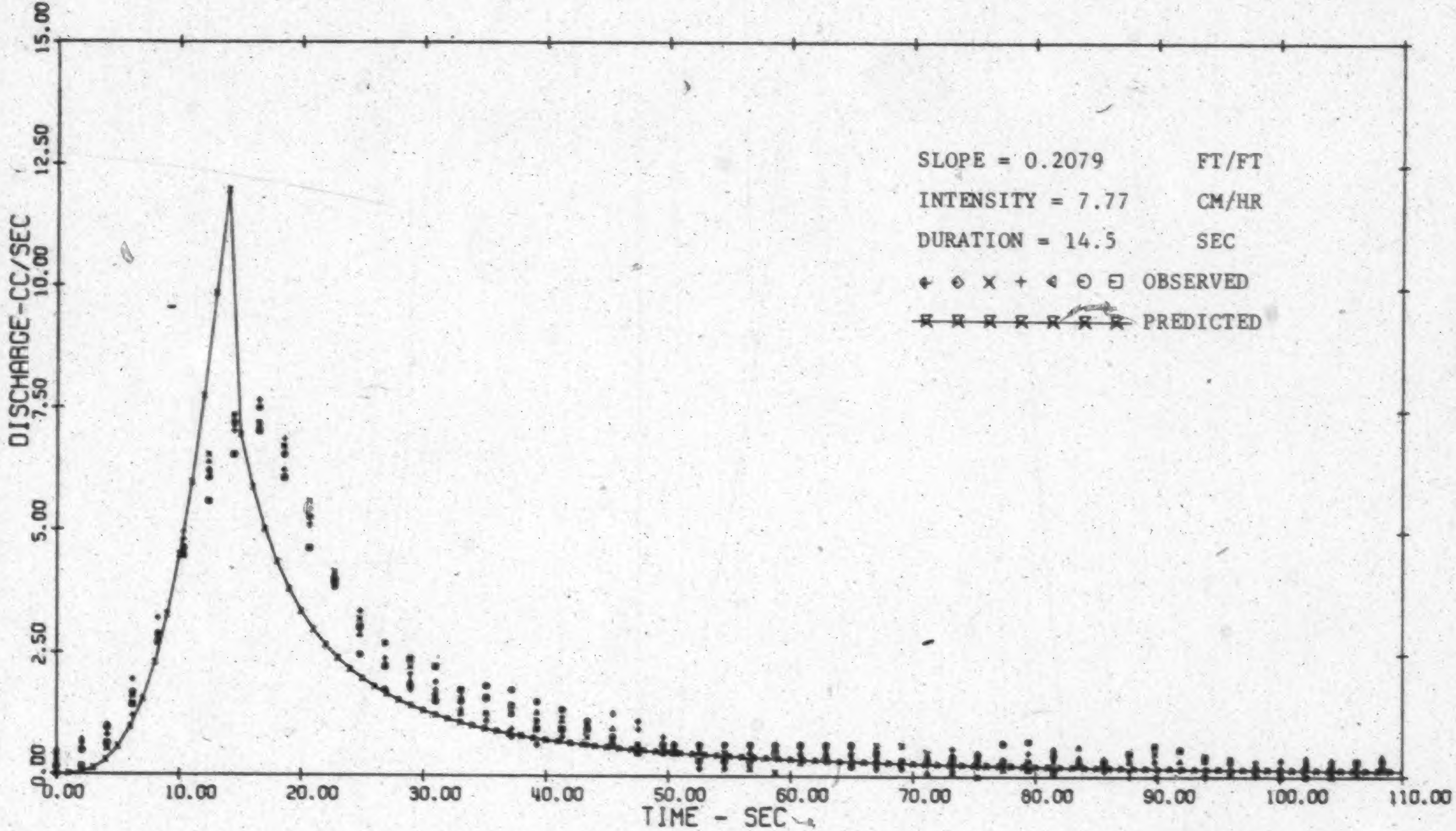

Figure 4-15. Observed and predicted hydrographs (kinematic wave model) for test 5, ($t_o \doteq t_s$).

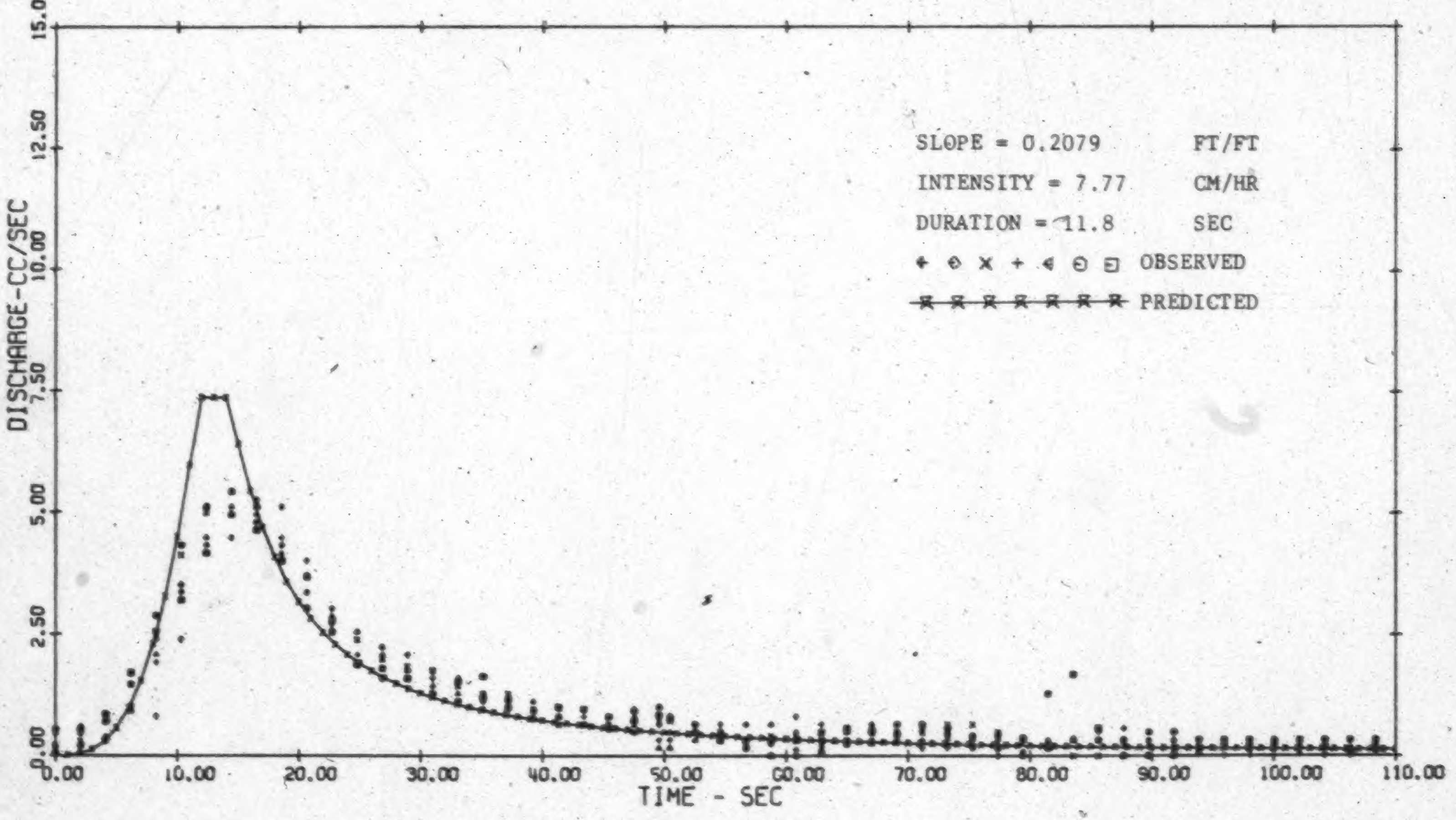

Figure 4-16. Observed and predicted hydrographs (kinematic wave model) for test 6, ($t_o < t_s$).

CHAPTER V

STATE VARIABLE MODEL OF SURFACE RUNOFF

5-1 Introduction

Observations of runoff from natural watersheds and from laboratory catchments, as well as theoretical considerations of fluid motion support the view that rainfall and runoff are related by a nonlinear relationship. For this reason, accurate predictions of runoff resulting from wide variations of rainfall cannot be achieved by a linear model. It was shown in Chapter III, for the case of a single reservoir that a linear approximation of a nonlinear process can be expected to be of an acceptable degree of accuracy only within a narrow range of fluctuations of the input variable (such as the rainfall intensity). There is a need to develop a nonlinear model of the rainfall-runoff phenomenon based on relevant physical laws.

The rainfall-runoff process is a part of a complex hydrological system which may have many inputs and many outputs, and these are related in a complicated manner. To analyze such a system, it is essential to reduce the complexity of the mathematical expressions, as well as to resort to computers for most of the tedious computations necessary in the analysis. The state-space approach to systems analysis, developed since around 1960, is best suited from this viewpoint (Ogata, 1970). The concept of state by itself is not new since it has been in existence for a long time in the field of classical dynamics (Ogata, 1967; MacFarlane, 1970), and other fields. In hydrology, many investigators (Minshall, 1960;

Amorocho, 1967; Kirkly, 1967) recognized that catchment runoff is related not only to the rainfall input but also to the past rainfall-runoff history of the catchment. Both the antecedent index of precipitation and the base flow have been used as indexes of the state of the catchment for the purpose of predicting future runoffs. However, this practice has been largely based on intuitive considerations.

In this chapter the state-space analysis is applied to the problem of simulating surface runoff due to rainfall distribution over an impervious uniformly sloping surface. The purpose of the analysis was to develop a mathematical model that could be used as a basis for a subsequent empirical evaluation to simulate runoffs from natural watersheds.

5-2 State Space Analysis of Systems

The state-space method has been developed in modern system control theory. Modern control theory, states Ogata (1970), is contrasted with conventional theory in that the former is applicable to multiple-input-multiple-output systems, which may be linear or nonlinear, time-invariant or time-varying, while the latter is applicable only to linear time-invariant single-input-single-output systems. Also, modern control theory is essentially a time-domain approach and thus particularly suited for digital computer computations, while conventional control theory is a complex frequency-domain approach.

From a mathematical viewpoint, the state-space approach to systems analysis and synthesis is the use of matrix and vector methods to handle the large number of variables which enter into such problems. As such, states Derusso (1967), these are not new methods, but rather they are the rediscovery of existing mathematical techniques. They aid considerably in the solution of linear multivariable problems. More important, however, the state-space approach aids conceptual thinking about these problems, and nonlinear problems as well. Furthermore, it provides a unifying basis for consideration of linear and nonlinear problems.

5-2-1 Dynamic Systems

For the purpose of further discussion it is convenient to define dynamic and instantaneous systems. Schwartz (1965) states that a system is classified as instantaneous if its output at any instant t depends at most on the input value at the same instant but not on past or future values of the input. The input-output relation for an instantaneous system may be expressed by

$$\underline{z}(t) = \underline{f}\ (\underline{u}[t],t) \tag{5-1}$$

where $\underline{u}$ = the input vector

$\underline{z}$ = the output vector

$\underline{f}$ = the vector-valued function

On the other hand, a system is said to be dynamic if the output at any instant depends not only on the present input, but also on at least some of the past input values. A system whose output at time t is completely determined by the input in the interval t-T to t, ($T \geq 0$), is said to have a memory of length T. The input-output relation for a dynamic system may be expressed by

$$\underline{z}(t) = \underline{g}(\underline{x}[t],\underline{u}[t],t) \tag{5-2}$$

where $\underline{x}$ = the state vector

$\underline{g}$ = the vector-valued function

All the relevant information concerning the past history of the system required to determine the response for any input is contained in the state vector $\underline{x}$.

5-2-2 State and State Variables

Ogata (1970) defines the state of a dynamic system as the smallest set of variables (called state variables) such that the knowledge of these variables at $t = t_o$, together with the input for $t \geq t_o$, completely determines the behaviour of the system for any time $t \geq t_o$. Thus, the state of a dynamic system at time t is uniquely determined by the state at time t_o and the input for $t \geq t_o$, and it is independent of the state and input before to.

If n state variables are needed to completely describe the behaviour of a given system, then these n state variables can be considered to be the n components of a vector $\underline{x}(t)$ and accordingly such a vector is called a state vector. A state vector is thus a vector which determines uniquely the system state $\underline{x}(t)$ for any $t \geq t_o$, once the input $\underline{u}(t)$ for $t \geq t_o$, is specified.

5-2-3 State Space

The n-dimensional space whose coordinate axes consist of the x_1 axis, x_2 axis, ... x_n Axis is called a state space. Any state, determined by the state vector $\underline{x}(t)$, can be represented by a point in the state space. As the state of the system changes with time the locus of the points, representing the states of the system at different instants of time, follows a curve called the trajectory of the state vector.

5-2-4 State Space Representation of Systems

The state variable method of systems analysis applies to systems described by ordinary differential equations. Such systems are said to be lumped. Systems which require the use of partial differential equations to describe their dynamic behaviour are said to be distributed. In the strict sense, states Schwartz (1965), all physical systems are distributed, but for practical purposes it is generally possible to approximate the behaviour of many by means of ordinary differential equations.

The basic concept of the state variable method may be developed from the general equation

$$\overset{(n)}{z} + a_1 \overset{(n-1)}{z} + \ldots + a_{n-1}\dot{z} + a_n z = u(t) \qquad (5\text{-}3)$$

where $\dot{z} = \frac{dz}{dt}$, $\ddot{z} = \frac{d^2z}{dt^2}$, ... , $\overset{(n-1)}{z} = \frac{d^{n-1}z}{dt^{n-1}}$, $\overset{(n)}{z} = \frac{d^n z}{dt^n}$

Equation (5-3) is general in the sense that it represents systems which may be classified in terms of the a_i coefficients $(i = 1, 2, \ldots, n)$ into the following three general categories (Langill, 1965): (1) linear systems, if all the coefficients, i.e. $a_1, a_2, \ldots, a_n$, are constant, (2) linear time-varying systems, if any of the coefficients a_i is a function of the independent variable time t, e.g. sin t, 3t, e^{-2t}, etc., (3) nonlinear systems, if one or more of the coefficients a_i is a function of the dependent variable z, e.g. sin z, 3z, cos $\dot{z}$, etc.

The state space representation of systems is based on the description of dynamical system behaviour in terms of n first-order differential equations. This may be done in a straightforward way, and without loss of generality, by adopting Moigno's device of introducing auxiliary variables (Moigno, 1844). To illustrate this technique on the example of Equation (5-3), let us define new variables $x_1, x_2, \ldots, x_n$ such that

$$
\begin{aligned}
x_1 &= z \\
x_2 &= \dot{z} \\
&\cdots\cdot \\
x_n &= z^{(n-1)}
\end{aligned}
\qquad (5\text{-}4)
$$

Since the specification of the values of these variables at a given reference time will determine a unique solution to the given equation, Equation (5-3), they are taken as the system state variables. Substitution of these variables then gives a set of n first-order differential equations which are equivalent to the given nth-order equation. These are

$$
\begin{aligned}
\dot{x}_1 &= x_2 \\
\dot{x}_2 &= x_3 \\
\vdots\ &\quad \vdots \\
\dot{x}_{n-1} &= x_n \\
\dot{x}_n &= -a_n x_1 - a_{n-1} x_2 - \dots - a_1 x_n + u
\end{aligned}
\qquad (5\text{-}5)
$$

or

$$
\underline{\dot{x}} = \underline{A}\,\underline{x} + \underline{B}\,u \qquad (5\text{-}6)
$$

where

$$
\underline{x} = \begin{bmatrix} x_1 \\ x_2 \\ \cdot \\ \cdot \\ \cdot \\ x_{n-1} \\ x_n \end{bmatrix}, \quad
\underline{A} = \begin{bmatrix}
0 & 1 & 0 & \dots & 0 \\
0 & 0 & 1 & \dots & 0 \\
\cdot & \cdot & \cdot & & \cdot \\
\cdot & \cdot & \cdot & & \cdot \\
\cdot & \cdot & \cdot & \dots & \cdot \\
0 & 0 & 0 & \dots & 1 \\
-a_n & -a_{n-1} & -a_{n-2} & \dots & -a_1
\end{bmatrix}, \quad
\underline{B} = \begin{bmatrix} 0 \\ 0 \\ \cdot \\ \cdot \\ \cdot \\ 0 \\ 1 \end{bmatrix}
$$

The output equation becomes

$$\underline{z} = [1\ 0\ \ldots\ 0]\begin{bmatrix} x_1 \\ x_2 \\ \cdot \\ \cdot \\ x_n \end{bmatrix}$$

or

$$\underline{z} = \underline{C}\ \underline{x} \qquad (5\text{-}7)$$

where

$$\underline{C} = [1\ 0\ \ldots\ 0]$$

The first-order differential equation, Equation (5-6), is the state equation, and the algebraic equation, Equation (5-7), is the output equation.

Whereas in the above example there was only one driving force, u(t), in a more general case m separate forces $u1, u_2, \ldots, u_m$ will be present. In this more general case, the set of first-order differential equations will thus read

$$\begin{aligned} \dot{x}_1 &= f_1(x_1, x_2, \ldots, x_n; u_1, u_2, \ldots, u_m) \\ \dot{x}_2 &= f_2(x_1, x_2, \ldots, x_n; u_1, u_2, \ldots, u_m) \\ &\cdot \\ &\cdot \\ &\cdot \\ \dot{x}_n &= f_n(x_1, x_2, \ldots, x_n; u_1, u_2, \ldots, u_m) \end{aligned} \qquad (5\text{-}8)$$

Integrating Equation (5-8) from time t_o to t gives

$$x_i(t) = x_i(t_o) + \int_{t_o}^{t} f_i(x_1, x_2, \ldots, x_n; u_1, u_2, \ldots, u_m)dt \qquad (5\text{-}9)$$

for $i = 1, 2, \ldots, n$. From Equation (5-9) it can be concluded, states Elgerd (1967), that each of the n x_i variables can be determined uniquely at any moment of time t if and only if:

(1) Each variable x_i is initially known, i.e. if n initial

conditions $x_i(t_o)$ are specified.

(2) All m driving forces u_j ($j = 1, 2, \ldots, m$) are specified throughout the interval t_o to t.

The n x_i variables can thus be interpreted as carriers of the full information about the transient state of the system. Initially, at $t = t_o$, the total system state can be expressed by the n numbers $x_1(t_o)$, $x_2(t_o)$, ..., $x_n(t_o)$. Under the influence of the m driving forces and the bonds of interaction, given by the equations describing the system, the state of the system will change. The updated state expressed by the n numbers $x_1(t)$, $x_2(t)$, ..., $x_n(t)$ can be continuously obtained from Equation (5-9). In consequence of this interpretation, the state of the system is defined as the n-dimensional vector $\underline{x}(t)$, which has as its components the n numbers or state variables $x_1(t)$, $x_2(t)$, ..., $x_n(t)$.

5-2-5 Second Order Systems and the Phase Plane

The state space with only two dimensions reduces to a state plane, also known as a phase plane. The phase plane applies to those systems for which the differential equation is of the form

$$\ddot{z} + a_1\dot{z} + a_2 z = u \qquad (5\text{-}10)$$

Although the phase plane analysis is limited to first and second order systems it is important for several reasons. Firstly, it allows easy visualization, since a trajectory on a plane can be readily traced, and thus it enables better understanding of the concept of state and state space. Secondly, many practically important and dynamically complex systems can be reasonably well approximated by second-order systems. Finally, because of its simplicity, many significant results and conclusions have been obtained, and several important theorems concerning system phase trajectories have been formulated (Hsu, 1968).

The phase plane method is a method for obtaining graphically the solution of a first or second order equation given by Equation (5-10), which may be linear or nonlinear. The solution, i.e. the phase trajectory, is displayed in a phase plane which most commonly is the z-$\dot{z}$ plane. The procedure is basically the same as that for the state space. Equation (5-10) is rewritten in terms of a set of first-order differential equations by introducing the state variables $x_1 = z$, and $x_2 = \dot{z}$. Equation (5-10) may be then written as

$$\begin{aligned} \dot{x}_1 &= x_2 \\ \dot{x}_2 &= u - a_1x_2 - a_2x_1 \end{aligned} \qquad (5\text{-}11)$$

or

$$\frac{\dot{x}_2}{\dot{x}_1} = \frac{dx_2}{dx_1} = \frac{u - a_1x_2 - a_2x_1}{x_2} \qquad (5\text{-}12)$$

Equation (5-12) defines the slope of the phase plane trajectory, dx_2/dx_1, in terms of functions x_2 and x_1. To find the curve which is the phase trajectory, this slope equation must be integrated. This integration may be performed analytically, graphically, or numerically. The trajectory does not show time information explicitly. If needed, however, the trajectory can be graduated in time units (Thaler, 1962; Ogata, 1970).

For examples of the phase plane representation of second order systems the reader is refered to Appendix G. Definition of a conservative system is given and the graphical method of isoclines is explained. The analytical and graphical methods of solution are illustrated on the following solved problems:

1. Analytical Solution.
   (a) Determination of phase trajectories for a linear conservative system.
2. Graphical Solution by the Method of Isoclines.
   (a) Determination of phase trajectories for a linear non-conservative system.
   (b) Determination of phase trajectories for a nonlinear system.

Further examples can be found in Thaler (1962) and Ogata (1970).

5-2-5-1 Phase Plane Analysis of Nonlinear Reservoir

Approximation of outflow from a nonlinear reservoir by the transfer function of a linearized equation of the reservoir was presented in Chapter III. In the following the same reservoir is analyzed by the phase plane method. The dynamic behaviour of the reservoir is described by Equation (3-4), restated here for convenience

$$\frac{dS}{dt} + K\sqrt{S} = i(t) \tag{5-13}$$

or more generally by Equation (3-3)

$$\frac{dS}{dt} + q(t) = i(t) \tag{5-14}$$

where S is the storage, K is the reservoir constant, i is the inflow input, and q is the reservoir outflow. In the analysis of the given reservoir two separate cases may be distinguished depending on a zero or non-zero forcing function, i(t), during the considered time interval $T(t_o, t)$.

Case 1. Forcing function is zero, $(i[t] = 0)$. The initial condition at time $t = t_o$ is given by $S = S_o$, and the equation of the reservoir is

$$\frac{dS}{dt} + K\sqrt{S} = 0 \tag{5-15}$$

Taking S to be the state variable, the term dS/dt defines the slope of the trajectory in the S - t plane at a given instant of time t, for $t \geq t_o$. Putting N = dS/dt, where N is a constant, yields an equation of a family of isoclines

$$S = (N/K)^2 \tag{5-16}$$

The isoclines are seen to be straight horizontal lines. By choosing different values of N, such as N_1, N_2, ..., N_k, a number of isoclines in the S-t plane can be determined. A particular trajectory can then be found by sketching a curve in the directional field of isoclines, starting from the point in the S-t plane given by the initial state S_o at the time $t = t_o$.

Three of the reservoir trajectories are shown in Figure 5-1. They fit very closely experimentally measured points. Since q = N (by comparison of Equations (5-13), (5-14), and (5-16)), both S and q can be determined from the same trajectory as functions of time.

The method of isoclines offers an interesting possibility of "identifying" the system given by Equation (5-15) from a single record of outflow q. The discharge, q, from the reservoir is related to the storage, S, by Equation (3-2).

$$q = K\sqrt{S} \tag{5-17}$$

Equation (5-17) defines a curve in the q-S plane. Slope N of this curve at any point P(q,S) is given by

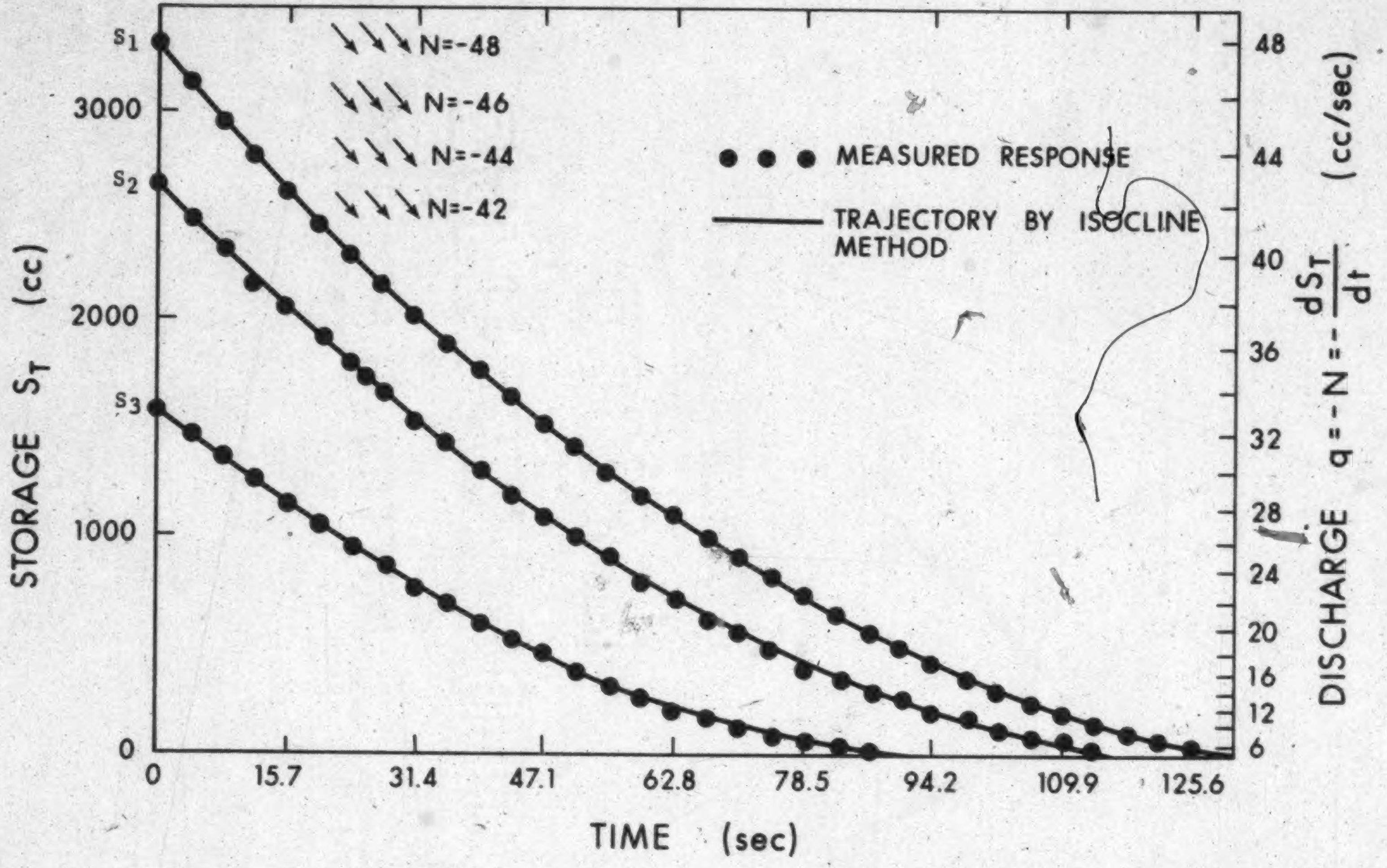

Figure 5-1. Graphical solution of storage equation of a nonlinear reservoir by the method of isoclines for the case of zero inflow and three initial storages S_1, S_2, S_3.

$$N = \frac{dq}{dS} \tag{5-18}$$

Suppose that the relation between q and S, given by Equation (5-17), is not known. Further suppose that a time record of outflow q is available in the range from $q = q_m$ to $q = 0$. Then for small increments of outflow q, Equation (5-18) may be approximated by

$$N \doteq \frac{\Delta q}{\Delta S} = \frac{q_2 - q_1}{\frac{q_1 + q_2}{2}\Delta T} \tag{5-19}$$

where q_1 = the outflow at the time t_1

q_2 = the outflow at the time t_2

$\Delta T = t_2 - t_1$, is the time increment

Equation (5-19) may be considered to define a family of isoclines in the q-S plane. Each isocline is a straight horizontal line given by the average outflow $(q_2 + q_1)/2$. When the isoclines are drawn the curve representing the relationship between q and S may be sketched and the parameters of the curve determined.

This procedure was verified experimentally by measuring the discharge q from a laboratory setup described in Chapter III. Table 5-1 shows the measured values of outflow q in discreet time intervals as well as the calculated average discharge q_{av} and the slope N (given by Equation (5-19)) for each time interval. The approximate curve determined by the method outlined above, shown in Figure 5-2, fits very closely the exact curve plotted from Equation (5-17) in the same figure. The time, which appears as a parameter on the curve, can be evaluated as follows. The q-S relationship is approximated by straight-line segments. For a particular segment its slope N may be determined as well as the average discharge, q_{av}, corresponding to the center of that segment.

TABLE 5-1

PHASE PLANE ANALYSIS OF A LABORATORY RESERVOIR FOR THE CASE OF RECEDING OUTFLOW AND ZERO INFLOW: APPROXIMATE SLOPES OF ISOCLINES CALCULATED BY EQUATION (5-19) FROM MEASURED VALUES OF DISCHARGE

Time (sec)	Discharge (cm^3/sec)	Average Discharge (cm^3/sec)	Slope N x(-10)$^{-3}$
0.00	47.7	47.0	7.6
3.93	46.3	45.7	7.4
7.86	45.0	44.4	7.5
11.79	43.7	43.0	7.6
15.72	42.4	41.8	7.8
19.65	41.1	40.5	7.6
23.58	39.9	39.3	7.7
27.51	38.7	38.1	8.6
31.44	37.4	36.8	8.6
35.39	36.2	35.6	8.7
39.30	34.9	34.3	8.8
43.23	33.7	33.1	9.5
47.16	32.5	31.9	9.4
51.09	31.3	30.7	11.1
55.02	30.0	29.4	10.4
58.95	28.8	28.1	11.4
62.88	27.5	26.9	12.0
66.81	26.2	25.6	13.4
70.74	24.9	24.3	12.3
74.67	23.7	23.0	14.8
78.60	22.3	21.7	16.1
82.53	21.0	20.3	16.9
86.46	19.7	19.0	17.7
90.39	18.3	17.6	21.6
94.32	16.8	16.1	23.6
98.25	15.3	14.6	24.4
102.18	13.9	13.3	22.9
106.11	12.7	11.9	34.7
110.04	11.1	10.3	38.1
113.97	9.6	8.8	45.3
117.90	8.0	7.1	63.2
121.83	6.2	5.3	94.8
125.76	4.3	2.9	243.0
129.69	1.5		

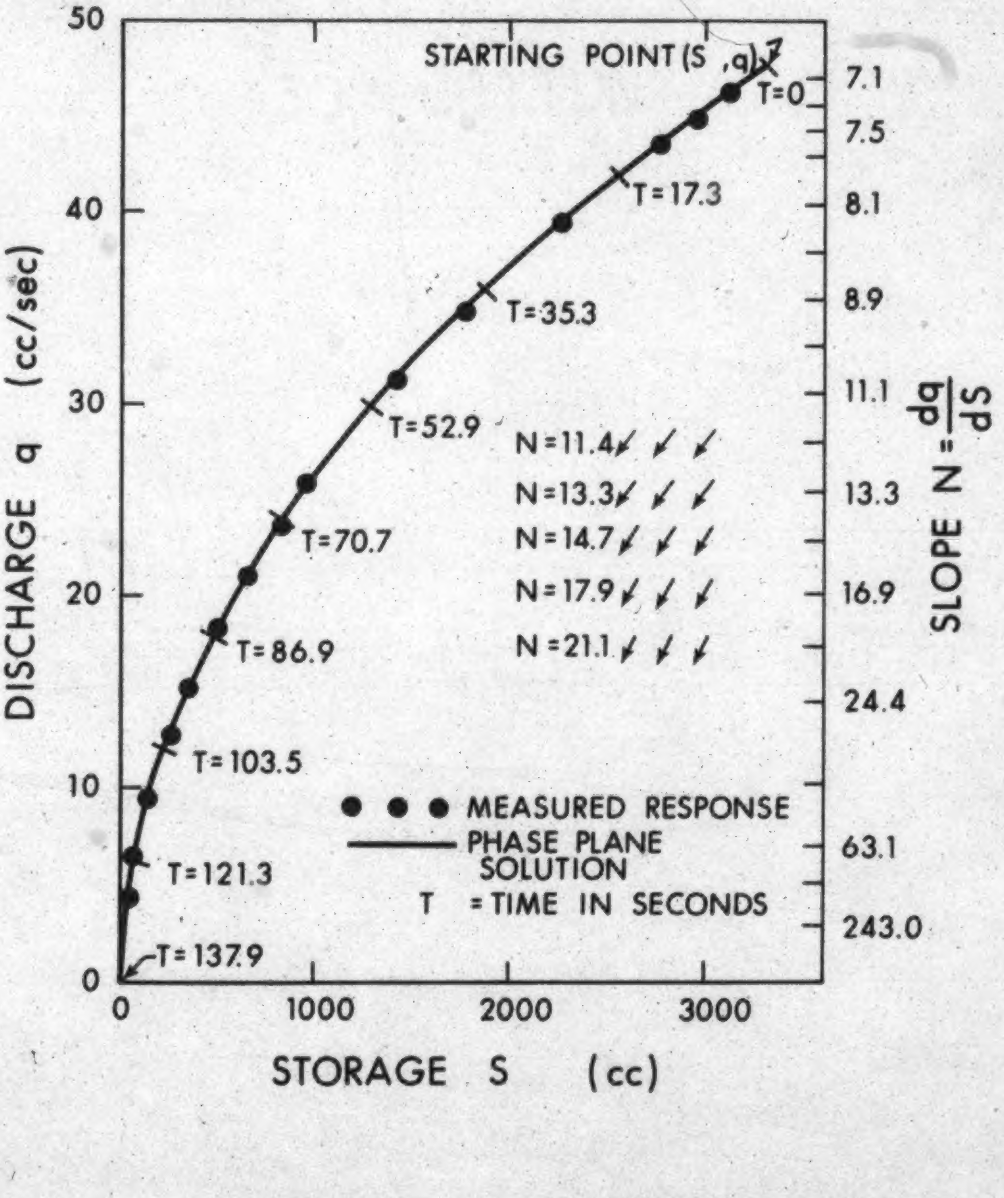

Figure 5-2. Phase plane solution of storage equation of a nonlinear reservoir for the case of zero inflow.

The displacement $\Delta q = q_2 - q_1$ can be measured over the length of the segment. Then from Equation (5-19) the time increment, ΔT, for that segment is

$$\Delta T = \frac{\Delta q}{N q_{av}} \tag{5-20}$$

Time for any point j on the phase trajectory may be calculated by summation of the time increments, ΔT_i, starting from the intial point, i.e., $t_j = \sum_{i=1}^{j} \Delta T_i$.

Equation (5-19) may be rearranged into

$$q_2 = q_1 \frac{2-N\Delta T}{2+N\Delta T} \tag{5-21}$$

which has the form of a well known depletion equation defining a recession curve of a hydrograph, usually written as

$$q_t = q_{t-1} K_r \tag{5-22}$$

where K_r is a recession constant. Equation (5-22) is often used in hydrograph analysis. It can be seen, by comparing Equations (5-21) and (5-22) that K_r can be constant only if N is a constant. However, a constant N implies a linear relationship between q and S (by Equation (5-18)) which is a questionable assumption with respect to watershed outflow. Thus, Equation (5-22) must be regarded as a gross linear approximation.

Case 2. Forcing function is not zero ($i(t) \neq 0$). This case was solved in Chapter III by the transfer function method for step inputs, using a linearized model of the reservoir. The initial conditions at time $t = t_o$ were: $S = S_*$, $i_* = q_*$, and for any time $t \geq t_o$ the input was $i = i_* + I$. The asterisk signifies a steady state value and I is the step increment of the input. Using the phase plane analysis the same problem may be solved graphically as follows.

The system equation is given by Equation (5-13), i.e.

$$\frac{dS}{dt} = i(t) - K\sqrt{S} \qquad (5\text{-}23)$$

The phase trajectory in the S-t plane may be approximated by short straight-line segments tangent to the trajectory. The slope of each tangent line segment is $N = \frac{dS}{dt}$, which can be calculated successively for small time (or storage) increments from Equation (5-23). This process, in principal similar to numerical solution of a differential equation, is organized in the following manner. Starting from the initial conditions at time $t = t_o$ the trajectory slope N at this time is calculated by Equation (5-23). A tangent line segment, having the slope N, is drawn. The length of the segment must be estimated so as to approximate closely the trajectory. A new value of S is read at the end of the segment. Substitution of this new value of S into Equation (5-23) yields a new value of the slope, N_2. Another tangent line segment is drawn, and the whole process is repeated. The tangent line segments form an envelope to the trajectory.

Responses of the reservoir to two step function inputs (the same problem as described in Chapter III) determined by the above method are compared to experimentally measured responses in Figure 5-3. The agreement between calculated and measured trajectories is very good. Further comparison of results obtained by the phase plane method and those obtained by the transfer function of a linearized reservoir indicates clearly the superiority of the former method.

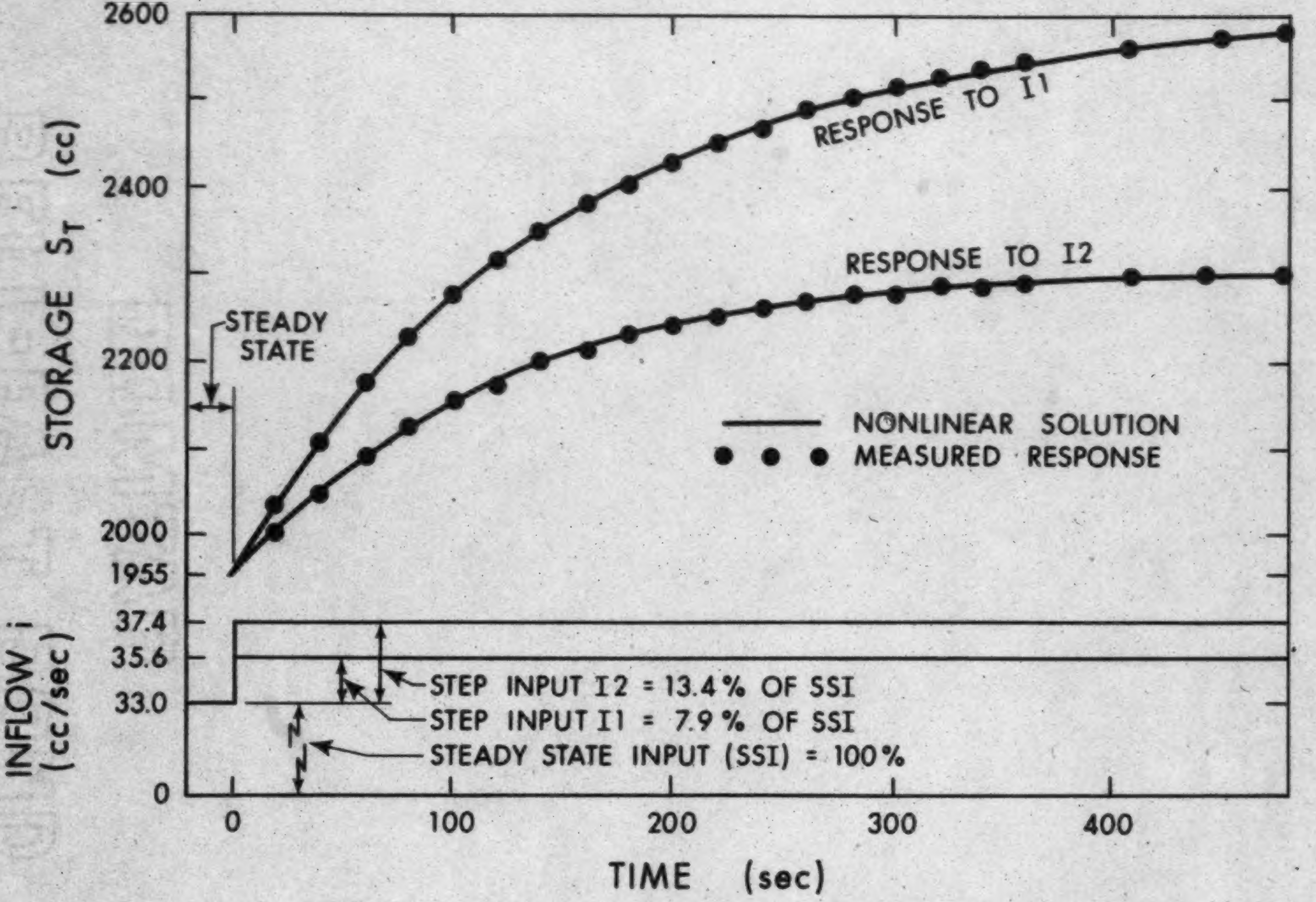

Figure 5-3. Comparison of measured responses of a nonlinear reservoir to two step function inputs, and those predicted by the phase plane method (nonlinear solution).

5-3 State Variable Model of Spatially Varied Overland Flow

Overland flow on a watershed is essentially a three-dimensional free-surface unsteady spatially varied flow phenomenon. However, unless there is a well defined channel, surface runoff can be approximated as two-dimensional (Yen, 1968). Thus, for the analysis of overland flow resulting from rainfall, consider an idealized impermeable surface shown in Figure 5-4. The surface is of length L, slope $S_o = \sin\theta$, and of unit width. The x axis is taken along AB with the origin at A. When rain of a constant intensity i begins to fall the discharge changes with time and the flow is unsteady. A time of equilibrium will eventually be reached. At this time the discharge is equal to the rate of rainfall and the runoff becomes steady. When rainfall ceases, the subsiding runoff becomes unsteady again. The objective was to develop a mathematical model (using the state space formulation) of this one-dimensional, spatially varied unsteady surface flow.

5-3-1 Unsteady Spatially Varied Flow - Basic Equations

The equations of two-dimensional unsteady spatially varied flow are the continuity equation

$$\frac{\partial y}{\partial t} + \frac{\partial (Uy)}{\partial x} = i \cos\theta \qquad (5\text{-}24)$$

and the dynamic equation

$$\frac{\partial U}{\partial t} + U\frac{\partial U}{\partial x} + g\frac{\partial y}{\partial x} = g(S_o - S_f) - \frac{i}{y}(U-u) \qquad (5\text{-}25)$$

In the above equations x is the longitudinal direction of the flow along the x-axis of the runoff plane. The average longitudinal velocity component of the flow is U. The lateral inflow is i, in terms of volume per unit time t per unit surface area on the runoff plane. This lateral

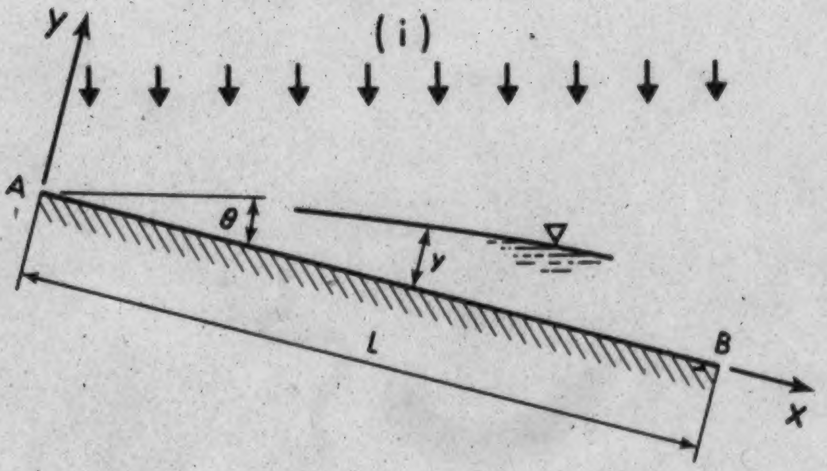

Figure 5-4. Definition sketch for surface flow over a sloping plane.

inflow has a horizontal velocity component u in the x-direction, y is the depth of flow normal to the plane and the slope of the runoff plane is S_o, S_f is the friction slope.

These equations were first derived by de Saint-Venant in 1871, and therefore, are sometimes referred to as the de Saint-Venant equations. Derivation of the equations with their assumptions may be found elsewhere (Rouse, 1957; Chow, 1959; Chen, 1968; Yen, 1968).

5-3-2 Unsteady Spatially Varied Flow - Approximation by Lumped Parameters

While the de Saint-Venant equations describe the unsteady spatially varied flow in a rigorous manner, their practical usefulness for simulating overland flow from watersheds is somewhat limited. This is because of the complexity of the equations. Their analytical solutions have been obtained only for restricted, simplified cases. The only available general method of solution are finite difference techniques (Chow, 1959; Strelkoff, 1970; Brutsaert, 1971). However, these methods have a major disadvantage for continuous simulation since substantial amounts of computer time are needed. Furthermore, areal variations in the rainfall inputs as well as the surface parameters of natural watersheds, such as the infiltration rate, surface roughness, length and slope, require the use of average values. Thus, while reasonably accurate methods are justified, the accuracy to be gained by using finite difference methods for overland flow, states Crawford (1966), is still subject to question because of the limited accuracy of the basic data.

It is thus desirable to develop a model based on simplified mathematical relations. This can be achieved by approximating the distributed system by lumped parameters. In the following the continuity and dynamic equations of surface runoff, based on lumped parameters, are derived.

5-3-2-1 The Continuity Equation

Equation of continuity of overland flow, considered as a distributed system shown in Figure 5-5(a), may be written as

$$\frac{\partial q}{\partial x} + \frac{\partial y}{\partial t} = i \cos \theta \qquad (5\text{-}26)$$

where $q = Uy$ is the discharge per unit width. Dynamics of this distributed system can be approximated by a lumped parameter model, shown in Figure 5-5(b), in which the runoff plane is substituted by a series of interacting reservoirs. The distributed parameters $i(x,t)$ and $q(x,t)$ indicating the rate of rainfall and discharge respectively, have been lumped into a finite number of input and output variables, P_j and O_j, respectively, where $j = 1, 2, \ldots, n$. This lumped model is of a "distributized" character since it consists of a number of lumped parameter units or subsystems. The equation of continuity, generally valid for each of the reservoirs, can be written in terms of the ordinary differential equation

$$\frac{dS_j}{dt} = X_j \cos \theta \frac{dh_j}{dt} = P_j - (O_j - O_{j-1}) \qquad (5\text{-}27)$$

where S_j = the storage in the j-th reservoir per unit width

X_j = the length of the j-th reservoir in the x-direction

h_j = the depth of water in the j-th reservoir

The lumped input P_j is given by

$$P_j = i X_j \cos \theta \qquad (5\text{-}28)$$

and the output O_j is to be determined by the dynamic equation. Continuity of the whole model consisting of n reservoirs is then described by the set of n ordinary differential equations

$$\begin{aligned} X_1 \cos\theta\frac{dh_1}{dt} &= P_1 - O_1 \\ X_2 \cos\theta\frac{dh_2}{dt} &= P_2 - (O_2 - O_1) \\ \vdots \quad & \quad \vdots \\ X_n \cos\theta\frac{dh_n}{dt} &= P_n - (O_n - O_{n-1}) \end{aligned} \tag{5-29}$$

More refined approximation to the distributed system may be achieved by routing the flow through n hypothetical reaches instead of reservoirs, as shown in Figure 5-5(c). Mechanism of outflow from these reaches is assumed to be such that the water surface remains parallel to the bottom at all times. The set of continuity equations characterizing the model is

$$\begin{aligned} X_1 \frac{dy1}{dt} &= P_1 - O_1 \\ X_2 \frac{dy2}{dt} &= P_2 - (O_2 - O_1) \\ \vdots \quad & \quad \vdots \\ X_n \frac{dy_n}{dt} &= P_n - (O_n - O_{n-1}) \end{aligned} \tag{5-30}$$

The approximation to the distributed system becomes progressively better as the number of reaches, n, in the lumped model increases. This can be proved by letting n increase to infinity, i.e. X_j approaches zero ($j = 1, 2, \ldots, n$). The left hand side of any of the equations (5-30) is then

$$\lim_{X_j \to 0} (X_j \frac{dy_j}{dt}) = \delta x \frac{\partial y}{\partial t} \tag{5-31}$$

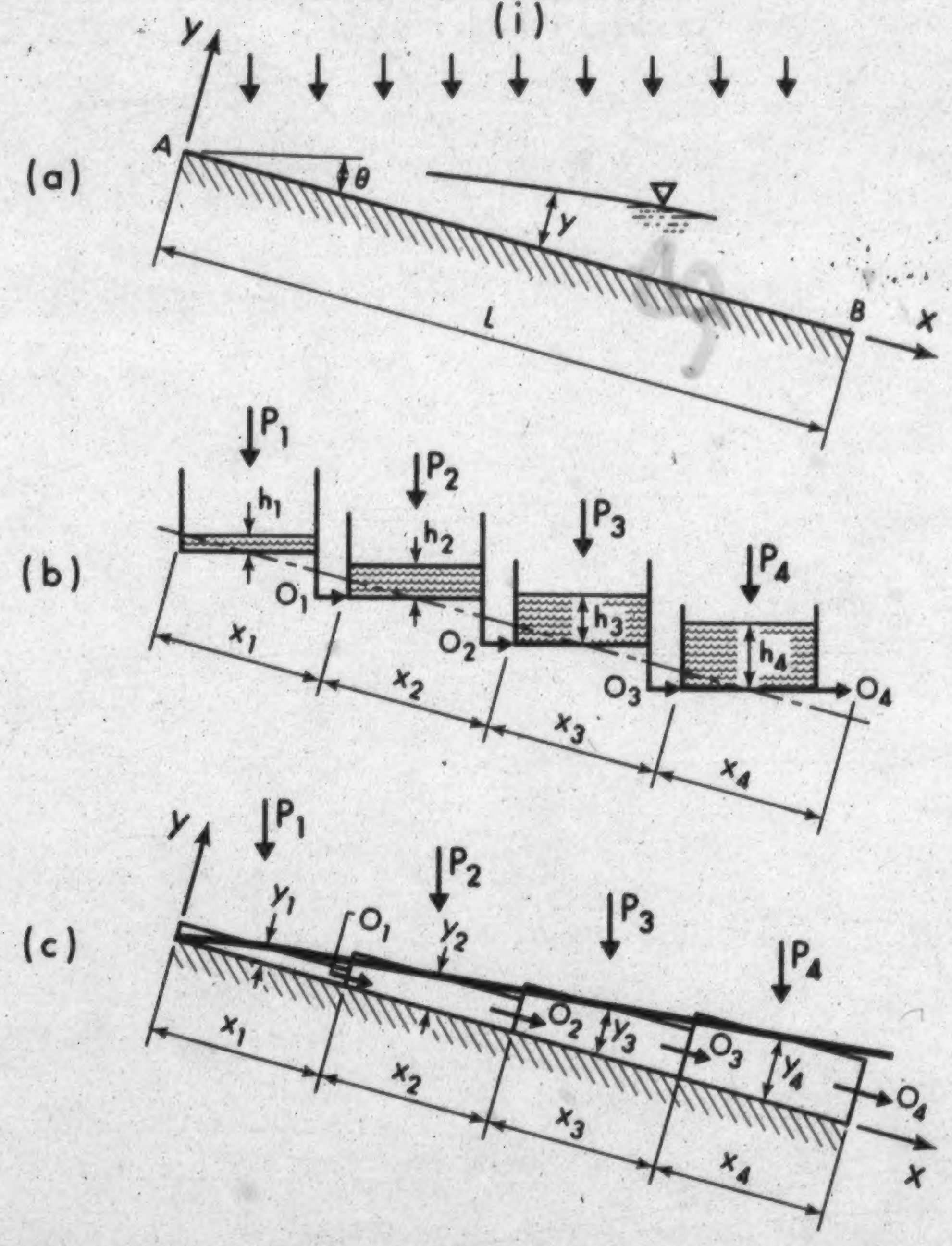
(i)
(a)
y
A
θ
y
L
B
x
(b)
P1
P2
P3
P4
h1
h2
h3
h4
O1
O2
O3
O4
x1
x2
x3
x4
(c)
y
P1
P2
P3
P4
y1
y2
y3
y4
O1
O2
O3
O4
x1
x2
x3
x4
x

Figure 5-5. Surface runoff over a sloping plane: (a) definition sketch, (b) simulation by a 4th-order lumped system of interacting reservoirs in series, (c) simulation by a 4th-order lumped system consisting of hypothetical uniform flow reaches.

and the right hand side is

$$\lim_{X_j \to 0} [P_j - (O_j - O_{j-1})] = i\delta x \cos\theta - \frac{\partial q}{\partial x}\delta x \tag{5-32}$$

By comparison of both sides one obtains

$$\frac{\partial y}{\partial t} + \frac{\partial q}{\partial x} = i \cos\theta \tag{5-33}$$

which is the continuity equation, Equation (5-26) of the distributed system.

5-3-2-2 The Dynamic Equation

Since the lumped model assumes uniform flow within every reach, discharge may be calculated by any type of resistance formula. In general terms the dynamic equation has the form

$$O = \alpha y^{m} \tag{5-34}$$

The parameters α and m are given as follows:

(1) Laminar flow (derivation can be found in Chow (1959)):

$$\alpha = \frac{gS}{3\nu}, \; m = 3$$

(2) Turbulent flow:

Chezy equation: $\alpha = C_1 S^{1/2}$, $m = 3/2$

Manning equation: $\alpha = C_2 S^{1/2}$, $m = 5/3$

where g = the acceleration of gravity

S = the total energy line gradient

ν = the kinematic viscosity of water

C_1 = Chezy resistance coefficient

C_2 = Manning resistance coefficient $(1.49/n)$

The Reynolds criterion for stability of flow on changing from laminar to turbulent may be used to determine the appropriate formula. More discussion about the Reynolds criterion follows in Section 4.

5-3-2-3 The Energy Equation as a Bond of Interaction

Definition of the slope S in the parameter α is of basic importance. Consider a prismatic channel in which the flow is gradually varied, shown in Figure 5-6. The total energy at the channel section 1 is

$$H_1 = z_1 + y_1 \cos\theta + \frac{U_1^2}{2g} \tag{5-35}$$

and at the channel section 2 is

$$H_2 = z_2 + y_2 \cos\theta + \frac{U_2^2}{2g} \tag{5-36}$$

The energy gradient, denoted by S_f, between the sections 1 and 2 is

$$S_f = \frac{H_2 - H_1}{L} = \frac{\Delta z}{L} + \frac{\Delta y}{L} \cos\theta + \frac{\Delta(\frac{U^2}{2g})}{L} \tag{5-37}$$

The water surface slope, S_w, is

$$S_w = \frac{\Delta z}{L} + \frac{\Delta y}{L} \cos\theta \tag{5-38}$$

and the channel bottom slope, S_o, is defined as

$$S_o = \frac{\Delta z}{L} = \sin\theta \tag{5-39}$$

In uniform flow, $S_f = S_w = S_o = \sin\theta$ (Chow, 1959).

Now, if the slope S_o is used in the dynamic equation, Equation (5-34) in conjunction with the set of continuity equations, Equation (5-30), to simulate surface runoff, the following situation will result. With reference to Figure 5-7(a) the actual steady state flow at cross-section j is

$$q_j = L\ i = \alpha y_j^m \tag{5-40}$$

where L is the distance in the x-axis direction from the origin to the

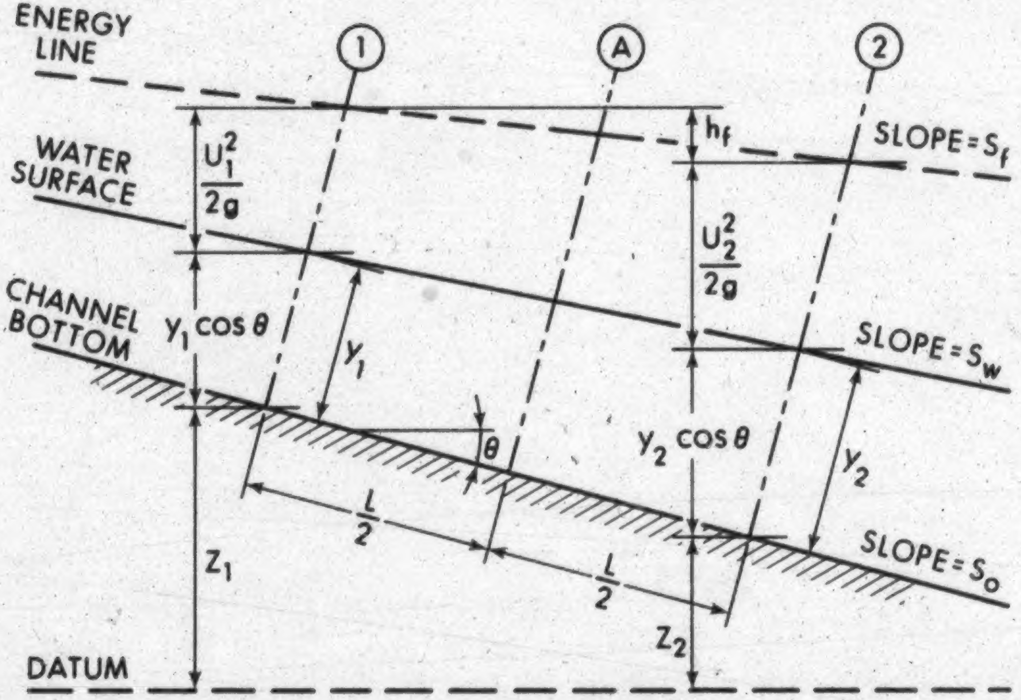
ENERGY LINE
WATER SURFACE
CHANNEL BOTTOM
DATUM
①
Ⓐ
②
$\frac{U_1^2}{2g}$
h_f
SLOPE = S_f
$\frac{U_2^2}{2g}$
SLOPE = S_w
$y_1 \cos\theta$
y_1
θ
$y_2 \cos\theta$
y_2
SLOPE = S_o
$\frac{L}{2}$
$\frac{L}{2}$
Z_1
Z_2

Figure 5-6. Energy in gradually varied overland flow.

(a) ACTUAL

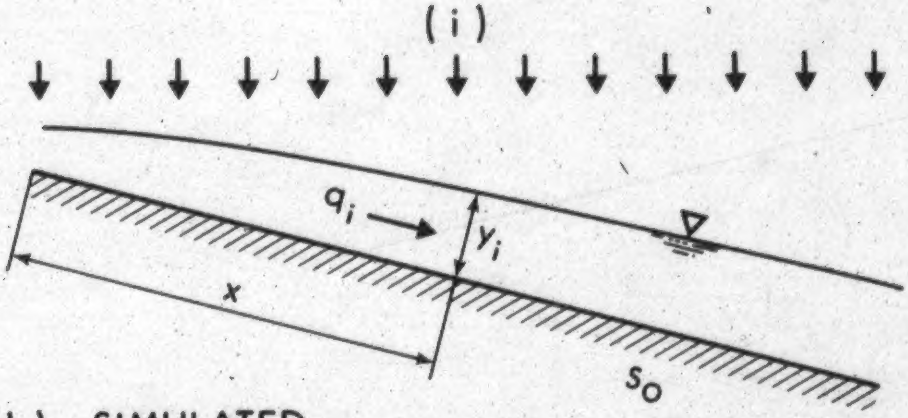

(b) SIMULATED

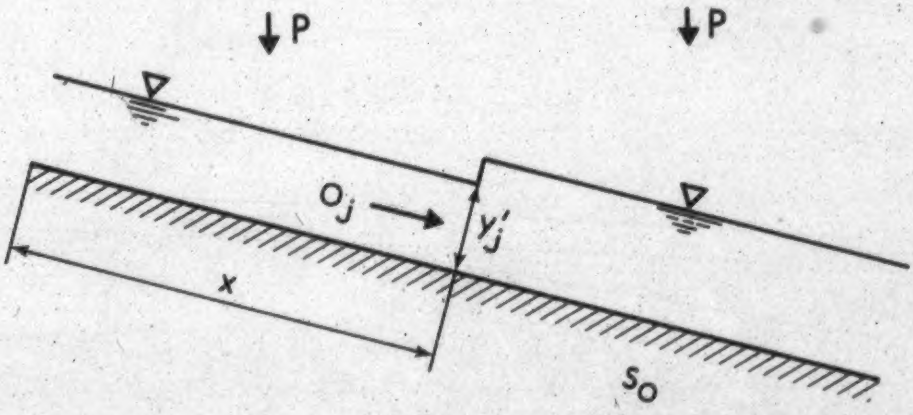

Figure 5-7. Definition sketch for comparison of: (a) actual flow, and (b) flow simulated by noninteracting reaches.

j-th cross-section. The same discharge will appear in the simulated flow shown in Figure 5- 7 (b), assuming that the dynamic equation is correct. Thus, the depth of the actual and simulated flow at the j-th cross-section will be the same, i.e., $q_j = O_j$, and $y_j = y_j'$. The geometrical interpretation of this result is that the simulated steady state profile will approximate the actual profile by a step-like curve. The depth at the lower boundary of every reach will correspond to the actual depth but because greater storage is required in the model to reach the steady state, the time to equilibrium will be longer for the simulated flow than for the actual runoff.

While the use of the channel bottom slope, S_o, in the model simplifies greatly the computation, it has one serious disadvantage. The model is not capable of simulating backwater curves because there is no interaction between the reaches. This can be corrected by using the energy gradient, S_f, in the dynamic equation. Definition of this slope for the lumped parameter model is apparent from Figure 5-6 Considering the cross-section A, the slope of the energy gradient is

$$S_f = \frac{z1-z2}{L} + \frac{\cos\theta(y1-y2)}{L} + \frac{U_1^2-U_2^2}{2gL} \tag{5-41}$$

Equation (5-41) may be considered as a bond of interaction between the two reaches. Similar equations apply to all interfaces between the reaches of the model. It is conceivable that in some cases of gradually varied flow the last term in Equation (5-41), representing the difference in velocity heads, may be negligible and the slope of water surface

$$S_w = \frac{z1-z2}{L} + \frac{\cos\theta(y1-y2)}{L} \tag{5-42}$$

can be used in the dynamic equation.

5-3-3 The State Variable Model

The lumped parameter model of surface runoff based on the continuity, dynamic, and energy equations given by Equations (5-30), (5-34), and (5-37), may be described mathematically in a compact matrix form using the state space representation of systems. The state and output equations of the lumped parameter surface runoff model are defined as follows. The state equation is

$$\underline{\dot{y}} = \underline{A}\ \underline{y} + \underline{B}\ \underline{P} \qquad (5\text{-}43)$$

where

$$\underline{y} = \begin{bmatrix} y_1 \\ y_2 \\ \cdot \\ \cdot \\ \cdot \\ y_{n-1} \\ y_n \end{bmatrix}, \quad \underline{A} = \begin{bmatrix} -\alpha\frac{y_1^2}{X_1} & 0 & 0 & \cdots & 0 & 0 \\ \alpha\frac{y_1^2}{X_1} & -\alpha\frac{y_2^2}{X_2} & 0 & \cdots & 0 & 0 \\ \vdots & \vdots & \vdots & & \vdots & \vdots \\ 0 & 0 & 0 & \cdots & -\alpha\frac{y_{n-1}^2}{X_{n-1}} & 0 \\ 0 & 0 & 0 & \cdots & \alpha\frac{y_{n-1}^2}{X_{n-1}} & -\alpha\frac{y_n^2}{X_n} \end{bmatrix}$$

$$\underline{B} = \begin{bmatrix} \frac{1}{X_1} & 0 & 0 & \cdots & 0 & 0 \\ 0 & \frac{1}{X_2} & 0 & \cdots & 0 & 0 \\ \vdots & \vdots & \vdots & & \vdots & \vdots \\ 0 & 0 & 0 & \cdots & \frac{1}{X_{n-1}} & 0 \\ 0 & 0 & 0 & \cdots & 0 & \frac{1}{X_n} \end{bmatrix}$$

and $\underline{P}$ is the precipitation input vector.

The output equation is

$$\underline{O} = \underline{C}\,\underline{y} \tag{5-44}$$

where

$$\underline{O} = \begin{bmatrix} O_1 \\ O_2 \\ \cdot \\ \cdot \\ \cdot \\ O_{n-1} \\ O_n \end{bmatrix}, \quad \underline{C} = \begin{bmatrix} \alpha y_1^2 & 0 & 0 & \cdot & \cdot & \cdot & 0 & 0 \\ 0 & \alpha y_2^2 & 0 & \cdot & \cdot & \cdot & 0 & 0 \\ \cdot & \cdot & \cdot & \cdot & \cdot & \cdot & \cdot & \cdot \\ \cdot & \cdot & \cdot & \cdot & \cdot & \cdot & \cdot & \cdot \\ \cdot & \cdot & \cdot & \cdot & \cdot & \cdot & \cdot & \cdot \\ 0 & 0 & 0 & \cdot & \cdot & \cdot & \alpha y_{n-1}^2 & 0 \\ 0 & 0 & 0 & \cdot & \cdot & \cdot & 0 & \alpha y_n^2 \end{bmatrix}$$

Operation of the lumped parameter runoff model, given by Equation (5-43) and (5-44) may be visualized in the following steps:

(1) The runoff plane is subdivided into a number of n sub-areas which constitute the elements of the lumped model. The flow within each element is assumed to be uniform at all times.

(2) The outflow from each of the n elements of the model is determined for small increments of time, ΔT, by solving simultaneously the set of continuity equations, Equation (5-43), followed by simultaneous solution of the set of output equations, Equation (5-44).

(3) The input into each element j ($j = 1, 2, \ldots, n$) at the beginning of a particular time interval ΔT is assumed to be an impulse of a magnitude equal to the sum of the rainfall input, P_j, the surface inflow, O_{j-1}, and the surface outflow, O_j. The impulse input causes an instantaneous change in the depth of flow. However, the water surface remains parallel to the bottom. Thus, the flow within each element may be characterized as uniform unsteady flow.

(4) The response of each element to the impulse input determines the outputs and the state of each element at the end of the time interval ΔT; the new states are the initial conditions for the following time increment.

(5) Each of the elements operates essentially as the nonlinear reservoir analyzed in Chapter V, Section 2-5-1, by the phase plane method. Since the lumped parameter runoff model consists of n elements the solution is performed in n-dimensional state space rather than in a two-dimensional phase plane.

5-4 Modification of the Dynamic Equation for Raindrop Impact Effect

In overland flow with rainfall, drops after striking the surface water layer generate a local disturbance, which results in high resistance to flow, Although the raindrop impact effect has been observed, its mechanics as yet has not been fully explained. The problem of rainfall impact effect, as related to surface flow, was investigated in the present study for the purpose of testing the state variable runoff model.

5-4-1 General

The retarding influence of rainfall impact effect on surface flow has been observed by many investigators. Early experimental studies by Izzard (1943; 1944, 1947) confirmed the existence of the effect of drop impact, which demonstrated itself by a momentary increase in the discharge after cessation of rainfall. This phenomenon was attributed to the fact that during rainfall the amount of detention is greater, due to the raindrop impact effect, than the amount required to cause the same rate of runoff after cessation of rainfall. Wenzel and Yoon (1971) measured surface flow depth with rainfall and recognized that it is substantially deeper than that without rainfall at the same flow rate.

The rainfall impact effect also influences the transition of flow from laminar to turbulent region. Reynolds number, which is used as a criterion for distinguishing the laminar and turbulent flow, is defined for overland flow as

$$Re = \frac{Uy}{\nu} \tag{5-45}$$

where U is the average flow velocity. Yu and McNown (1964) found from their analysis of the Los Angeles airfield drainage data that the transitional range of the Reynolds number is 200 and 1000 for flow on a concrete surface with and without rainfall respectively.

5-4-2 The Relationship Between Rainfall Intensity and Friction Factor

The friction factor is a measure of the resistance to the flow, and for flow in pipes or open channels it gives the relationship between the energy gradient slope (S_f), mean velocity (U), and the depth (y) or hydraulic radius (R) of the flow. It can be expressed in a number of different forms including the Darcy-Weisbach equation

$$f = \frac{8gyS_f}{U^2} \tag{5-46}$$

For flows in pipes and in rigid boundary open channels the friction factor depends primarily on the relative roughness (ε/y) in the hydraulically rough regime, on the Reynolds number of the flow (Uy/ν) in the hydraulically smooth regime, and on both these parameters when the flow is transitional between the two regimes. However, it appears that in case of sheet flow under rainfall the friction factor also depends to some extent on the rainfall characteristics such as the rainfall intensity, size and spacing of raindrops, and their impact velocity.

Woo and Brater (1962) carried out sheet flow experiments with controlled rainfall in which they studied the relationship of the friction factor of flow under rainfall, f_r, Reynolds number, Re, and the runoff surface slope, S_o. They made the following conclusions:

(1) The raindrop impact effect is greater for small depths and small values of Re.

(2) For rough surfaces the relationship between f_r and Re differs from the steady flow relationship more than for smooth surfaces (because turbulence is more easily generated on rough surfaces).

(3) The f_r values for a particular Re decrease with increasing slope for small slopes ($S_o \leq 0.006$), but do not follow this rule for slopes steeper than 0.008.

(4) For small slopes, values of f_r are larger than the corresponding values of f for uniform flow without rainfall.

Yoon and Wenzel (1971) confirmed the findings of Woo and Brater in their report on mechanics of sheet flow under simulated rainfall. They found that for $R_e < 2000$ the rainfall intensity increased the resistance of flow at a constant Reynolds number. Above $R_e = 2000$, the intensity effect decreased rapidly until it became insignificant. For $R_e \leq 1000$ the results could be described for practical purposes by straight lines, parallel to the theoretical $f = 24/Re$ which is valid for laminar flow. The parallel lines were thus given by a general relationship $f = C/Re$, in which the authors expressed C as a function of channel slope and rainfall intensity.

The same authors also studied effects of changes in the impact velocity, from 8.8 ft/sec to 22.3 ft/sec, and raindrop spacing of one and two inches, on the friction factor. These changes were found to be insignificant. Similarly, the Froude number did not yield any significant correlation with the friction factor.

5-4-2-1 Dimensional Analysis

The objective of dimensional analysis is to express the behaviour of a phenomenon in the form of functional equations relating non-dimensional parameters. These equations can then be evaluated empirically to determine the relative importance of individual parameters and to formulate the relationship between these parameters.

The method of dimensional analysis may be used in the development of the relation defining the friction factor, f_r, of flow under rainfall. Considering the case of runoff due to rainfall from an impervious surface, the physical variables which most likely effect the flow phenomenon may be expressed in a functional form as

$$f_r = F_n(U,y,S_o,\mu,\rho,g,\varepsilon,i,d,u_r,\eta,\lambda) \quad (5\text{-}47)$$

where f_r = the friction factor of flow under rainfall

U = the local mean flow velocity

y = the local depth measured normal to the channel bottom

S_o = the channel slope or $\sin\theta$

θ = the angle between the x direction and the horizontal

μ = the dynamic viscosity of water

ρ = the density of water

g = the acceleration of gravity

ε = the equivalent surface roughness

i = the rainfall intensity

d = the mean drop size

u_r = the raindrop impact velocity

$$\left.\begin{matrix}\eta\\ \lambda\end{matrix}\right\} = \left\{\begin{matrix}\text{the dimensionless parameters describing the drop impact}\\ \text{pattern and shape}\end{matrix}\right\}$$

The last four terms in Equation (5-47) were neglected in further analysis because they were kept constant during experiments, and furthermore were shown by Yoon and Wenzel (1971) to have little significance. Thus, the functional relationship of Equation (5-47) simplifies into

$$f_r = \text{Fn}\ (U, y, S_o, \mu, \rho, g, \varepsilon, i) \qquad (5\text{-}48)$$

Application of Buckingham theorem of dimensional analysis (Blench, 1969) leads to

$$f_r = \text{Fn}\ \left(\frac{\rho U y}{\mu}, \frac{U}{\sqrt{gy}}, S_o, \frac{\varepsilon}{y}, \frac{i\nu}{U^2 y}\right) \qquad (5\text{-}49)$$

The effects of the Froude number and the slope S_o were considered to have only secondary effects, thus giving

$$f_r = \text{Fn}\ \left(\frac{Uy}{\nu}, \frac{\varepsilon}{y}, \frac{i\nu}{U^2 y}\right) \qquad (5\text{-}50)$$

Equation (5-50) is a general functional relationship describing the flow from an impervious surface caused by rainfall. Since all flows in the experimental part of the present study occurred within the laminar region, further attention was given specifically to the relationship

$$f_r = \text{Fn}\ \left(\frac{Uy}{\nu}, \frac{i\nu}{U^2 y}\right) \qquad (5\text{-}51)$$

which applies to laminar flow under rainfall

For laminar flow without rainfall the functional relationship is known to be (Blench, 1969)

$$f = Fn(\frac{Uy}{\nu}) \tag{5-52}$$

which can be expressed by a general equation

$$f = \frac{C}{Re} \tag{5-53}$$

A theoretical value of C can be found from the Darcy-Weisbach equation, written for an infinitely wide channel

$$f = \frac{8gS_oy}{U^2} \tag{5-54}$$

which is valid for both uniform and nearly uniform flows (Chow, 1959). Comparison of Equation (5-53) and Equation (5-54) gives

$$C = \frac{8gS_oy^2}{U\nu} \tag{5-55}$$

The theoretical mean velocity of laminar sheet flow (Chow, 1959) is

$$U = \frac{gS_oy^2}{3\nu} \tag{5-56}$$

which after substitution into Equation (5-55) gives

$$C = 24 \tag{5-57}$$

Solving Equation (5-55) for the mean velocity and substituting into the relation for specific discharge, $O = Uy$, yields

$$O = \frac{8gS_oy^3}{C\nu} \tag{5-58}$$

It was hypothesized that the raindrop impact effect on laminar flow can be included in the friction factor f_r, expressed as

$$f_r = \frac{Cr}{Re} \tag{5-59}$$

where

$$Cr = \frac{8gS_oy^2}{U\nu} + Fn(\frac{i\nu}{U^2y}) \tag{5-60}$$

or

$$C_r = C + C_i \tag{5-61}$$

Thus, Equation (5-58) is modified for the case of runoff under rainfall into

$$O = \frac{8gS_o y^3}{C_r \nu} \tag{5-62}$$

The rainfall intensity term

$$C_i = Fn\left(\frac{i\nu}{U^2 y}\right) \tag{5-63}$$

becomes zero when rain ceases, and C_r is then equal to C. The impact effect diminishes with increasing depth and velocity of flow, whereas increasing rain intensity and higher viscosity of the fluid tend to enhance the impact effect. These relations are in accordance with intuitive expectations.

5-4-2-2 Empirical Evaluation

The functional relationship given by Equation (5-63) has to be evaluated empirically. Because of very small depth of flow involved in the experiments, the depth and velocity could not be measured directly. An approximate method was therefore used, which was based on measured amounts of water detained on the runoff plane during steady flows, for various rainfall intensities.

With reference to Figure 5-8 a steady state discharge Q from a runoff plane of length X and width B is

$$Q = B\ i\ X \tag{5-64}$$

and also

$$Q = B\alpha \frac{y^3}{C_r}\ , \quad \text{where } \alpha = \frac{8gS_o}{C_r \nu} \tag{5-65}$$

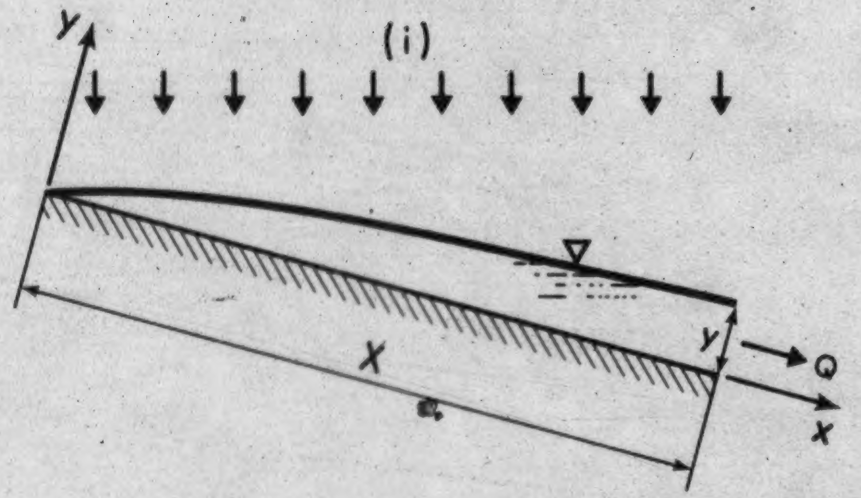

Figure 5-8. Definition sketch for steady discharge condition ($Q = BiX = B\alpha y^3/C_r$) from a plane of length X and width B.

Solving both Equation (5-64) and Equation (5-65) for y gives

$$y = (\frac{iXC_r}{\alpha})^{1/3} \tag{5-66}$$

which is an equation of the water surface profile at steady state flow conditions.

The volume of water temporarily detained on the runoff plane is given by

$$S = B \int_0^X y dx \tag{5-67}$$

Substituting for y from Equation (5-66) yields

$$S = B \int_0^X (\frac{iC_r}{\alpha})^{1/3} x^{1/3} dx \tag{5-68}$$

Equation (5-68) is an integral equation expressing the amount of detained water, S, during the steady runoff as a function of distance x, rainfall intensity i, and the coefficient C_r. The coefficient C_r depends on the rainfall intensity i and the depth of flow y, and thus it is an implicit function of distance x. Exact integration of Equation (5-68) is therefore not possible.

To evaluate the coefficient C_r approximately, an "average" depth of flow, $\overline{y}$, in the reach of length X was substituted into Equation (5-67). Solution of Equation (5-65) yields an equivalent coefficient $\overline{C}_r$

$$\overline{C}_r = B\alpha\frac{\overline{y}^3}{Q} \tag{5-69}$$

The equivalent coefficient $\overline{C}_r$ is representative of an equivalent uniform steady flow of depth $\overline{y}$ and discharge Q within the reach of length X. The method thus involves approximation of actual non-uniform flow by an "equivalent" uniform flow, with the same output discharge, and one might classify the method as lumping of parameters.

Experimental evaluation of the parameters $\overline{C}_r$, S, Q, and $\overline{y}$ for different rainfall intensities and for three slopes of the runoff plane was carried out by dividing the runoff plane into four reaches of equal length X = 19.6 cm, as shown in Figure 5-9. In the first measurement of discharge Q_1 (Figure 5-9(a)) the rain was allowed to fall on the first reach only. The amount of detained water, S_1, at steady flow was determined graphically from the vertical distance between the recorded curves of cumulative input and output, after the steady flow was reached, as illustrated in Figure 5-10.

In the second measurement the rain was allowed to fall on the first and second reach, and the total amount of stored water, S_T, was determined by the same graphical method. The term S_2, representing the amount of stored water on the second reach, was found by subtracting S_1 from S_T. By successive adding one more reach in each measurement, the amount of stored water in each reach was determined from the general formula

$$S_n = S_T - S_{n-1} \tag{5-70}$$

Measurements were repeated for several rainfall intensities, and for the three slopes: 12° ($S_o = 0.20791$), 6° ($S_o = 0.1051$), 2°56' ($S_o = 0.05143$). The intensity factor, C_i, was evaluated from the rearranged Equation (5-61)

$$C_i = C_r - 24 \tag{5-71}$$

The C_i factor was plotted in Figure 5-11 against the dimensionless

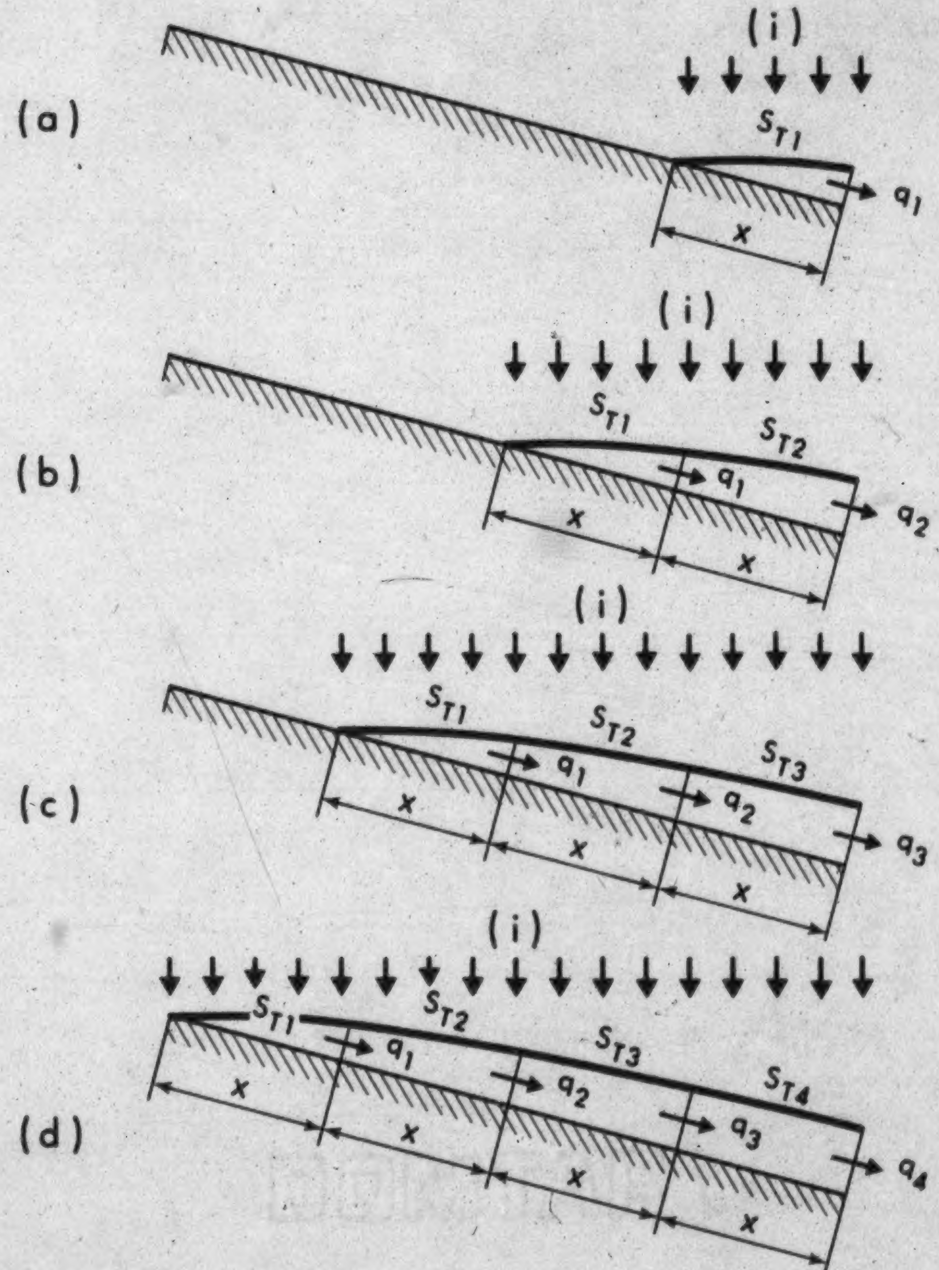
(a)
(i)
S_{T1}
q_1
x
(b)
(i)
S_{T1}
S_{T2}
q_1
q_2
x
x
(c)
(i)
S_{T1}
S_{T2}
S_{T3}
q_1
q_2
q_3
x
x
x
(d)
(i)
S_{T1}
S_{T2}
S_{T3}
S_{T4}
q_1
q_2
q_3
q_4
x
x
x
x

Figure 5-9. Definition sketch for determination of storage terms S_n, $(n = 1, 2, 3, 4)$.

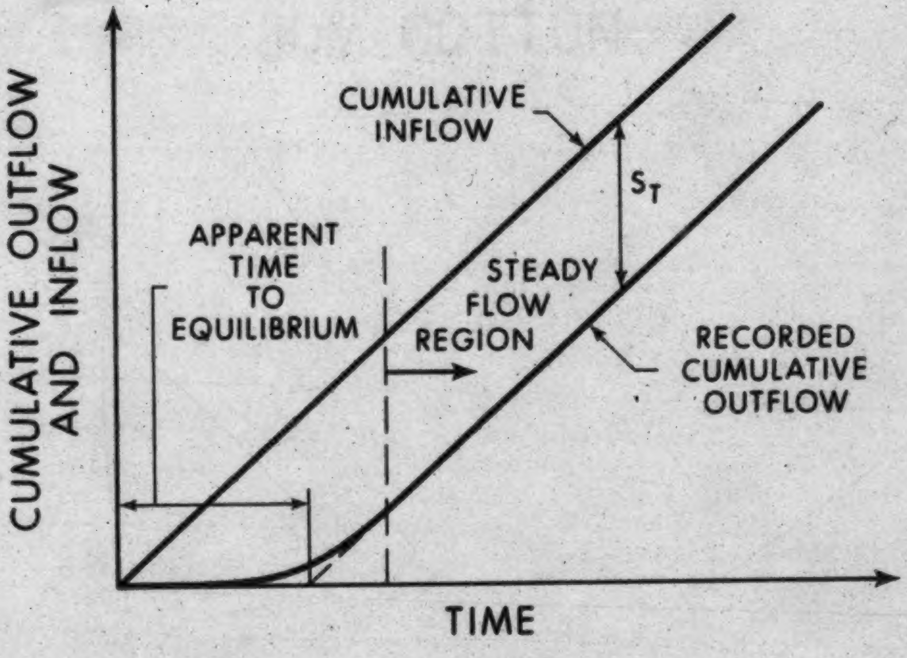

Figure 5-10. Determination of the amount of stored water, S_T, on the runoff plane by means of mass curves of inflow and outflow.

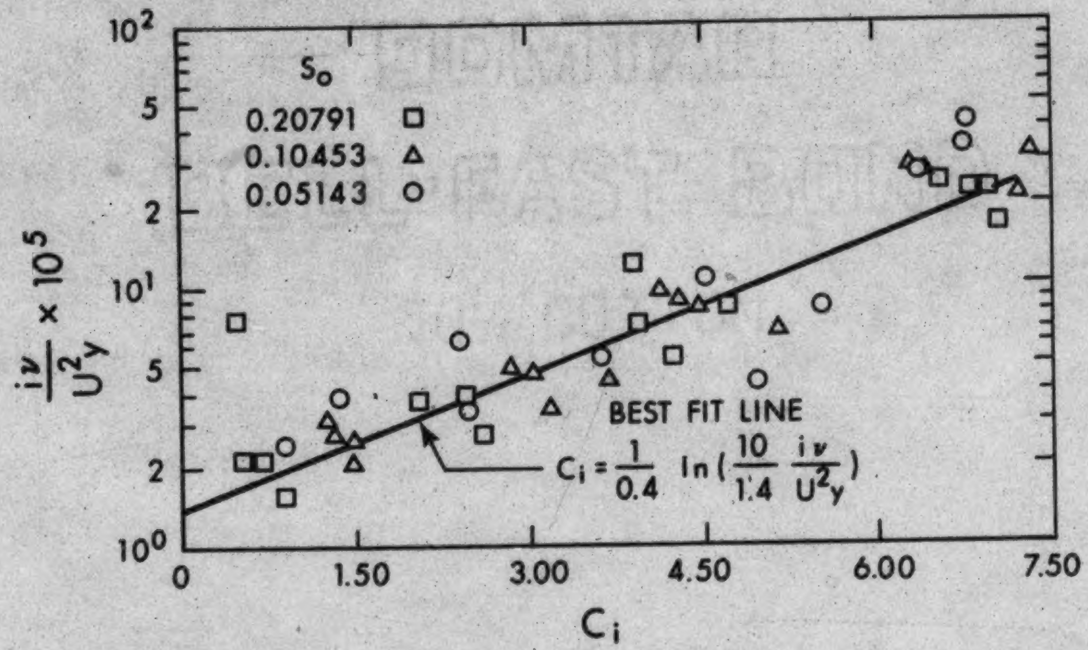

Figure 5-11. Best fit line of the relationship between the intensity factor C_i and the dimensionless parameter $i\nu/U^2y$.

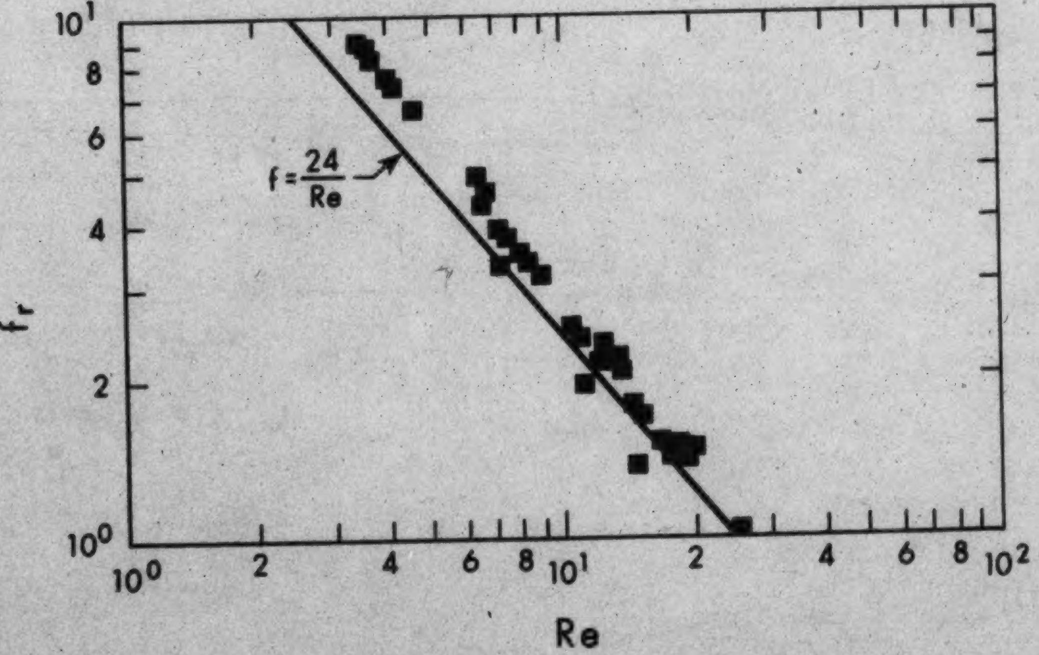

Figure 5-12. Friction factor, f_r, for laminar sheet flow under rainfall versus Reynold's number Re.

parameter $\frac{i}{ReU}$, Equation (5-63), on a semilogarithmic paper with C_i values on the arithmetic scale. A best fit straight line, fitted to the data by the least square method, is given by the equation

$$C_i = \frac{1}{0.4}\ln\left(\frac{10^5}{1.4}\,\frac{i\nu}{U^2y}\right) \qquad (5\text{-}72)$$

with the correlation coefficient r = 0.922. Substituting the above expression into the equation for friction coefficient under rainfall, Equation (5-59), yields

$$f_r = \frac{1}{Re}\left[\frac{8gS_oy^2}{U\nu} + \frac{1}{0.4}\ln\left(\frac{10^5}{1.4}\,\frac{i}{ReU}\right)\right] \qquad (5\text{-}73)$$

or for a laminar sheet flow

$$f_r = \frac{1}{Re}\left[24 + \frac{1}{0.4}\ln\left(\frac{10^5}{1.4}\,\frac{i}{ReU}\right)\right] \qquad (5\text{-}74)$$

A summary of all experimentally determined, and calculated parameters is given in Appendix C. Values of f_r and Re, plotted in the form of a friction diagram, are shown in Figure 5-12. The plotted points, following approximately a parallel line to the theoretical $f = \frac{24}{Re}$, indicate higher values of the friction coefficient then for laminar flow without rainfall. The analyses presented in this thesis is based on the premise that laminar flow prevailed on the model independent of rainfall impact effects and therefore the equation: $Q \alpha y^3$ was valid. All values of Re based on depths of flow calculated from Equation (5-67)(or $\overline{y} = S/BX$) and the average velocities of flow calculated from $\overline{U} = Q/B\overline{y}$ were < 30. This value of Re is well within the laminar flow limits suggested by other investigators (Yoon, 1971; Schreiber, 1972). Further, the results presented in Figure 5-12 give additional credence to this assumption because of the close agreement between the experimental results and the theoretical curve: f = 24/Re.

5-4-3 Comparison of Results with Existing Knowledge

Examining Equation (5-74), one might expect that for the same Reynold's number the friction coefficient should vary with the rainfall intensity. This was found to be the case by Yoon and Wenzel(1971) for $Re < 2000$. The authors presented a friction diagram, where experimentally found values for f_r followed parallel lines to $f = \frac{24}{Re}$, each parallel for a given rainfall intensity. In the present study such distinction due to different intensities could not be made, most likely because of the approximate method used to determine f_r and Re, and because the small depth of flow, ranging from about 0.2 mm to 0.5 mm. It is probable that for such small depths the effect of varying intensity of rainfall is not apparent.

The experiments conducted by Yoon and Wenzel also showed, that for $Re>2000$, the rainfall intensity effect decreases rapidly with increasing Re until it becomes insignificant. The authors suggested that the retardation effect of the rainfall intensity on flow can be explained on the basis of momentum considerations. If raindrops strike almost normal to the water surface, the component of momentum carried by raindrops in the mean flow direction is almost negligible. Therefore, a portion of mean flow momentum has to be transferred to accelerate the raindrop mass from almost zero velocity in the x-direction to the point velocities at various depths. The velocity of mean flow is thus somewhat retarded below the velocity that it would have if no rainfall were present. Because the raindrops strike the water surface first and then diffuse vertically as well as laterally, transfer of mean flow momentum is greatest near the surface at high Reynold's numbers than for the low ones and the fact that the rate of raindrop impact is constant for a given intensity and drop size, the relative magnitude of transfer of mean flow momentum decreases with increasing Reynold's number.

The findings in the present study are in general agreement with results of recent investigation conducted by Schreiber and Bender (1972), who obtained overland hydrographs from a laboratory plane catchment 8 ft by 16 ft, with a lightweight-concrete surface. The rainfall was generated by rows of nozzles. The hydrographs were simulated by a mathematical model based upon the simultaneous solution of the continuity equation, Equation (5-26), and the dynamic equation, Equation (5-34), by a finite-difference method. The resistance coefficient K (corresponding to the coefficient Cr in the present study) in Equation (5-59) was determined for each hydrograph by parameter optimization, i.e., the unknown parameter K was varied systematically to obtain the best fit between the computed and observed hydrographs. However, this procedure assumed that K is constant over the entire flow plane at a particular instant in time.

The coefficient K was plotted against various dimensionless parameters. The most successful plottings involved K, Weber number W, and precipitation number P. The latter parameter is the volume rate of precipitation divided by the product of mean velocity of flow and the square of the depth of flow. Values of K appeared to be dominated by P during rainfall and by W after rainfall.

The magnitude of K ranged from 29 to 40 for the rainfall intensity around 3 in/hr, and from 20 to 25 for the intensity around 1 in/hr. Optimal values of K for the recession periods ranged from 13 to 18. The resistance coefficient, C_r, proposed in the present study ranged from 24 to 32 for the rainfall intensity range from 0 to around 4.5 in/hr. The value of C_r for the recession periods was 24. The coefficient C_r is based on physical reasoning whereas the parameter K was determined more or less by a trial method. The most significant objection to the method discussed above is the assumption of constant K over the entire flow plane at an instant in time. In fact, as the authors pointed out themselves, the friction factor f, and therefore also K, varies with Reynolds number, and thus K cannot be constant along the flow plane for non-uniform flow.

The dimensionless precipitation number, P, which the authors correlated with the coefficient K does not include the kinematic viscosity of fluid. The kinematic viscosity was considered significant in the present study. The parameter P also includes a rather awkward quantity - the volume rate of precipitation. The expression for the friction coefficient derived in the present study, Equation (5-73), is considered more meaningful physically.

5-5 Comparison of Predicted and Measured Hydrographs

The detailed description of experimental techniques was given in Chapter II. Basically, the laboratory catchment hydrographs were recorded in the form of discrete time series, which were further processed by a computer. The end product of the computer analysis were plots of runoff hydrographs delineated by a series of points plotted at the sampling intervals of the discrete data. Each runoff event for a particular set of conditions (rainfall intensity, temporal and spatial rainfall distribution, slope of the runoff surface, and initial wetness of the surface) was repeated seven times to obtain a better estimate of the measured values.

Recorded hydrographs were simulated by a seven order state variable runoff model (thus the length of each of the seven reaches was 13.06 cm (5.14 in)). The dynamic, or discharge formula of the model was given by Equation (5-34), which included the derived relationship for raindrop impact effect on laminar flow, Equation (5-74), in the form of an extended friction factor, $f_r = C_r/Re$. Figure 5-13 shows the effect the factor f_r has on the solution as compared to the solution when the raindrop impact effect is not included, i.e., for $f = 24/Re$. The theoretical value of the resistance coefficient for laminar flow with no rainfall, $C = 24$, was used for simulation of all recession curves.

The effect of a number of stages (reaches) in the mathematical model (i.e., the order of the simulating system) on the model's response is illustrated in Figure 5-14. As the number of stages increases, the S-shaped response of the model (series of interacting nonlinear stages with a distributed input) steepens and approaches a limit, given by the response curve of a completely distributed system, as was proven in Chapter V, Section 3-2-1.

The experiments were divided, according to temporal and spatial distribution of the rainfall input, into the following three categories:

(1) Experiments with uniformly distributed rainfall input.

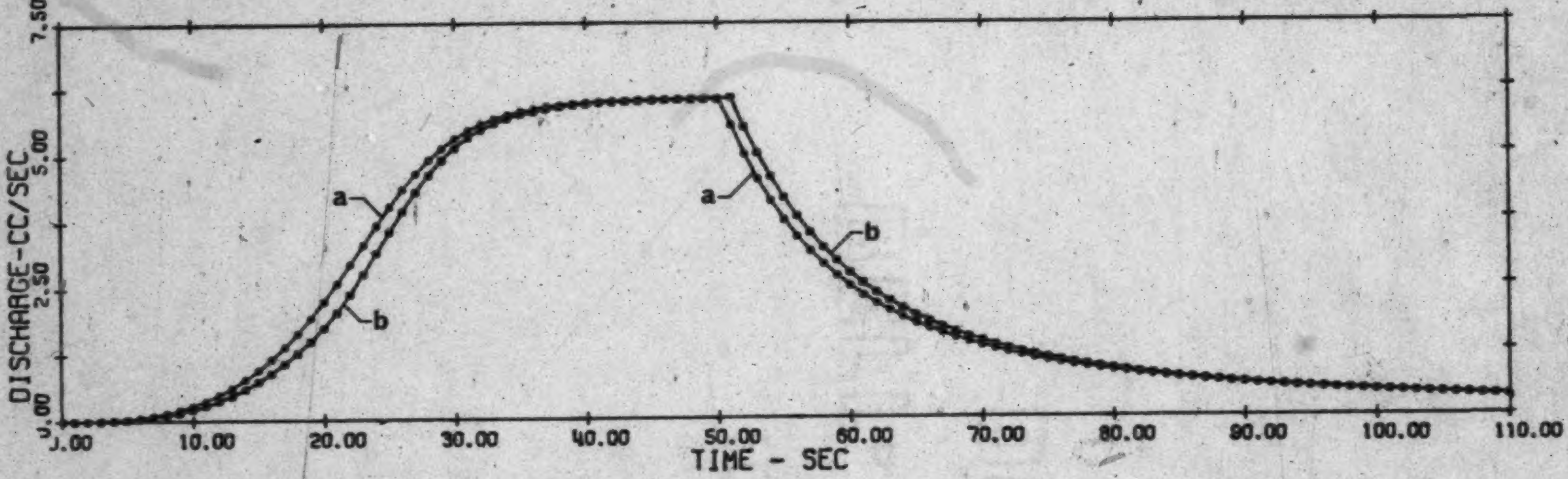

Figure 5-13. Comparison between hydrographs generated by the state variable model for the case: (a) raindrop impact effect not included, (b) raindrop impact effect included.

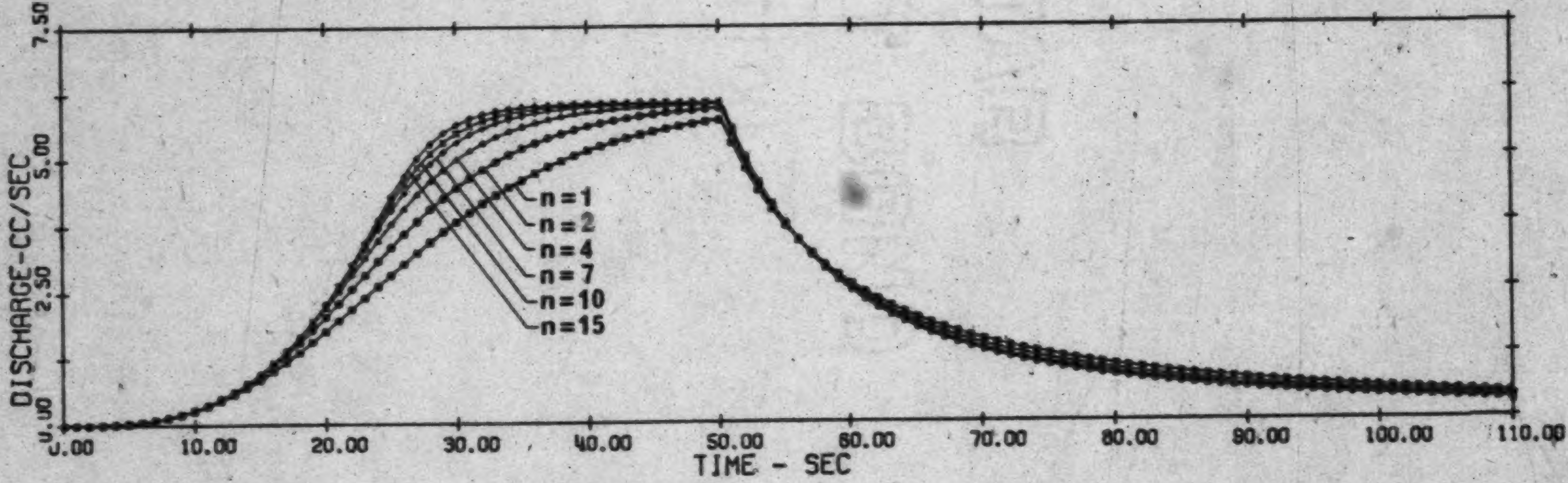

Figure 5-14. Responses of state variable models of nth-order (n = 1, 2, 4, 7, 10, and 15) to identical inputs of uniform rainfall with duration of 50 seconds.

(2) Experiments with temporally varied rainfall input.

(3) Experiments with spatially varied rainfall input.

Plotting of the experimental data and the state variable model simulation into a common plot for each event has been used as a means of displaying and appraising the results. Statistical analysis of the experimental data for accuracy are given in Chapter VI.

5-5-1 Experiments with Uniformly Distributed Rainfall Input

Hydrographs of the surface runoff, generated by temporally and spatially uniform rainfall inputs, formed the bulk of the laboratory catchment experiments. Three factors were varied in the experiments: (1) slope of the runoff plane (approximately 3, 6 and 12 degrees), (2) rainfall intensity (low, $i \doteq 40.0$ mm/hr; medium, $i \doteq 75.0$ mm/hr; high, $i \doteq 115.0$ mm/hr), and (3) duration of the rainfall input (two short durations, 8 to 31 sec, which were shorter than time to equilibrium, and one long duration of 200 sec).

Exact rainfall intensity in every event was calculated from steady flow conditions resulting from the long duration (200 sec) rainfalls.

The laboratory catchment experiments with uniformly distributed rainfall inputs were carried out in the following manner. For each of the three slopes the catchment hydrographs were measured for three rainfall intensities (low, medium and high). Further, hydrographs resulting from three rainfall durations were measured for each of the rainfall intensities. Thus, 27 different runoff events existed, and since each was repeated seven times, the total number of recorded hydrographs was 189. Summary of the runoff events is given in Table 5-2.

TABLE 5-2

SUMMARY OF LABORATORY CATCHMENT EXPERIMENTS WITH UNIFORMLY DISTRIBUTED RAINFALL INPUTS

Run No.	Rainfall Duration * (sec)	Rainfall Intensity (cm/hr)	Bed Slope $S_o = \sin\theta$
1	50.0	11.53	0.20791
2	11.5	"	"
3	8.8	"	"
4	50.0	7.77	"
5	14.5	"	"
6	11.8	"	"
7	50.0	3.84	"
8	23.0	"	"
9	19.0	"	"
10	50.0	11.47	0.10450
11	14.5	"	"
12	11.5	"	"
13	50.0	7.42	"
14	17.5	"	"
15	14.5	"	"
16	50.0	3.91	"
17	23.5	"	"
18	18.5	"	"
19	50.0	11.04	0.05117
20	14.5	"	"
21	11.5	"	"
22	50.0	7.51	"
23	17.5	"	"
24	14.5	"	"
25	50.0	3.65	"
26	30.5	"	"
27	23.5	"	"

Simulated hydrographs by the state variable model for low rainfall intensity and slopes 12° and 2°56', compared to the recorded hydrographs, are shown in Figures 5-15 to 5-20. The rest of the simulated events (Table 5-2) are shown in Appendix E.

In most cases, the simulated hydrographs agree very well with the recorded events, generally following an "average" curve indicated by the scatter diagram of the recorded hydrographs. The scatter of points sometimes becomes larger, or the simulated peak discharge is higher than the recorded one, such as can be seen in Figures E-3 and E-19, Appendix E. These facts can be partly attributed to errors of recorded data which were due to: (1) long sampling interval - about 2 seconds, (2) internal noise of the data acquisition system, and (3) manual control of the on and off commands for rainfall input.

The recorded data were smoothed during computer processing and then differentiated numerically. Numerical differentiation is sensitive to data fluctuation and can become an unstable process. Hence the scatter of points. Because of this scatter the comparison between actual and simulated hydrographs cannot be carried into fine details. The results could be improved by increasing the sampling rate. Unfortunately, this was not possible because, as pointed out in Chapter II, the data acquisition system malfunctioned during faster rate of sampling. Accuracy and error estimation problems are further discussed in Chapter VI.

The retarding effect of rainfall on sheet flow is particularly evident in the simulated hydrograph shown in Figure 5-18. Cessation of rainfall caused a sudden increase of discharge. Although this increase in discharge could not be confirmed by the experimental data (because of their scatter), such phenomena have been observed (Izzard, 1944;

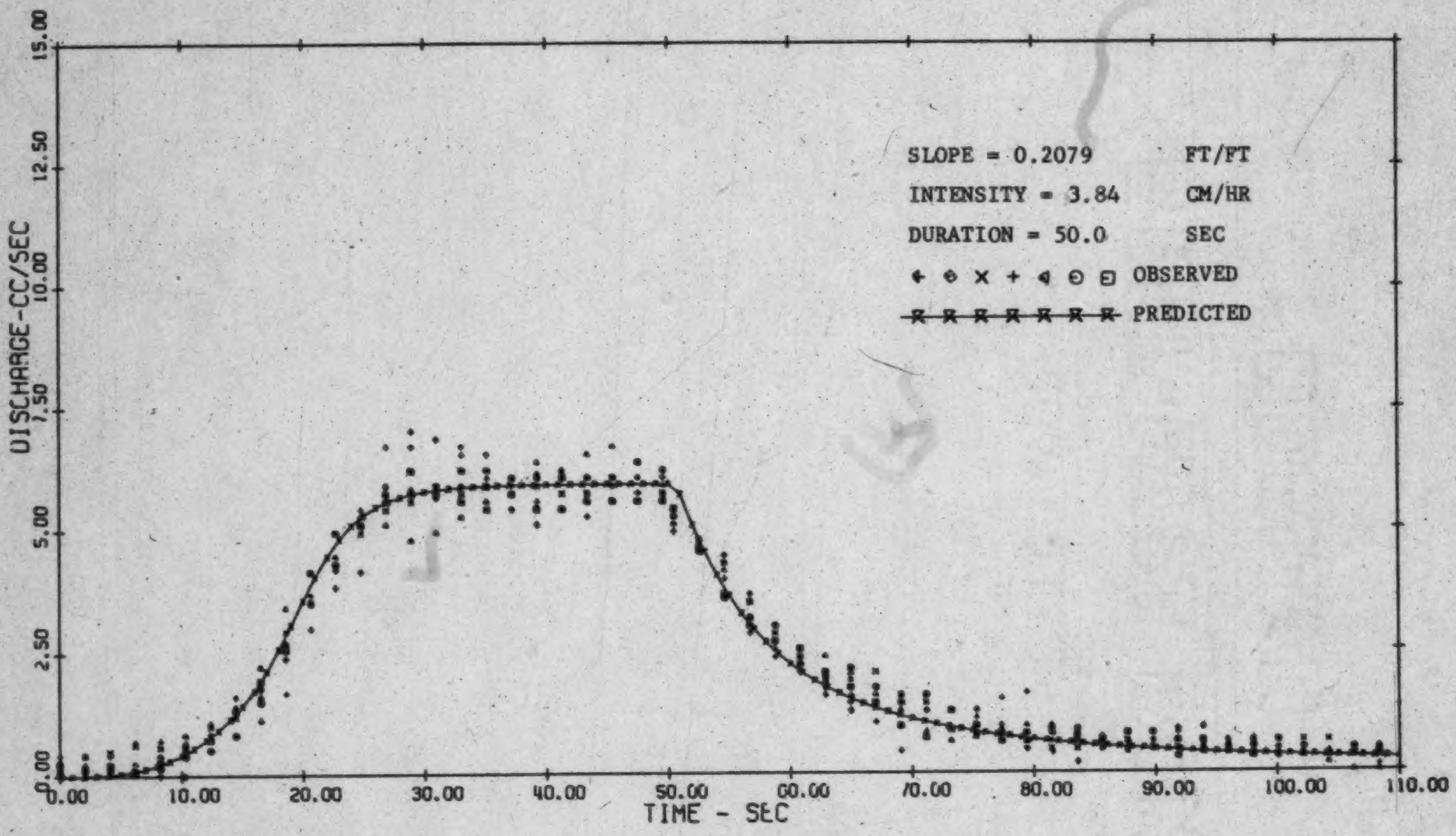

Figure 5-15. Observed and predicted hydrographs (state variable model) for test 7 with uniform rainfall input.

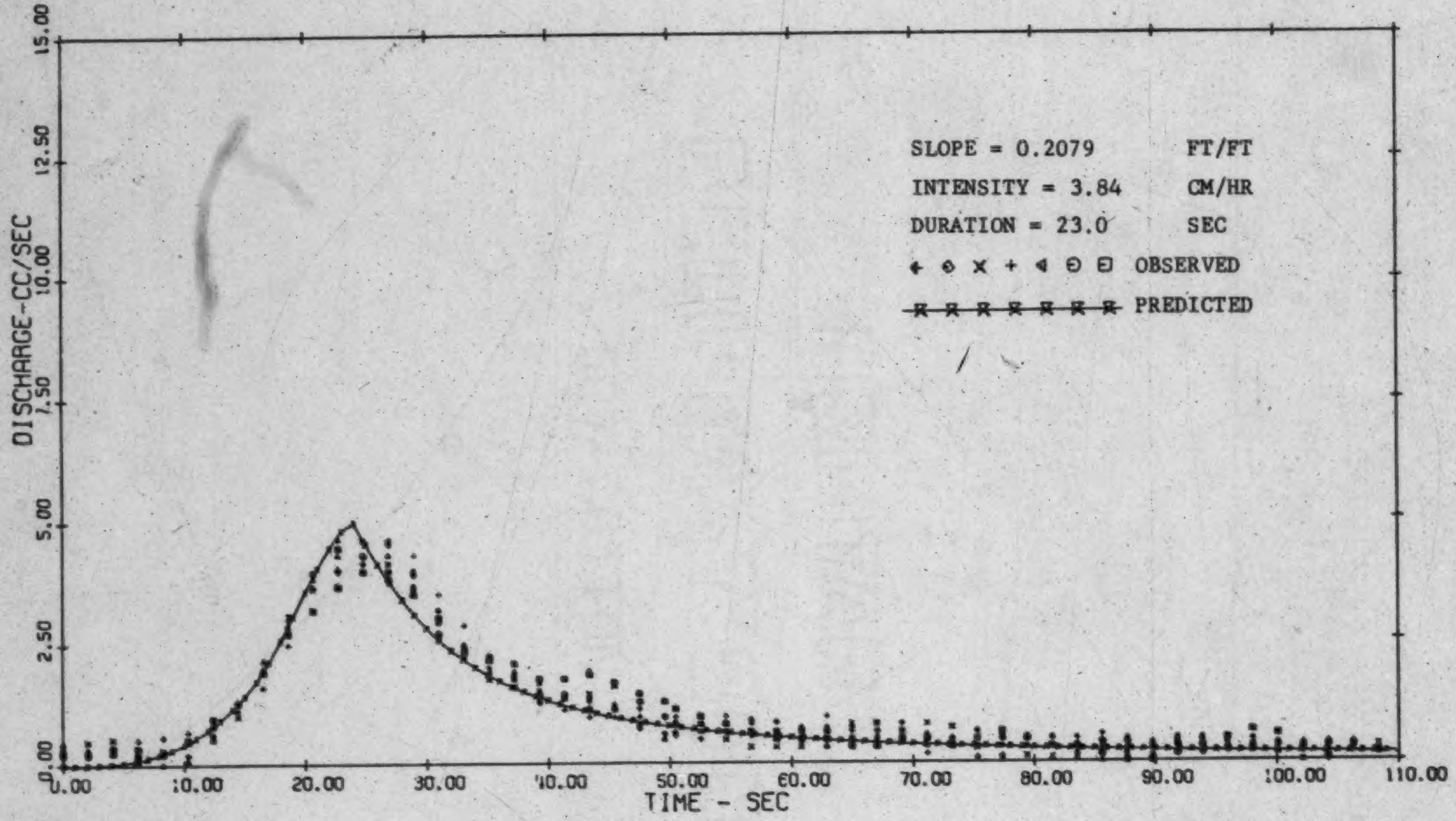

Figure 5-16. Observed and predicted hydrographs (state variable model) for test 8 with uniform rainfall input.

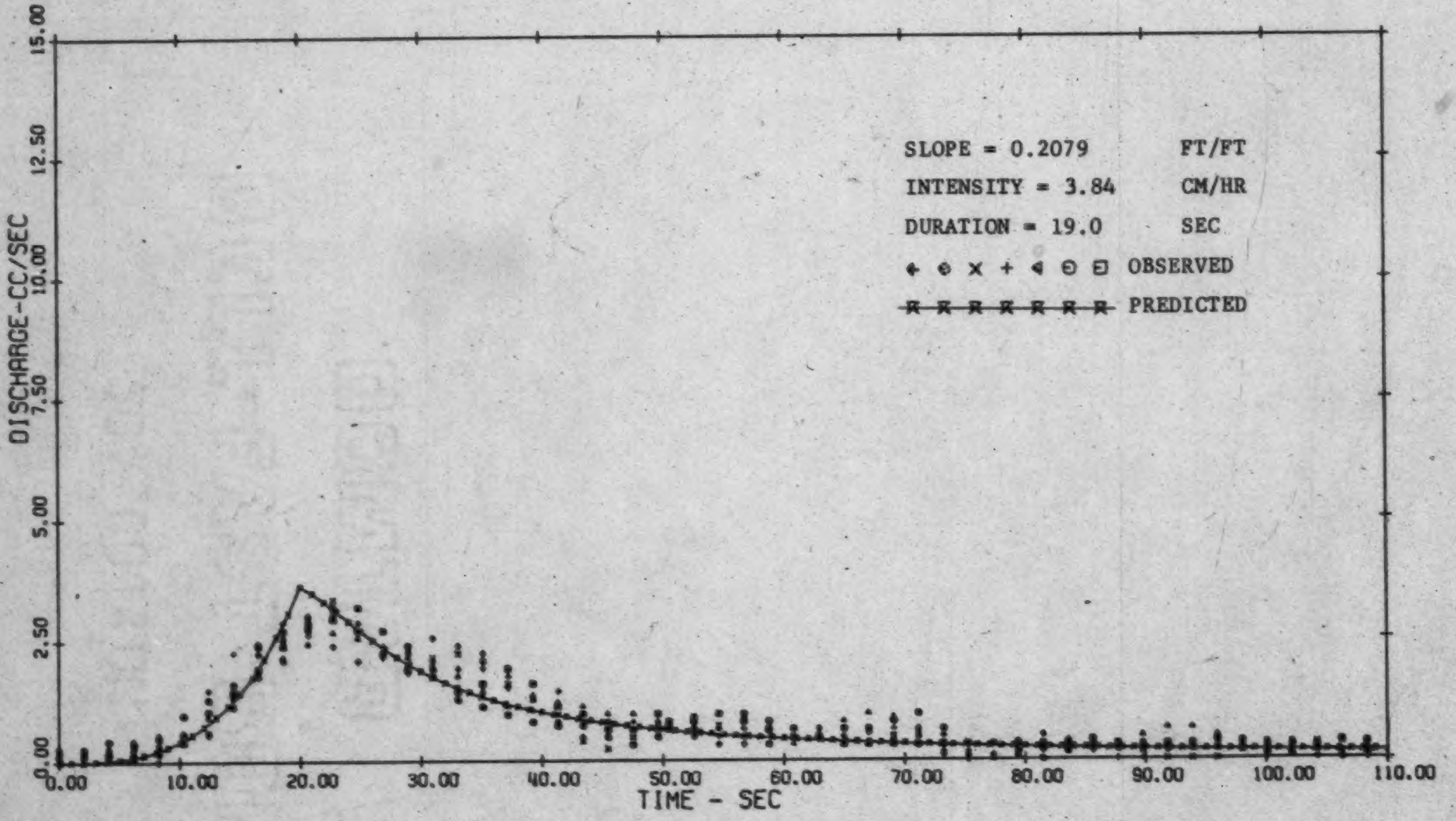

Figure 5-17. Observed and predicted hydrographs (state variable model) for test 9 with uniform rainfall input.

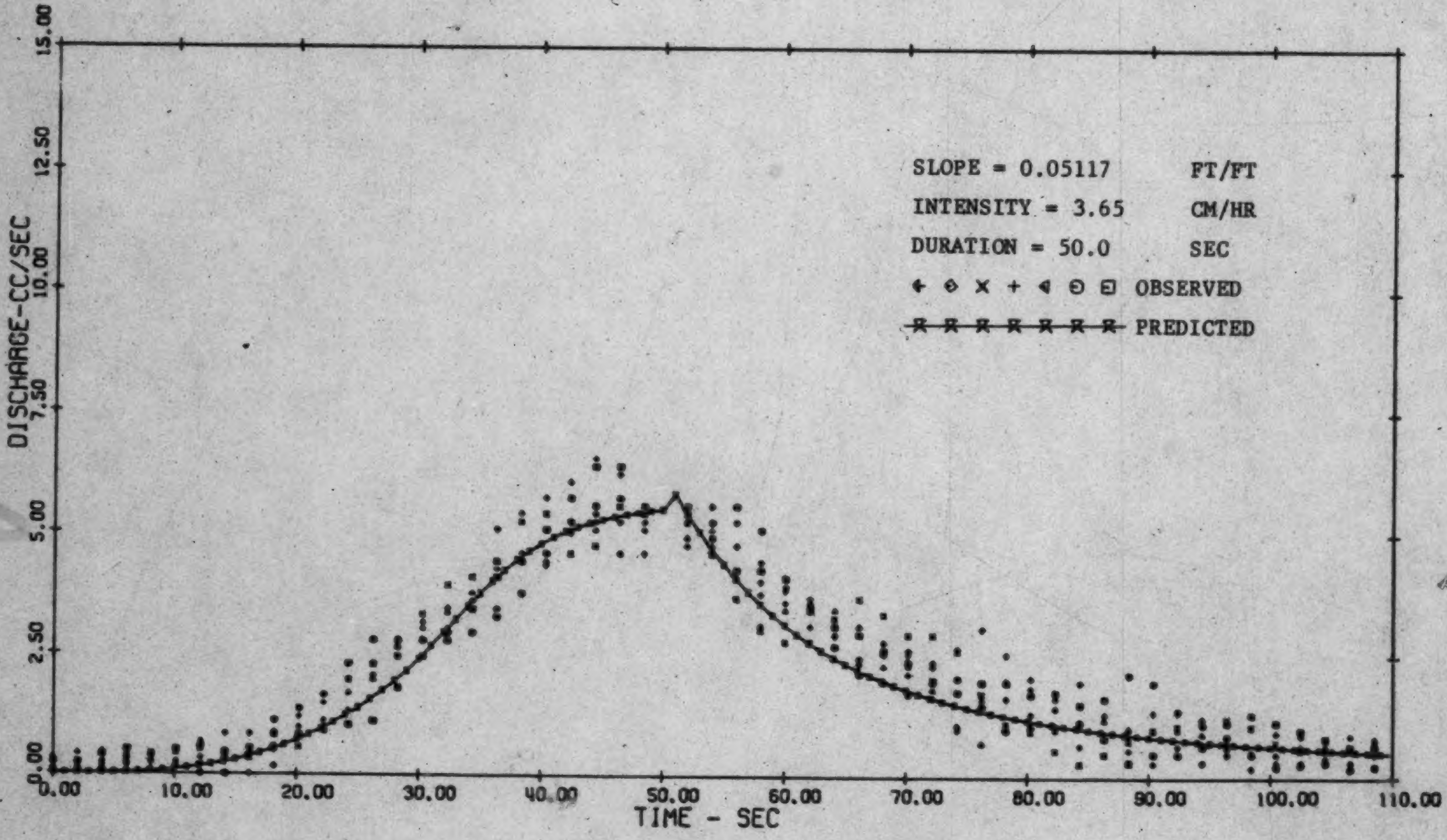

Figure 5-18. Observed and predicted hydrographs (state variable model) for test 25 with uniform rainfall input.

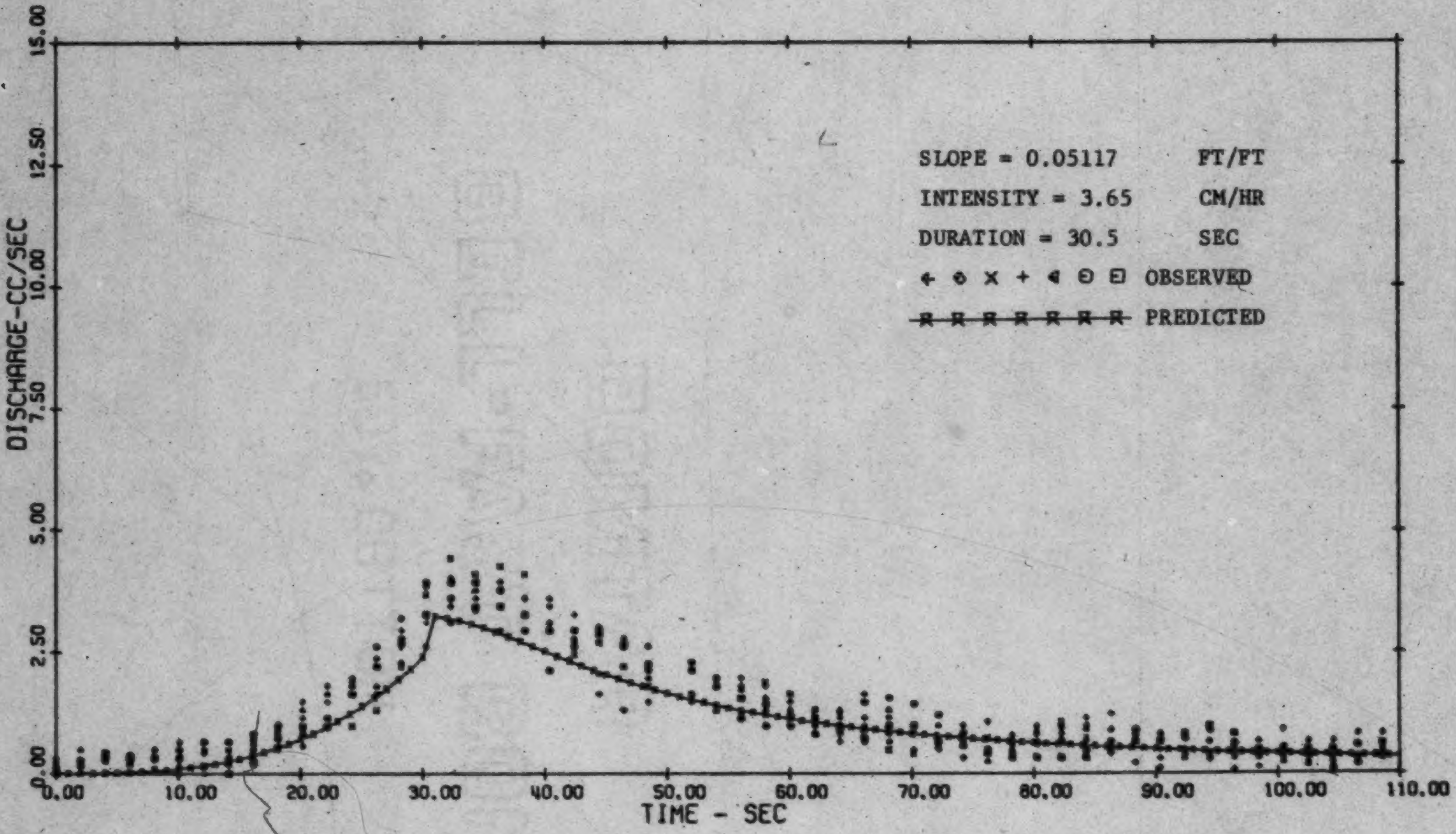

Figure 5-19. Observed and predicted hydrographs (state variable model) for test 26 with uniform rainfall input.

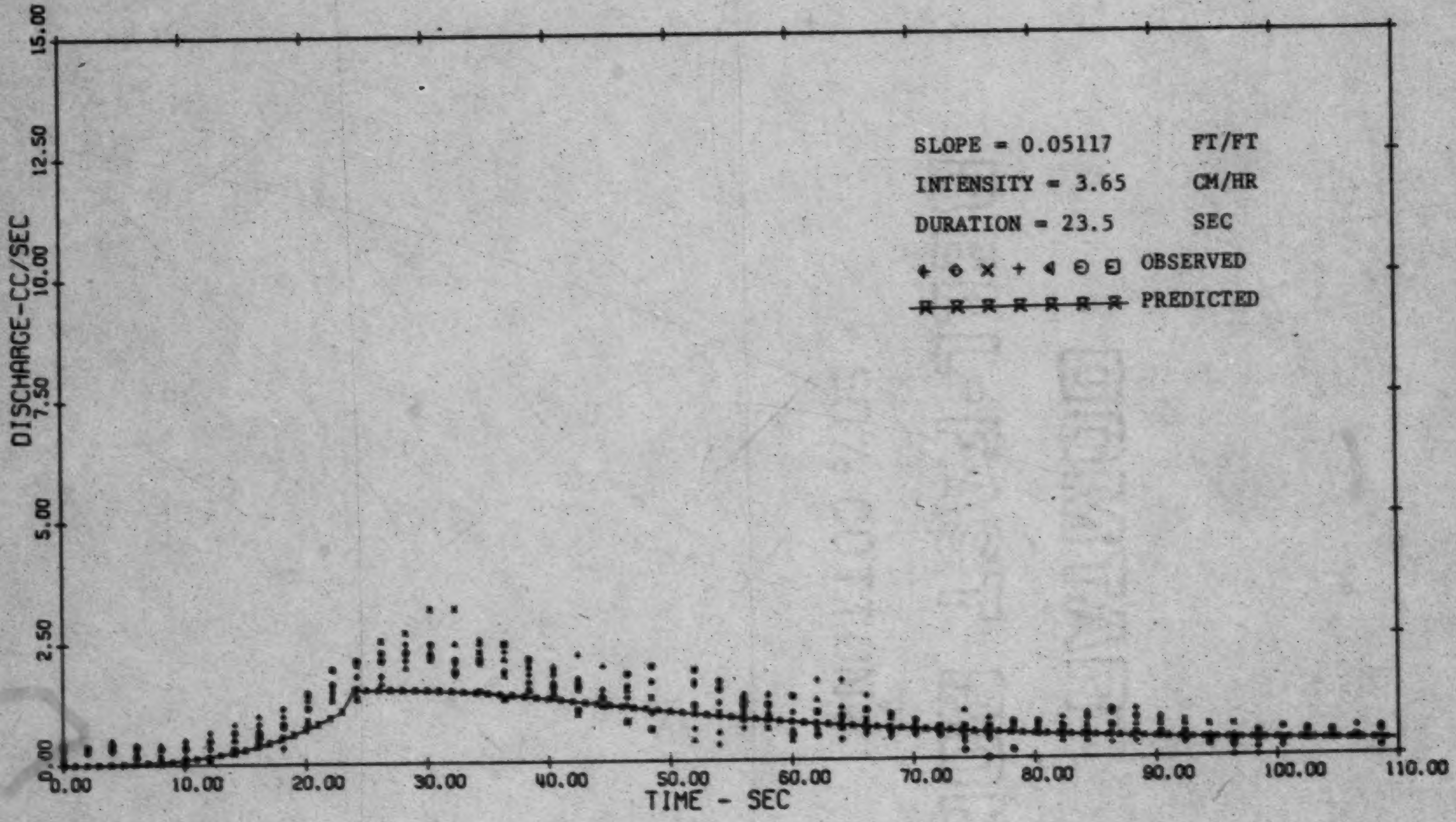

Figure 5-20. Observed and predicted hydrographs (state variable model) for test 27 with uniform rainfall input.

Woo and Brater, 1962; Yu and McNown, 1964; Das, 1970; Morgali, 1970; Schreiber and Bender, 1972). The increase of discharge does not always happen to the same degree. It basically depends on the flow velocity, rainfall intensity, and possibly on the surface roughness. Surfaces with mild slopes tend to produce greater increase in discharge after cessation of rainfall than those with steep slopes.

5-5-2 Experiments with Temporally Varied Rainfall Input

Two types of the temporally varied rainfall input were tested: (1) ramp function input, and (2) two consecutive pulse function inputs, separated by a "no input" time interval.

Results of the ramp function input experiment are shown in Figure 5-21. The simulated hydrograph is a good approximation to the laboratory data.

The two pulse function inputs produced a double peak hydrograph, shown in Figure 5-22. The fit of the simulated hydrograph to the experimental data is good. One phenomenon, not observed in the laboratory data (again possibly because of the scatter of the data and because of too long a sampling interval), is the sudden drop in discharge at the beginning of the second pulse input. This is due to increased friction factor, caused by the raindrop impact effect.

5-5-3 Experiments with Spatially Varied Rainfall Input

The physical phenomenon of surface runoff from a catchment under spatially distributed rainfall differs from that under uniform rainfall by the difference in distribution of the local inputs and consequently by the difference in the time distribution of the output.

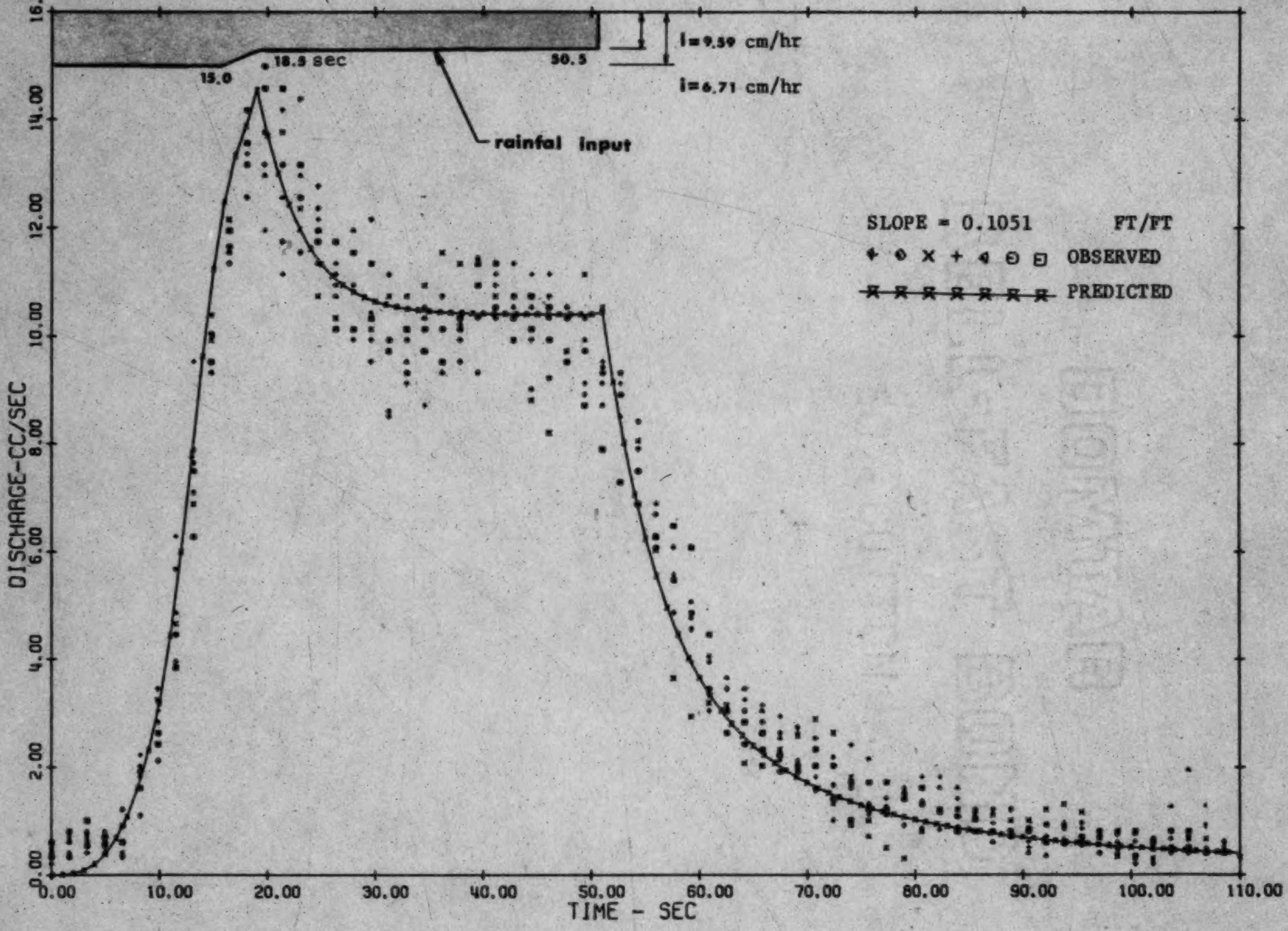

Figure 5-21. Observed and predicted hydrographs (state variable model) for test with temporally varied rainfall input (ramp function).

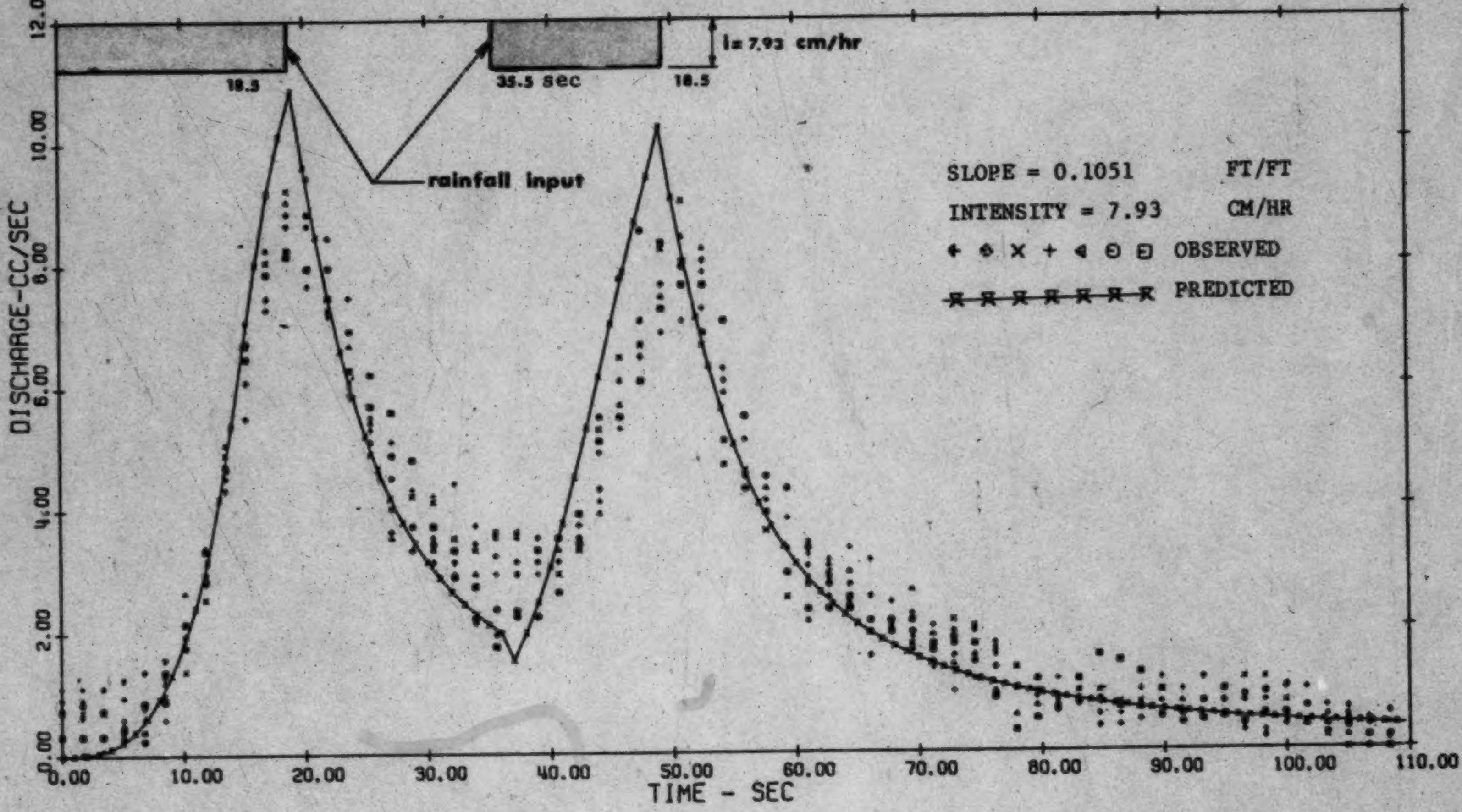

Figure 5-22. Observed and predicted hydrographs (state variable model) for test with temporally varied rainfall input (double pulse function).

For experimental purposes two basic patterns of spatially distributed rainfall input can be distinguished: (1) moving rainstorm with uniform rainfall intensity, and (2) stationary rainstorm with non-uniform spatial intensity. The former type was studied by Yen and Chow (1968). Combination of the two types will result in both spatially and temporally varied input. If on such input still another temporal variation is superimposed the result is then the most general case of rainfall input, such as most likely occurs in nature.

From the point of view of runoff simulation, any type of spatially varied rainfall input may present a difficult problem. The spatially distributed input induces an uneven depth of flow in various parts of the test basin, which may eventually lead to formation of waves moving over the runoff plane. Simulated outflow from the basin under such circumstances, by the state variable model or any lumped parameter model, could become significantly distorted. The state variable model treats the wave input into a particular reach of the model in the same manner as the rainfall input, i.e. as an impulse resulting in an immediate response in the form of increased outflow from that reach. Such response approximates the actual situation very closely when the significant input is in the form of rainfall, but in the case of a wave entering the upper part of the reach there is a time lag involved, equal to the travel time of the wave through the reach, before there can be any apparent response.

A similar situation arises in the case of receding flow when there is no input due to rainfall. The flow is varied gradually and the inputs and outputs for a particular reach are of the same order of magnitude.

Such gradually varied flow obviously does not present any problem during simulation, as can be seen from the very good fit of most of the simulated recession hydrographs.

One can therefore reason that unless there are extreme spatial differences in the rainfall intensity, able to induce formation of waves with depths several times the magnitude of the flow depth in the rest of the basin, the state variable model should provide reasonably good approximations to runoff caused by spatially varied rainfall inputs. Such extreme conditions, however, are unlikely to occur in overland flow situations.

To examine the effect of spatially distributed rainfall input on the simulated hydrograph by the state variable model a stationary rainstorm with alternating regions of "rain" and "no rain" input, as shown schematically in Figure 5-23, was generated over the test catchment. The simulated hydrograph approximates reasonably well the experimental data. Unfortunately, the exact shape of the hydrograph, especially at the beginning of the rising stage and after cessation of rainfall when a sudden increase of discharge occurs in the simulated hydrograph, could not be confirmed by the experimental data because of the scatter of points.

Although the detailed form of the response could not be confirmed, the experiment demonstrated the ability of the state variable model to simulate the hydrograph. It was not attempted to determine to what extent, or extremes in spatial distribution of the input, this would hold true. It was reasoned that the size of the laboratory catchment (2 ft by 3 ft) was not sufficient for this purpose.

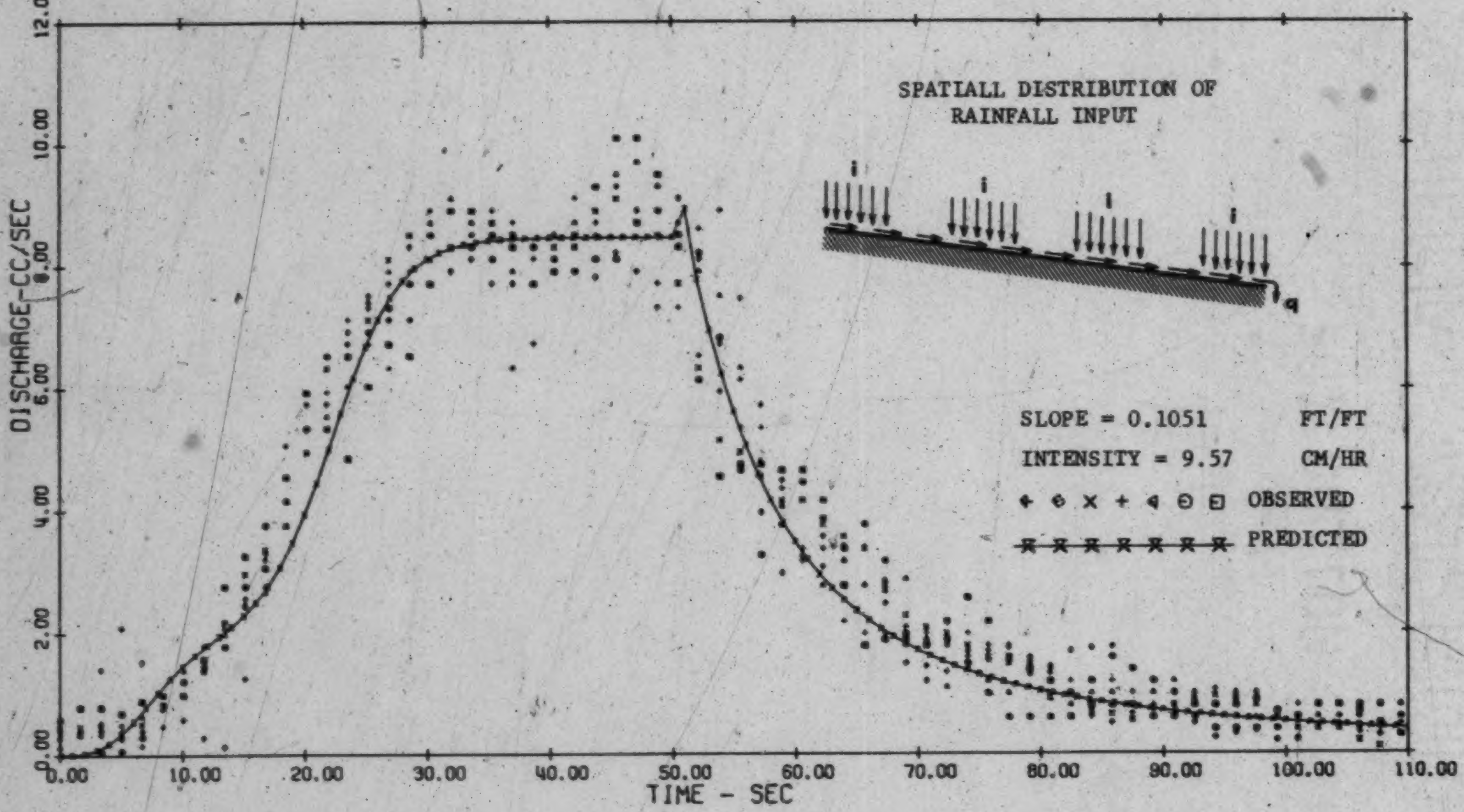

Figure 5-23: Observed and predicted hydrographs (state variable model) for test with spatially varied rainfall input (stationary rainstorm).

CHAPTER VI

DISCUSSION OF EXPERIMENTAL RESULTS AND SIMULATION METHODS

6-1 General

A question that may be raised in connection with the significance of the results obtained in the present study relates to the accuracy of the method of measuring the outflow rates by numerical differentiation of the cumulative outflow. Sufficient accuracy of measured hydrographs is necessary to lend significance to the conclusions related to the simulating techniques, made through comparison of the measured and simulated hydrographs. In this chapter estimates of the accuracy of the experimental techniques used in the present study are discussed.

This chapter also deals with the comparison of the mathematical models of surface runoff presented in this study, i.e., the state variable model, kinematic wave model, and the instantaneous unit hydrograph model. The aim of the discussion is to investigate the physical validity of the basic concepts of each of the above mathematical models. Comparison of the output hydrographs of the models simulating the same rainfall event serves to depict properties characteristic to each mathematical model and to discuss these properties in terms of the underlying concepts.

The last section of this chapter deals with the possible application of the state variable model in simulation of natural watersheds.

It is shown that the concept of state and state variables, applied in the present study to the elementary case of runoff from an impervious surface, is not only useful but perhaps indispensable in the formulation of watershed models based on physical principles. This conclusion was arrived at by reviewing the present state of the art of digital simulation in hydrology.

6-2 Accuracy of Experimental Techniques

In the following analysis the dispersion of the computed discharges is discussed in the case when the number of repetitions in each run was seven. The usual procedure is to establish a confidence band of the experimental curve given by the average values of the repetitions. Because the instantaneous outflow rates were obtained from the measured cumulative outflows by numerical differentiation, which is an unstable process, the calculation of confidence bands for the instantaneous outflow rate hydrographs must consider possible errors due to differentiation. Typical results of calculation of the confidence limits for both cumulative and instantaneous outflows are presented in the following sections.

6-2-1 Cumulative Outflow Hydrographs

Cumulative outflow hydrographs were obtained by recording the weight of accumulated water from surface runoff. Accuracy of the cumulative outflow hydrographs depends directly on the following two factors: (1) the experimental technique, and (2) the overall performance of the data recording system, discussed in more detail below.

The experimental technique of measurement involved a manual operation of a sliding tray by means of which the duration of rainfall over the laboratory catchment was regulated. It was estimated that the maximum error in timing due to the manual operation was about ±0.5 second. Thus the cumulative outflow hydrographs could be shifted along the time axis by a maximum amount of ±0.5 second from the true position which then results in corresponding differences or errors in values of the cumulative outflow. The errors increase with increasing slope of the catchment and with increasing rainfall intensity. This is due to higher velocities of flow induced by steeper slope and higher intensity, which result in larger runoff volumes, and therefore greater errors, during the same time interval. Estimated maximum errors in cumulative outflows, corresponding to different intensities, are given in Table 6-1.

The second factor influencing the accuracy of the experimental data is a function of the overall performance of the data recording system which consisted of the strain gauge transducer that measured cumulative weight of water and the data acquisition system. It was determined that the error in the reading was ±2.0 grams for static weight measurement. The error of reading, however, increased to ±3.0 grams when the weight increase was due to inflowing water from the laboratory catchment. The impact of inflowing water into the collecting tank caused slight vibrations and waves which were reflected in wider fluctuation of the transducer's output signal.

Estimated maximum errors in the experimental values of cumulative outflow are given by the sum of errors due to the two factors discussed above. The estimates of maximum errors for three typical rainfall intensities are given in Table 6-1.

Statistical analyses of the actual test series were also performed. Typical results of these computations are presented in Appendix F.

TABLE 6-1

ESTIMATED MAXIMUM ERRORS IN CUMULATIVE OUTFLOW

Rainfall Intensity cm/hr	11.5	7.8	3.9
Error Due To 0.5 Sec Time Shift (grams)	± 8.6	±6.0	±3.0
Error Due To Recording (grams)	± 3.0	±3.0	±3.0
Total Error (grams)	±11.6	±9.0	±6.0

In general, at the 95 per cent confidence level, the cumulative outflow values determined from seven runs could be considered accurate within about 0.9 to 5.5 cc. Figure 6-1(b) shows the 95% confidence bands for the series of experiments of run no. 7 (Table 5-2). These results are within the maximum values estimated in Table 6-1.

Figure 6-1(b) also shows the cumulative flow hydrograph predicted by the state variable model. It can be seen that the predicted hydrograph is within the 95% confidence zone of the experimental hydrograph. The close fit of the predicted hydrograph to the experimental values was utilized in the following section for estimation of errors due to differentiation.

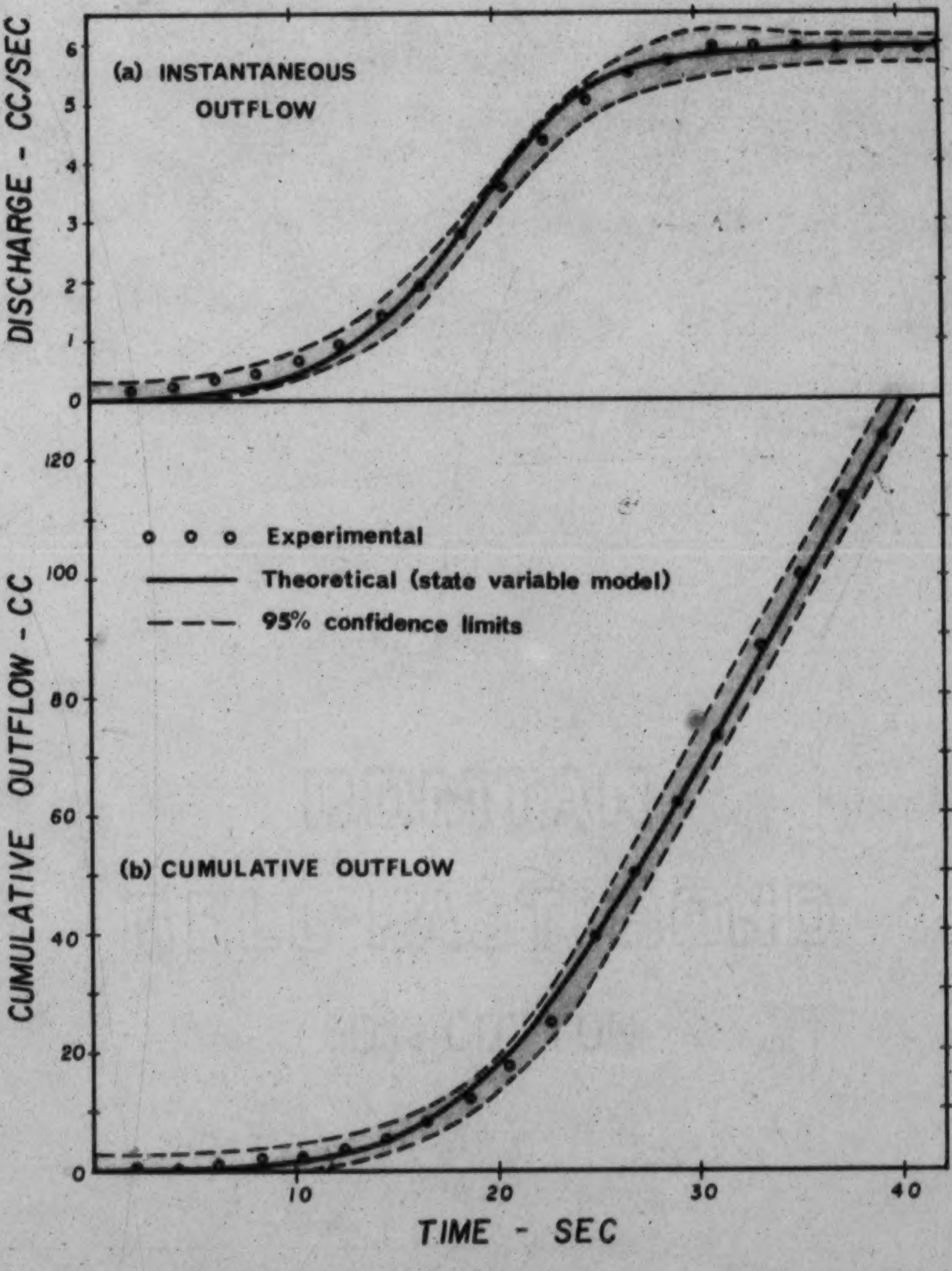

Figure 6-1. 95% confidence bands of experimental hydrographs for test 7.

6-2-2 Instantaneous Outflow Hydrographs

Determination of the confidence intervals of the instantaneous outflow hydrographs consisted essentially of the following steps:

(1) Fitting a smooth theoretical curve to the experimental cumulative outflow hydrograph.

(2) Differentiation of the fitted theoretical curve and determination of the errors due to numerical differentiation.

(3) Comparison of the theoretical and experimental differential curves and estimation of the confidence interval of the experimental curve.

As pointed out in the previous section, the cumulative outflow hydrograph simulated by the state variable model gave a very good fit to the experimental curve (Figure 6-1(b)). The simulated hydrograph was therefore taken as a theoretical curve fitted to the cumulative outflow. The theoretical values of outflow were known at equidistant time intervals of 0.1 second. The errors due to differentiation of the theoretical curve were determined in the Appendix F, and were found to be less than or equal to 0.0007 cc/sec. Since the measured steady outflows were of the order of 5 to 18 cc/sec the error in the theoretical curve was negligible.

The theoretical and experimental curves of instantaneous outflow rates are plotted in Figure 6-1(a) for comparison. Also plotted is the 95% confidence interval determined from the experimental data after differentiation. Typical results of the confidence interval calculations are presented in Appendix F. Since the theoretical curve lies within the 95% confidence limits the interval was accepted as valid. The curves shown in Figure 6-1 are typical results obtained in this investigation. It can be noted that the experimental hydrograph has relatively high values at the beginning of runoff, where they should be close to zero. Also the experimental curves tend to be rounded off at the time of rain cessation, where there should be a sharp break between the end of steady runoff and the beginning of recession. These inaccuracies were attributed to the smoothing procedure applied to data prior to differentiation. For the same reason it is suspected that the experimental values of peak outflow rates were in some cases distorted and the confidence limits around the peak are unreliable.

In summary, it was found that with sets of seven consecutive experiments the outflow rates could be estimated with 95% confidence within approximately 0.1 to 0.4 cc/sec. This represents between 2 to 8% of the measured steady flow rates. In general the outflow rates for various inputs differed from each other by much more than these percentages and it was concluded that the method based on the numerical differentiation of the cumulative curves was adequate for detecting the kinds of responses normally encountered in the investigation. The evaluation became uncertain only when the contrasts between responses were smaller than about 5%.

A more efficient means of regulation and control of the rainfall input would improve accuracy of reading substantially. Also the high sensitivity of the strain gauge transducer was somewhat countered by vibrations of the collecting tank.

6-3 Comparison of the Studied Models

Simulations of the experimental runs number 13, 14, and 15 (Table 5-2) were chosen for comparison of the state variable, the kinematic wave, and the instantaneous unit hydrograph models. The specific conditions of the runs were: $S_o = 0.1045$, rainfall intensity $i = 7.42$ cm/hr, rainfall duration $t = 50.0$ sec, 17.5 sec, and 14.5 sec. The hydrographs, simulated by the above mathematical models, were plotted for each run on a common plot, without the experimental hydrographs. The plots show typical results of simulation by the individual models, and provide a suitable ground for discussion of the concepts and assumptions which form the basis of a particular model.

6-3-1 The Instantaneous Unit Hydrograph Model

The basic issue in discussion of the instantaneous unit hydrograph model is not the concept itself. The concept of convolution is correct and valid, but only for linear processes. Thus, the main concern of the investigation was to find whether surface runoff can be approximated by the linear unit hydrograph model to such a degree that the method would be of practical value.

It was shown in Chapter IV that two instantaneous unit hydrographs of the laboratory catchment, derived from two different runoff events, differed considerably in peak values, time to peak, and total time base. To facilitate discussion in the present section, another two instantaneous unit hydrographs were derived from runs number 13 ($i = 7.42$ cm/hr) and 16 ($i = 3.91$ cm/hr). The derived IUH-1 and IUH-2 are shown in Figures 6-2 and 6-3 respectively. The large difference between the two IUH's indicates a high degree of nonlinearity of the runoff process and confirms the results presented in Chapter IV.

To understand the implications of these results it is convenient to recall at this point some of the deductions concerning nonlinear

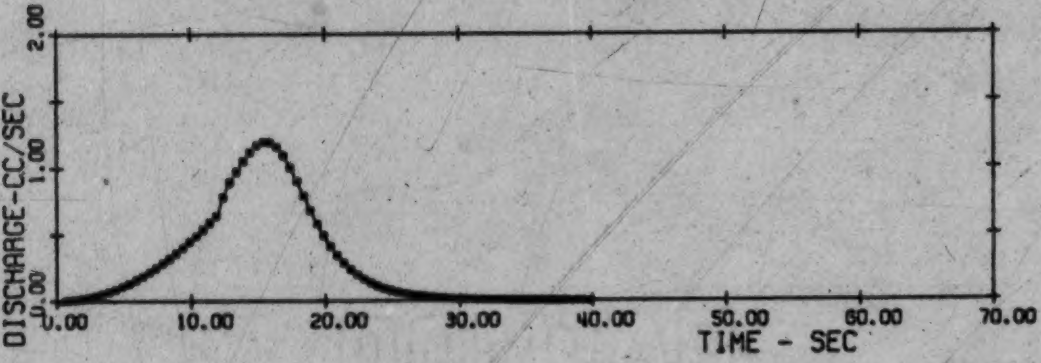

Figure 6-2. Instantaneous unit hydrograph (corresponding to unit rainfall intensity i = 7.42 cm/hr) derived from test 13.

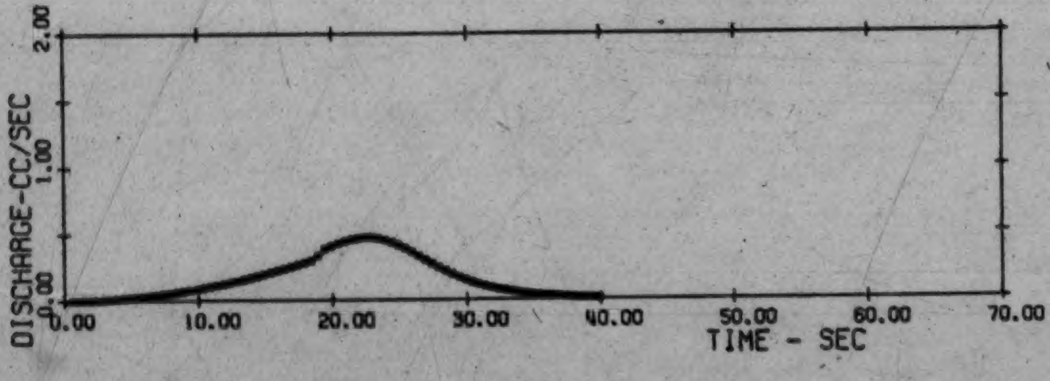

Figure 6-3. Instantaneous unit hydrograph (corresponding to unit rainfall intensity i = 3.91 cm/hr) derived from test 16.

systems, made earlier in this study when dealing with the analysis of a nonlinear reservoir. In Chapter III it was shown that a nonlinear process can be approximated by a linearized relationship of the process variables around a steady state, and that the approximation is then reasonably good only within a narrow range of fluctuations of the process variables about the particular steady state. This general conclusion can be applied in the case of surface runoff as described below.

Results of the laboratory catchment experiments indicate that the surface runoff is a nonlinear process. The experimental evidence also indicates that when deriving the laboratory catchment IUH from measured hydrographs generated by rainfalls of different intensities, one obtains a number of different IUH. It follows then that there exists an infinite number of instantaneous unit hydrographs for a particular catchment, and each of these hydrographs is in effect a steady state linear approximation (i.e. an approximation valid for a particular value of rainfall intensity with infinite duration) of the nonlinear rainfall-runoff relationship. Hence, the instantaneous unit hydrograph model is capable of simulating only that runoff hydrograph from which the IUH used in the model during simulation was derived. When the input amplitude, i.e., the rainfall intensity, increasingly deviates from the original "steady state" value, the simulation becomes more and more unrealistic.

Results of the instantaneous unit hydrograph model simulation, using the two instantaneous unit hydrographs derived from runs number 13 and 16 are compared with hydrographs simulated by the kinematic wave and state variable models in Figures 6-4, 6-5, and 6-6. Simulated hydrographs for the case when rainfall duration was longer than the time to equilibrium (run 13) are shown in Figure 6-4. It should be noted that the IUH-1 was derived from the state variable model hydrograph shown in the figure because the latter was judged to be a very good fit to the experimental data. It is seen that the original state variable model hydrograph is reproduced perfectly by the instantaneous unit hydrograph model (using IUH-1) up to the time of rainfall cessation. When the IUH-2 was used in the simulation the reproduction was very poor.

Simulated hydrographs with rainfall durations shorter than the time to equilibrium (runs 14 and 15) are shown in Figures 6-5 and 6-6. The IUH-1 was used in the simulation. It is seen that the original (state variable) hydrographs are reproduced again correctly up to the time of rainfall cessation. Simulation of the recession curves is unsuccessful in all cases. The cause of this failure can be found in the shape of the IUH, which is not suited for reproduction of the recession curves by means of a convolution integral, and the reason can be attributed to the nonlinearity of the runoff process.

In summary, the performance of the instantaneous unit hydrograph model was found unsatisfactory. The main reason for the poor simulation results was found to be the incorrect theoretical assumption of linearity.

6-3-2 Kinematic Wave and State Variable Models

Results of the present study have shown that the kinematic wave and state variable models were able to simulate reasonably well rainfall-runoff events within the laboratory conditions encountered in the investigation. In the following the properties of the kinematic wave model by the way of comparison with the state variable model are discussed. This method of discussion was selected primarily because the principle of

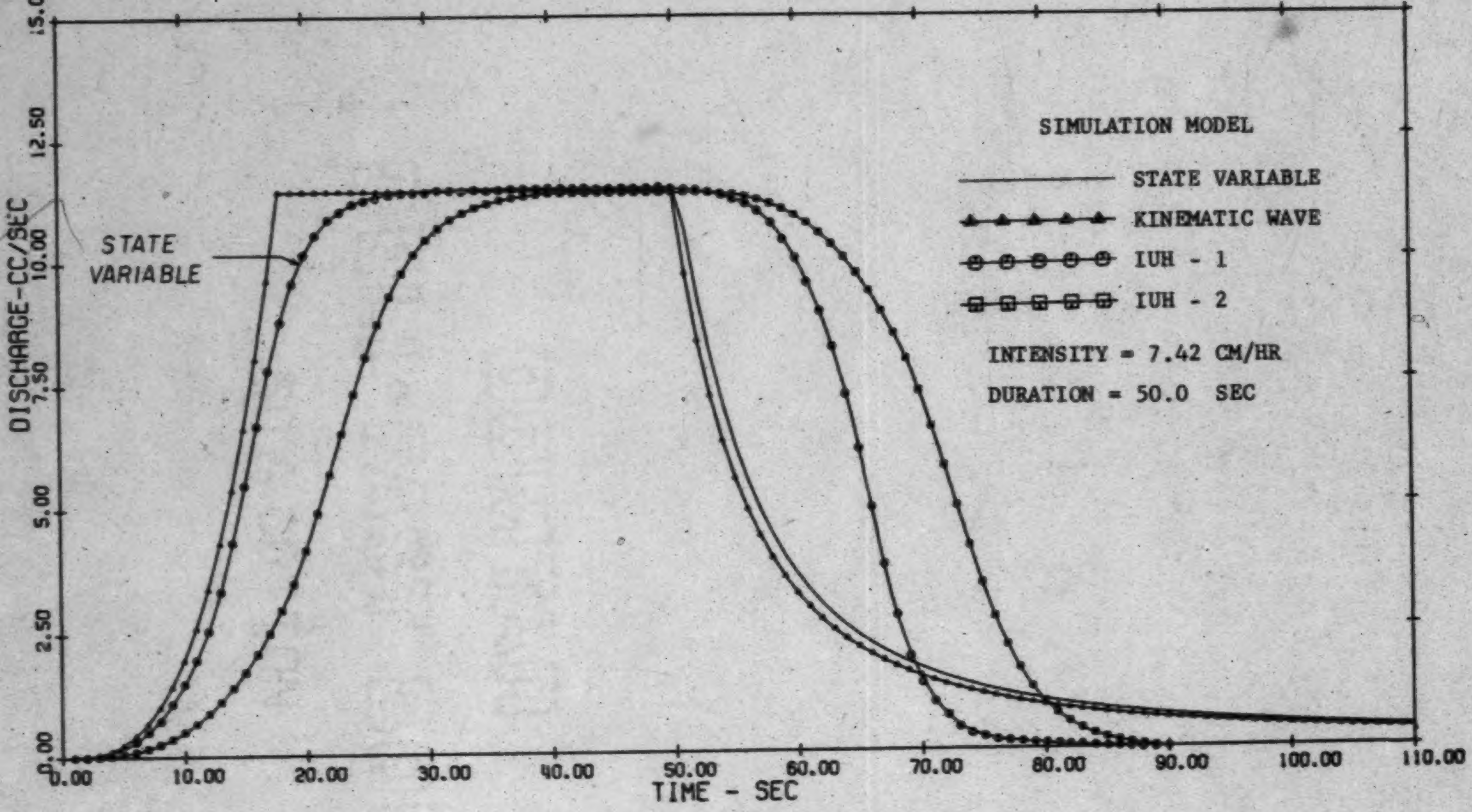

Figure 6-4. Comparison of simulated hydrographs for test 13.

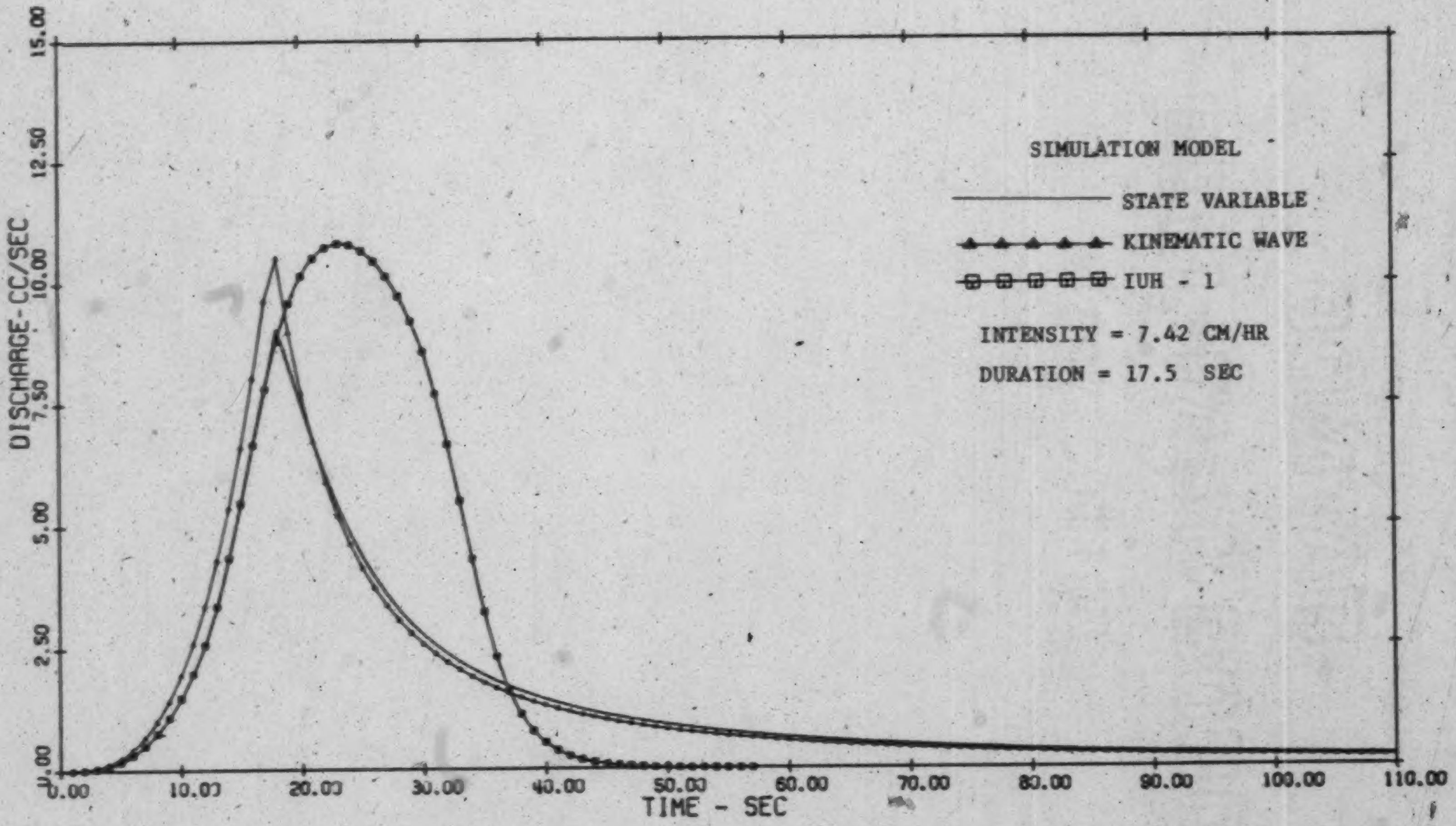

INTENSITY = 7.42 CM/HR

DURATION = 17.5 SEC

Figure 6-5. Comparison of simulated hydrographs for test 14.

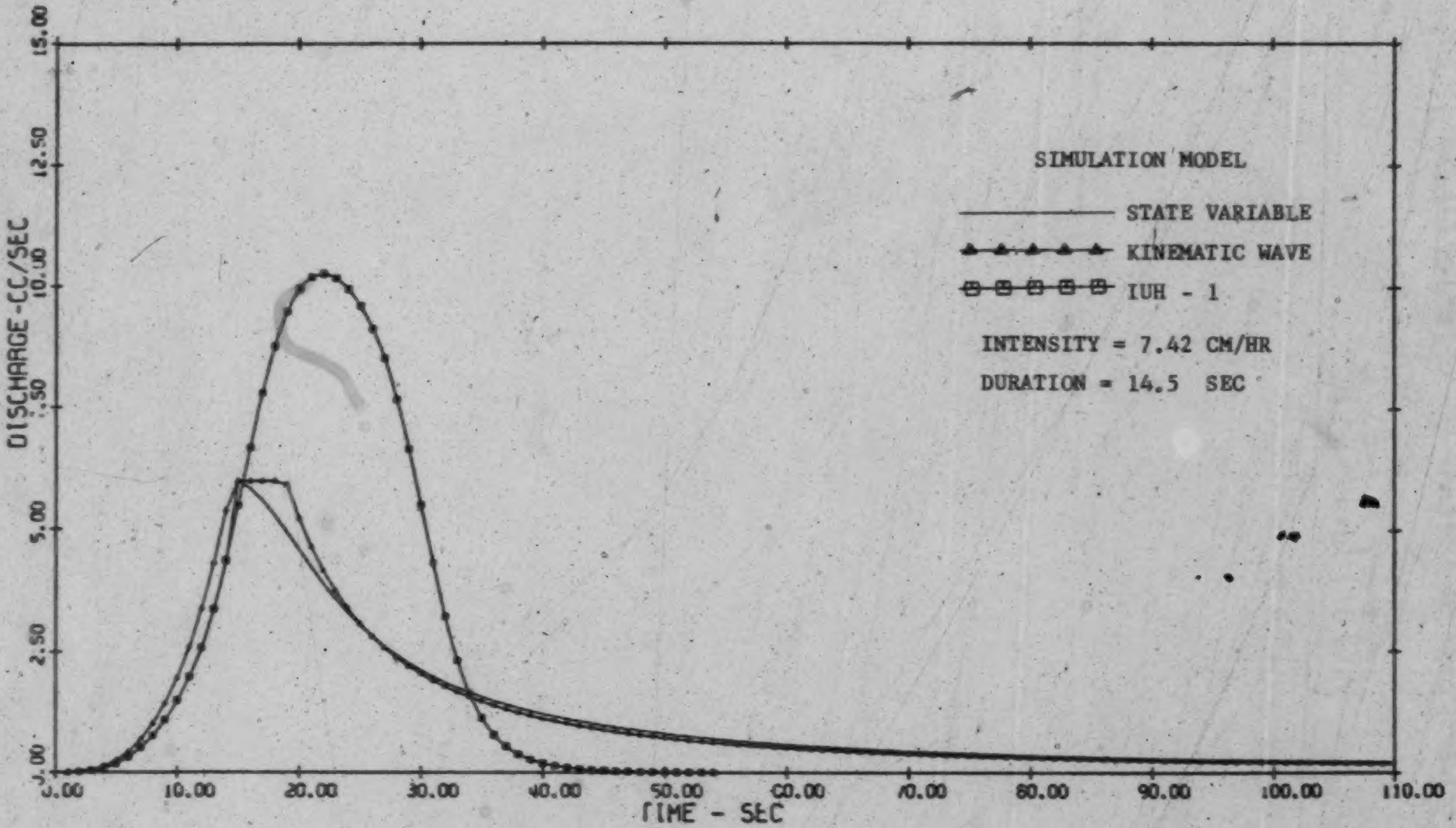

Figure 6-6. Comparison of simulated hydrographs for test 15.

the state variable model is simple to the degree that many flow situations can be easily visualized.

The kinematic wave model as well as the state variable model of surface runoff are based on the assumption that the discharge of overland flow can be described with a reasonable accuracy by a uniform flow formula. The two models, however, differ in the mathematical manipulation of the equation of continuity of the unsteady spatially varied flow.

In the mathematical development of the kinematic wave model the equation of continuity was written as a total derivative of depth of flow [Equations (4-13), (4-16), and (4-18)]. Validity of the new equation thus derived was based on the assumption that discharge is a function of depth only, and was restricted to a new set of co-ordinates. Analytical solution of the surface runoff problem then followed from the application of the method of characteristics.

The state variable model is based on the assumption that the partial differential equation of continuity can be approximated by a finite number of simultaneous ordinary differential equations of continuity. The set of such equations can be written in the form of state equations. It was shown in Chapter V that as the number of equations in the set increases to infinity, the set approaches the partial differential equation of continuity of the flow in the limit. This property makes the state variable model physically meaningful, and suitable to represent the actual flow very closely. As a result, the state variable model was used in the following to estimate the validity of some of the relations given by the kinematic wave model.

Two characteristic properties of the kinematic wave model discussed in this section are the following: (1) the absence of a point of inflection on the rising limb of a hydrograph, and (2) the steady rate of receding outflow for the period of time t_p, when $t_o < t_s$.

The first of the above properties is illustrated in Figure 6-4. The absence of a point of inflection is the result of the kinematic wave relationship specifying the depth of flow during the rising stage as $y = it$ (or $dy/dt = i$) given by Equation (4-19). The peak of the simulated hydrograph is then always sharp crested as illustrated in Figures 6-4 and 6-6. Such a shape of hydrographs has never been observed in actual outflows and the validity of the relationship $y = it$ is therefore questionable.

In the following, the elementary case of runoff, i.e., runoff from a uniformly sloping plane under uniformly distributed rainfall, is analysed by means of the state variable approach to assess approximately the validity of the relation given by $y = it$ for $t \leq t_s$.

Consider for a moment an infinite runoff plane. The state variable model simulating runoff from this plane would consist of an infinite number of identical elements in series, basically operating as a series of interacting reservoirs (Chapter V). Since the rainfall is uniformly distributed, each of the elements receives exactly the same rainfall input, and the depth in all elements rises initially (in the first time increment) to the same depth. Consequently, the outflows from the elements are identical. Therefore, during the following time increments the surface outflow and inflow components of the continuity equations of the elements are all equal, and the storage components are made up only of the precipitation input, i.e. $y = it$.

Consider now a runoff plane of a finite length. The first (upstream) element in the series does not receive any surface inflow but only the precipitation input. Because the outflow from the element, q, is a function of the third power of the depth, y, i.e., $q \propto y^3$, the response of the element to a step function input has the form of an S-curve. Let Q_1 be the rate of outflow from the first element corresponding to the point of inflection of the S-shaped outflow curve from the element. The S-shaped outflow function is routed through the rest of the series, which disturbs the equality of inflow and outflow, described for the case of infinite series. Consequently, the process results in differentiation of depths in the individual elements of the series. The outflow hydrograph simulated by the kinematic wave model corresponds to the outflow from the last element in the series representing the state variable model. It is reasoned that for the last element in the series the relationship given by $y = it$ remains valid for the time required to route the discharge Q_1 through the entire series. After the discharge Q_1 reached the n-th and last element of the series, the rate of increase of the surface inflow into the n-th element begins to decrease, thus marking the point of inflection of the total outflow hydrograph. The total outflow then approaches assymptotically a steady state rate of outflow. Table 6-2 illustrates the described process on an example of the run number 4 (Table 5-2), simulated by the state variable model with $n = 7$. The rows of the table give the simulated water surface profiles at small increments of time.

The discussion presented above leads to the conclusion that both the kinematic wave and state variable models, simulating a particular

TABLE 6-2

DIFFERENTIATION OF THE DEPTH OF FLOW IN THE SEGMENTS OF THE 7-ORDER STATE VARIABLE MODEL DURING SURFACE RUNOFF SIMULATION FOR TEST 4

Time Since the Beginning of Rainfall (sec)	Rainfall Intensity (cm/hr)	Discharge (cc/sec)	Depth of Flow (cm) in Segments 1 to 7						
			H_1	H_2	H_3	H_4	H_5	H_6	H_7
0.1	7.77	0.0	0.000216	0.000216	0.000216	0.000216	0.000216	0.000216	0.000216
1.0	7.77	0.002585	0.002157	0.002158	0.002158	0.002158	0.002158	0.002158	0.002158
2.0	7.77	0.024320	0.004299	0.004315	0.004315	0.004315	0.004315	0.004315	0.004315
3.0	7.77	0.086475	0.006391	0.006471	0.006473	0.006473	0.006473	0.006473	0.006473
4.0	7.77	0.210324	0.008373	0.008618	0.008630	0.008631	0.008631	0.008631	0.008631
5.0	7.77	0.417140	0.010182	0.010731	0.010785	0.010788	0.010788	0.010788	0.010788
6.0	7.77	0.728199	0.011761	0.012761	0.012924	0.012944	0.012946	0.012946	0.012946
7.0	7.77	1.164767	0.013076	0.014636	0.015017	0.015091	0.015102	0.015104	0.015104
8.0	7.77	1.748084	0.014125	0.016280	0.017002	0.017206	0.017252	0.017260	0.017261
9.0	7.77	2.499560	0.014929	0.017642	0.018791	0.019232	0.019373	0.019409	0.019417
10.0	7.77	3.616761	0.015526	0.018710	0.020281	0.021039	0.021384	0.021518	0.021561
11.0	7.77	5.031344	0.015958	0.019505	0.021374	0.022506	0.023155	0.023492	0.023645
12.0	7.77	6.662226	0.016264	0.020043	0.022151	0.023583	0.024551	0.025174	0.025543

runoff event, will compute the same values of discharge up to the time of occurrence of a point of inflection on the hydrograph simulated by the state variable model. For illustration, hydrographs of run number 13 (Table 5-2), simulated by the kinematic wave and the state variable models are plotted in Figure 6-4. It can be seen that the hydrographs do not differ in their shape significantly up to the time of occurrence of a point of inflection on the hydrograph simulated by the state variable model. The faster rate of rising of the kinematic wave hydrograph is due to neglected raindrop impact effect. Only after the time to the inflex point do the two hydrographs differ in their shape significantly.

The second property of the kinematic wave model listed previously is typical for the case when the duration of rainfall, t_o, is shorter than the time to equilibrium, t_s. In this case, after cessation of rainfall the discharge remains constant for the time period t_p. A typical outflow hydrograph is shown in Figure 6-6. Considering this case from the point of the state variable model, the constant outflow could occur only if the depth of flow, at the time of rain cessation, is the same in two or more elements of the series. Referring to the previous analysis of flow by the state variable approach, this means that in order for the receding flow to remain constant for a certain period of time, t_p, the rain must cease before the occurrence of a point of inflection on the hydrograph of total outflow, caused by rain of duration $t_o \geq t_s$. The flow during the time period t_p can be visualized as propagation of a negative wave through the remaining elements of the series. Clearly, the time period t_p depends on the chosen number n of the elements in the series, and on the time interval used in the calculation. These two factors must be determined through experience, and will require the use of an empirical coefficient in the outflow equation (Equation (5-51)). Such a coefficient should be determined by a parameter optimization technique. In actual flow the time period t_p, if it exists at all, most likely depends on the slope of the runoff plane and on the energy losses due to friction. The faster the flow the shorter the t_p will be. Hydrographs simulated by the state variable model (Chapter IV and Appendix E) do not show any time period t_p of a significant duration throughout which the flow would remain strictly constant. However, some of the recession curves are S-shaped, and on very mild slopes the rate of decrease of discharge is so small for an appreciable duration that it is almost constant. A typical case is shown in Appendix E, Figures E-15 and E-21.

Recession curves of equilibrium hydrographs, i.e., the case when $t_o \geq t_s$, simulated by the kinematic wave and state variable models are practically identical, as illustrated in Figure 6-4. The state variable model recession curve is only shifted horizontally due to increased runoff caused by decreased friction factor at the time of rain cessation.

6-4 Application of the State Variable Approach in Hydrologic Simulation

With the rapidly increasing rate of urban development in the present technological society there is an ever growing need for better and more effective methods of water resources management, flood regulation, streamflow forecasting, pollution control, and power regulation. All these needs require development of more reliable techniques of hydrologic forecasting. Taking as an example the problem of flood forecasting, the simplest method of obtaining a flood forecast at a downstream point would consist of monitoring river and reservoir levels upstream and routing the flood hydrograph downstream. In many instances, however, the travel time of the flood waves through the channel reaches is short. Thus, there would be insufficient time to prepare and disseminate the forecast before the onset of flooding. Any effective forecasting system must give a much earlier warning and this implies the necessity of basing forecasts on measured or forecasted rainfall which must then be routed mathematically through the watershed as well as the river channel and reservoir system (City of Calgary Flood Study, 1972).

The transformation of measured or forecasted hydrometeorological data into a flood forecast may be achieved by means of a watershed simulation system which "models" the behaviour of the watershed. A brief review of the state of art of hydrologic simulation is given in the following.

6-4-1 Traditional Approach

In the simplest case of a fairly small uniform watershed in its natural state affected by fairly uniform rain only, one of the traditional and most common flood forecasting procedures would involve, for example:

(1) Determination of the storm rainfall on the watershed and its duration by plotting all measured rainfall data on a map, sketching in the isohyets and planimetering them to obtain the estimated watershed rainfall.

(2) Determination of the current antecedent precipitation index (API).

(3) Determination of the storm runoff volume from a coaxial

rainfall-runoff diagram using watershed rainfall, its duration, API, and time of year.

(4) Determination of the flood hydrograph at a gauged point for which a unit hydrograph is available.

(5) Determination of the flood hydrograph at the forecast point by routing the flood hydrograph determined through the intervening reach by the Muskingum or other routing procedures.

The traditional approach to flood forecasting is deceptively simple in appearance but involves considerable effort in practice when complications arise from the non-uniformity of meteorological and surface conditions and the resulting hydrologic complexity. Aside from these considerations, the method involves principles which are known to be incorrect. The coaxial diagram is a very crude model of the runoff process and involves statistically fitted curves of best fit to data which are widely scattered. The principle of the unit hydrograph has been questioned for many years. The investigation in the present study has revealed that the unit hydrograph concept is theoretically unsound. Most of the traditional methods therefore, are not suitable for operational flood forecasting.

6-4-2 Modern Approach - Digital Hydrologic Simulation

The advent of high speed digital computers has removed the traditional limitation of calculating speed. The object of today's research is to develop a general system of quantitative analysis for hydrologic regimes by establishing continuous mathematical relationships between elements of the hydrologic cycle. The operation of these mathematical relationships is observed and improved by using digital computers to carry the calculation forward in time. Precipitation and potential evapotranspiration are the basic inputs for these digital models and actual evapotranspiration, streamflow, and soil moisture levels are generally obtained as outputs. Calculations are made on selected time intervals and are carried continuously, whether or not precipitation is occurring, to simulate the entire spectrum of watershed behaviour.

A review of the literature has indicated that there are a dozen watershed simulation systems presently in existence. Most of them, however, are either in the development stage or are specifically intended for some purpose. An example of such "dedicated" model is the streamflow simulation and Reservoir Routing Model developed by the U.S. Corps of Engineers and the Portland River Forecast Centre for use on the Columbia River Basin. It is essentially a flood routing model which lacks adequate simulation of the land surface runoff process.

Perhaps the best known digital hydrologic model is the Stanford Watershed Model (Crawford, Linsley, 1966). The authors have developed the model over the last 12 years into a powerful program known as the Hydrologic Simulation Program (HSP). HSP programming is divided into three load modules designated Library, Lands, and Channels. The Library module handles the hydro-meteorological data files. The Lands module simulates land surface processes such as infiltration, evaporation, soil moisture storage and overland flow. The Channels module simulates depth and velocity of flows in the stream channel system, and spillway discharges and reservoir levels.

Two main steps are required to bring HSP into operation. These are "installation" and "calibration". Installation comprises establishing the basic mode of operation, selecting the data network stations which will provide input to the program, subdividing the watershed into "segments" and the channel network into "sections", and establishing rule curves and operating policies for each reservoir.

Calibration refers to the selection of the parameter values to be used in the program and their successive adjustment during trial runs to the point where the simulated record fits the observed records as closely as possible. A minimum of five years data is required for this purpose. This program is extremely versatile and practical, and finds applications in flood forecasting and water resources management.

6-4-3 Potential of the State Variable Approach

The state variable approach to system analysis appears to be suited to digital hydrologic simulation. The advantages of the method and its practical application are discussed in the following.

Because of the almost unlimited diversity of the boundary and initial conditions characteristic to the hydrological processes occurring in natural watersheds, pure distributed hydrologic models are not practical. Instead, the behaviour of a watershed must be simulated by lumped parameter models. The state variable method is in many instances the most efficient method of lumped parameter systems analysis. The method is extremely versatile and enables the mathematical characterization of lumped systems in a compact matrix form suitable for digital computer calculations. The concept of state itself is invaluable for development of a hydrologic model that operates using physically relevant components.

Application of the state variable method in simulating surface runoff under laboratory conditions was investigated in the present study.

To apply the method to natural watershed conditions, the state equations must be expanded to include evapotranspiration, infiltration and surface detention terms. Equations relating these terms in the state and output equations must be carefully considered, and will involve empirical coefficients determined by parameter optimization.

Continuous simulation of inflow into the channel network of a watershed requires simulation of the subsurface components of this inflow. The state variable model of the subsurface flow would not differ in its structure from the surface runoff model. The infiltration amounts, which are outputs of the surface flow model, will become inputs into the subsurface flow model. It is anticipated that the density of subdivision, or the number of elements required for subsurface flow simulation, would be less than for the surface flow model because of smaller flow velocities within the porous media. A block diagram of the state variable model simulating the lateral inflow into the watershed channel network is shown in Figure 6-7. The subsurface flow model can be further subdivided into two subsystems simulating the interflow and groundwater flow respectively. The channel flow can be simulated in principle by the state variable model, however, its application to large velocities and depths of flow in the unsteady channel flow would require further investigation. Various other methods of channel flow routing, however, which have been used successfully are available, such as the kinematic wave or Muskingum methods.

In the practical application of the state variable model the watershed will be divided, for the purpose of installation and calibration and subsequent operation of the model, into a number of segments and the

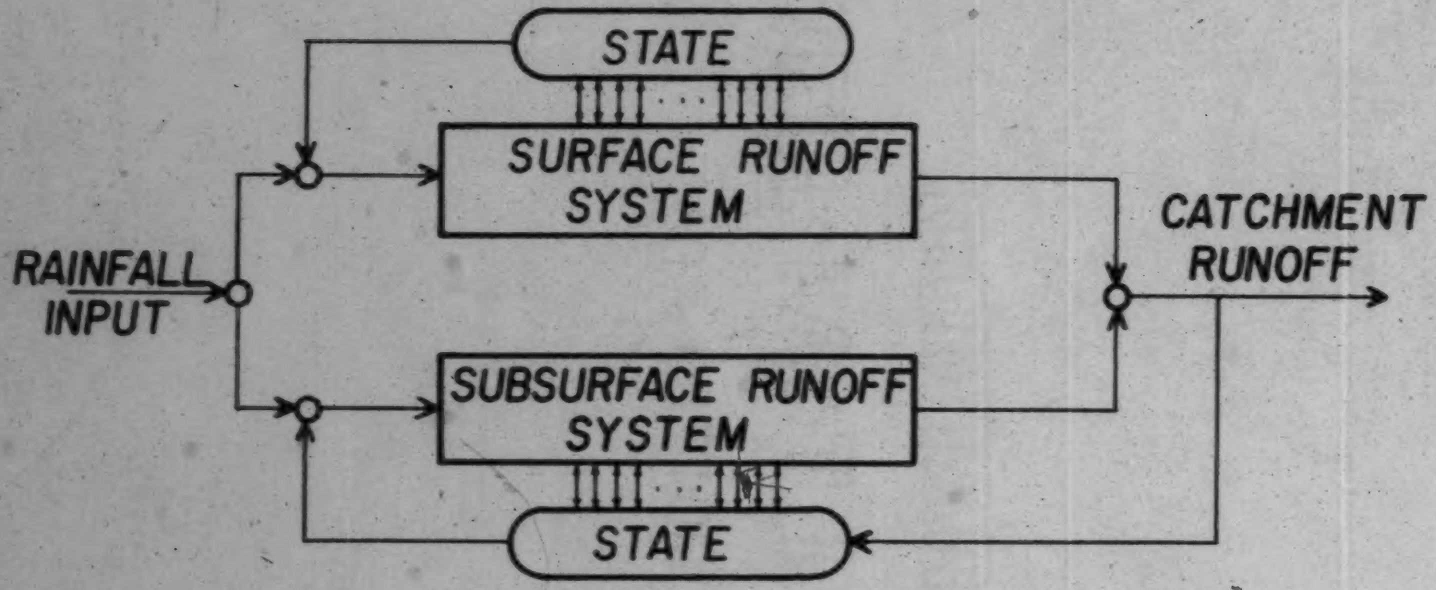
STATE
SURFACE RUNOFF SYSTEM
RAINFALL INPUT
CATCHMENT RUNOFF
SUBSURFACE RUNOFF SYSTEM
STATE

Figure 6-7. Block diagram of the state variable model simulating natural watershed.

channel network of the watershed into a number of reaches. A definition sketch of the watershed components used in the model is shown in Figure 6-8. Each segment and each reach has its characteristic parameter values used in the state and output equations of the model. For example, the state variable model of surface runoff developed in the present study contains only one parameter, α, [Equations (5-60) and (5-61)], which depends on the discharge formula and the time and space increments used in the calculation. State variable model simulating both surface and subsurface flow will contain more parameters to account for subsurface flow conditions, infiltration, evaporation, etc. The parameters will be estimated from existing information on the geology, topography, vegetation, channel cross-sections, etc. Almost all this information can be derived from existing maps, aerial photographs, bridge surveys, dam surveys, etc. The estimated parameters will be optimized to provide best fit to observed hydrographs.

Surface runoff from each segment will be calculated by the state variable model of surface flow fitted to each segment individually. As mentioned previously, the subsurface flow model of each segment will likely consist of a smaller number of elements than the corresponding surface flow model, i.e. each element of the subsurface flow model will receive inputs in the form of infiltration from several elements of the surface flow model.

The general state variable model will continuously calculate the streamflow from rainfall in each successive watershed segment, and from flows measured or calculated at upstream flowpoints. All calculations will be carried independently for each segment so that areal variations

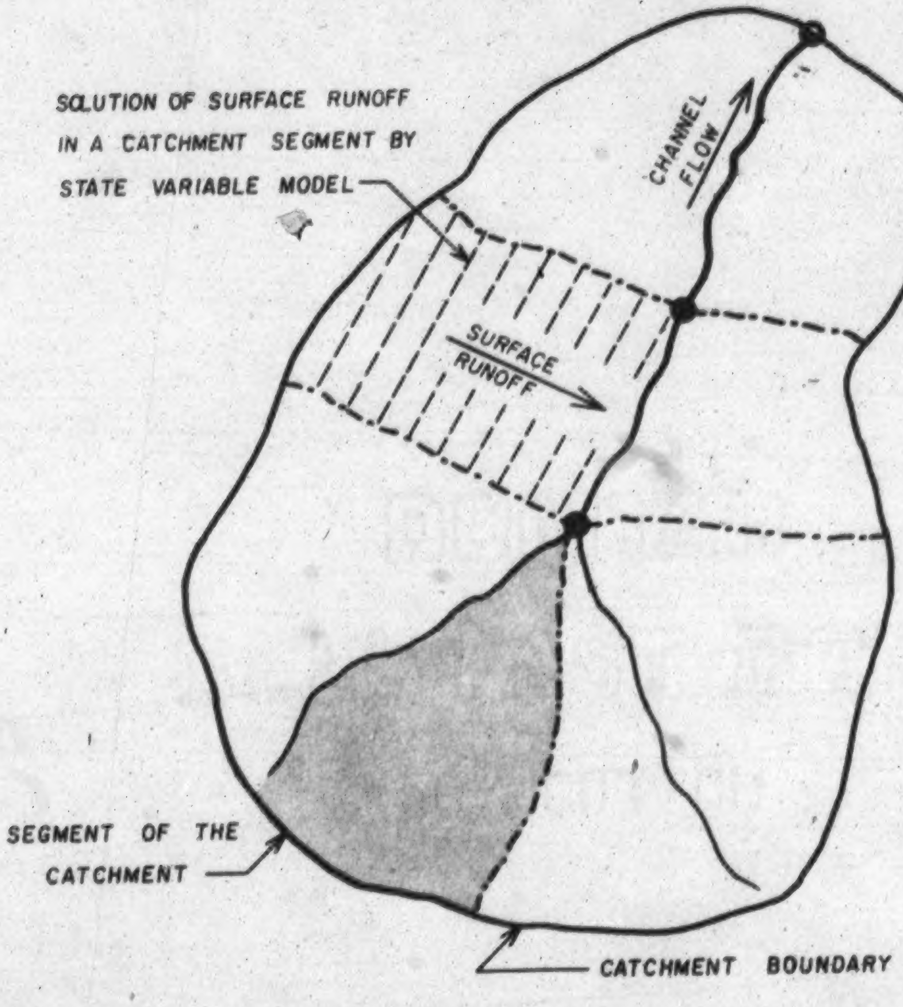
SOLUTION OF SURFACE RUNOFF IN A CATCHMENT SEGMENT BY STATE VARIABLE MODEL
CHANNEL FLOW
SURFACE RUNOFF
SEGMENT OF THE CATCHMENT
CATCHMENT BOUNDARY

Figure 6-8. Definition sketch for application of the state variable model in simulating surface runoff from a natural watershed.

in rainfall and topographic features can be represented. There will be no limit to the number of segments that can be used.

In summary, the concept of state and the state variable method form a skeleton of a practical and physically relevant hydrologic model. The state variable model can reasonably well represent spatial and temporal variations of rainfall and topography, and is suitable for continuous simulation by a digital computer. The structure of the model allows for improvement of the performance of the model by: (1) changing the inter-relationships between individual components, such as the infiltration, evapotranspiration, etc., as they become better understood, (2) optimizing parameters during the simulation, and (3) increasing the number of segments or elements into which the watershed has been subdivided. The property (3) gives the state variable model considerable flexibility since it can be easily applied to different watersheds. For the same reason the state variable model has also potential for use in simulation of ungauged watersheds.

CHAPTER VII

CONCLUSIONS AND RECOMMENDATIONS

7-1 Conclusions

The study shows that unsteady spatially varied overland flow from an impervious plane can be simulated by a number of interacting elements operating as reaches with uniform flow subjected to impulse inputs. Mathematically the simulation model is conveniently described by the state space method of system representation.

The concept of state enables expression of the antecedent conditions, i.e., to determine the state of a watershed, by means of a set of state variables which have a clear physical interpretation, such as the depth of flow. The mathematical form of the model is suitable for computer solution.

The state variable model developed in the present study contains only one parameter, α, which depends primarily on the discharge formula used (for laminar or turbulent flow) and also on the time and space increments used in the calculation. No attempt has been made to derive a criterion for the choice of the time and space increments because of the experimental limitations imposed by the size of the laboratory catchment. It was found, however, that the calculated hydrographs did not differ significantly for time increments of 0.1 sec and 0.01 sec respectively. With respect to the number of segments used in simulation it was found that increasing the number of segments resulted in a faster response to a given input. Theoretically, there could be an infinite number of segments. For practical reasons, however, it was concluded that some judgement must be used to find an optimum number of segments which would be consistent with the accuracy of other input parameters, computer storage availability, etc. The use of a finite number of segments may require empirical evaluation of a correction factor applied to the discharge (output) equation.

The study shows that rainfall affects the mechanics of overland flow on a hydraulically smooth boundary. The rainfall intensity is the strongest single parameter affecting the flow. The relationship $f_r = C_r/Re$ describes adequately the flow resistance of overland flow under rainfall within the range of experimental conditions covered in the investigation, i.e., $Re \leq 30$, $U \leq 10$ cm/sec, $3 \leq i \leq 12$ cm/hr, and for the galvanized wrought iron runoff surface treated with hydrochloric acid, having Manning's n approximately equal to 0.015. The coefficient C_r is a function of rainfall intensity, Reynold's number and the velocity of flow.

Simulated hydrographs by the state variable model showed increased outflow rates after rain cessation in the form of a sudden peak. This increase in discharge was attributed to the change in the friction factor fr; this coefficient is a function of rainfall intensity.

The state variable model is capable of defining overland flow for both cases of uniformly distributed rainfall and temporally and spatially varied rainfall. The results showed that the calculated hydrographs were in good agreement with the experimental data. The fit of the simulated hydrographs to the experimental data was slightly better for milder slopes and lower rainfall intensities.

The experimental results showed the surface runoff from an impervious surface to be highly nonlinear. The apparent time to equilibrium, a measure of the time required to reach steady state outflow, for fixed physical parameters of the catchment (length and roughness) was found to be a function of rainfall intensity, contrary to the unit hydrograph theory which assumes a constant time to equilibrium.

Instantaneous unit hydrographs (IUH) derived by differentiation from observed experimental equilibrium hydrographs (S-curves) differed from each other by as much as 50 per cent in peak values, time to peak, and total time base. Accordingly, computed hydrographs by the instantaneous unit hydrograph model were unrealistic. It was concluded that there exists an infinite number of IUH for for a given catchment, and each represents a linear approximation of the rainfall-runoff process for a given rainfall intensity. As the rainfall intensity changes the particular linear approximation becomes progressively worse.

The kinematic wave model of surface runoff was found to predict the experimental hydrographs quite satisfactory. The model was able to respond correctly to changes in rainfall intensity and slope of the runoff plane. However, the model was not suitable to account for temporal and spatial variations of rainfall. It also did not include a factor for the raindrop impact effect. Hydrographs simulated by the kinematic wave model are sharp crested owing to the lack of a point of inflection on the rising limb of the hydrograph. It was concluded that because of this peculiarity the time to equilibrium, predicted by the kinematic wave model would be generally shorter than the observed time.

7-2 Recommendations

From the results of the foregoing study the following recommendations can be made:

(1) Surface runoff experiments should be carried out on a larger laboratory catchment. A procedure employing direct outflow rate measurement and a more efficient means of regulation and control of the input could reduce the number of consecutive runs necessary and also produce a better definition of details.

(2) Detailed experimental studies are needed to examine the role of the rainfall impact effect and surface roughness in overland flow. The transition range of overland flow under rainfall from laminar to turbulent need to be investigated in order that a proper discharge formula can be selected.

(3) Experiments should be carried out to simulate surface runoff from urban areas by the state variable model and to determine criteria for finding an optimum number of segments into which a simulated catchment need be subdivided.

(4) The results describing the scope of existing experimental conditions and performance of the state variable model should be carefully considered in the design of a future general hydrologic model. Application of the concepts of state and state variables in general hydrologic simulation will result in a worthwhile expansion of the theory and experimental data presented herein.

LIST OF REFERENCES

Amorocho, Y., Orlob, G.T., "Nonlinear analysis of hydrologic systems", Water Resources Center Contribution No. 40, University of California, 1961.

Amorocho, Y., Hart, W.E., "The use of laboratory catchments in the study of hydrologic systems", Journal of Hydrology, Vol. 3, 1965.

Amorocho, Y., "The nonlinear prediction problem in the study of the runoff cycle", Water Resources Research, Vol. 3, No. 3, 1967.

Amorocho, Y., Brandstetter, A., "Determination of nonlinear functional response functions in rainfall-runoff processes", Water Resources Research, Vol. 7, No. 5, October, 1971.

Balakrishnan, A.V., "A general theory of nonlinear estimation problems in control systems", Journal of Mathematical Analysis and Applications, February, 1963.

Balakrishnan, A.V., "Stochastic system identification technique," Proceedings of an Advance Seminar Conducted by the Mathematics Research Center and the United States Army at the University of Wisconsin, Madison, October 2-4, 1967.

Barre de Saint Venant, A.J.C., "Etudes theoriques et practiques sur le mouvement des eaux courantes", Paris, 1848.

Bell, F.C., Kar, S.O., "Characteristic response times in design flood estimation", Journal of Hydrology, Vol. 8, 1969.

Bendat, Y.S., Piersol, A.G., Measurement and Analysis of Random Data, John Wiley & Sons, Inc., New York, 4th printing, 1968.

Blench, T., Dimensional Analysis and Dynamical Similarity for Hydraulic Engineers, University Bookstore, Edmonton, Alberta, Canada, 1969.

Brutsaert, W., "De Saint Venant equations experimentally verified", Journal of the Hydraulics Division, ASCE, Vol. 97, No. HY9, September, 1971.

Byars, E.F., Snyder, R.D., Engineering Mechanics of Deformable Bodies, 2nd edition, International Textbook Co., Scranton, Pennsylvania, 1969.

Chen, CH.L., Chow, V.T., "Hydrodynamics of mathematically simulated surface runoff", Hydraulic Engineering Series No. 18, Department of Civil Engineering, University of Illinois, Urbana, Illinois, August, 1968.

Chery, D.L., "Construction, instrumentation, and preliminary verification of a physical hydrologic model", Joint Report of the U.S. Department of Agriculture and the Utah State University, July, 1965.

Chery, D.L., "Design and test of a physical watershed model", Journal of Hydrology, Vol. 4, pp-224-235, 1966.

Chery, D.L., "A review of rainfall-runoff physical models as developed by dimensional analysis and other methods", Water Resources Research, Vol. 3, No. 3, 1967.

Chiw, Ch.L., Huang, J.T., "Nonlinear time varying model of rainfall-runoff relation", Water Resources Research, Vol. 6, No. 5, October, 1970.

Chow, V.T., Open Channel Hydraulics, McGraw-Hill Co., 1959.

Chow, V.T., Harbaugh, T.E., "Raindrop production for laboratory watershed experimentation", Journal of Geophysical Research, Vol. 70, No. 24, December, 1965.

Chow, V.T., Hydrologic Determination of Waterway Areas for the Design of Drainage Structures in Small Drainage Basins, University of Illinois Engineering Experimental Station Bulletin 462, 1962.

Chow, V.T., Handbook of Applied Hydrology, McGraw-Hill Co., New York, pp. 14-14, 1964.

Chow, V.T., "Laboratory study of watershed hydrology", Proceedings of the International Hydrology Symposium, Fort Collins, Vol. 1, September, 1967.

City of Calgary Flood Study, Report by Montreal Engineering Co., 1972.

Conte, S.D., Elementary Numerical Analysis, McGraw-Hill Co., 1965.

Coughanowr, D.R., Koppel, L.B., Process Systems Analysis and Control, McGraw-Hill Co., 1965.

Crawford, N.H., Linsley, R.K., "Digital simulation in hydrology: Stanford watershed model IV", Technical Report No. 39, Department of Civil Engineering, Stanford University, July, 1966.

Das, K.C., "Laboratory modeling and overland flow analysis", Ph.D. thesis presented to Purdue University at LaFayette, Indianna, 1970.

Derusso, P.M., Roy, R.J., and Close, Ch.M., State Variables for Engineers, John Wiley & Sons, Inc., New York, 1967.

Diskin, M.H., A Basic Study of the Linearity of the Rainfall-Runoff Process in Watersheds, Ph.D. thesis, University of Illinois, Urbana, Illinois, 1964.

Dooge, J.C.I., "A general theory of the unit hydrograph", Journal of Geophysical Research, Vol. 64, No. 1, 1959.

Elgerd, O.I., Control Systems Theory, New York, McGraw-Hill Co., 1967.

Grace, R.A., Eagleson, P.S., "Similarity criteria in the surface runoff process", Laboratory Report No. 77, Massachusetts Institute of Technology, Hydrodynamics Laboratory, July, 1965.

Grace, R.A., Eagleson, P.S., "The modeling of overland flow", Water Resources Research, 1966.

Grace, R.A., Eagleson, P.S., "Construction and use of a physical model of the rainfall-runoff process", Technical Note No. 11, Massachusetts Institute of Technology, Hydrodynamics Laboratory, June, 1966.

Grace, R.A., Eagleson, P.S., "Scale model of urban runoff from storm rainfall," Journal of the Hydraulics Division, ASCE, Vol. 93, No. HY3, May, 1967.

Hall, M.J., "A critique of methods of simulating rainfall", Water Resources Research, Vol. 6, No. 4, August, 1970.

Harbaugh, T.E., "Time distribution of runoff from watersheds", Ph.D. thesis presented to the University of Illinois, Urbana, Illinois, 1966.

Harbaugh, T.E., Chow, V.T., "A study of conceptual watershed roughness", Paper presented at the XIIth I.A.H.R. Congress, Fort Collins, Colorado, September, 1967.

Henderson, F.M., Wooding, R.A., "Overland flow and groundwater flow from a steady rainfall of finite duration", Journal of Geophysical Research, Vol. 69, No. 8, April, 1964.

Henderson, F.M., Open Channel Flow, MacMillan Co., 1969.

Hildebrand, F.B., Introduction to Numerical Analysis, McGraw-Hill Inc., 1956.

Hsu, J.C., Meyer, A.U., Modern Control Principles and Applications, McGraw-Hill Inc., 1968.

International Hydrology Symposium - Proceedings, Fort Collins, Colorado, September, 1967.

Izzard, C.F., Agustine, M.T., "Preliminary report on analysis of runoff from simulated rainfall on a paved plot", Trans. AGU, Vol. 24, No. 500, 1943.

Izzard, C.F., "The surface profile of overland flow", Trans. AGU, Vol. 25, 959, 1944.

Izzard, C.F., "Hydraulics of runoff from developed surfaces", Highway Research Board, Proceedings, 26, 129, 1947.

Kerby, W.S., "Time of concentration for overland flow", Civil Engineering, Vol. 29, No. 3, March, 1959.

Kirkly, M.Y., Chorley, R.Y., "Throughflow, overland flow and erosion", Bulletin of the International Association of Scientific Hydrology, XII, No. 3, September, 1967.

Kirpich, Z.P., "Time of concentration of small agricultural watersheds", Civil Engineering (New York), Vol. 10, No. 6, June, 1940.

Kulandaiswang, V.C., A Basic Study of the Rainfall Excess-Surface Runoff Relationship in a Basin System, Ph.D. thesis, University of Illinois, Urbana, Illinois, 1964.

Langill, A.W., Automatic Control Systems Engineering, Englewood Cliffs, N.J., Prentice-Hall, 1965.

Laws, Y.O., "Measurement of the fall velocity of water drops and raindrops", Trans. AGU, 22, 709, 1941.

Laws, Y.O., Parsons, D.A., "The relation of raindrop size to intensity, Trans. AGU, 24, 452, 1943.

Lighthill, M.J., Whitham, G.B., "On kinematic waves: I - flood movement in long rivers", Proceedings Royal Society (London), Vol. 229, No. 1178, May, 1955.

Linsley, R.K., Kohler, M.A., and Paulhus, Y.L.H., Hydrology for Engineers, McGraw-Hill Inc., 1958.

MacFarlane, A.G.J., Dynamical System Models, George G. Harrap & Co., London, 1970.

Mariotte, E., Traite du Mouvement des eaux et des autres corps fluides, E. Michallet, Paris, 1686.

Minshall, N.E., Predicting storm runoff on small experimental watersheds", Journal of the Hydraulics Division, ASCE, Vol. 86, No. HY8, August, 1960.

Moigno, F.L.N.M., Lecons de Calcul d'apres Cauchy, Paris, 1844.

Morgali, J.R., "Laminar and turbulent overland flow hydrographs", Journal of the Hydraulics Division, ASCE, Vol. 96, No. HY2, February, 1970.

Nash, J.E., "Determining runoff from rainfall", Proceedings, Institute of Civil Engineers, Vol. 10, June, 1958.

Naslin, P., The Dynamics of Linear and Nonlinear Systems, Blackie, London, 1965.

O'Donnell, T., "Methods of computation in hydrograph analysis and synthesis", Recent trends in Hydrograph Synthesis, Committee for Hydrological Research T.N.O., Proceedings and Information No. 13, Hague, Netherlands, 1966.

Ogata, K., State Space Analysis of Control Systems, Prentice-Hall Inc., Englewood Cliffs, N.J., 1967.

Ogata, K., Modern Control Engineering, Prentice-Hall Inc., Englewood Cliffs, N.J., 1970.

Perrault, P., De L'origin des fontaines, Pierre e Petit, Paris, 1674.

Ragan, R.M., Duru, J.O., "Kinematic wave monograph for times of concentration", Journal of the Hydraulics Division, ASCE, Vol. 98, No. HY10, October, 1972.

Ross, C.N., "The calculation of flood discharge by the use of time contour plan", Trans. Institute Engineers (Australia), Vol. 2, pp. 85-92, 1921.

Rouse, Hunter, and Simon, History of Hydraulics, Iowa Institute of Hydraulic Research, State University of Iowa, 1957.

Schreiber, D.L., Bender, D.L., "Obtaining overland flow resistance by optimization", Journal of the Hydraulics Division, ASCE, Vol. 98, No. HY3, March, 1972.

Schwartz, R.J., Friedland, B., Linear Systems, McGraw-Hill Co., New York, 1965.

Seddon, J., "River hydraulics", Trans. ASCE, Vol. 43, pp. 217-229, 1900.

Sherman, L.K., "Streamflow from rainfall by the unit-graph method", Engineering News-Record, Vol. 108, pp. 501-505, 1932.

Singh, K.P., "Non-linear instantaneous unit hydrograph theory", Journal of the Hydraulics Division, ASCE, Vol. 90, No. HY2, 1964.

Synder, F.F., "Synthetic unit hydrographs", Transactions American Geophysical Union, Vol. 19, part 1, 1938.

Stein, P.K., Measurement Engineering, Vol. II, "Non-self generating transducers", Stein Engineering Services, Inc., 1962.

Strelkoff, T., "Numerical solution of Saint-Venant equations", Journal of the Hydraulics Division, ASCE, Vol. 96, No.HY9 , September, 1970.

System Approach to Hydrology, Proceedings of the first bilateral U.S.-Japan Seminar in Hydrology held at the East-West Center of the University of Hawaii, Honolulu, Water Resources Publication, Fort Collins, Colorado, January, 1971.

Taylor, A.B., Schwartz, H.E., "Unit hydrograph lag and peak flow related to basin characteristics", Trans. AGU, Vol. 38, April, 1952.

Thaler, G.J., Pastel, M.P., Analysis and Design of Nonlinear Feedback Control Systems, McGraw-Hill Co., 1962.

Toebes, C., "Hydrology - a changing science", Soil & Water, published by the Soil Conservation & Rivers Control Council of New Zealand, Vol. 4, No. 3, March, 1968.

Vemuri, V., Vemuri, N., "On the system approach in hydrology", Bulletin of the International Association of Scientific Hydrology, XV, No. 2, July, 1970.

Wenzel, H.G., Wang, R.Ch.T., "The mechanics of a drop after striking a stagnant water layer", Research Report No. 30, Department of Civil Engineering, University of Illinois, Urbana - Champaign, 1970.

Woo, D.C., Brater, E.R., "Spatially varied flow from controlled rainfall", Journal of the Hydraulics Division, ASCE, Vol. 88, No. HY6, November, 1962.

Yen, B.Ch., Chow, V.T., "A study of surface runoff due to moving rainstorms", Civil Engineering Studies, Hydraulic Engineering Series No. 17, Department of Civil Engineering, University of Illinois, Urbana, Illinois, June, 1968.

Yoon, Y.N., Wenzel, H.G., "Mechanics of sheet flow under simulated rainfall", Journal of the Hydraulics Division, ASCE, Vol. 97, No. HY9, September, 1971.

Yu, Y.S., McNown, J.S., "Runoff from impervious surfaces", Journal of Hydraulic Research, International Association for Hydraulic Research, Vol. 2, No. 1, 1964.

Zadeh, L.A., Desoer, Ch.A., Linear System Theory, McGraw-Hill Co., 1963.

APPENDIX A

LOAD BEAM:

STRAIN - RESISTANCE RELATIONSHIP

A-1 Load Beam: Stress - Strain Relationship

Consider a beam with two symmetrically acting forces of equal magnitude P, as shown in Figure A-1. It is seen from the stress diagram shown in Figure A-2 that

$$\frac{\sigma_y}{y} = \frac{\sigma_a^{max}}{a} = k \qquad \text{(A-1)}$$

or

$$\sigma_y = ky \qquad \text{(A-2)}$$

where σ_y is the normal stress at the distance y from the neutral axis.

With respect to the cross-section diagram shown in Figure A-2 it is seen that the resultant normal force is

$$R_n = \int_{area} \sigma_y \, dA = k \int_{area} y \, da = 0 \qquad \text{(A-3)}$$

and the resultant internal moment M is

$$M = \int_{area} y \, \sigma_y \, dA = k \int_{area} y^2 \, dA = kI \qquad \text{(A-4)}$$

where I denotes the second moment of the cross-sectional area about the horizontal centroidal axis. Thus,

$$k = \frac{M}{I} \qquad \text{(A-5)}$$

The stress - strain relationship for a uniaxial state of stress is expressed by Hooke's Law

$$\sigma = E\varepsilon \qquad \text{(A-6)}$$

where E is the modulus of elasticity and ε is the strain. Combining Equations (A-2) and (A-6) gives

$$\varepsilon = \frac{My}{EI} \qquad \text{(A-7)}$$

or

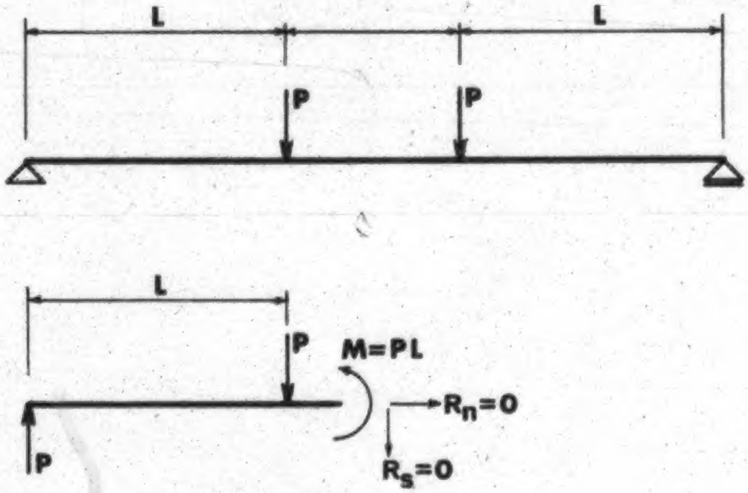
L
L
P
P
L
P
M=PL
$R_n=0$
P
$R_s=0$

Figure A-1. Definition sketch of a beam in bending.

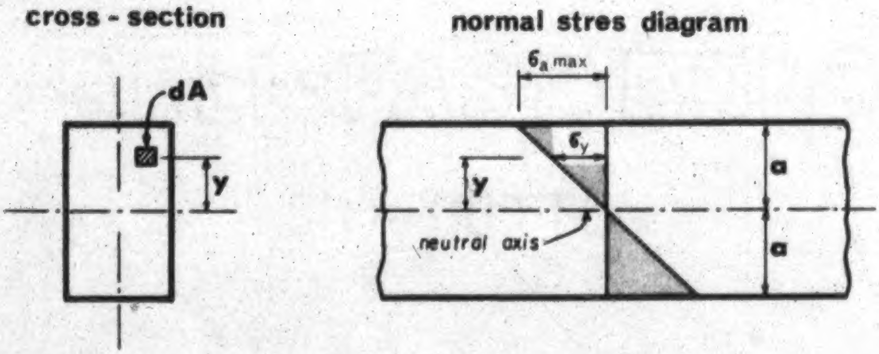
cross - section
normal stres diagram
dA
y
$\sigma_{a\,max}$
σ_y
y
neutral axis
a
a

Figure A-2. Stress distribution diagram.

$$\varepsilon = \frac{PLy}{EI} \tag{A-8}$$

and

$$\varepsilon \propto P \tag{A-9}$$

It is thus shown that in the case of elastic bending of a beam with symmetrical sections the strain is linearly proportional to the applied force P.

A-2 Strain Gauge: Strain - Resistance Relationship

The mechanical strain ε in a beam will give rise to consequent electrical resistance change, ΔR, in a strain gauge mounted on the beam in accordance with the relationship

$$\frac{\Delta R}{R} = \varepsilon K \tag{A-10}$$

where K is a gauge factor. Gauge factor (G.F.) is a property of the strain gauge which relates output resistance change to input mechanical strain and is defined as

$$\text{G.F.} = \frac{\text{unit resistance change in the strain gauge}}{\text{mechanical strain in the specimen beneath the gauge}}$$

A-3 Sensitivity of Load Transducer

When the instrument with which the strain gauge circuit output is measured is a voltage-sensing device, the circuit output sensitivity may be expressed according to Stein (1962) as

$$S_V = \frac{v}{\varepsilon} n_c \, n_m \tag{A-11}$$

Also

$$v = i \, R_g \, K \, \varepsilon \tag{A-12}$$

and

$$V = i \, R_g \tag{A-13}$$

Thus,

$$S_V = V\ K\ n_c\ n_m \qquad \text{(A-14)}$$

where

S_V = system voltage sensitivity in units of microvolts circuit output per microstrain in the speciment beneath the gauge

V = voltage output from the transducer at reference applied P

v = incremental voltage output produced by the action of P (or ε)

i = current in amperes passing through the gauge

R_g = gauge resistance in Ohms

n_c = efficiency of the circuit of which the gauge is part

n_m = efficiency of signal transfer from the circuit to the voltage measuring instrument

It can be concluded, by examining Equation (A-14), that the sensitivity of a voltage-sensing device used for strain gauge transducers can be increased, for a given applied current i, by using strain gauges with higher resistance R_g and higher gauge factor K.

For further reference see Byars (1969) and Stein (1962).

APPENDIX B

DERIVATION OF A UNIT IMPULSE RESPONSE OF (1) SINGLE RESERVOIR, (2) SERIES OF RESERVOIRS

B-1 Unit Impulse Response of a Single Reservoir

The system under consideration is shown in Figure B-1. The relationship between storage, S, and discharge, q, is linear and has the form

$$q = \frac{S}{k} \tag{B-1}$$

where k is a constant. Equation of continuity of the reservoir is

$$\frac{dS}{dt} = i - q \tag{B-2}$$

or

$$\frac{dS}{dt} = i - \frac{S}{k} \tag{B-3}$$

where i is the volumetric rate of inflow.

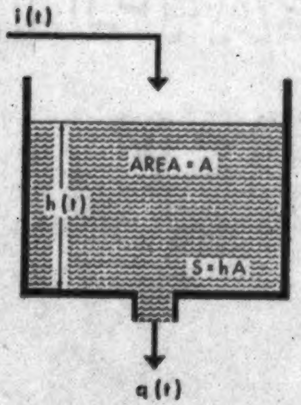

$q = \frac{S}{k}$

k = constant

S = storage

Figure B-1. Definition sketch of a single linear reservoir.

When the system described by Equation (B-3) operates at a steady state, Equation (B-3) becomes

$$\frac{dS_*}{dt} = 0 \tag{B-4}$$

and

$$i_* - \frac{S_*}{k} = 0 \tag{B-5}$$

where the asterisk denotes steady state values. Subtracting Equation (B-4) and (B-5) from Equation (B-3) gives

$$\frac{d(S-S_*)}{dt} = (i-i_*) - \frac{1}{k}(S-S_*) \tag{B-6}$$

or

$$\frac{dZ}{dt} = I - \frac{Z}{k} \tag{B-7}$$

where $Z = S-S_*$ and $I = i-i_*$ are deviation variables.

Taking Laplace transform of Equation (B-7) gives a transfer function between input and storage

$$\frac{Z(s)}{I(s)} = \frac{1}{s + \frac{1}{k}} \tag{B-8}$$

The transfer function relating outflow and inflow can be obtained as follows. The discharge-storage relationship at a steady state is

$$q_* = \frac{S_*}{k} \tag{B-9}$$

which subtracted from

$$q = \frac{S}{k} \tag{B-10}$$

gives

$$q-q_* = \frac{1}{k}(S-S_*)$$

Substitution of the deviation variables, $Q = q-q_*$ and $Z = S-S_*$ gives

$$Q = \frac{Z}{k} \tag{B-11}$$

Laplace transform of Equation (B-11) is

$$\frac{Q(s)}{Z_{(s)}} = \frac{1}{k} \qquad \text{(B-12)}$$

Multiplying Equation (B-8) by Equation (B-12) gives the desired transfer function between input and output

$$\frac{Q(s)}{I_{(s)}} = \frac{1}{ks + 1} \qquad \text{(B-13)}$$

For a unit impulse input $I_{(s)} = 1$ the transfer function given by Equation (B-13) becomes

$$Q_{(s)} = \frac{1}{ks + 1} \qquad \text{(B-14)}$$

Inversion of Equation (B-14) into the time domain gives the unit impulse response of a single reservoir

$$u(t) = Q(t) = \frac{1}{k} e^{-t/k} \qquad \text{(B-15)}$$

Response of the system to an input i(t) can be found by application of the convolution integral

$$q(t) = \int_{o}^{t} i(t)\, u(t-\tau) d\tau \qquad \text{(B-16)}$$

For an input of a constant magnitude i one obtains

$$q(t) = i \int_{o}^{t} \frac{1}{k}\, e^{\frac{-t-\tau}{k}} d\tau \qquad \text{(B-17)}$$

which integrates into

$$q(t) = i[e^{-t/k}\, e^{\tau/k}]_{o}^{t} \qquad \text{(B-18)}$$

or

$$q(t) = i(1 - e^{-t/k}) \qquad \text{(B-19)}$$

B-2 Unit Impulse Response of a Series of Reservoirs

The system under consideration is shown in Figure B-2. Transfer function of a system consisting of n identical linear non-interacting reservoirs can be derived by induction. The transfer function between input and output for each tank is given by Equation (B-13) and the input into the second, third, etc., reservoir is the output from the first, second, etc., reservoir. Thus, the transfer function relating the output from the nth reservoir, q_n, to the input i is

$$\frac{Q_n(s)}{I(s)} = \left(\frac{1}{ks + 1}\right)^n \qquad \text{(B-20)}$$

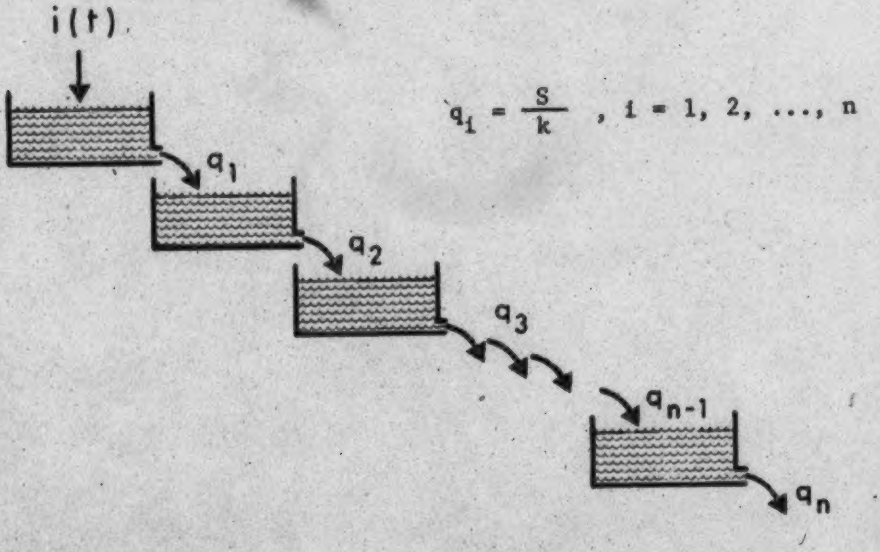

$$q_i = \frac{S}{k} \quad , \; i = 1, 2, \ldots, n$$

Figure B-2. Definition sketch of a series of linear non-interacting reservoirs.

The unit impulse response of the system can be derived conveniently by induction. Consider a system consisting of two reservoirs in series. The transfer function of the system is

$$\frac{Q_2(s)}{I(s)} = \left(\frac{1}{ks + 1}\right)^2 \tag{B-21}$$

Substituting I(s) = 1 for a unit impulse gives

$$Q_2(s) = \frac{1}{k^2} \frac{1}{(s + \frac{1}{k})^2}. \tag{B-22}$$

Applying partial fraction technique yields

$$Q_2(s) = \frac{1}{k^2}\left[\frac{A}{(s + \frac{1}{k})^2} + \frac{B}{(s + \frac{1}{k})}\right] \tag{B-23}$$

Inversion into time domain gives

$$Q_2(t) = \frac{1}{k^2} e^{-t/k}(At + B) \tag{B-24}$$

The constants A and B can be determined from combined Equations (B-22) and (B-23)

$$\frac{1}{(s + \frac{1}{k})^2} = \frac{A}{(s + \frac{1}{k})^2} + \frac{B}{s + \frac{1}{k}} \tag{B-25}$$

Multiplying Equation (B-25) by a factor $(s + \frac{1}{k})^2$ gives A = 1, and differentiation of Equation (B-25) with respect to s gives B = 0. Thus, the solution of Equation (B-24) is

$$Q_2(t) = \frac{t}{k^2} e^{-t/k} \tag{B-26}$$

Similarly, for a system consisting of three reservoirs in series, one obtains

$$Q_3(s) = \frac{1}{k^3} \frac{1}{(s + \frac{1}{k})^3} \tag{B-27}$$

which can be expanded into

$$Q_3(s) = \frac{1}{k^3}\left[\frac{A}{(s+\frac{1}{k})^3} + \frac{B}{(s+\frac{1}{k})^2} + \frac{C}{s+\frac{1}{k}}\right] \qquad \text{(B-28)}$$

and inversion into time-domain gives

$$Q_3(t) = \frac{1}{k^3}\frac{1}{2!}\, e^{-t/k}[At^2 + Bt + C] \qquad \text{(B-29)}$$

Rewriting Equations (B-27) and (B-28) as one equation gives

$$\frac{1}{(s+\frac{1}{k})^3} = \frac{A}{(s+\frac{1}{k})^3} + \frac{B}{(s+\frac{1}{k})^2} + \frac{C}{s+\frac{1}{k}} \qquad \text{(B-30)}$$

Multiplying Equation (B-30) by the factor $(s + \frac{1}{k})^3$ gives $A = 1$, and differentiating twice with respect to s gives $B = 0$ and $C = 0$. Thus, the solution for three reservoirs in series is

$$Q_3(t) = \frac{t^2}{k^3}\frac{1}{2!}\, e^{-t/k} \qquad \text{(B-31)}$$

By induction the formula for a unit impulse response of a system consisting of n linear non-interacting tanks is derived as

$$Q_n(t) = \frac{t^{n-1}}{k^n}\frac{1}{(n-1)!}\, e^{-t/k} \qquad \text{(B-32)}$$

APPENDIX C

RAINDROP IMPACT EFFECT ANALYSES - TABLE OF MEASURED AND CALCULATED FLOW PARAMETERS

LIST OF SYMBOLS

CI = CR-24 EQ.(5-88)
CR = ALPHA*B*(H**3)/Q EQ.(5-86)
FF = FRICTION FACTOR OF LAMINAR FLOW UNDER RAINFALL. FF=CR/RE EQ.(5-76)
FR = FROUDE NUMBER
H = EQUIVALENT DEPTH OF UNIFORM FLOW. H=ST/(B*X). WHERE B AND X ARE THE WIDTH AND LENTH OF THE RUNOFF PLANE
I = RAINFALL INTENSITY
I/RE*U = DIMENSIONLESS PARAMETER EQ.(5-90)
Q = STEADY DISCHARGE FROM THE RUNOFF PLANE (CC/SEC)
RE = REYNOLD NUMBER
ST = AMOUNT OF DETAINED WATER ON THE RUNOFF PLANE DURING STEADY DISCHARGE Q (CC)
U = MEAN FLOW VELOCITY IN THE X-DIRECTION (CM/SEC)

TABLE C-1
FLOW PARAMETERS FOR SLOPE S = 0.2079

Q (CC/SEC)	ST (CC)	CR	CI	FF	H (CM)	U (CM/SEC)	RE	FR	I (CM/SEC)	I/RE*U
3.60	26.00	31.05	7.05	4.89	0.022	2.70	6.35	0.58	30.26	17.66
7.11	31.60	28.22	4.22	2.25	0.027	4.39	12.53	0.86	29.89	5.44
10.78	35.60	26.61	2.61	1.40	0.030	5.90	19.00	1.09	30.21	2.69
15.16	39.00	24.88	0.88	0.93	0.033	7.58	26.72	1.34	31.86	1.57
2.31	22.40	30.94	6.94	7.60	0.019	2.01	4.07	0.47	19.42	23.72
4.63	27.30	27.94	3.94	3.42	0.023	3.31	8.16	0.70	19.46	7.21
6.24	29.60	26.43	2.43	2.40	0.025	4.11	11.00	0.83	17.49	3.87
9.60	33.40	24.68	0.68	1.46	0.028	5.60	16.92	1.07	20.18	2.13
2.29	22.30	30.79	6.79	7.63	0.019	2.00	4.04	0.47	19.25	23.82
3.76	25.70	28.71	4.71	4.33	0.022	2.85	6.63	0.62	15.80	8.36
6.86	30.40	26.04	2.04	2.15	0.026	4.40	12.09	0.88	19.22	3.61
9.32	33.00	24.52	0.52	1.49	0.028	5.51	16.43	1.06	19.59	2.16
2.07	21.50	30.53	6.53	8.37	0.018	1.88	3.65	0.45	17.40	25.40
4.11	25.10	24.47	0.47	3.38	0.021	3.19	7.24	0.70	17.28	7.47
6.33	28.00	22.05	-1.95	1.98	0.024	4.41	11.16	0.92	17.74	3.61
8.35	29.80	20.15	-3.85	1.37	0.025	5.46	14.72	1.10	17.55	2.18

TABLE C-2
FLOW PARAMETERS FOR SLOPE S = 0.1051

Q (CC/SEC)	ST (CC)	CR	CI	FF	H (CM)	U (CM/SEC)	RE	FR	I (CM/SEC)	I/RE*U
3.57	32.60	31.20	7.20	4.96	0.027	2.14	6.29	0.41	30.01	22.33
7.01	39.90	29.13	5.13	2.36	0.034	3.43	12.36	0.60	29.47	6.96
10.43	44.50	27.16	3.16	1.48	0.037	4.57	18.39	0.75	29.23	3.48
14.15	48.20	25.44	1.44	1.02	0.041	5.72	24.94	0.91	29.74	2.08
2.58	29.00	30.39	6.39	6.68	0.024	1.73	4.55	0.35	21.69	27.49
5.06	35.50	28.42	4.42	3.19	0.030	2.78	8.92	0.51	21.27	8.58
7.44	40.00	27.65	3.65	2.11	0.034	3.63	13.11	0.63	20.85	4.38
10.25	43.30	25.46	1.46	1.41	0.036	4.62	18.07	0.77	21.54	2.58
2.33	28.00	30.29	6.29	7.37	0.024	1.62	4.11	0.34	19.59	29.39
4.75	34.70	28.28	4.28	3.38	0.029	2.67	8.37	0.50	19.97	8.93
7.06	39.00	27.01	3.01	2.17	0.033	3.53	12.44	0.62	19.78	4.50
9.56	42.20	25.27	1.27	1.50	0.035	4.42	16.85	0.75	20.09	2.70
2.02	27.00	31.32	7.32	8.80	0.023	1.46	3.56	0.31	16.98	32.69
4.11	33.00	28.11	4.11	3.88	0.028	2.43	7.24	0.47	17.28	9.82
6.02	36.90	26.83	2.83	2.53	0.031	3.18	10.61	0.58	16.87	5.00
8.15	40.00	25.24	1.24	1.76	0.034	3.97	14.37	0.69	17.13	3.00

TABLE C-3
FLOW PARAMETERS FOR SLOPE S = 0.05143

Q (CC/SEC)	ST (CC)	CR	CI	FF	H (CM)	U (CM/SEC)	RE	FR	I (CM/SEC)	I/RE*U
3.75	41.70	30.42	6.42	4.60	0.035	1.75	6.61	0.30	31.53	27.20
7.58	52.20	29.52	5.52	2.21	0.044	2.83	13.36	0.43	31.86	8.42
11.16	59.00	28.95	4.95	1.47	0.050	3.69	19.67	0.53	31.27	4.31
15.44	62.50	24.87	0.87	0.91	0.053	4.82	27.22	0.67	32.45	2.48
2.59	37.00	30.76	6.76	6.74	0.031	1.36	4.57	0.25	21.77	34.94
5.06	45.10	28.52	4.52	3.20	0.038	2.19	8.92	0.36	21.27	10.90
7.60	51.10	27.62	3.62	2.06	0.043	2.90	13.40	0.45	21.30	5.48
10.17	55.50	26.44	2.44	1.47	0.047	3.57	17.93	0.53	21.37	3.34
1.94	33.60	30.76	6.76	8.99	0.028	1.13	3.42	0.21	16.31	42.36
4.21	42.10	27.88	3.88	3.76	0.035	1.95	7.42	0.33	17.70	12.23
6.27	47.20	26.38	2.38	2.39	0.040	2.59	11.05	0.42	17.57	6.14
8.48	51.50	25.34	1.34	1.70	0.043	3.21	14.95	0.49	17.82	3.71

APPENDIX D

LIST OF COMPUTER PROGRAMS USED IN THE ANALYSIS

Program Name: MAIN (including subroutines STATE and WAVE)

Description: MAIN is designed to perform the following operations:

(1) Derivation of IUH (MAIN)

(2) Simulation of surface runoff hydrographs by:

  (a) IUH model (MAIN)

  (b) State variable model (subroutine STATE)

  (c) Kinematic wave model (subroutine WAVE)

Output from MAIN includes printed tables of time and discharge coordinates (1 sec time increment), and Cal Comp plots of derived IUH and simulated hydrographs. Subroutine CGPL (available at the Computing Center, University of Alberta) was used for plotting.

MAIN generates an S-hydrograph (using state variable model) of surface runoff from a plane of given slope and size, and for the given rainfall duration and intensity (alternatively time and discharge coordinates of S-hydrograph could be supplied). IUH is derived from smoothed S-hydrograph (subroutine SE15) by numerical differentiation (subroutine DET3). Subsequently the S-hydrograph (or any other hydrograph) is reproduced (simulated) by convolution using the derived IUH. Subroutines SE15 and DET3 are available from standard IBM subroutine package.

Subroutines STATE and WAVE simulate surface runoff hydrographs for the same conditions (duration and intensity of rainfall, slope and size of runoff plane) as specified in MAIN program.

LIST OF SYMBOLS

A = SPACE INCREMENT
AA = ADMISSABLE ERROR OF ITERATION
ALP = PARAMETER ALPHA
B = WIDTH OF THE RUNOFF PLANE
CH = DURATION OF SIMULATED RAINFALL
C(I) = FRICTION FACTOR
FC = UPPER LIMIT OF C(I).
H(I) = DEPTH OF FLOW IN THE I-TH ELEMENT
HO = DEPTH OF FLOW AT B
K = TOTAL TIME OF SIMULATION (10*SEC)
L = LENGTH OF THE RUNOFF PLANE
M = ORDER OF THE STATE VARIABLE MODEL
ND = TOTAL TIME OF THE IUH BASE (10*SEC)
P = RAINFALL INTENSITY (CM/SEC)
PPP = INTENSITY OF SIMULATED RAINFALL
Q = DISCHARGE FROM THE RUNOFF PLANE (CC/SEC)
Q(J) = ORDINATE OF SIMULATED HYDROGRAPH (CC/SEC)
QU(I)= ORDINATE OF THE IUH (CC/SEC)
R(I) = DISCHARGE FROM THE I-TH ELEMENT
S = SLOPE OF THE RUNOFF PLANE
T = TIME (SEC)
T = TIME INCREMENT (SEC)
TO = DURATION OF RAINFALL (SEC)
TOT = TOTAL TIME OF SIMULATION (SEC)
TS = TIME TO STEADY STATE RUNOFF (SEC)
TT = TIME INCREMENT (SEC)
TT(J)= ABSCISSA OF SIMULATED HYDROGRAPH (SEC)

MAIN PROGRAM
IUH GENERATION AND CONVOLUTION

```
      REAL A(10),B(10),H(10),BB(25),RR(25),R(10),Q(800),TI(400),
     1DERY(10),DH(10),ALPHA(20),Y(40),Z(40),U(400),QU(100),TU(100),
     1POP(200,9),ZZ(400),C(30),QS(200),TA(800),UQ(400)
      CCMMON MK,S,ALPHA,CH,PPP,LK,IVA
      READ(5,33) (ALPHA(I),I=1,20)
   33 FORMAT(20A4)
      IVA=1
      MK=129
      DO 350 JIM=1,2
      M=7
      G=981.
      V=.0093
      S=0.1045
      TT=.1
      DO 60 I=1,M
      A(I)=91.4*61./M
   60 CONTINUE
```

```
      ALP=8.*G*S/V
      FC=31.
      DO 2 J=1,M
      C(J)=FC
      H(J)=0.
    2 CONTINUE
      P=0.0012
      IF(JIM.EQ.2) P=0.002060838
      PRE=P
      N=1
      II=1
      T=0.
      K=400
      DO 200 L=1,K
      DO 50 I=1,M
      R(I)=ALP*61.*(H(I)**3.)/C(I)
      IF(R(I).EQ.0.) GO TO 50
      QC=R(I)/61.
      ABC=2.5*ALOG((100000.*P*V*H(I))/(1.4*QC*QC))
      C(I)=24.+ABC
      IF(C(I).GT.FC) C(I)=FC
   50 CONTINUE
      DO 51 I=1,M
      IF(P.EQ.0.) C(I)=24.
      R(I)=ALP*61.*(H(I)**3.)/C(I)
   51 CONTINUE
      Q(L)=R(M)
      TA(L)=T
      DERY(1)=P-R(1)/A(1)
      DO 70 I=2,M
      DERY(I)=P+(R(I-1)-R(I))/A(I)
   70 CONTINUE
      DO 100 I=1,M
      DH(I)=DERY(I)*TT
      H(I)=H(I)+DH(I)
  100 CONTINUE
      T=T+TT
      IF(L.LT.II) GO TO 200
      WRITE(6,301) T,R(7),H(7),C(7)
      TI(N)=T
      QS(N)=R(7)
      N=N+1
      IF(II.GE.5) GO TO 188
      II=II+9
      GO TO 200
  188 II=II+10
  200 CONTINUE
      ND=K
      CALL DET3(TT,Q,U,ND,IER)
      CALL SE15(U,Q,ND,IER)
      DO 700 I=1,ND
      IF(JIM.EQ.2) GO TO 230
      U(I)=Q(I)
      GO TO 700
  230 UQ(I)=Q(I)
  700 CONTINUE
      KU=ND/5
      DO 124 I=1,KU
      QU(I)=U(I*5)
      TU(I)=TA(I*5)
      WRITE(6,501) TU(I),QU(I)
  124 CONTINUE
  301 FORMAT('0',5X,F5.1,3F10.3)
  501 FORMAT('0',5X,F5.1,10X,F10.3)
      CALL CGPL(TU,QU,TU,KU,MK,1,1,3,1,0.,10.,12.,0.,1.,2.,ALPHA,6)
  350 CONTINUE
      MK=MK+1
      DO 300 LK=1,3
      READ(6,35) CH,PPP
   35 FORMAT(F6.1,F12.9)
      MK=129
      DO 210 IV=1,2
      NN=CH+ND/10
      P=PPP
      DO 208 J=1,NN
      NI=10*J
      IN=1
      SUM=0.
      IF(J.GT.ND/10) NI=ND
      IF(J.GT.CH) IN=10*J-10*CH
      DO 201 JJ=IN,NI
      IF(IV.EQ.2) GO TO 211
      SUM=SUM+U(JJ)
      GO TO 201
  211 SUM=SUM+UQ(JJ)
  201 CONTINUE
      Q(J)=.1*SUM*P/PRE
  208 CONTINUE
      TI(1)=1.
      DO 202 J=2,120
      TI(J)=TI(J-1)+1.
  202 CONTINUE
  299 CONTINUE
      CALL CGPL(TI,Q,TI,NN,MK,1,1,3,1,0.,10.,12.,0.,2.5,8.,ALPHA,6)
      MK=MK+1
  210 CONTINUE
      CALL STATE
      CALL WAVE
  300 CONTINUE
      STOP
      END
      SUBROUTINE STATE
      COMMON MK,S,ALPHA,CH,PPP,LK,IVA
      REAL H(30),DERY(30),R(30),A(30),RR(30),BB(30),C(30),MULT,DH(30),
     1QS(200),TI(200),ALPHA(20),N2,F(7),QX(200),QY(200),QZ(200)
      M=7
      G=981.
      V=.0093
      ALP=8.*G*S/V
      TT=.1
      DO 60 I=1,M
      A(I)=61.*91.4/M
   60 CONTINUE
      K=1200
      FC=31.
      DO 2 J=1,M
      C(J)=FC
      H(J)=0.
    2 CONTINUE
      T=0.
      II=1
      N=1
      DO 200 L=1,K
      P=0.
      IF(T.LE.CH) P=PPP
      IF(P.EQ.0.) GO TO 50
      DO 50 I=1,M
      R(I)=ALP*61.*(H(I)**3.)/C(I)
      IF(R(I).EQ.0.) GO TO 50
      QC=R(I)/61.
      ABC=2.5*ALOG((100000.*P*V*H(I))/(1.4*QC*QC))
      C(I)=24.+ABC
      IF(C(I).GT.FC) C(I)=FC
   50 CONTINUE
      DO 51 I=1,M
      IF(P.EQ.0.) C(I)=24.
      R(I)=ALP*61.*(H(I)**3.)/C(I)
   51 CONTINUE
      DERY(1)=P-R(1)/A(1)
      DO 70 I=2,M
      DERY(I)=P+(R(I-1)-R(I))/A(I)
   70 CONTINUE
      DO 100 I=1,M
      DH(I)=DERY(I)*TT
      H(I)=H(I)+DH(I)
  100 CONTINUE
  199 T=T+TT
      IF(L.LT.II) GO TO 200
      WRITE(6,301) T,R(7),H(7),C(7)
      TI(N)=T
      QS(N)=R(7)
      N=N+1
      IF(II.GE.5) GO TO 188
      II=II+9
      GO TO 200
  188 II=II+10
  200 CONTINUE
      ND=N-1
      CALL CGPL(TI,QS,TI,ND,MK,1,1,4,1,0.,10.,12.,0.,2.5,8.,ALPHA,6)
      MK=MK+1
  400 CONTINUE
  301 FORMAT(' ',F20.1,3F20.5,F30.3)
      RETURN
      END
      SUBROUTINE WAVE
      CCMMON MK,S,ALPHA,CH,PPP,LK,IVA
      REAL N,QS(200),TI(200),HH(200),ALPHA(20)
      F(H)=(ALP*(H**N)/VO)+N*ALP*TA*(H**(N-1.))-L
      L=91.4
      B=61.
      G=981.
      NEW=.0093
      AA=.00005
      N=3.
      TOT=120.
      TO=CH
      VO=PPP
      ALP=G*S/(3.*.0093)
      LL=1
      I=1
      T=.1
      TS=(L/(ALP*(VC**(N-1.))))**(1./N)
      WRITE(6,100) TS
  100 FORMAT('0',10X,'TS=',F5.2)
      IF(TO.LE.TS) GO TO 30
   76 IF(T.GT.TO) GO TO 77
      IF(T.LE.TS) Q=ALP*(VO**N)*(T**N)*B
      IF(T.GT.TS) Q=L*VC*B
      IF((10*I).GT.LL) GO TO 80
      QS(I)=Q
      TI(I)=T
      I=I+1
   80 T=T+.1
      LL=LL+1
      GO TO 76
   77 HO=(Q/(B*ALP))**(1./N)
      WRITE(6,84) HO
   84 FORMAT('0','HO=',F10.7)
      HO=VO*TS
      WRITE(6,84) HO
      GO TO 79
   30 IF(T.GT.TO) GO TO 330
      Q=B*ALP*((VO*T)**N)
      IF((10*I).GT.LL) GO TO 31
      QS(I)=Q
      TI(I)=T
      I=I+1
   31 T=T+.1
      LL=LL+1
      GO TO 30
  330 HO=(Q/(B*ALP))**(1./N)
      WRITE(6,84) HO
      HO=VO*TO
      WRITE(6,84) HO
      TOS=L/(ALP*(H0**(N-1.)))
      TP=(TOS-TO)/N
      WRITE(6,101) TP
  101 FORMAT('0',10X,'TP=',F5.2)
   78 IF(T.GT.(TO+TP)) GO TO 79
      Q=Q
      IF((10*I).GT.LL) GO TO 81
      QS(I)=Q
      TI(I)=T
      I=I+1
   81 T=T+.1
      LL=LL+1
      GO TO 78
   79 TT=0.1
      T=T-.1
      IM=1
   99 CONTINUE
      TA=TT
      IF(TO.LT.50.) TA=TP+TT
      J=0
      H0=H0
      H1=0.01
   12 H2=((H0*F(H1))-(H1*F(H0)))/(F(H1)-F(H0))
      Z=ABS(H2-H1)/ABS(H2)
      IF(Z.LE.AA) GO TO 10
      IF(J.EQ.100) GO TO 11
      J=J+1
      H0=H1
      H1=H2
      GO TO 12
   11 WRITE(6,4)
    4 FORMAT(' ',3X,'FAILED TO CONVERGE')
   10 IF(IM.EQ.2) GO TO 13
      IF((10*I).GT.LL) GO TO 83
   13 Q=ALP*B*(H2**N)
      HH(I)=H2
      QS(I)=Q
      TI(I)=T+TT
      I=I+1
      IM=2
      TT=TT+1.
      GO TO 82
   83 TT=TT+.1
   82 LL=LL+1
      IF(TT.LE.(TOT-T)) GO TO 99
      ND=I
      DO 92 J=1,ND
      WRITE(6,90) TI(J),QS(J),HH(J)
   92 CONTINUE
   90 FORMAT(' ',5X,F10.2,5X,2F8.4)
   50 CONTINUE
```

```
      IVA=IVA+1
      IF(IVA.EQ.4) MK=-MK
      CALL CGPL(TI,QS,TI,ND,MK,1,1,2,1.0,10.,12.,0.,2.5,8.,ALPHA,6)
      RETURN
      END
```

APPENDIX E

MEASURED AND SIMULATED HYDROGRAPHS BY THE STATE VARIABLE MODEL

RUNS NO. 1 TO 6, AND 10 TO 24

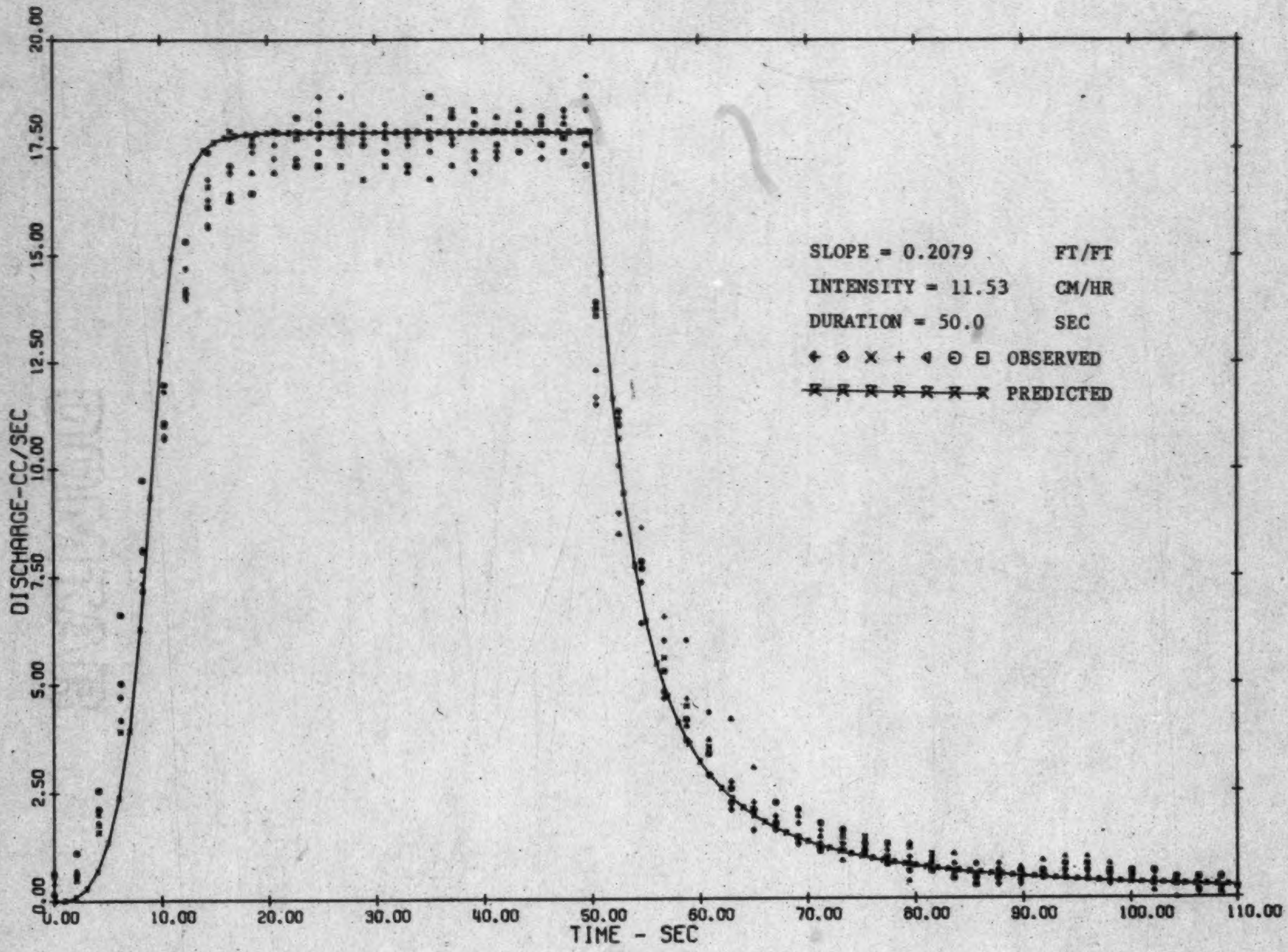

Figure E-1. Observed and predicted hydrographs (state variable model) for test 1 with uniform rainfall input.

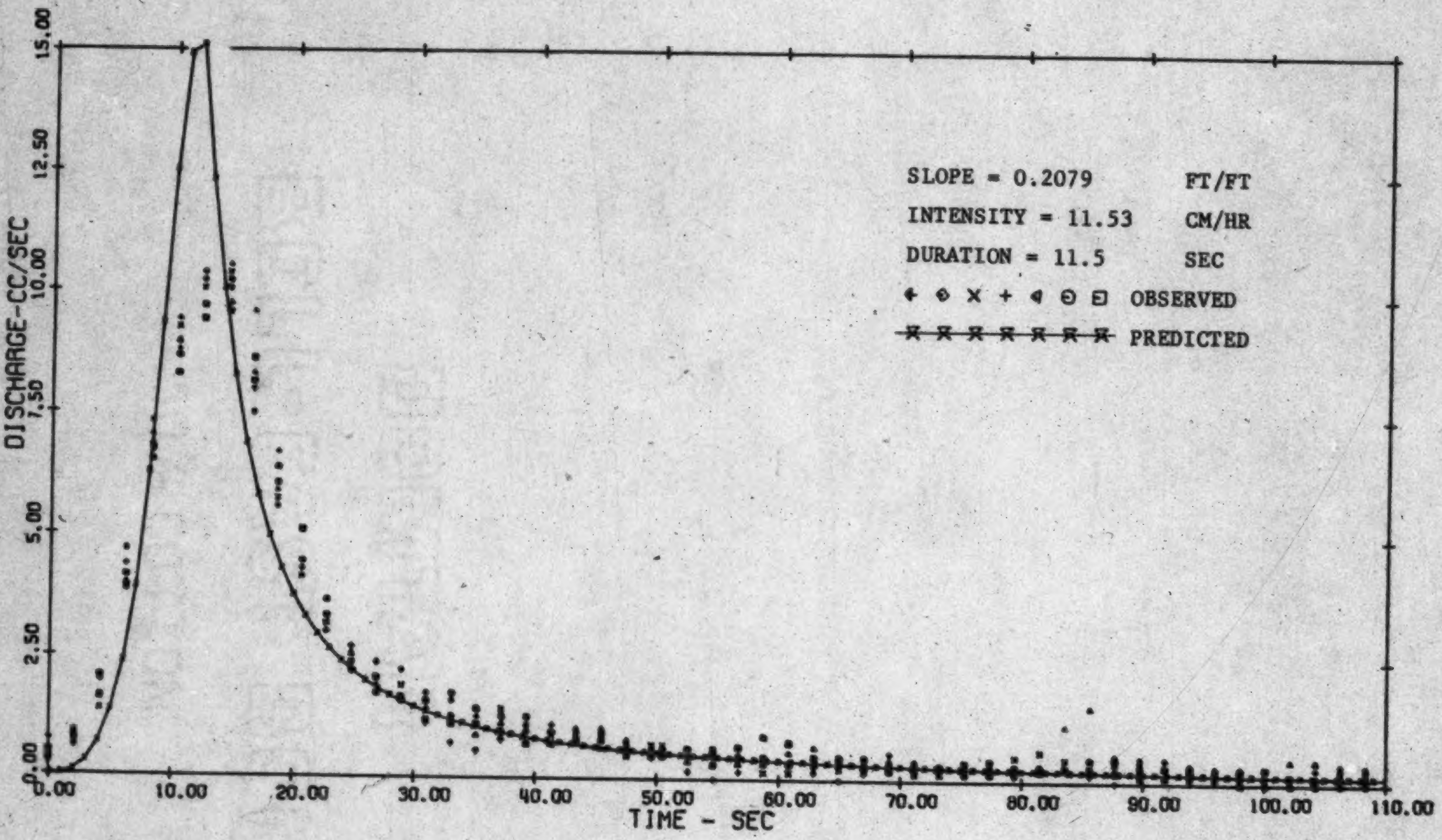

Figure E-2. Observed and predicted hydrographs (state variable model) for test 2 with uniform rainfall input.

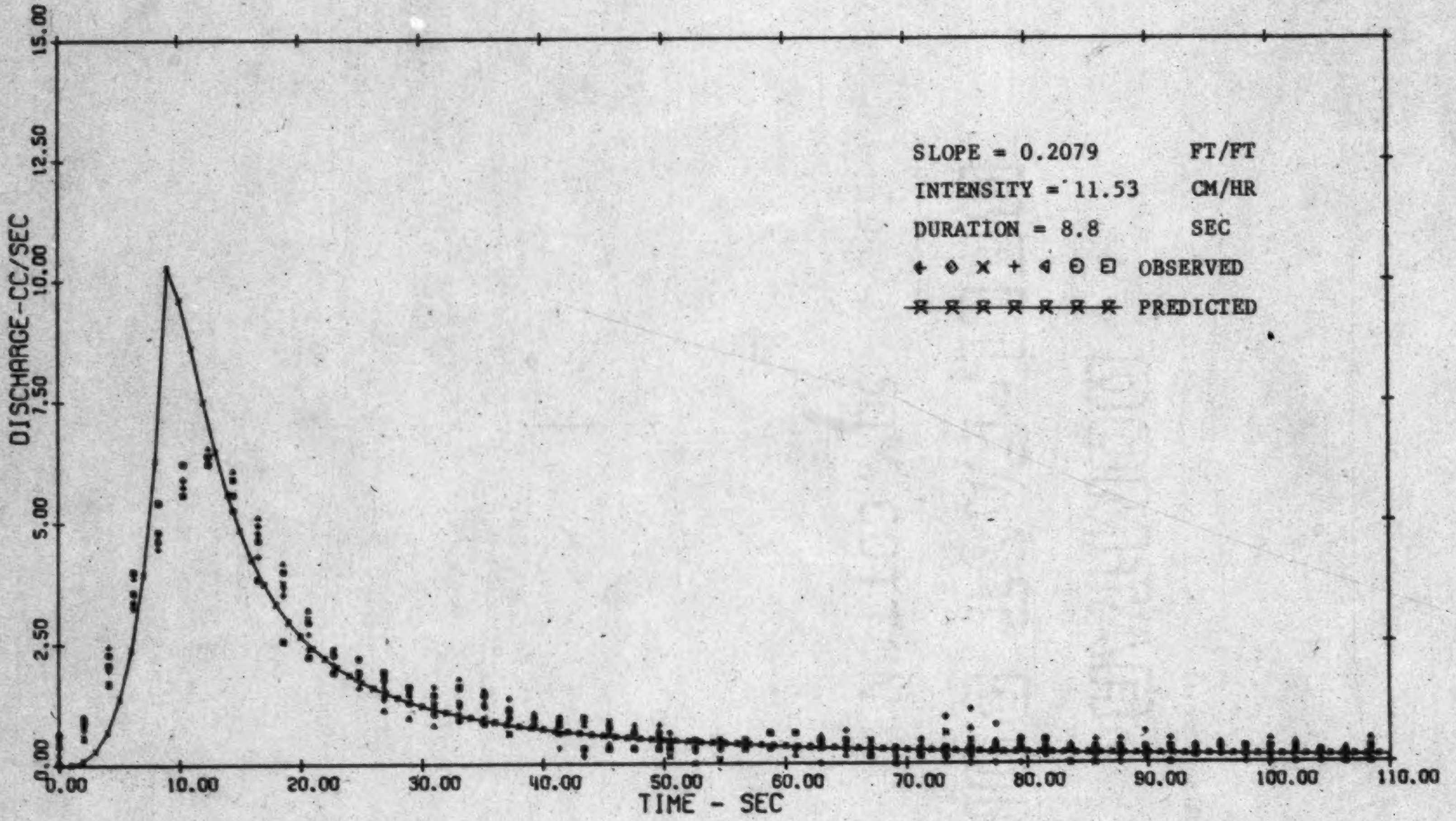

Figure E-3. Observed and predicted hydrographs (state variable model) for test 3 with uniform rainfall input.

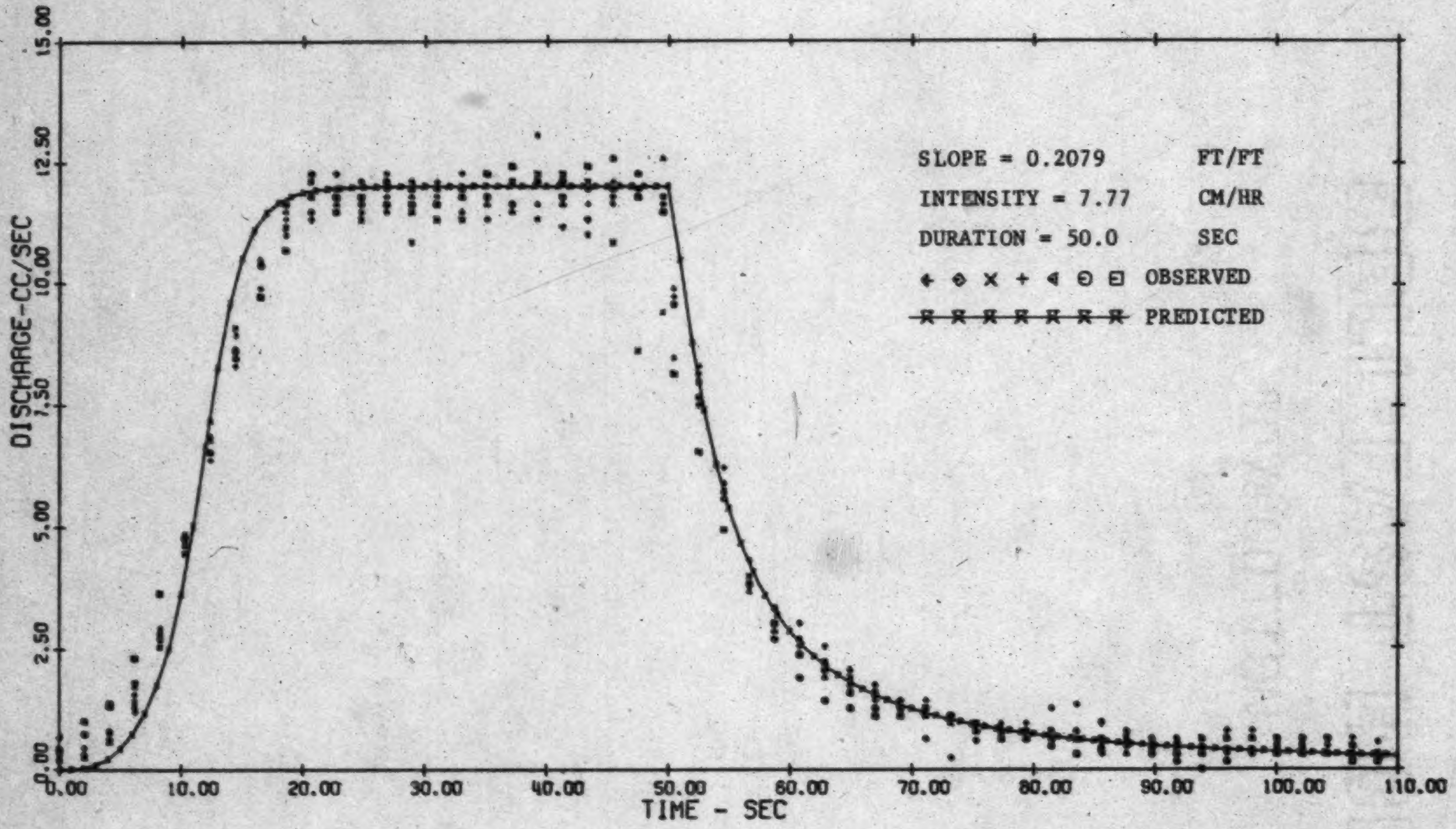

Figure E-4. Observed and predicted hydrographs (state variable model) for test 4 with uniform rainfall input.

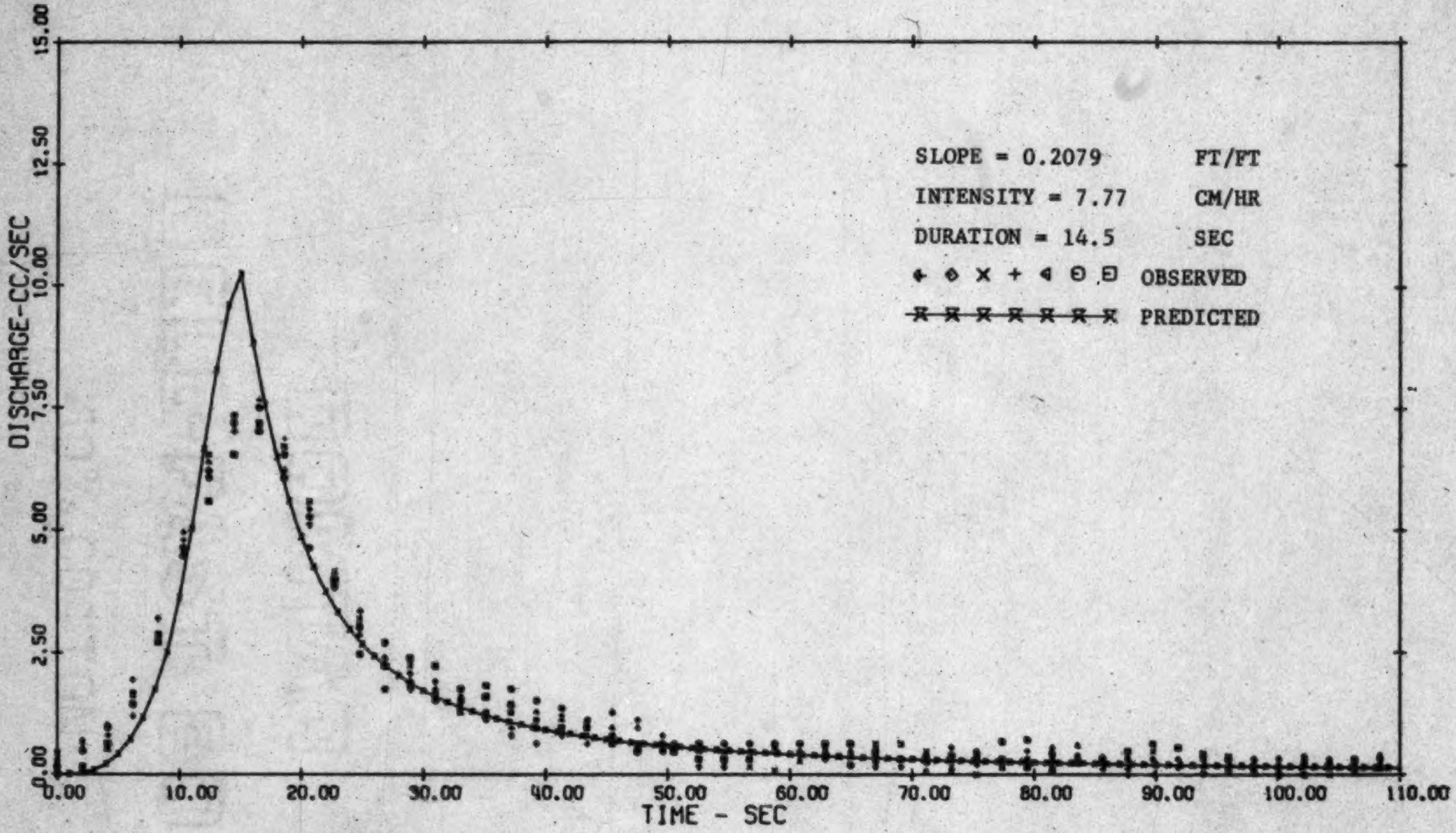

Figure E-5. Observed and predicted hydrographs (state variable model) for test 5 with uniform rainfall input.

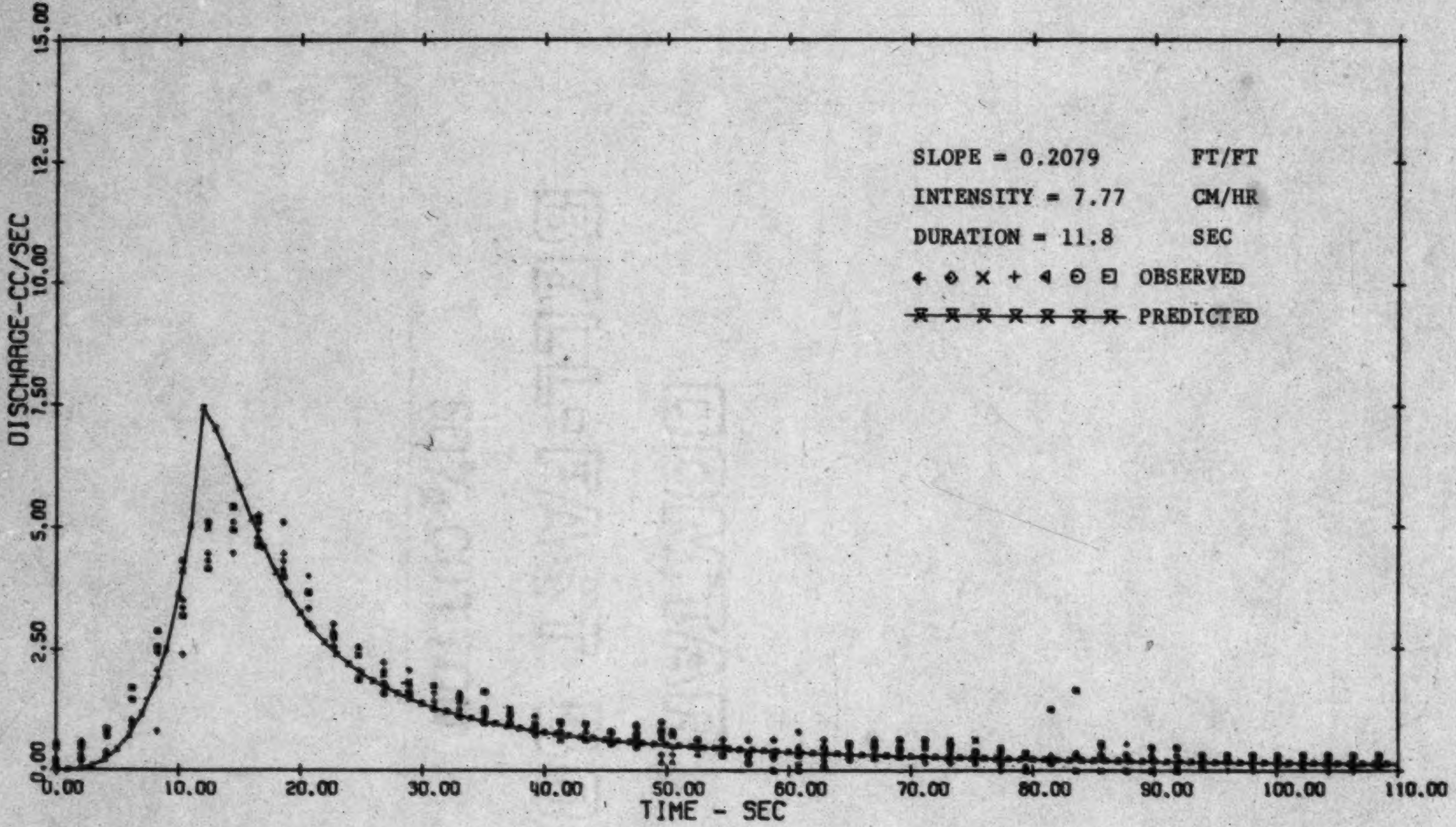

Figure E-6. Observed and predicted hydrographs (state variable model) for test 6 with uniform rainfall input.

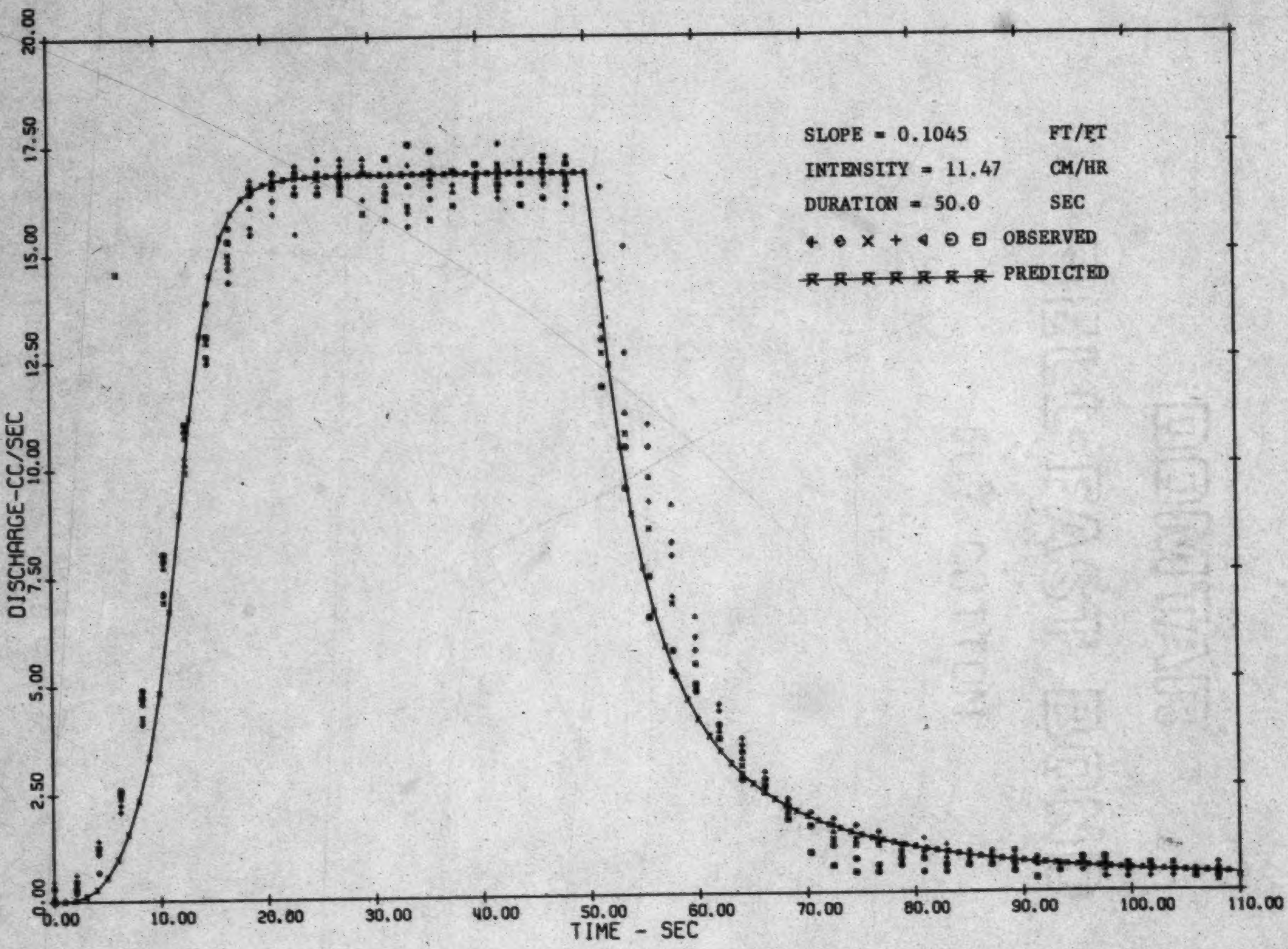

Figure E-7. Observed and predicted hydrographs (state variable model) for test 10 with uniform rainfall input.

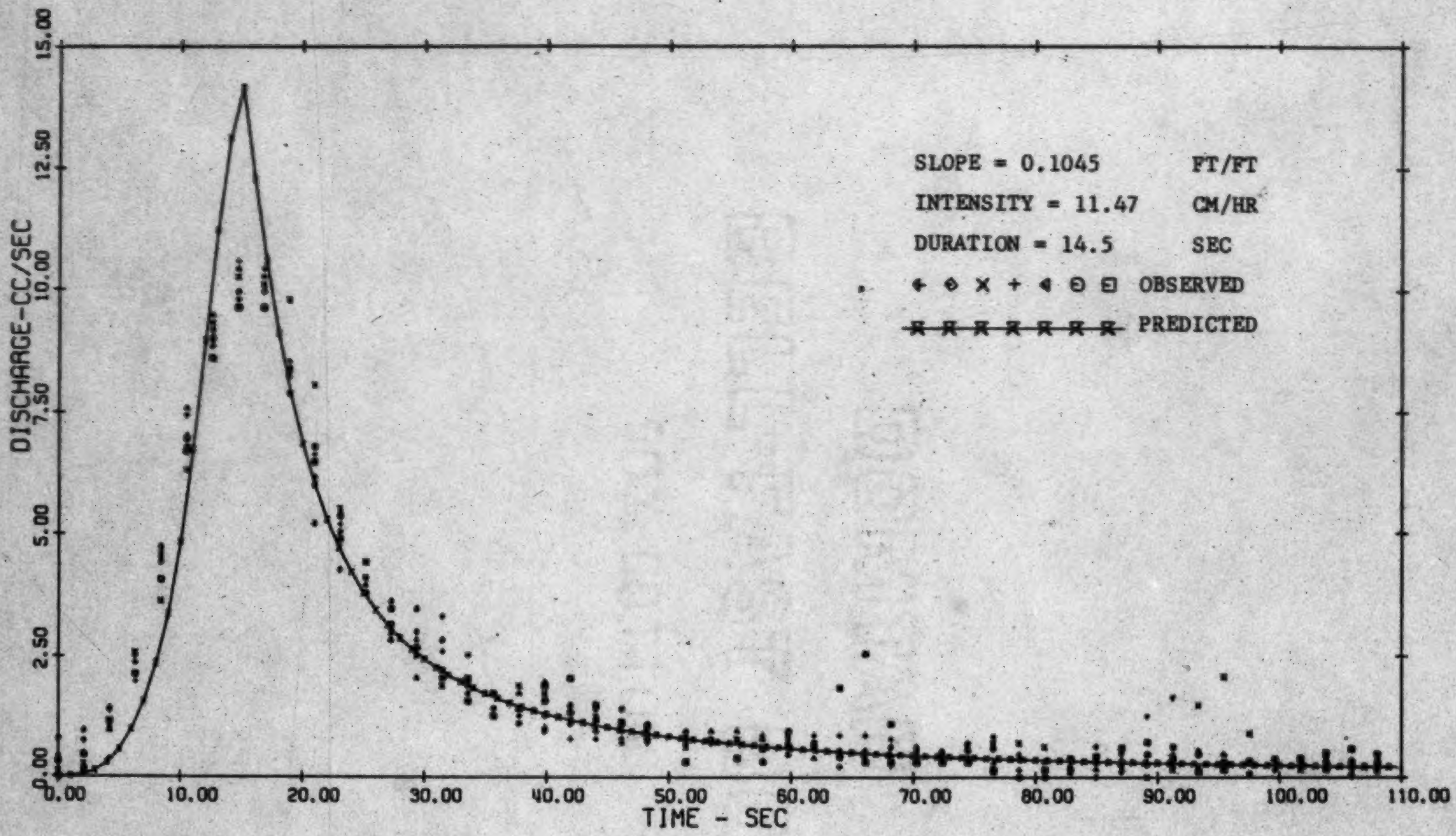

Figure E-8. Observed and predicted hydrographs (state variable model) for test 11 with uniform rainfall input.

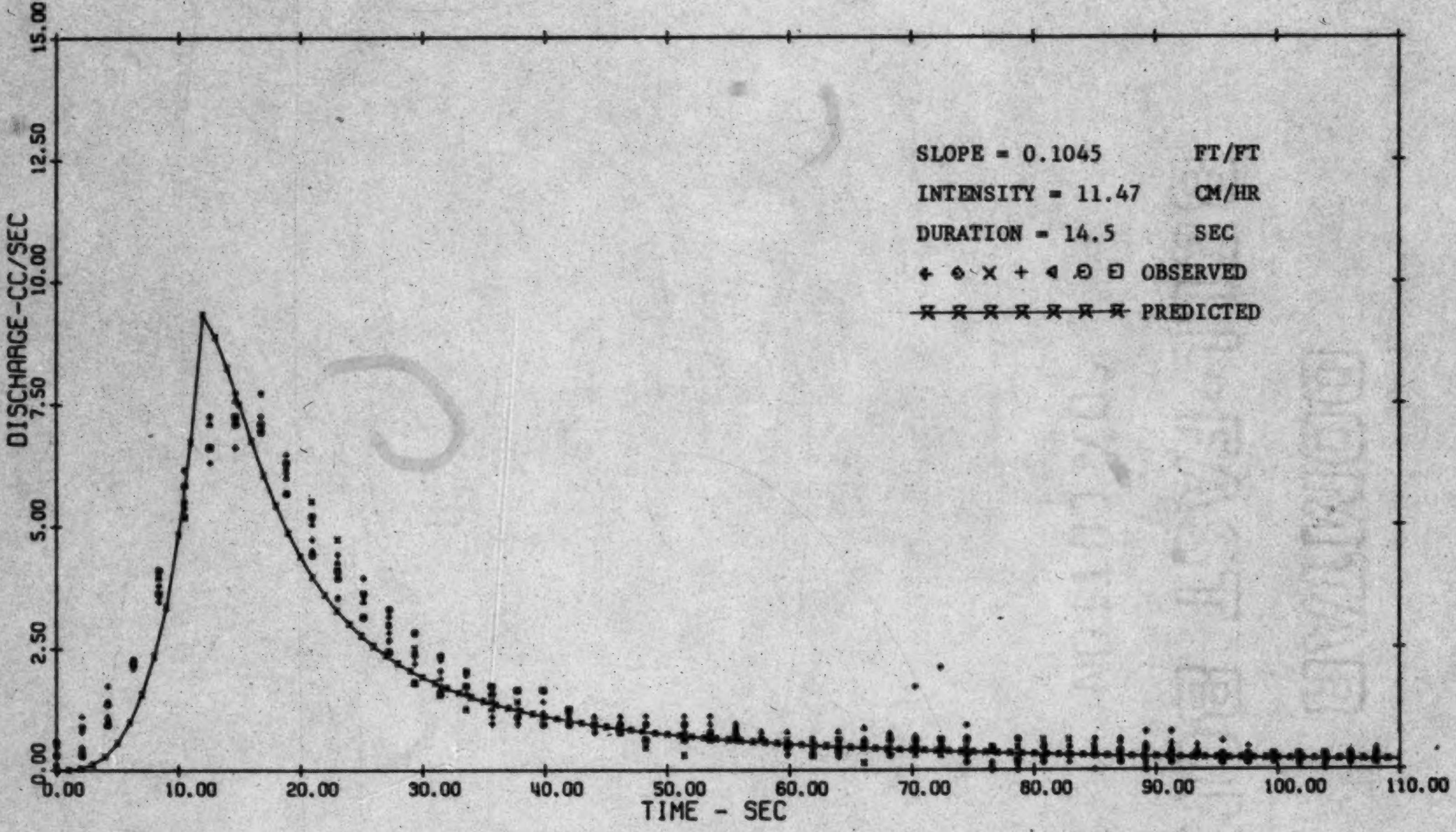

Figure E-9. Observed and predicted hydrographs (state variable model) for test 12 with uniform rainfall input.

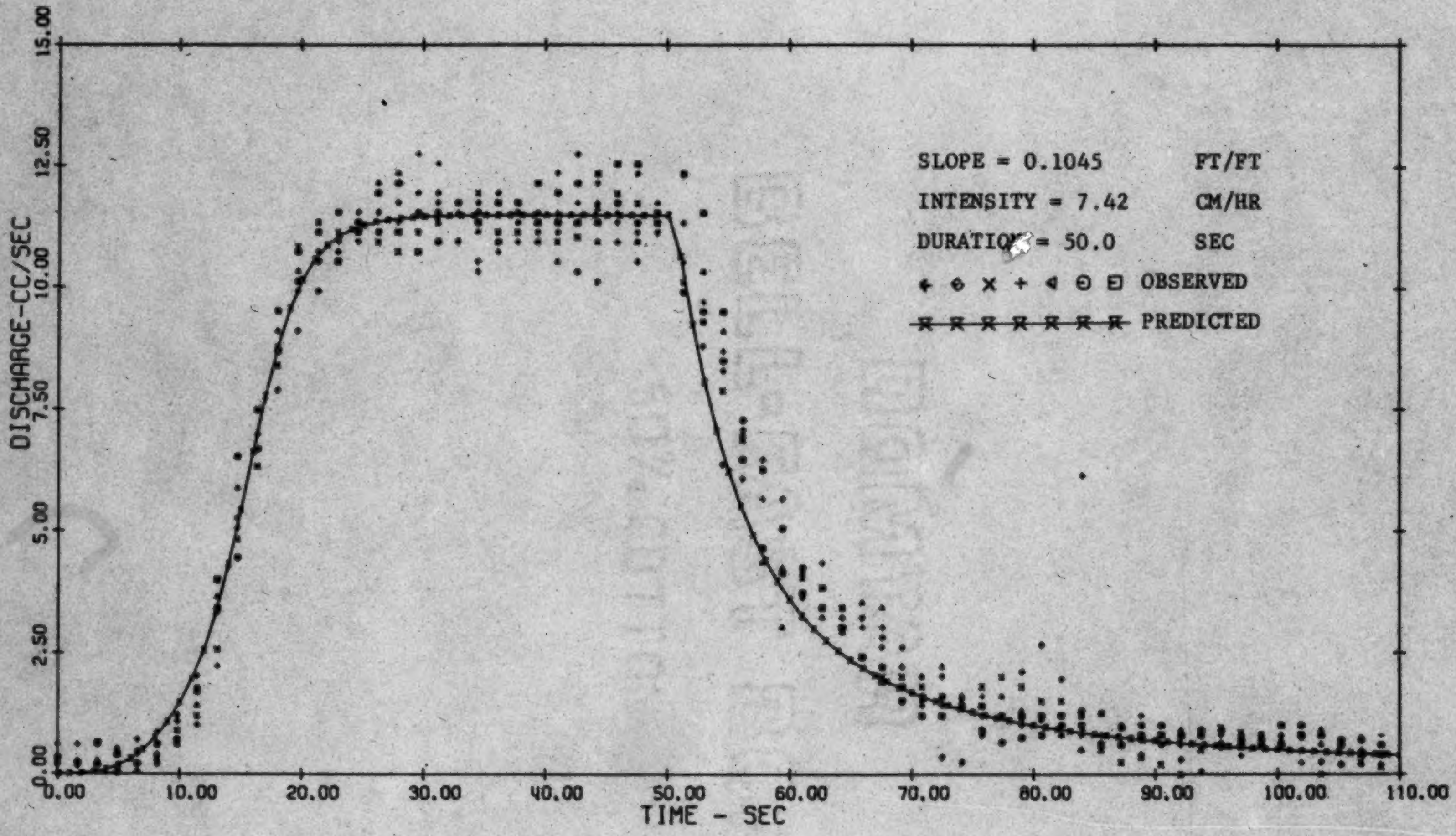

Figure E-10. Observed and predicted hydrographs (state variable model) for test 13 with uniform rainfall input.

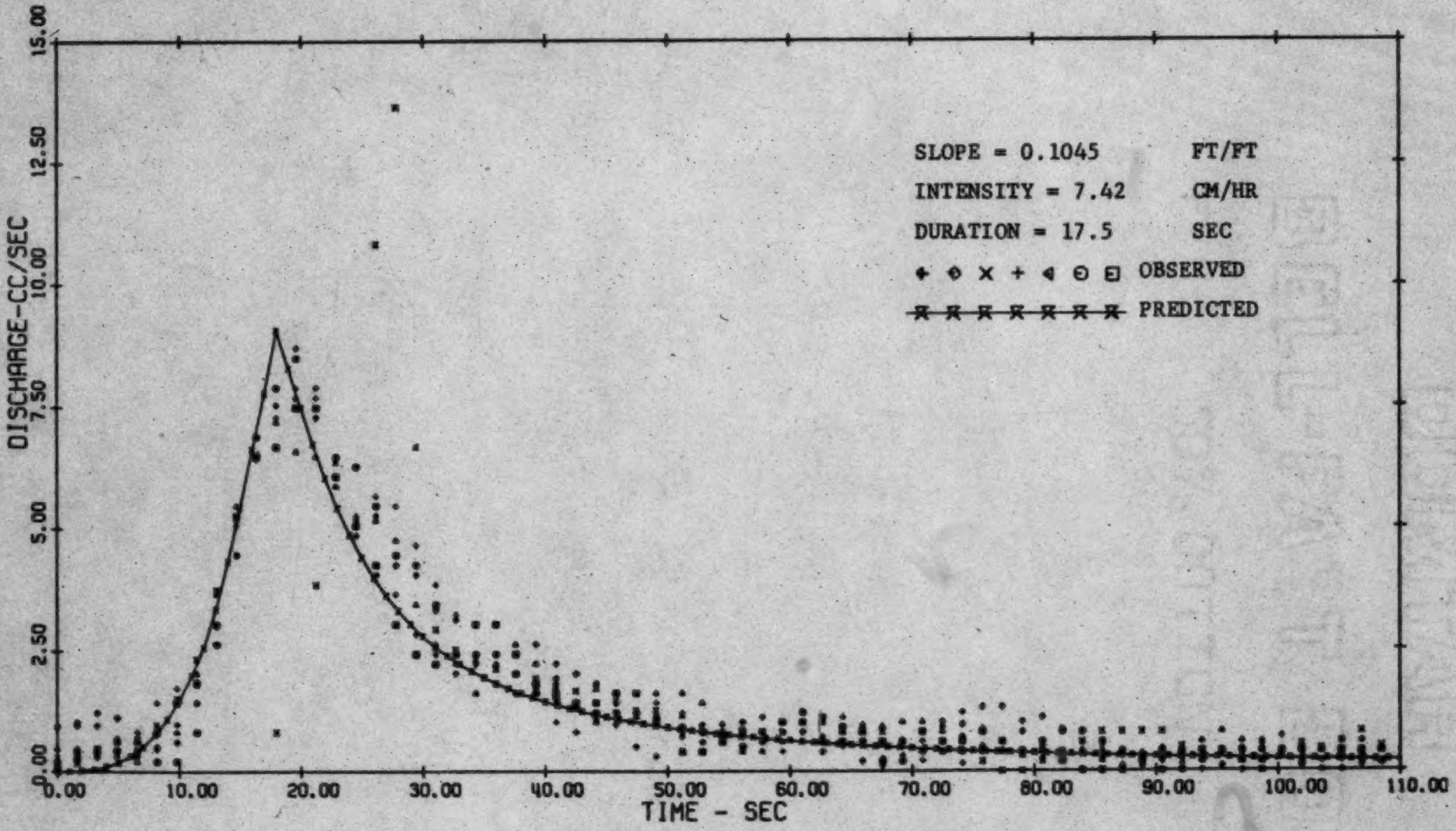

Figure E-11. Observed and predicted hydrographs (state variable model) for test 14 with uniform rainfall input.

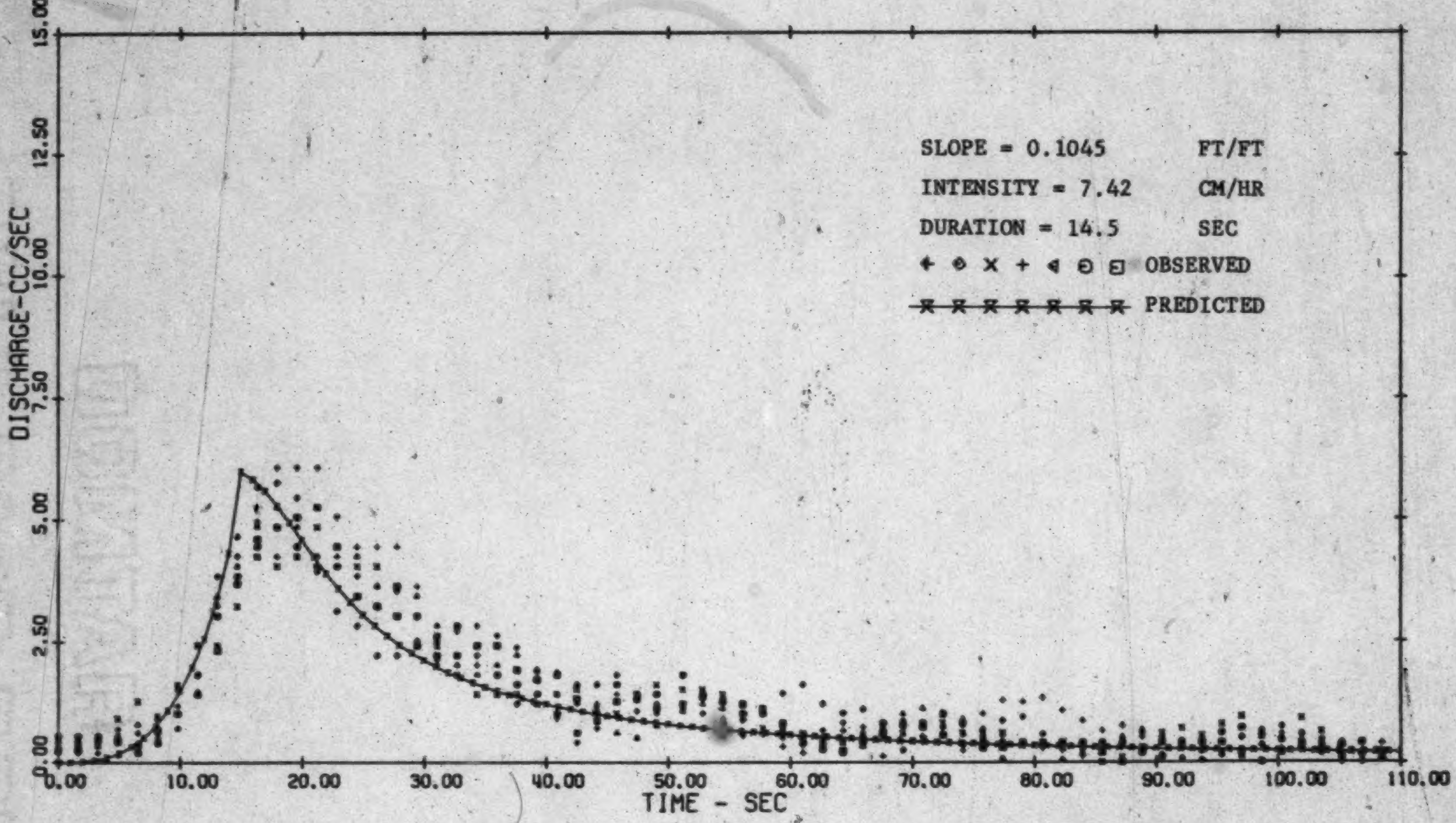

Figure E-12. Observed and predicted hydrographs (state variable model) for test 15 with uniform rainfall input.

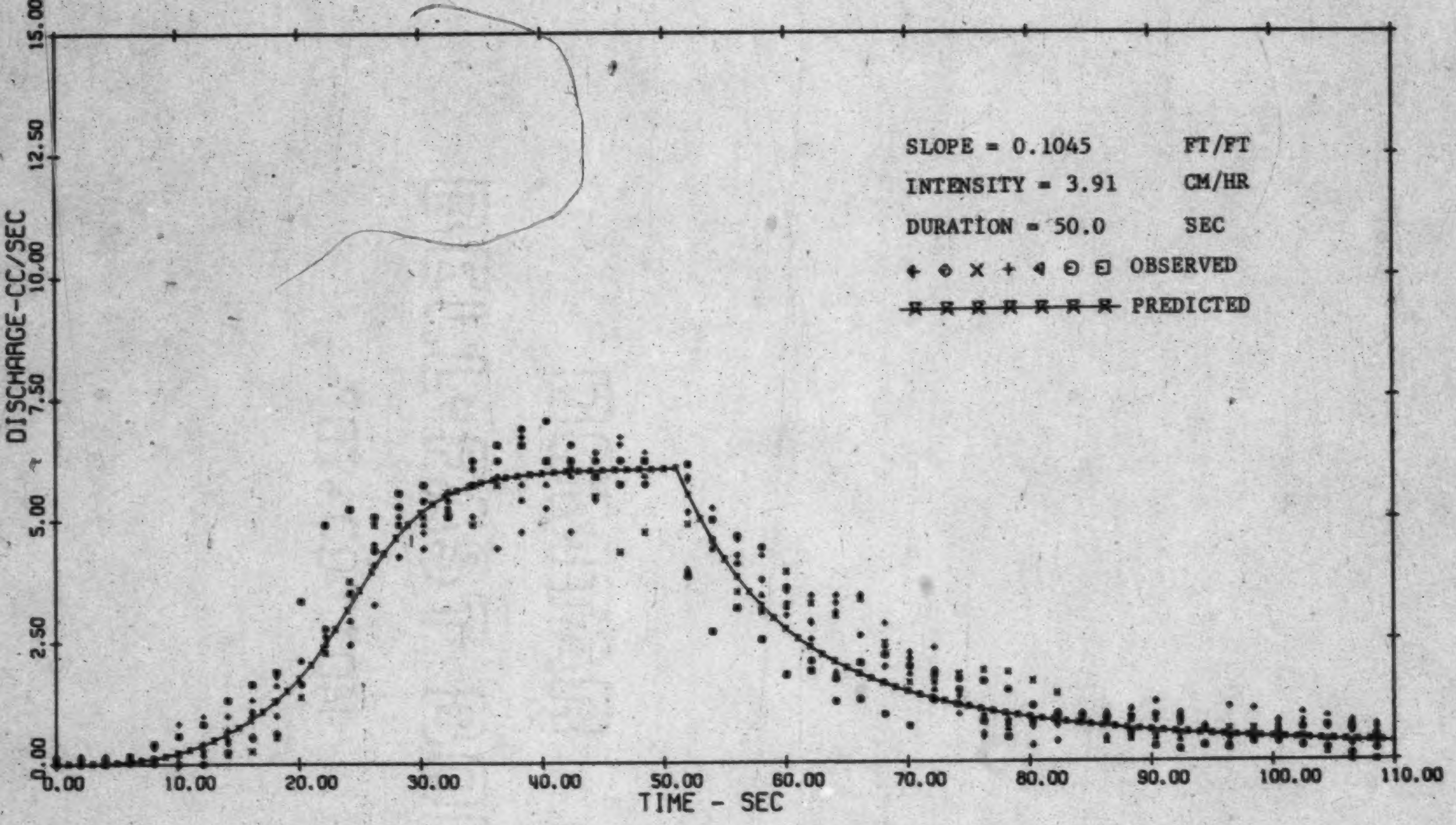

Figure E-13. Observed and predicted hydrographs (state variable model) for test 16 with uniform rainfall input.

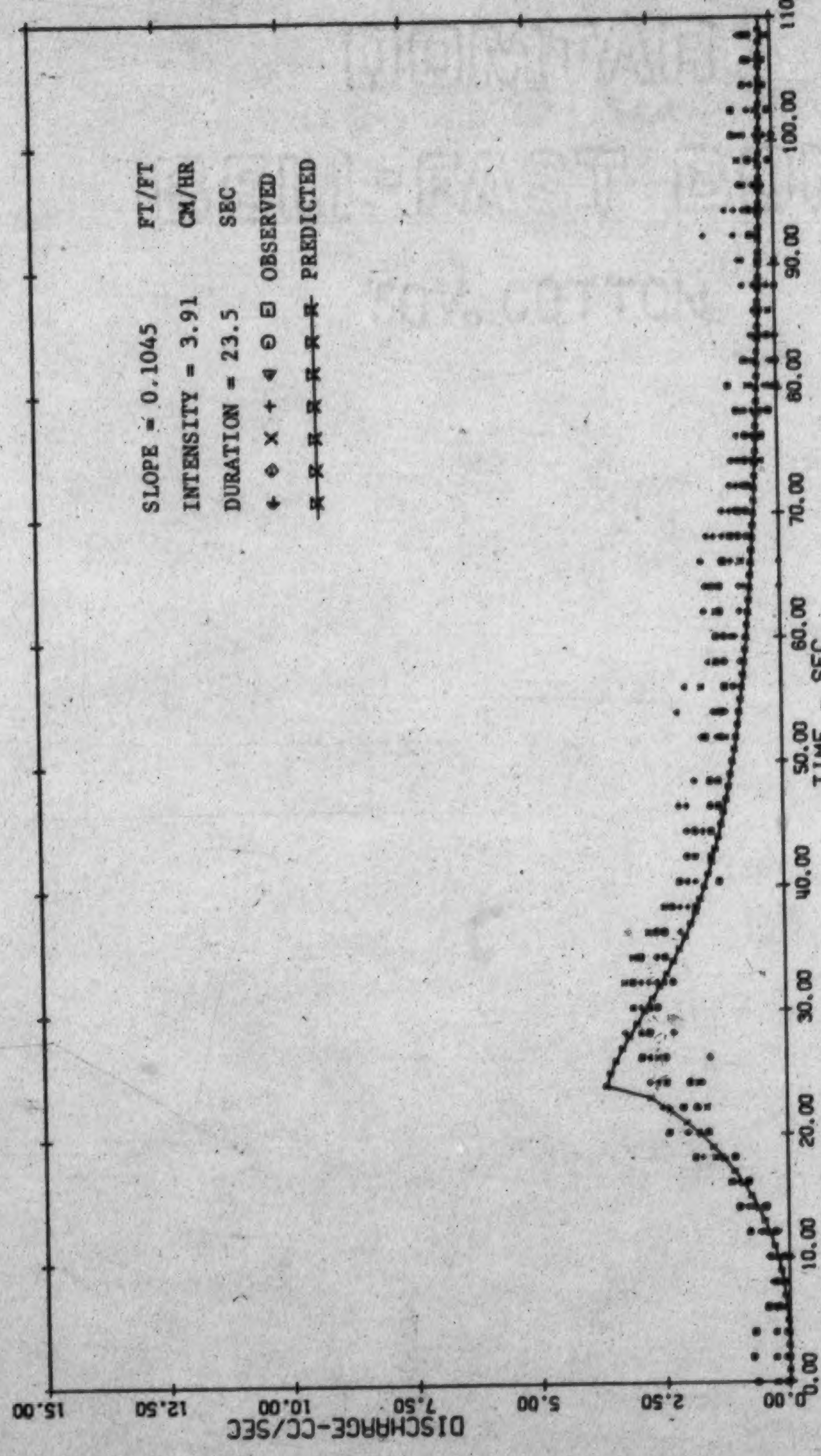

Figure E-14. Observed and predicted hydrographs (state variable model) for test 17 with uniform rainfall input.

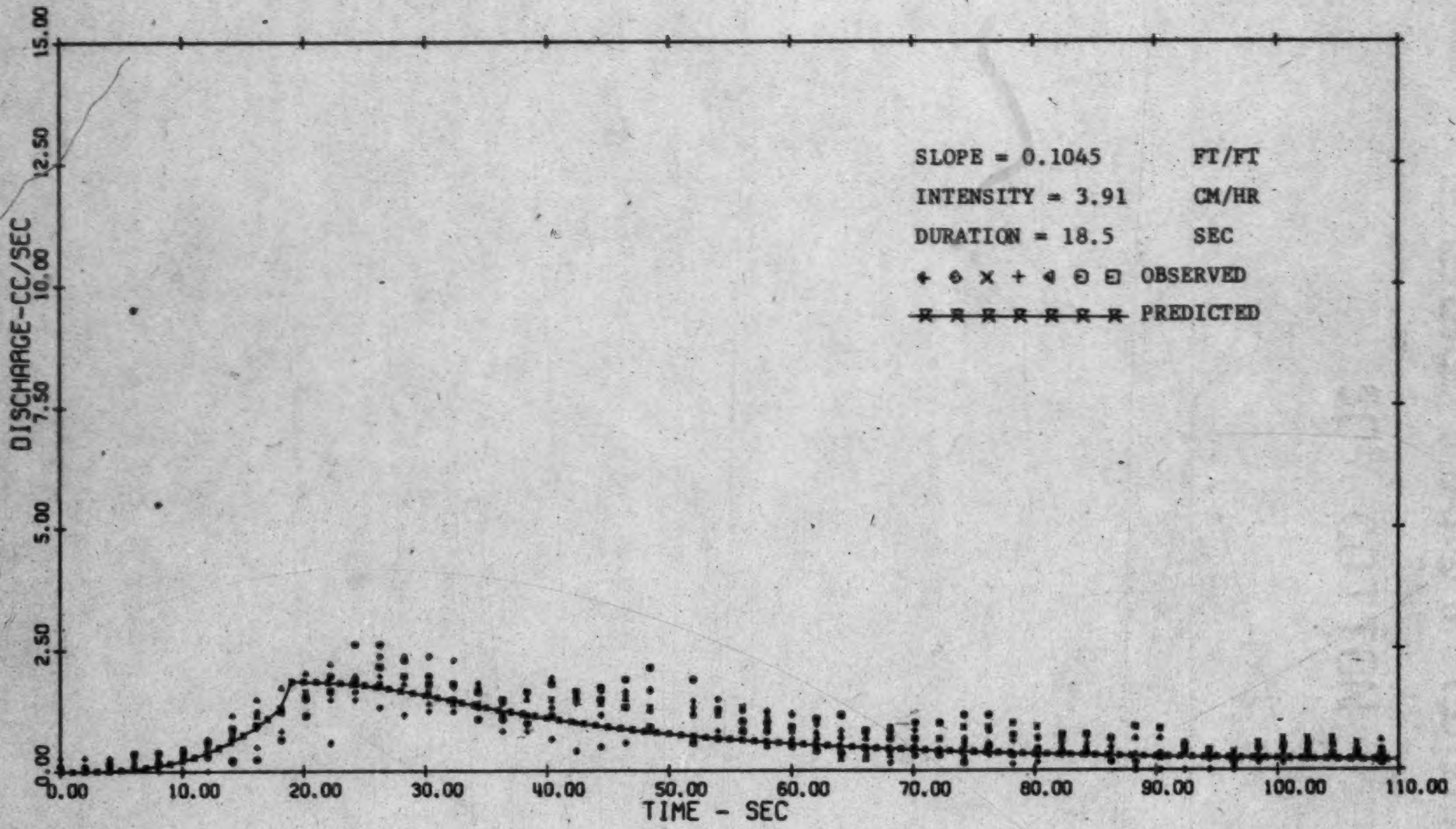

Figure E-15. Observed and predicted hydrographs (state variable model) for test 18 with uniform rainfall input.

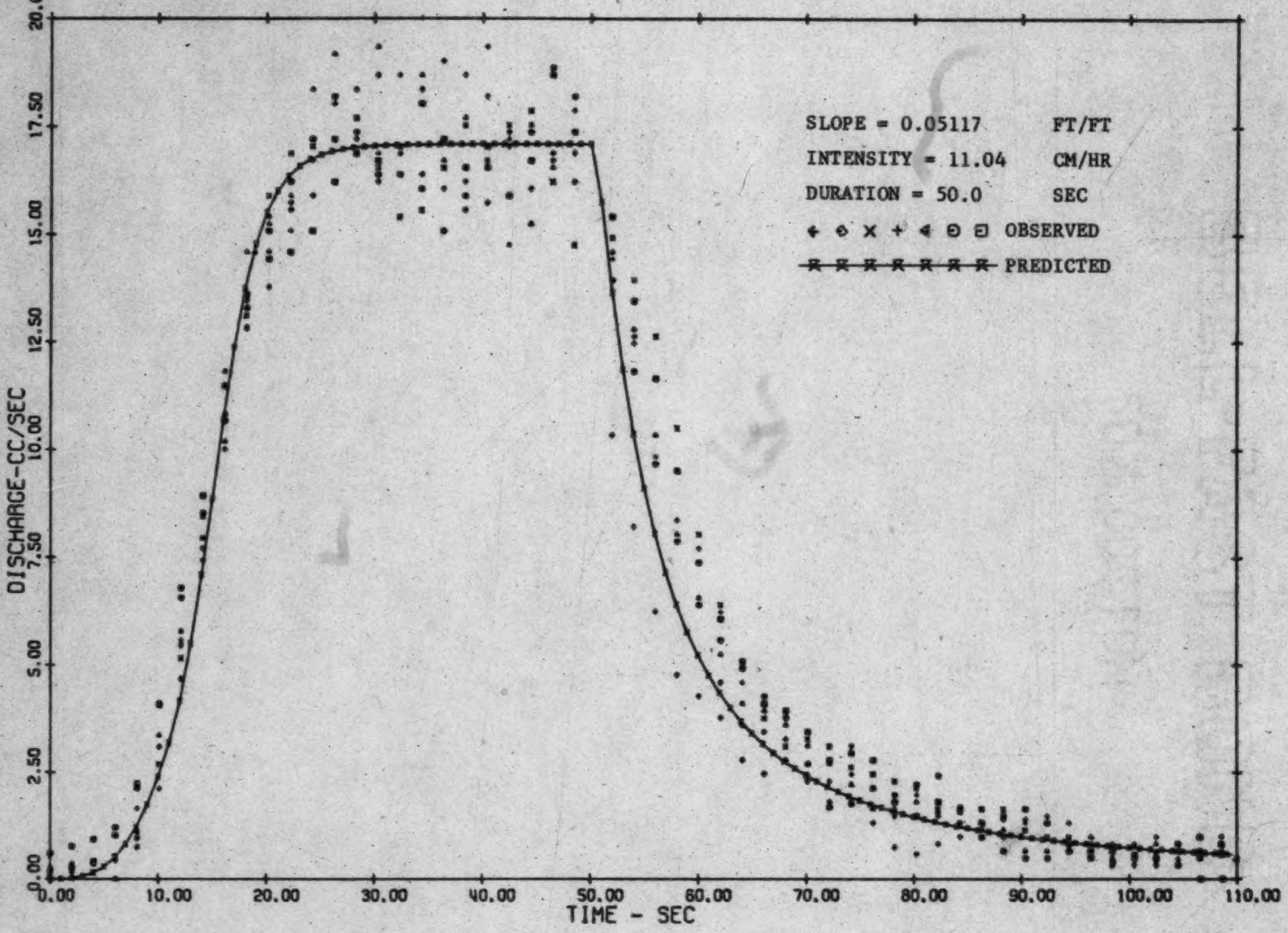

Figure E-16. Observed and predicted hydrographs (state variable model) for test 19 with uniform rainfall input.

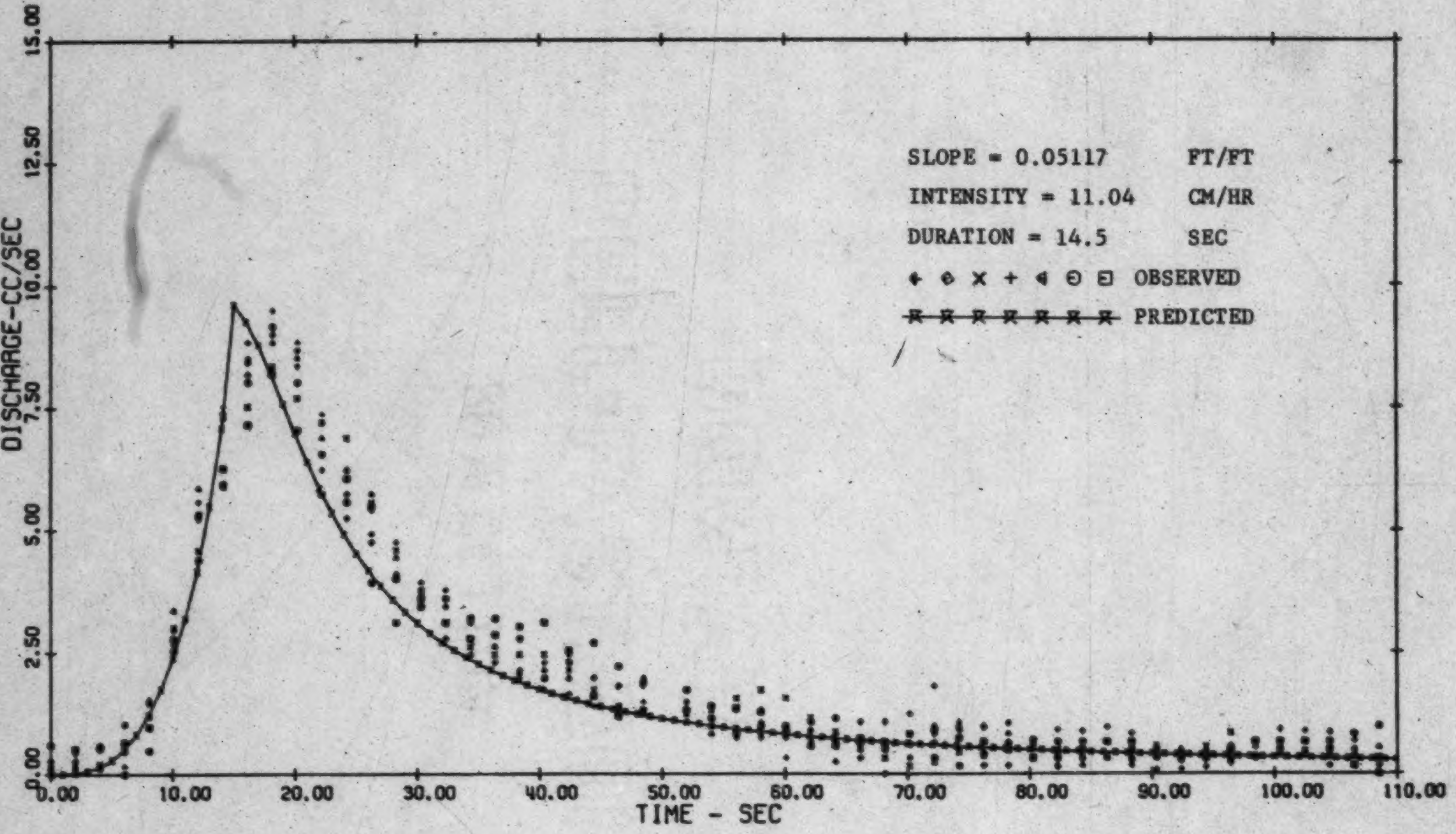

Figure E-17. Observed and predicted hydrographs (state variable model) for test 20 with uniform rainfall input.

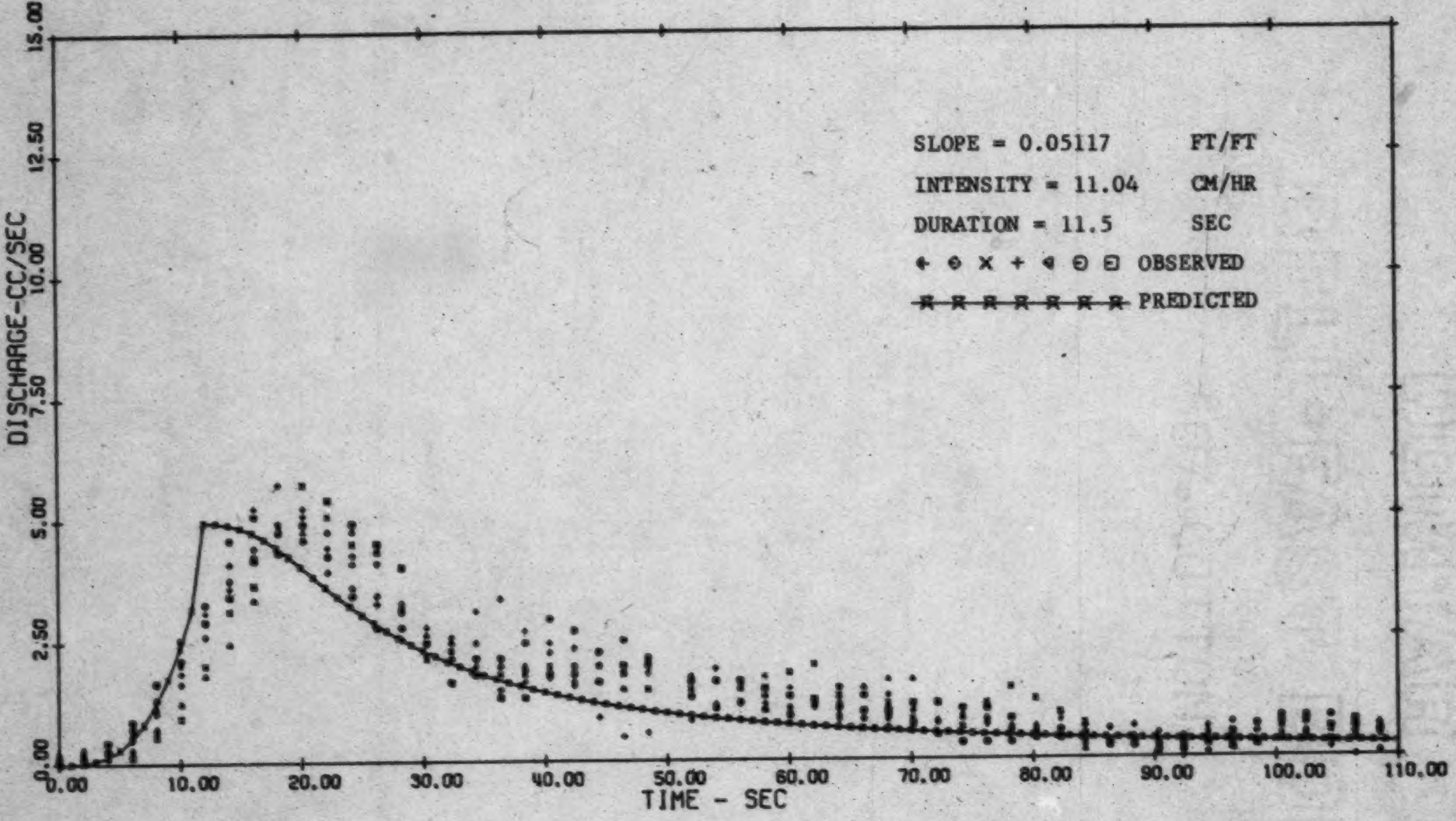

Figure E-18. Observed and predicted hydrographs (state variable model) for test 21 with uniform rainfall input.

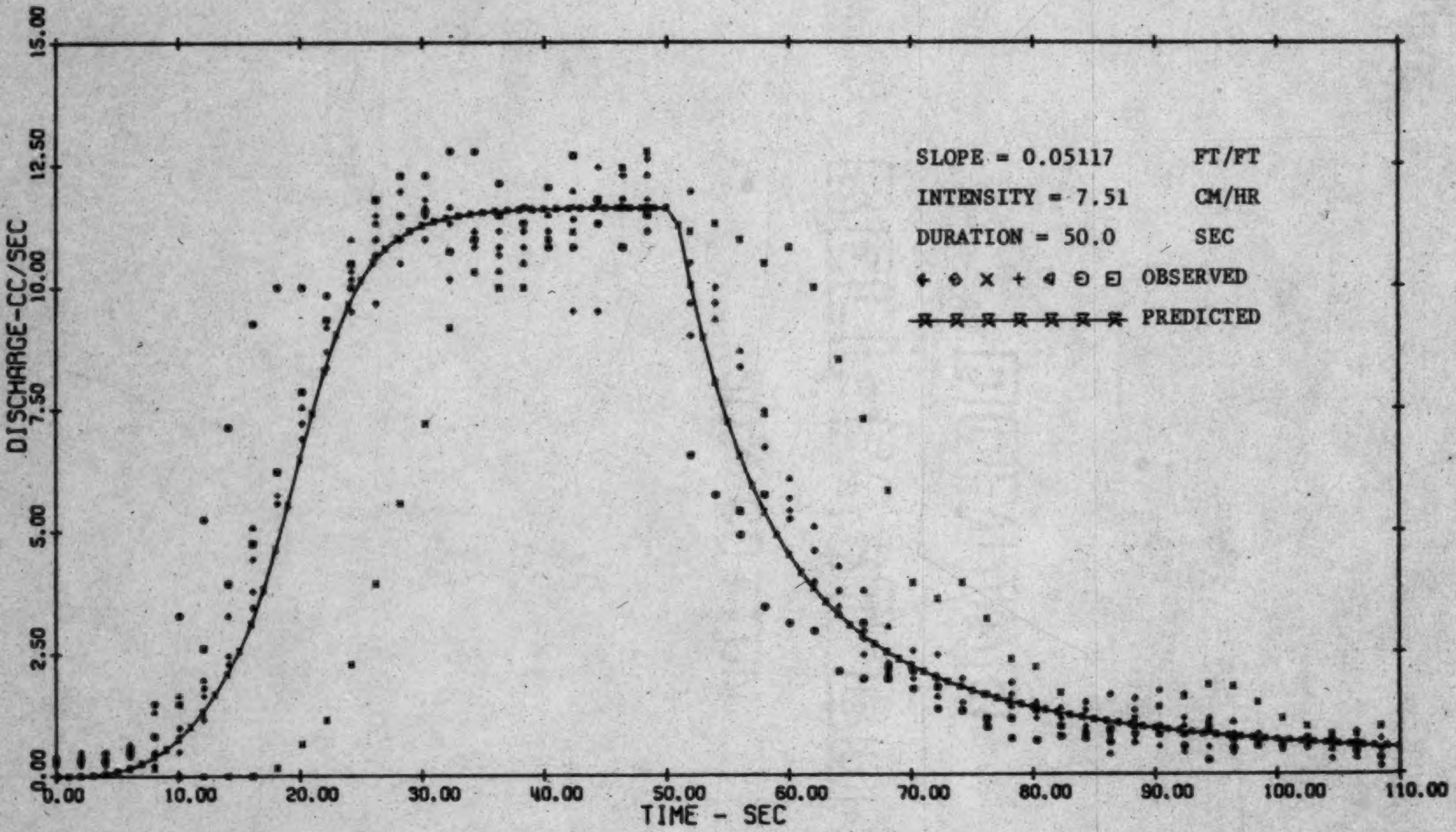

Figure E-19. Observed and predicted hydrographs (state variable model) for test 22 with uniform rainfall input.

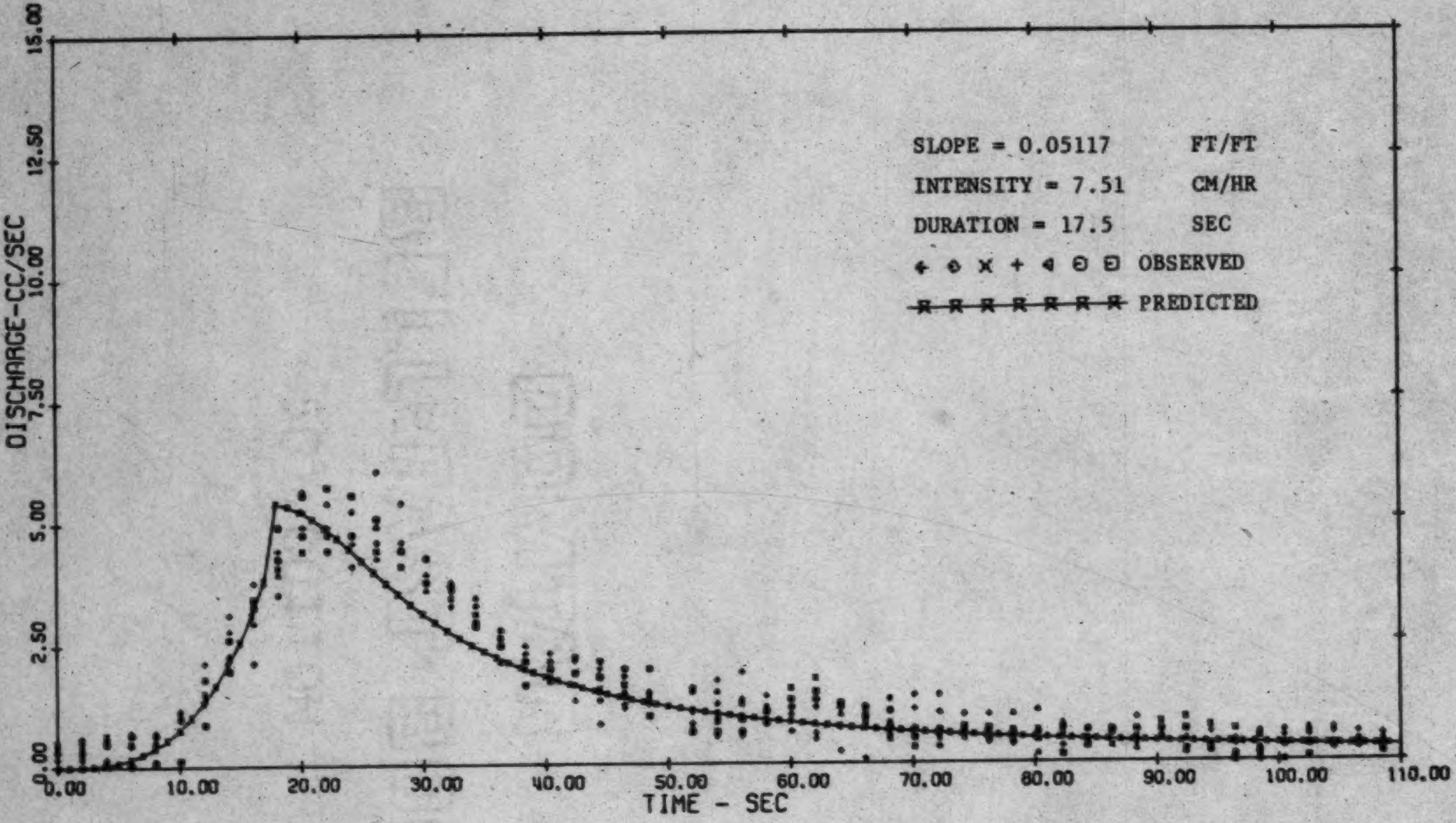

Figure E-20. Observed and predicted hydrographs (state variable model) for test 23 with uniform rainfall input.

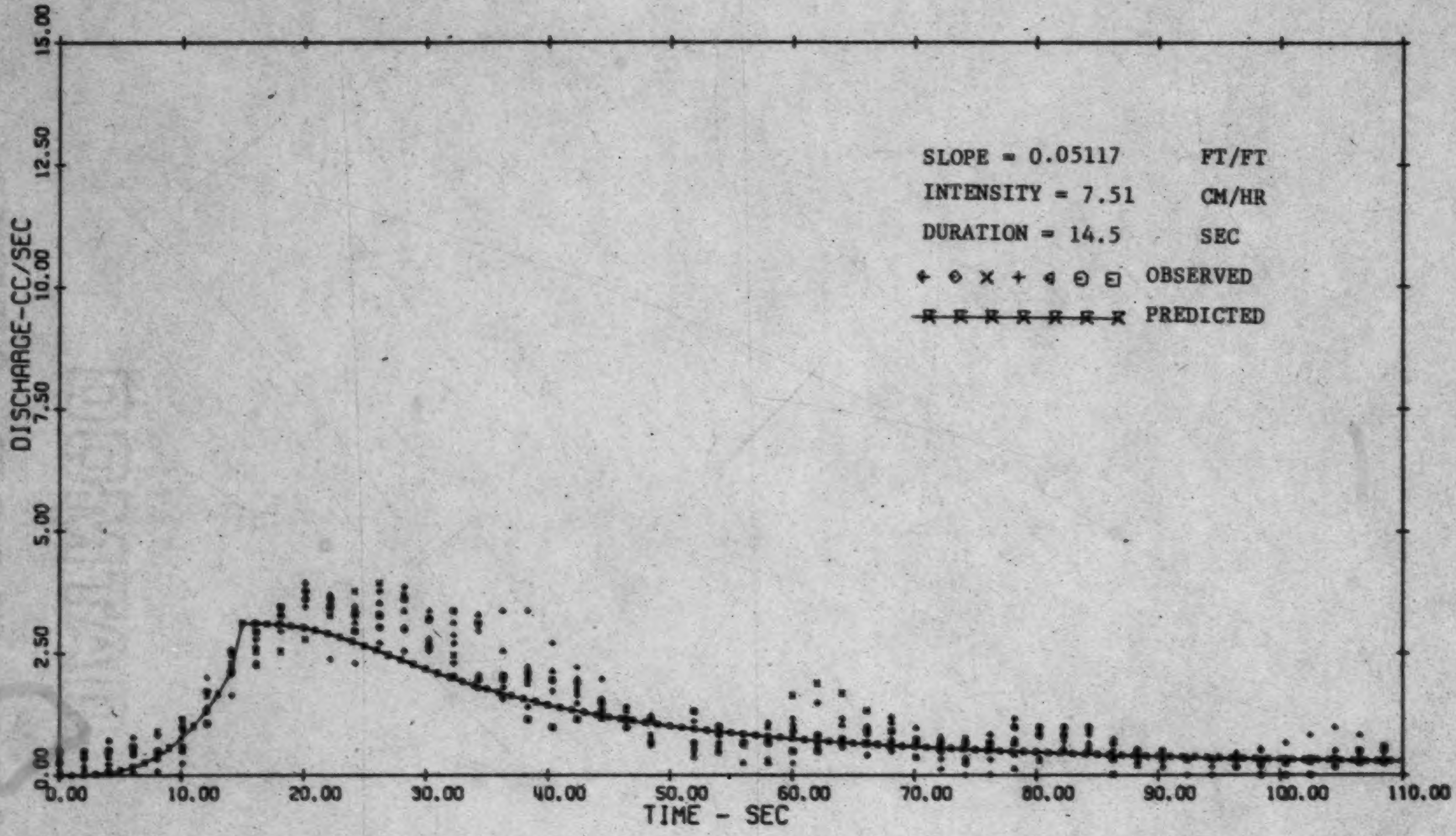

Figure E-21. Observed and predicted hydrographs (state variable model) for test 24 with uniform rainfall input.

APPENDIX F

SAMPLE STATISTICAL ANALYSES

F-1 Confidence Intervals of Cumulative Hydrographs

Cumulative outflows recorded during experiments performed on a laboratory catchment (single pulse rainfall inputs) were analysed statistically as described in Chapter VI. As a sample of the analyses, Table F-1 shows a computation of the 95% confidence intervals of the mean $\bar{x}$ (mean of 7 tests) of the accumulated outflow for the run number 7. The confidence intervals were computed for Student's t = 2.447 and n = 7 according to the formula

$$\bar{x} \pm \varepsilon = \bar{x} \pm \frac{st}{\sqrt{n-1}} \qquad \text{(F-1)}$$

where s is the estimate of the standard deviation. The largest value of ε was found to be ± 5.49 cc which is less than the estimated maximum error of 6 cc given in Table 6-1 in Chapter VI.

Table F-1 also contains values of accumulated outflow as predicted by the state variable model. It can be seen that the predicted values are within the confidence interval of the experimental cumulative hydrograph. Because of the very good fit the cumulative hydrograph predicted by the state variable model was taken as a theoretical smooth curve representing the experimental data.

F-2 Confidence Intervals of Instantaneous Outflow Hydrographs

The instantaneous outflow rates were obtained from the measured cumulative outflow hydrographs by numerical differentiation. The computation of confidence intervals of these determined instantaneous outflow rates for the run number 7 is shown in Table F-2.

Because numerical differentiation involves trunkation and round-off errors, it was necessary to establish the effect of differentiation on the confidence intervals given in Table F-2.

For this purpose, the theoretical curve of the cumulative outflow (predicted by the state variable model) was differentiated and the truncation error was determined (runoff error was neglected). The theoretical and experimental instantaneous outflow hydrographs were than compared to check the validity of the confidence intervals based on the differentiated experimental data.

F-2-1 Determination of the Truncation Error

Numerical differentiation was carried out on the IBM model 360-67 computer using the subroutine DET3 described in the System/360 Scientific Subroutine Package (PL/I). The subroutine computes a vector $Z = (z_1, z_2, \ldots, z_n)$ of derivative values, given a vector $Y = (y_1, y_2, \ldots, y_n)$ of function values whose components y_i correspond to n equidistantly spaced argument values x_i with $x_i - x_{i-1} = h$ for $i = 1, 2, \ldots, n$. The resultant value z_i involves a truncation error T_i where (Hildebrand, 1956)

$$T_i = \begin{cases} \frac{h^2}{3}\, y^{(3)}\,(\xi_1),\ \xi_1 \varepsilon [x_1, x_3] \text{ if } i = 1 \\ -\frac{h^2}{6}\, y^{(3)}\,(\xi_i),\ \xi_i \varepsilon [x_{i-1}, x_{i+1}] \text{ if } i = 2, \ldots, n-1 \\ \frac{h^2}{3}\, y^{(3)}\,(\xi_n),\ \xi_n \varepsilon [x_{n-2}, x_n] \text{ if } i = n \end{cases} \qquad \text{(F-2)}$$

Typical values of the theoretical curve of cumulative outflow, known at discreet time intervals with $h = 0.1$ sec, are shown in Table F-3. The third derivative, $y^{(3)}$, of the curve was determined from a relationship between differences and derivatives of a function (Conte, 1965). In general

$$\Delta^k f(x) = h^k f^{(k)} (\xi) \qquad \text{(F-3)}$$

for $x < \xi < x + k\,h$

where $\Delta^k f(x)$ is the kth difference of a function and $f^{(k)}(\xi)$ is the kth derivative of a function. The truncation error T_i in terms of differences is then given by

$$T_i = \begin{cases} \dfrac{\Delta^3 y(\xi_1)}{3h}, & \xi_1 \in [x_1, x_3] \text{ if } i = 1 \\ -\dfrac{\Delta^3 y(\xi_i)}{6h}, & \xi_i \in [x_{i-1}, x_{i+1}] \text{ if } i = 2, \ldots, n-1 \\ \dfrac{\Delta^3 y(\xi_n)}{3h}, & \xi_n \in [x_{n-2}, x_n] \text{ if } i = n \end{cases} \qquad \text{(F-4)}$$

Table F-3 also contains the computed first, second and third differences and the truncation errors given by Equation (F-4). The maximum error was found to be 0.0007 cc/sec, which is insignificant in comparison with the confidence limits given in Table F-2 and which ranged from 0.1 to 0.5 cc/sec. Since the theoretical curve of the instantaneous outflow lies within the confidence band of the experimental curve, the confidence band was accepted as valid.

TABLE F-1

SAMPLE CALCULATION OF THE CONFIDENCE BAND OF THE CUMULATIVE OUTFLOW HYDROGRAPH

RUN NO. 7

	Cumulative Outflow (cc)										
	Test										
Time (sec)	1	2	3	4	5	6	7	State Variable Model	$\bar{x}$	s	$\pm\varepsilon$
0.0	0	0	0	0	0	0	0	0	0	0	0
2.07	3.03	1.65	0.00	1.10	0.55	0.83	0.83	0.002	1.14	0.97	0.97
4.14	1.24	2.48	0.00	2.75	1.10	-0.41	1.24	0.03	1.20	1.16	1.16
6.20	0.34	1.24	1.65	3.58	2.75	0.62	1.44	0.153	1.66	1.15	1.15
8.27	3.20	0.62	0.83	3.99	4.40	1.14	1.55	0.645	2.25	1.58	1.58
10.33	1.32	1.96	2.06	4.40	6.05	1.65	1.60	1.19	2.72	1.79	1.79
12.40	3.69	3.30	1.03	7.70	6.88	3.30	1.65	2.482	3.93	2.49	2.49
14.47	4.87	4.95	7.12	7.70	5.64	4.95	1.65	4.615	5.27	1.95	1.95
16.54	6.05	5.78	10.16	7.70	11.62	8.25	9.90	7.93	8.49	2.18	2.18
18.60	12.65	6.60	13.20	12.65	14.61	11.55	14.03	12.865	12.18	2.65	2.65
20.67	19.25	13.20	19.80	17.60	17.60	18.15	18.15	19.920	17.68	2.14	1.14
22.74	25.85	23.10	29.70	20.90	34.10	21.45	21.45	28.970	25.22	5.01	5.00
24.8	39.05	39.60	49.50	34.10	40.70	37.95	37.95	39.292	39.83	4.70	4.70
26.87	58.85	46.20	56.10	50.60	50.60	47.85	41.25	50.5	50.21	5.94	5.93
28.94	62.15	56.10	62.70	67.10	67.10	61.05	57.75	62.3	62.0	4.21	4.20
31.0	75.35	69.30	75.90	80.30	70.40	77.55	64.35	74.224	73.31	5.51	5.50
33.07	88.55	82.50	81.20	94.00	93.50	84.15	93.50	86.3	88.2	5.59	5.58
35.14	105.05	99.00	99.00	103.40	96.80	95.70	103.95	98.5	100.41	3.7	3.70
37.21	111.65	108.90	108.90	123.20	116.60	107.25	117.15	110.7	113.4	5.8	5.79
39.27	124.85	122.10	118.80	129.80	119.90	123.75	120.45	122.9	122.8	3.75	3.75
41.34	134.75	132.00	135.30	143.00	129.80	127.05	136.95	135.3	134.12	5.19	4.18

TABLE F-2

SAMPLE CALCULATION OF THE CONFIDENCE BAND OF THE INSTANTANEOUS OUTFLOW HYDROGRAPH

RUN NO. 7

	Instantaneous Outflow (cc/sec) Test										
Time (sec)	1	2	3	4	5	6	7	State Variable Model	$\bar{x}$	s	±ε
0.0	0.16	0.13	0.07	0.26	0.23	0.06	0.11	0	0.14	0.08	0.08
2.07	0.15	0.15	0.10	0.36	0.34	0.09	0.13	0.01	0.19	0.11	0.11
4.14	0.15	0.15	0.18	0.43	0.43	0.16	0.12	0.03	0.23	0.14	0.14
6.20	0.23	0.19	0.31	0.46	0.52	0.29	0.18	0.1	0.31	0.13	0.13
8.27	0.34	0.27	0.49	0.51	0.64	0.44	0.35	0.23	0.43	0.13	0.13
10.33	0.56	0.41	0.75	0.64	0.75	0.68	0.60	0.46	0.63	0.12	0.12
12.40	0.93	0.68	1.17	0.79	1.01	0.97	0.93	0.80	0.93	0.16	0.16
14.47	1.44	1.16	1.78	1.06	1.50	1.39	1.46	1.28	1.40	0.24	0.24
16.54	2.17	1.82	2.48	1.64	2.09	1.97	2.03	1.96	1.89	0.46	0.46
18.60	3.03	2.59	3.21	2.46	2.79	2.66	2.56	2.89	2.76	0.27	0.27
20.67	3.79	3.45	3.94	3.38	3.60	3.45	3.15	3.90	3.54	0.26	0.26
22.74	4.55	4.26	4.51	4.47	4.31	4.29	3.94	4.74	4.33	0.21	0.21
24.8	5.25	4.89	4.78	5.49	4.82	4.97	4.74	5.28	4.99	0.28	0.28
26.87	5.56	5.34	4.91	6.19	5.29	5.40	5.40	5.57	5.45	0.38	0.38
28.94	5.68	5.72	5.04	6.56	5.55	5.72	6.07	5.74	5.76	0.47	0.47
31.0	5.84	5.94	5.14	6.64	5.62	5.75	6.51	5.83	5.92	0.52	0.52
33.07	5.84	6.03	5.33	6.45	5.68	5.65	6.55	5.87	5.93	0.44	0.44
35.14	5.68	6.10	5.65	6.16	5.75	5.72	6.23	5.90	5.90	0.25	0.25
37.21	5.62	6.13	5.91	5.88	5.72	5.81	5.94	5.92	5.86	0.16	0.16
39.27	5.62	6.10	6.16	5.62	5.72	5.78	5.72	5.93	5.82	0.22	0.22
41.34	5.56	6.07	6.39	5.52	5.84	5.88	5.52	5.93	5.82	0.33	0.33

TABLE F-3

SAMPLE CALCULATION OF THE TRUNCATION ERROR OF THE THEORETICAL INSTANTANEOUS OUTFLOW HYDROGRAPH, RUN NO. 7

Time (sec)	Cumulative Discharge (cc)	Δy	$\Delta^2 y$	$\Delta^3 y$	Truncation Error (cc/sec) $\frac{\Delta^3 y}{6h}$
15.0	5.213				
		0.14082			
15.1	5.354		0.00283		
		0.14365		0.00004	-0.00006
15.2	5.498		0.00286		
		0.14651		0.00004	-0.00006
15.3	5.644		0.00290		
		0.14941		0.00004	-0.00006
15.4	5.794		0.00294		
		0.15234		0.00004	-0.00006
15.5	5.946		0.00297		
		0.15532		0.00004	-0.00006
15.6	6.101		0.00301		
		0.15832		0.00004	-0.00006
15.7	6.259		0.00305		
		0.16137		0.00009	-0.00014
15.8	6.421		0.00313		
		0.16450		0.00042	-0.00070
15.9	6.585		0.00355		
		0.16805		0.00011	-0.00019
16.0	6.753		0.00366		
		0.17171		0.00006	-0.00010
16.1	6.925		0.00373		
		0.17544		0.00006	-0.00009
16.2	7.101		0.00378		
		0.17922		0.00006	-0.00009
16.3	7.280		0.00384		
		0.18306		0.00005	-0.00009
16.4	7.463		0.00389		
		0.18695		0.00005	-0.00009
16.5	7.650		0.00394		
		0.19089		0.00005	-0.00009
16.6	7.841		0.00400		
		0.19489		0.00005	-0.00009
16.7	8.036		0.00405		
		0.19894		0.00005	-0.00009
16.8	8.234		0.00410		
		0.20304		0.00005	-0.00009
16.9	8.438		0.00416		
		0.20720			
17.0	8.645				

APPENDIX G

EXAMPLES OF THE PHASE PLANE REPRESENTATION OF SECOND ORDER SYSTEMS

G-1 Determination of Phase Trajectories by Analytical Solution for a Linear Conservative System.

Consider a system described by the second-order differential equation

$$\ddot{z} + z = 0 \qquad \text{(G-1)}$$

Defining the state variables $x_1 = z$, and $x_2 = \dot{z}$, Equation (G-1) may be written as

$$\begin{aligned} \dot{x}_1 &= x_2 \\ \dot{x}_2 &= -x_1 \end{aligned} \qquad \text{(G-2)}$$

and

$$\frac{\dot{x}_2}{\dot{x}_1} = -\frac{x_1}{x_2} \qquad \text{(G-3)}$$

In this case the variables in Equation (G-3) can be separated, thus

$$x_2 dx_2 = -x_1\, dx_1 \qquad \text{(G-4)}$$

and by integration the equation of trajectories is

$$x_2^2 + x_1^2 = C \qquad \text{(G-5)}$$

Equation (G-5) defines phase trajectories which are concentric circles with radii $r = C^{\frac{1}{2}}$. Some of the trajectories are shown in Figure G-1. The constant C is given by the initial conditions at time t_o, $x_1(t_o)$ and $x_2(t_o)$.

The system given by Equation (G-1) in the above example belongs to the class of second-order systems of the form $\ddot{z} + f(z) = 0$, which is known as that of conservative systems. It is so named because $\dot{z}$, which generally represents a measure of damping or energy dissipation in the system, is missing (Hsu, 1968). For this class of systems therefore, energy is conserved. This fact is illustrated by closed trajectories, such as the circles in Figure G-1, or can be seen by writing Equation

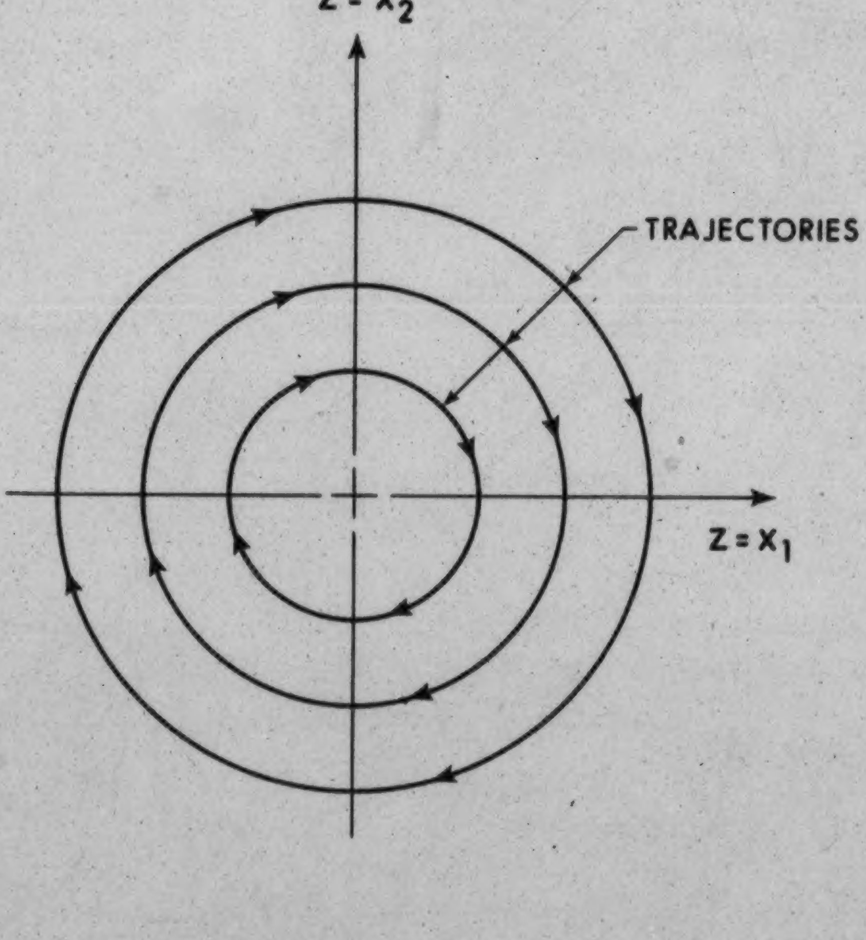
$\dot{Z} = X_2$
TRAJECTORIES
$Z = X_1$

Figure G-1.- Phase trajectories for a system described by $\ddot{z} + z = 0$.

(G-3) more generally as

$$\frac{dx_2}{dx_1} = \frac{-f(x_1)}{x_2} \tag{G-6}$$

Integrating Equation (G-6) yields

$$\frac{x_2^2}{2} + \int_{x_{1o}}^{x_1} f(x)dx = E \tag{G-7}$$

where E is the constant of integration. The first term of Equation (G-7) is seen to be a measure of the kinetic energy of the system, while the second term is a measure of the potential energy. x_{1o} is the equilibrium state in x_1 with reference to which the potential energy is measured. The value of the constant E is thus a measure of the total energy; it is seen to be dependent on the initial condition. For each given value of E, Equation (G-7) gives the trajectory for the system.

G-2 Determination of Phase Trajectories by the Method of Isoclines

If the system differential equation cannot be solved easily then the trajectory must be found by numerical or graphical methods. One of the graphical methods is the method of isoclines. To describe the method in general terms, consider a system of the form

$$\begin{aligned} \dot{x}_1 &= f_1(x_1, x_2) \\ \dot{x}_2 &= f_2(x_1, x_2) \end{aligned} \tag{G-8}$$

or

$$\frac{\dot{x}_2}{\dot{x}_1} = \frac{dx_2}{dx_1} = \frac{f_2(x_1, x_2)}{f_1(x_1, x_2)} \tag{G-9}$$

There are three variables in Equation (G-9), x_1, x_2, and $dx_2/dx_1 = N(x_1, x_2)$. As defined, $N(x_1, x_2)$ gives the slope of the local tangent of the trajectory passing through the point x_1, x_2. If a specific numerical value is chosen for N, such that $N = N_1$, then

$$N_1 = \frac{f_2(x_1, x_2)}{f_1(x_1, x_2)} \qquad \text{(G-10)}$$

Equation (G-10) is a function of x_1 and x_2 only, thus defining a curve on the $x_1 - x_2$ plane, and this curve has the special property of being the locus of all points for which the slope of the phase trajectory is N_1. The line is therefore called an isocline (Thaler, 1962). A suitable field of local tangents N_i, $i = 1, 2, \ldots, m$, is then constructed assuming that the tangent is constant over a small region near the point. From this, the system trajectories can be constructed, if the initial conditions are given. The construction procedure is shown in Figure G-2. The following example serves to illustrate the method.

G-2-2 Linear Non-conservative System

Consider a system represented by the linear differential equation

$$\ddot{z} + \dot{z} + z = 0 \qquad \text{(G-11)}$$

The state variables are again $x_1 = z$, and $x_2 = \dot{z}$. Equation (G-11) is then rewritten as

$$\begin{aligned} \dot{x}_1 &= x_2 \\ \dot{x}_2 &= -x_1 - x_2 \end{aligned} \qquad \text{(G-12)}$$

or

$$\frac{\dot{x}_2}{\dot{x}_1} = N = \frac{-x_1 - x_2}{x_2} \qquad \text{(G-13)}$$

from which

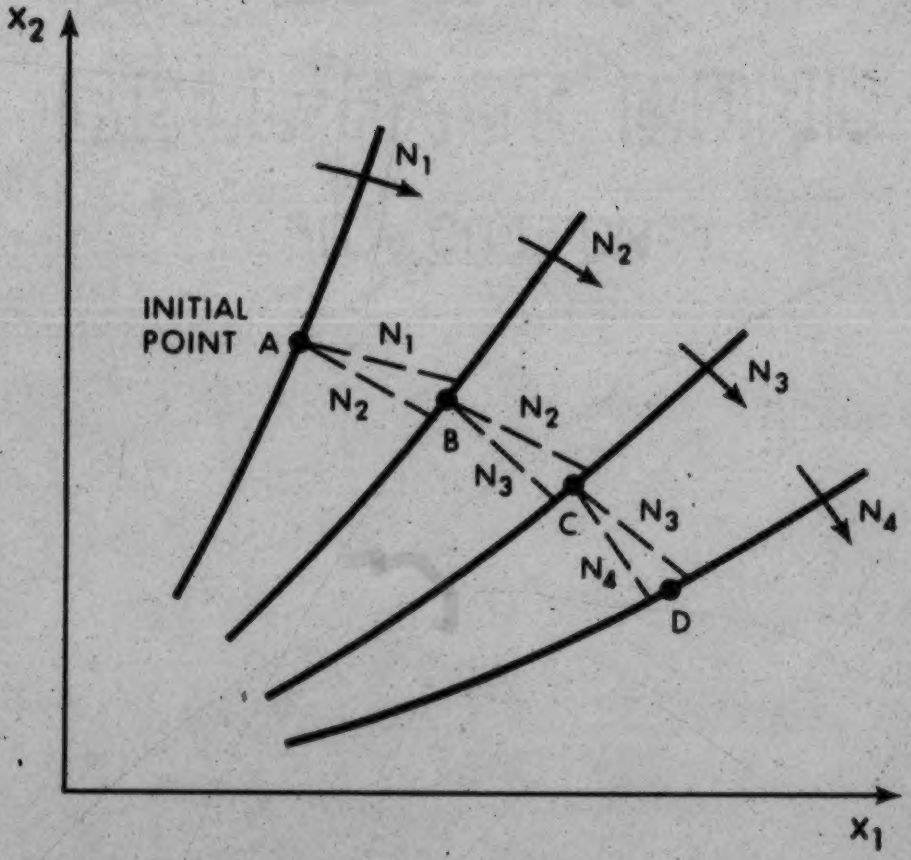
x_2
x_1
INITIAL
POINT A
B
C
D
N_1
N_2
N_3
N_4
N_1
N_2
N_2
N_3
N_3
N_4

Figure G-2. Construction of a trajectory (ABCD) using isoclines.

$$\frac{x_2}{x_1} = \frac{-1}{N + 1} \qquad \text{(G-14)}$$

Equation (G-14) defines the isoclines to be a family of straight lines passing through the origin of the phase plane. Figure G-3 shows isoclines and one particular trajectory for the system given by Equation (G-11).

G-2-3 Nonlinear System. For nonlinear systems the isoclines are curves which usually require the computation of a number of points for each isocline. Consider the nonlinear system described by the equation

$$\ddot{z} + z\dot{z} + z = 0 \qquad \text{(G-15)}$$

from which

$$\frac{\dot{x}_2}{\dot{x}_1} = \frac{-x_1(x_2 + 1)}{x_2} \qquad \text{(G-16)}$$

The isoclines are defined by

$$x_2 = \frac{-x_1}{N + x_1} \qquad \text{(G-17)}$$

Family of isoclines given by Equation (G-17) and several phase trajectories of the system defined by Equation (G-15) are shown in Figure G-4.

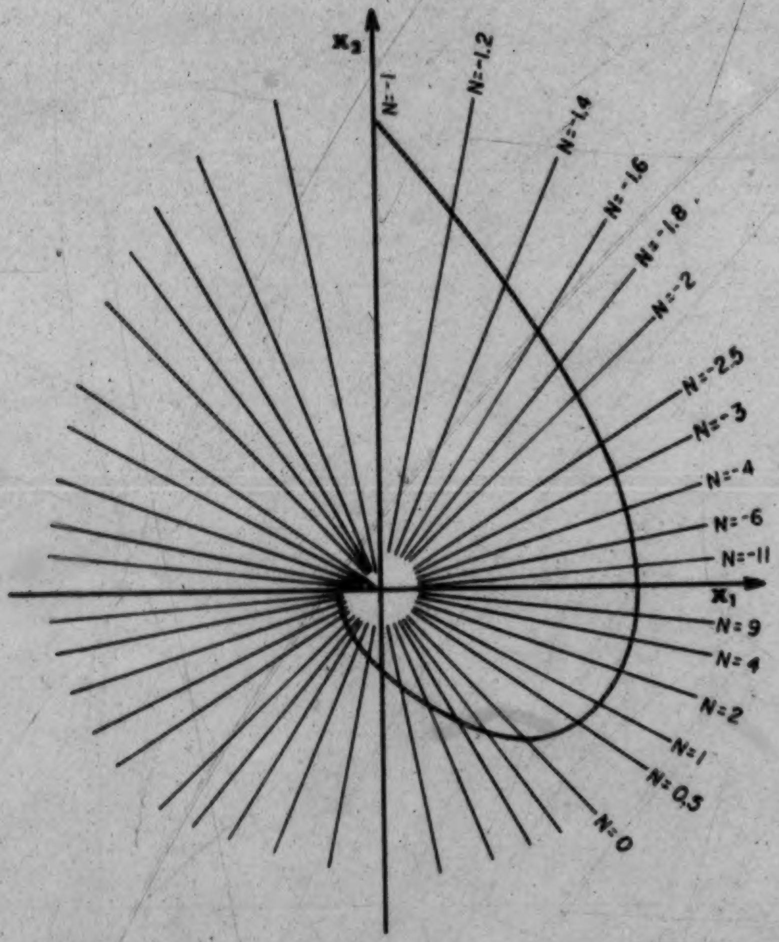
x_2
N=-1
N=-1.2
N=-1.4
N=-1.6
N=-1.8
N=-2
N=-2.5
N=-3
N=-4
N=-6
N=-11
x_1
N=9
N=4
N=2
N=1
N=0.5
N=0

Figure G-3. Phase plane diagram showing isoclines and a typical trajectory for a system described by $\ddot{x} + \dot{x} + x = 0$.

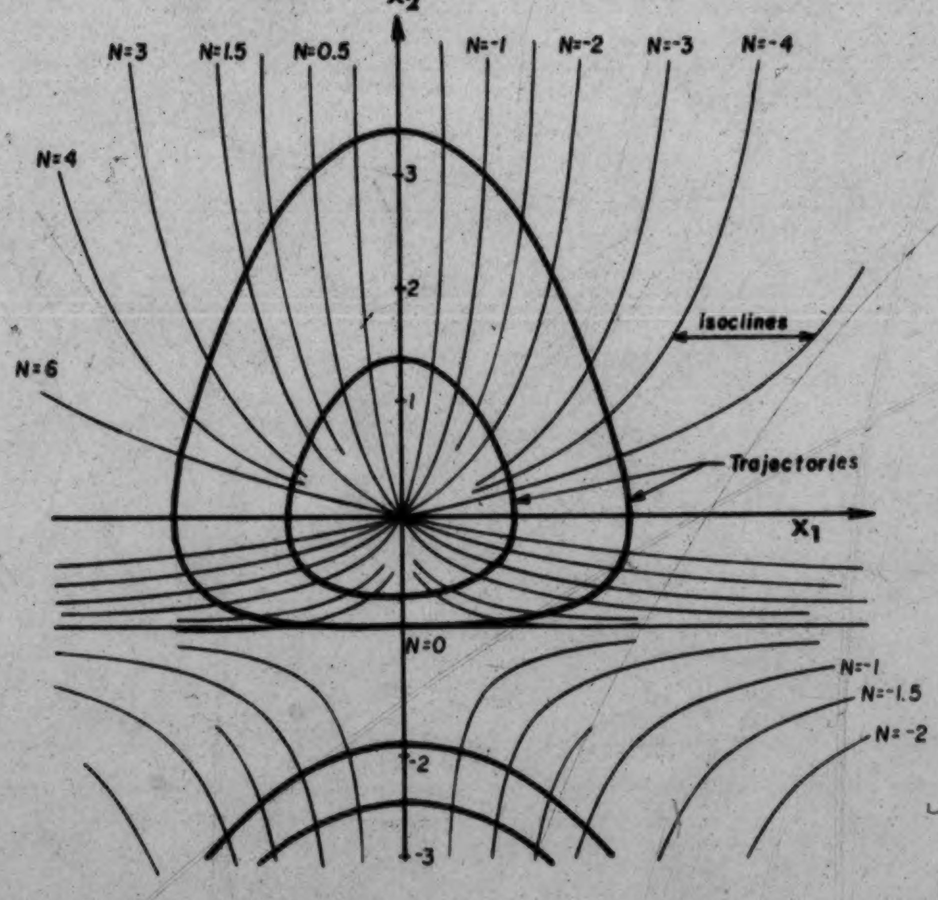
x_2
N=3
N=1.5
N=0.5
N=-1
N=-2
N=-3
N=-4
N=4
3
2
Isoclines
N=6
1
Trajectories
x_1
N=0
N=-1
N=-1.5
N=-2
-2
-3

Figure G-4. Phase plane diagram for a system described by $\ddot{x} + x\dot{x} + x = 0$.